Expression and Targeting of Voltage-Gated Ca^{2+} Channels in Neuroendocrine Cells and Pituicytes

A Thesis

Submitted to

The College of Graduate Studies and Research

In Partial Fulfillment of the Requirements

For the Degree of Doctor of Philosophy

In the Department of Physiology

University of Saskatchewan

Saskatoon

By

David Daoyi Wang

PERMISSION TO USE

In presenting this thesis in partial fulfillment of the requirements for a Postgraduate Degree from the University of Saskatchewan, I agree that the Libraries of this University may make it freely available for inspection. I further agree that permission for copying of this thesis in any manner, in whole or in part, for scholarly purposes may be granted by the professor or professors who supervised my thesis work or, in their absence, by the Head of the Department or the Dean of the College in which my thesis was done. It is understood that any copy or publication or use of this thesis or parts thereof for financial gain shall not be allowed without my written permission. It is also understood that due recognition shall be given to me and to the University of Saskatchewan in any scholarly use which may be made of any material in my thesis.

Requests for permission to copy or to make other use of material in this thesis in whole or part should be addressed to:

Head of the Department of Physiology,
University of Saskatchewan,
107 Wiggins Road,
Saskatoon, Saskatchewan,
Canada S7N 5E5

ABSTRACT

Magnocellular neurosecretory cells (MNCs) are neuroendocrine cells with somata located in the hypothalamus and nerve terminals in the posterior pituitary. They receive neuronal inputs from the brain and release vasopressin and oxytocin into the blood to regulate many important functions such as water balance, lactation, and parturition. The process of hormone release depends on Ca^{2+} influx mediated by voltage-gated Ca^{2+} channels (VGCCs) on the plasma membranes of neuroendocrine cells. To better understand the cellular and molecular components that are involved in regulating secretory vesicle exocytosis, this thesis work was conducted to investigate the expression and function of different subtypes of VGCCs in MNCs and pituicytes (the glial cells surrounding MNC nerve terminals).

Molecular biology, immunohistochemistry and cellular biology were used to detect expression and alternative splicing of different VGCC subtypes in MNCs, neurons, and pituicytes. First, the presence of $Ca_V2.2$ and $Ca_V2.3$ channels were detected on the pituicytes in situ. When the pituicytes were isolated and cultured for 14 days, more VGCC subtypes were expressed including $Ca_V1.2$ channels. Regulation of VGCC expression was measured in normal and dehydrated rats, and $Ca_V1.2$ channels were found to be selectively up-regulated in pituicytes after 24 hours of dehydration.

Second, two splice variants of $Ca_V2.1$ channels ($Ca_V2.1\Delta1$ and $\Delta2$) that lack a large portion of the synprint (synaptic protein interaction) site were detected in

the rat brain. To determine whether the splice variants were expressed in MNCs, we did immunocytochemistry using two antibodies (the selective and the inclusive antibody) that recognized the carboxyl-terminus of channels and the synprint site, respectively, in different cell types. We found that vasopressin MNCs, but not the oxytocin MNCs, and one type of endocrine cell (the melanotropes of the pituitary gland) expressed the synprint site deleted variants, whereas the hippocampal neurons mainly expressed the full-length isoform. The splice variants were properly distributed on the plasma membrane of the somata and nerve terminals of the MNCs, suggesting the synprint site is not essential for $Ca_V2.1$ channel targeting into the nerve terminals of neuroendocrine cells.

Third, expression and distribution of $Ca_V2.2$ channels were studied in the MNCs. All $Ca_V2.2$ isoforms we detected contained the full-length synprint site. To test the importance of the CASK/Mint1 binding site for $Ca_V2.2$ channel targeting, we over-expressed a peptide that inhibits the interaction between $Ca_V2.2$ channels and CASK/Mint1 in differentiated PC12 cells (a neuroendocrine cell line). We found that the distribution of $Ca_V2.2$ channels in the growth cones of PC12 cells were significantly decreased, suggesting that the CASK/Mint1 interaction is important for $Ca_V2.2$ channel targeting into the neuroendocrine terminals.

In conclusion, these results provide insights of VGCC expression in neuroendocrine cells, and also give rise to a better understanding of the molecular components that are involved in forming the exocytotic machinery in these cells.

ACKNOWLEDGEMENTS

I would like to give my thanks to Dr. Thomas E. Fisher, my supervisor, who gave me tremendous inspiration and support to pursue PhD degree and to explore the exciting world of neuroscience. His unfailing passion and patience always encourage me to find a better way to test scientific hypotheses. The way he shows his respect to people and care for people is just exemplary to whoever wants to pursue a career in the scientific world.

I would also want to extend my special thanks to other advisory committee members, Drs. Michel Desautels, Nigel West, Sean Mulligan, Jack Gray and Prakash Sulakhe, for their kind help and advice during years of my study. I appreciate their time and efforts to guide my program, give comments and discuss my thesis writing.

There are many names I want to give my appreciation, including Dr. Gerald W. Zamponi at the University of Calgary and Drs. Xin-Min Li, Darrell D. Mousseau and Bin Yan at the Department of Psychiatry, Dr.Yu Luo at the Department of Biochemistry, Drs. Wolfgang Walz, Francisco Cayabyab, John Howland, Lisa Kalynchuk in the Neural System and Plasticity Research Group, and my colleagues and fellows Dr. Wenbo Zhang, Dr. Kosala Rajapaksha,

Xiaoyu Xu, Xuan Vo, Zhicheng, Chen, Dr. Neil Fournier, Erin Sterner, Clare Florence, Ann Lam, Joanne Sitarski, Gabriel Stegeman, Dilip Singh, and Rene Mag-atas. Without their generous help and collaboration, I could not accomplish the academic goal.

During my PhD program I was supported by a scholarship from the College of Medicine, University of Saskatchewan. The work in this thesis was supported by grants from the Canadian Institutes of Health Research and Natural Sciences and Engineering Research Council of Canada.

DEDICATION

I dedicate this thesis to:

My wife Lily Bin Yan, for her love and understanding, and my son, Morgan Mingda, for the happiness he infuses in my life.

TABLE OF CONTENTS

PERMISSION OF USE STATEMENT……i

ABSTRACT……ii

ACKNOWLEDGEMENTS…….....iv

DEDICATION……...vi

TABLE OF CONTENTS…….....vii

LIST OF TABLES…….xi

LIST OF FIGURES…….....xii

LIST OF ABBREVIATIONS……..xv

1. **INTRODUCTION…….1**

1.1 Calcium signaling and physiology…….....3

1.1.1 Calcium influx, storage, and release…….4

1.1.2 Plasma membrane Ca^{2+} channels…….4

1.1.3 Intracellular Ca^{2+} storage and release…….....8

1.2 Neuronal Ca^{2+} signaling and SNAREs hypothesis…….12

1.2.1 Ca^{2+}-dependent exocytosis mediated by voltage-gated Ca^{2+} channels....12

1.2.1.1 Vesicles holding the neurotransmitter and hormones……13

1.2.1.2 SNARE proteins……...……...15

1.3 Voltage-gated Ca^{2+} channels (VGCCs)……..…….18

1.3.1 VGCCs and Ca^{2+} domains……..….....19

1.3.2 Classification of VGCCs…….……...……....20

1.3.3 The expression and function of subtypes of VGCCs in neural Systems……..25

1.4 VGCC molecular structure and regulation……30

1.4.1 Molecular structure of VGCCs ……..30

1.4.2 Neurotransmission and Ca_V2 channel activities regulated by SNARE proteins … ……..33

1.4.3 Mechanisms of Ca_V2 channel targeting……...36

1.4.3.1 β subunits regulation of the Ca_V2 channel targeting…..36

1.4.3.2 CASK/Mint1 regulation of the Ca_V2 channel targeting..37

1.4.3.3 G protein regulation of the Ca_V2 channel targeting……38

1.4.4 Alternative splicing of Ca_V2 α1 subunits…….……40

1.5 VGCCs expression and function of neuroendocrine cells and pituicytes in the hypothalamo-neurohypophysial system (HNS)……...45

1.5.1 Magnocellular neurosecretory cells (MNCs) in the HNS…….45

1.5.2 Pituicytes in the posterior lobe of the pituitary gland……..51

1.5.3 Ca^{2+} signalings in the pituicytes and glial cells in the CNS…….54

1.5.4 Melanotropes of the intermediate lobe of pituitary gland……...58

2. RATIONALE, HYPOTHESES AND OBJECTIVES……...…..59

3. MATERIAL AND METHODS……...63

3.1 Animal and Cell preparations…….63

3.2 RT-PCR and Molecular Cloning……66

3.3 Plasmid preparation…….68

3.4 Western-Blot……70

3.5 Immunohistochemistry and Immunocytochemistry…….71

3.6 Epifluorescent and Confocal Microscopy……..74

3.7 Statistics…….75

4. RESULTS……78

4.1 Expression and distribution of VGCCs on pituicytes……78

4.1.1 $Ca_V2.2$ and $Ca_V2.3$ channels are expressed on pituicytes of the NH…….....78

4.1.1.1 Identification of pituicytes……78

4.1.1.2 Identification of different subcellular components in the NH……81

4.1.1.3 Identifying VGCCs on the pituicytes…….....85

4.1.2 The $Ca_V1.2$ channels can be selectively up-regulated in the pituicytes after dehydration……...89

4.1.3 Multiple subtypes of VGCCs expressed on cultured pituicytes…….100

4.2 Targeting properties of the $Ca_V2.1$ and $Ca_V2.2$ channels in neuroendocrine cells……..107

4.2.1 RT-PCR results revealed the presence of the $Ca_V2.1$ splice variants in rats…….107

4.2.2 Immunohistochemical and immunocytochemical evidence showing the expression of the $Ca_V2.1$ splice variants……..113

4.2.2.1 Differential distributions of the $Ca_V2.1$ splice variants in OT-MNCs and VP-MNCs……..118

4.2.2.2 Expression of the $Ca_V2.1$ splice variants in the melanotropes of the IL……..127

4.2.3 Expression of the $Ca_V2.2$ channels in the SON and NH……...130

4.2.4 Terminal targeting of the $Ca_V2.2$ channels in differentiated PC12 cells……140

5. GENERAL DISCUSSION…….....149

5.1 VGCCs expressed in the glial cells of the neurohypophysis……149

5.1.1 Ca^{2+} signaling in pituicytes and cortical astrocytes…….....149

5.1.2 L-type Ca^{2+} channels are up-regulated in the pituicytes during dehydration…….153

5.2 Splice variants of the $Ca_V2.1$ channels lacking syntprint site are expressed in neuroendocrine cells…….....156

5.2.1 The regulation of the synprint site in fast neurotransmission and hormone release……..…….156

5.2.2 Targeting properties of the $Ca_V2.1$ channels and splice variants…….…….165

5.2.3 The $Ca_V2.2$ channels expressed in neuroendocrine cells contain the synprint site and exon 18a……..…….171

5.2.4 Functions of the $Ca_V2.1$ and $Ca_V2.2$ channels in MNCs……174

5.3 Future direction……..178

6. CONCLUSIONS……....180

7. REFERENCES……..182

8. APPENDIX ……**206**

LIST OF TABLES

Table 1-1 The α1 subunits of VGCCs and corresponding Ca^{2+} currents…….25

Table 1-2 Comparison of the genome information between the human $Ca_V2.1$ and $Ca_V2.2$ channels……44

Table 1-3 Comparison of alternative splicing sites between the human $Ca_V2.1$ and $Ca_V2.2$ channels……44

Table 4-1 Immunohistochemistry in the neurohypophysis. Single labeling of MNC nerve terminals, synaptic inputs and S100β positive pituicytes…….80

Table 4-2 Immunohistochemistry in the neurohypophysis. Double staining of the combinations among MNC terminals, synaptic inputs and pituicytes……..83

Table 4-3 Immunohistochemistry in the neurohypophysis. Double staining of VGCC α1 subunits and pituicytes by rabbit polyclonal α1 subunit antibodies (Alomones laboratories) and S100β……....87

Table 4-4 Immunohistochemistry in the neurohypophysis. Double staining of VGCC α1 subunits and pituicytes by goat polyclonal α1 subunit antibodies (Santa Cruz Biotechnology) and S100β……....88

LIST OF FIGURES

Figure 1.1 Calcium influx, storage, and release in a cell……12

Figure 1.2 Molecular model of a typical synaptic vesicle…….....14

Figure 1.3 Types of presynaptic Ca^{2+} signals……..19

Figure 1.4 Sequence similarities of VGCC α1 subunits and their major tissue distributions…….....24

Figure 1.5 Primary and accessory subunits of VGCCs on the plasma membrane…….31

Figure 1.6 Possible regulatory regions that affect channel activity and targeting……39

Figure 1.7 Schematic representation of human $Ca_V2.1$ molecular structure showing the loci of exons……..42

Figure 1.8 MNC soma in the SON of hypothalamus and terminals in the posterior pituitary…….46

Figure 1.9 Possible functions for VGCCs in the MNCs…….....49

Figure 1.10 Effects of plasma osmolality on vasopressin secretion and firing rate in VP-MNCs……50

Figure 4.1 Distribution of immunoreactivity to S100 β and synapsin I in the pituitary gland……81

Figure 4.2 Distribution of immunoreactivity to S100 β, the neurophysins, and synapsin I in the neurohypophysis……..84

Figure 4.3 Distribution of immunoreactivity to Ca^{2+} channels in the NH…….....86

Figure 4.4 Increased expression of $Ca_V1.2$ in the pituicytes during 24h dehydration…….....91

Figure 4.5 Quantitative measurement of immunofluorescence of the $Ca_V1.2$ channels in the pituicytes between control and dehydrated rats……..92

Figure 4.6 Negative control of immunostaining of the $Ca_V1.2$ antibody……..93

Figure 4.7 Expression level of the $Ca_V1.3$ channels in the pituicytes was unchanged during dehydration in comparison with normal condition…….95

Figure 4.8 Normalized immunofluorescence of the $Ca_V1.3$ channels in the pituicytes of control and dehydrated rats……..96

Figure 4.9 Expression level of $Ca_V2.3$ in the pituicytes was unchanged during dehydration in comparison with normal condition…….97

Figure 4.10 Normalized immunofluorescence of the $Ca_V2.3$ channels in the pituicytes of control and dehydrated rats……..…….....98

Figure 4.11 Expression levels of the $Ca_V2.2$ channels in the pituicytes was not changed during dehydration in comparison with normal condition……..…….99

Figure 4.12 Quantitative measurement of immunofluorescence of the $Ca_V2.2$ channels in the pituicytes between normal and dehydrated rats……...……100

Figure 4.13 Western-blot of VGCC expression in cultured pituicytes…1..02-103

Figure 4.14 Expression of multiple VGCCs in cultured pituicytes……104

Figure 4.15 Amino acid sequences of the splice variants of $Ca_V2.1$ channels…….110-111

Figure 4.16 Splice variants of $Ca_V2.1$ observed in RNA isolated from rat brains…….111

Figure 4.17 A representative RT-PCR image demonstrating that the $Ca_V2.1$ splice variants are found in isolated neuroendocrine cells…….…….113

Figure 4.18 Working mechanism of the inclusive and selective antibodies directed against different parts of the $Ca_V2.1$ channels……..…...116

Figure 4.19 Immunofluorescence in three different cell types using two antibodies directed against different portions of the $Ca_V2.1$ α1 subunit……117-119

Figure 4.20 Expression patterns of different isoforms of $Ca_V2.1$ channels in the rat SON……120-121

Figure 4.21 Distribution of the splice variants of $Ca_V2.1$ channels in OT-MNCs and VP-MNCs……...122

Figure 4.22 Localizations of the full-length and splice variants of $Ca_V2.1$ channels on nerve terminals of VP-MNC in the NH…….125-127

Figure 4.23 Localization of the splice variants of $Ca_V2.1$ channels on melanotropes in the IL…….....128-129

Figure 4.24 RT-PCR results of screening synprint site deletion isoforms of the $Ca_V2.2$ channels……131-132

Figure 4.25 Localization of $Ca_V2.2$ channels in soma and nerve terminals of acutely isolated MNCs, and cultured hippocampal neurons and PC12 cell lines…….134-135

Figure 4.26 Distribution of $Ca_V2.2$ channels in the SON…….....137-138

Figure 4.27 α-MSH releasing melanotrophs in the IL of pituitary express the full-length $Ca_V2.2$ channels…….....140

Figure 4.28 Illustration of interaction between CASK and the $Ca_V2.2$ Channels……..…….141-142

Figure 4.29 GFP-NC3 inhibitory peptides significantly decreased the terminal targeting of $Ca_V2.2$ channels in differentiated PC12 cells…143-145

Figure 5.1 Steady state inactivation curves obtained from the WT $Ca_V2.1$ Channels and the splice variants……..159-160

Figure 5.2 Exon 18a alternative splicing within the II-III loop of $Ca_V2.2$ and $Ca_V2.3$ channels……171

LIST OF ABBREVIATIONS

ACTH adrenocorticotropic hormone
AH Anterior lobe, or adenohypophysis
AID alpha-interaction domain
AKAP A-kinase anchoring protein
AMPA alpha- amino- 3-hydroxy-5-methyl-4-isoxazolepropionic acid
Arc arcuate nucleus
ARCs arachidonate-regulated Ca^{2+} channels
ATP adenosine triphosphate
ATPase adenosine triphosphatase
BID beta-interaction domain
CaM calmodulin
CaMKII Ca^{2+}/calmodulin-dependent protein kinase II
CaMKIV Ca^{2+}/calmodulin-dependent protein kinase IV
cAMP cyclic adenosine monophosphate
CASK "calcium, calmodulin associated serine kinase"
CBP Ca^{2+} binding protein
cDNA Complementary DNA
cGMP 3'5' cyclic guanosine monophosphate
CIC3 voltage-gated chloride channel 3
CNS central nervous system
CRAC Ca^{2+} release-activated Ca^{2+} channel
CREB cAMP-responsive element binding
CRH corticotrophin releasing hormone
CSP cysteine string protein
DHP dihydropyridine
EC excitation-contraction
ECF extracellular fluid
ER endoplasmic reticulum
FSH follicle-stimulating hormone
GABA gamma-aminobutyric acid
GH growth hormone
GK guanylate kinase

GPCR G-protein coupled receptor
GTP Guanosine triphosphate
HNS hypothalamo-neurohypophsial system
HVA high voltage activated
Hz Hertz
IEG immediate early gene
IL intermediate lobe
IP_3 inositol 1,4,5-trisphosphate
LDCVs large dense-core vesicles
LH luteinizing hormone
LVA low voltage activated
MAPK/ERK mitogen-activated protein kinase
MDCK Madin-Darby canine kidney
Mint1 Munc-18-interacting protein 1
MNCs magnocellular neurosecretory cells
MNCX motochodrial Na^+/ Ca^{2+} exchanger
MNTB medial nucleus of the trapezoid body
mRNA messenger RNA
MSH melanocyte-stimulating hormone
NCX Na^+/ Ca^{2+} exchanger
$NFATc_4$ nuclear factor of activated T-cells, cytoplasmic, calcineurin-dependent 4
NH neural lobe, neurohypophysis
NMDA N-methyl D-aspartate
NSF N-ethylmaleimide–sensitive factor
Orail1 calcium release-activated calcium channel protein 1
ORL1 opioid receptor like receptor 1
OT oxytocin
PC12 pheochromocytoma cells
PDZ postsynaptic density-95 (PSD-95)/Discs large/Zona occludens 1
PI3K Phosphoinositide 3-kinase
PMCA plasma membrane Ca^{2+} ATPase
POMC proopiomelanocortin
PP1 protein phosphatase 1
PV parvalbumin

PVN paraventricular nuclei
RRP readily releasable pool
RyR ryanodine receptors
SCAMP secretory carrier membrane proteins
SCGN sympathetic gangion neurons
SERCA sarcoplasmic-endoplamic type ATPase
SH3 Src homology 3
Shank SH3 and ankyrin repeat-containing protein
SNAP soluble NSF attachment protein
SNAP25 soluble NSF attachment protein 25
SNAP29 soluble NSF attachment protein 29
SNARE soluble NSF attachment protein receptor
SOC store-operated channels
SON supraoptic nuclei
SR sarcoplasmic reticulum
STIM1 stromal interaction molecule 1
SVs synaptic vesicles
TRP transient receptor potential
TSH thyroid- stimulating hormone
t-SNARE SNARE in target membrane
VAMP vesicle-associated membrane protein
VAMP4 vesicle-associated membrane protein 4
V-ATPase vacuolar ATP synthase subunit H
VGCCs voltage-gated calcium channel
VGLUT vesicular glutamate transporter
VP vasopressin
VS versus
v-SNARE SNARE in vesicles
WT **w**ild type or full-length

INTRODUCTION

Ca^{2+} ions are important intracellular messenger and impact nearly all aspects of cellular function. Exocytosis, which triggers neurotransmitter release from neurons and hormone secretion from neuroendocrine cells, is dependent on influx of Ca^{2+} through voltage-gated Ca^{2+} channels (VGCCs). The locations and the properties of VGCCs determine where Ca^{2+} influx occurs and therefore how the exocytotic machinery senses the Ca^{2+} signal. To better understand the differences between fast neurotransmission of neurons and slower neurosecretion of neuroendocrine cells, this thesis work is to investigate the molecular properties of VGCCs expressed in one type of neuroendocrine cell, the magnocellular neurosecretory cells (MNCs), that release oxytocin and vasopressin into the blood through their nerve terminals in the posterior pituitary gland (neurohypophysis). To better understand the importance of the synaptic proteins that are involved in the regulation of exocytosis in both neurons and neuroendocrine cells, this thesis work addresses whether the P/Q- and N-type Ca^{2+} channels of MNCs have the synaptic protein binding sites as these channels do in neurons, and how their molecular properties will affect channel targeting and distribution. The expression and regulation of VGCCs in the glial cells within the neurohypophysis were studied to better understand the interaction between pituicytes and MNC terminals and how these glial cells respond to the hyperosmolality that triggers the vasopressin release from the MNC terminals.

In this introductory part I will firstly describe calcium signaling and its physiological roles. Different ion channels and proteins that may be involved in mediating Ca^{2+} ions flow will be introduced. The SNARE hypothesis, which is important for Ca^{2+}-dependent exocytosis, will be also described. Secondly, I will introduce the history of VGCC discovery and their classification system. In this section, more information will be given in terms distributions of VGCCs in neurons and neuroendocrine cells. I will describe how the neurosecretion of MNCs is related to functions of VGCCs in the hypothalamo-neurohypophysial system. Next, Ca_V2 channel targeting and alternative splicing within the synaptic protein interaction site will be introduced, especially for the $Ca_V2.1$ and $Ca_V2.2$ channels in neurons and neuroendocrine cells. The introductory parts above lead to our first main hypothesis of the expression of splice variants of the $Ca_V2.1$ and $Ca_V2.2$ channels in the hypothalamo-neurohypophysial system. These variants are hypothesized to be involved with the alternatively splicing of synaptic protein interaction sites. Finally, I will describe the physiology of the pituitary gland and in particular the pituicytes, the glial cells of the neurohypophysis. A comparison between Ca^{2+} signaling of glial cells in the CNS and in pituicytes will also be introduced. This will lead to our second main hypothesis of the expression of VGCCs in the pituicytes.

1.1 Calcium signaling and physiology

In 1883, physiologist Sydney Ringer accidentally discovered that the frog heart failed to contract normally if he prepared the saline solution with distilled water rather than regular tap water. Soon, he realized that the substance in London tap water that was responsible for the contraction was Ca^{2+} (Ringer 1883). The concept of Ca^{2+} signaling only started to gain much attention in the 1940s, when Heilbrunn and Baily published their landmark findings on muscles. Heilbrunn found the isolated frog muscle fibers only contracted when the Ca^{2+} was applied to their cut ends, but not to their surfaces (Carafoli 2003). Bailey showed that Ca^{2+} stimulated the ATPase (adenosine triphosphatase) activity of myosin, and suggested that the presence of Ca^{2+} in close proximity to the myosin filaments was important for muscle contraction (Bailey 1942). Later on, Fatt and Katz published their work on the electrical properties of crustacean muscle fibers, which suggested that Ca^{2+} could be responsible for transforming electrical signal to a chemical or mechanical response (Fatt & Katz 1953a). Later, numerous great discoveries proved that the Ca^{2+} ion functions as a carrier or messenger to fulfill diverse important biological processes (Neher 1992). It is now very clear that intracellular Ca^{2+} signaling regulates diverse neuronal functions such as neuronal survival, axonal pathfinding, neurotransmission, and synaptic plasticity (Bear & Malenka 1994; Bliss & Collingridge 1993; Burgoyne 2007; Franklin & Johnson 1992).

1.1.1 Calcium influx, storage, and release

If Ca^{2+} is to deliver signals to the targets that control essential processes, its intracellular concentration must be precisely regulated. In response to certain extracellular stimuli, the concentration of intracellular Ca^{2+} rises and falls and the concentration achieved is determined by three aspects of Ca^{2+} ion flow: influx, storage, and release. In most of the mammalian cells, the extracellular Ca^{2+} concentration is at mM level, whereas the intracellular Ca^{2+} concentration is typically ~0.2 μM and, therefore, there is a large Ca^{2+} gradient that allows Ca^{2+} influx to occur and act as a signaling mechanism.

1.1.2 Plasma membrane Ca^{2+} channels

Cells increase their intracellular Ca^{2+} concentration in two ways: by allowing Ca^{2+} influx through the cell membrane, or by releasing Ca^{2+} from intracellular stores. The physical entities allowing ions to flow into the cell are proteins called ion channels. There are several types of ion channels found to be able to mediate Ca^{2+} flux into the plasma membrane, such as VGCCs, N-methyl D-aspartate receptors (NMDARs), Ca^{2+} release-activated Ca^{2+} channels (CRACs), arachidonate- regulated Ca^{2+} channels (ARC), and TRP (transient receptor potential) channels.

VGCCs are members of a gene superfamily of transmembrane proteins that includes voltage-gated potassium and sodium channels (Yu & Catterall 2004). They are highly selective for Ca^{2+}, with permeability to Ca^{2+} being about 1000-fold greater than that of Na^{+} (Nestler et al 2008). VGCCs are found in the plasma membrane of many excitable cells (neurons, neuroendocrine cells, etc.) and are activated by membrane depolarization (Catterall 2000). One of the major functions of VGCCs is to contribute to the depolarization phase of action potentials in cells. VGCCs mediate Ca^{2+} influx in response to membrane depolarization of the cell, and regulate intracellular responses such as contraction in cardiac and skeletal muscle cells, secretion in endocrine cells, neurotransmission in neurons, and gene expression in many types of cells.

Ligand-gated non-selective cation channels lead to membrane depolarization by providing relatively non-selective passage of the major cations such as Na^{+}, K^{+} and Ca^{2+}. Channels of this type may have significant permeability for Ca^{2+} and include neuronal acetylcholine receptors, ionotropic glutamate receptors (NMDA and AMPA, or alpha- amino-3-hydroxy- 5-methyl- 4-isoxazolepropionic acid receptors), cyclic nucleotide- gated channels, and P2X receptors. They have significant physiological effects, particularly in neural systems. NMDA and AMPA receptors contribute to long-term potentiation and depression in the central nervous system (CNS) and are believed to contribute to learning and memory (Collingridge et al 2004; Malenka &

Bear 2004). Ca^{2+} overload mediated by NMDARs had been found to be related to excitotoxic neuronal cell death (Choi et al 1988; Franklin & Johnson 1992; Ghosh & Greenberg 1995). Cyclic nucleotide-gated channels (CNGs) are important for the process of vision, in which cGMP-gated channels (cGMP, 3′5′ cyclic guanosine monophosphate) carry the light-sensitive currents (Kaupp & Seifert 2002). In the dark, the $[cGMP]_i$ is high within the photoreceptor cytoplasm and keeps CNGs open. Light stimulates the phosphodieasterase and thus decreases the $[cGMP]_i$, then reduces the numbers of opened CNGs, which in turn hyperpolarizes the photoreceptor and passes a visual signal to the retinal neurons (Boron & Boulpaep 2005). P2X receptors are sensors for extracellular adenosine triphosphate (ATP) and are expressed in both CNS and peripheral systems (North 2002). In sensory neurons, they are involved in the initiation of afferent signals in sensing the inflammatory stimuli. In some endocrine organs, ATP signaling through P2X receptors acts in a paracrine fashion, a signal transduction process from one cell to adjacent cells often seen in the hormonal regulation of surrounding cells by hormone releasing cells (North 2002).

CRACs can be selectively activated by a fall of Ca^{2+} concentration within the endoplasmic reticulum (ER) (Parekh 2006), and their molecular identities were quite elusive. The Ca^{2+} entry process through CRACs is mysterious because the links between ER Ca^{2+} release and the subsequent initiation of a slower and sustained influx from the plasma membrane are not known. The decrease in luminal Ca^{2+} triggers

store-operated channels (SOCs) present in the plasma membrane, which mediate the Ca^{2+}-selective Ca^{2+} release–activated Ca^{2+} current (I)$_{CRAC}$ observed in many cell types, particularly in B immune cells (Parekh & Putney 2005). Because of the small current amplitude, it is very difficult to characterize these Ca^{2+} currents. Recently, ER membrane proteins like Orai1 (Calcium release-activated calcium channel protein 1), STIM1 (Stromal interaction molecule 1), and IP_3 (inositol 1,4,5- trisphosphate) receptors were found to be expressed or translocated into the plasma membrane where they mediate the CRAC currents (Dellis et al 2006; Feske et al 2006; Gill et al 2006; Roos et al 2005). The arachidonate-regulated Ca^{2+} channel (ARC) is closely related to CRAC, but plays different roles on the plasma membrane including the regulation of the frequency of Ca^{2+} oscillations. Activation of ARC channels is specifically dependent on arachidonic acid acting at the intracellular surface of the membrane and is totally independent of any depletion of internal Ca^{2+} stores (Shuttleworth 2009). TRP channels are important for sensory systems. They can be activated by light, temperature or pH stimuli and mediate Ca^{2+} influx into cells at hyperpolarized membrane potentials. Most TRP channels are relatively nonselective to cations and therefore depolarize cells from their resting membrane potential and raise $[Ca^{2+}]_i$ (Clapham et al 2001; Ramsey et al 2006).

In the following section, I will briefly introduce the intracellular Ca^{2+} storage and release, which helps to regulate and maintain Ca^{2+} homeostasis in all cells.

1.1.3 Intracellular Ca^{2+} storage and release

Intracellular Ca^{2+} ions are mainly stored by Ca^{2+} binding proteins that act in cytosol and ER. These proteins account for 90-95% of the total Ca^{2+} load in a cell (Clapham 2007).

Mobile Ca^{2+} buffering proteins in the cytosol are acidic proteins that can store large amounts of Ca^{2+} with affinities that range from low to high. They belong to the EF-hand family, which contains characteristic helix-loop-helix binding motifs that are highly conserved in sequence, and includes parvalbumin (PV), calmodulin, and troponin C (Cates et al 1999). Parvalbumin has high affinity for Ca^{2+} and is found in high concentration in the sarcoplasm of fast contracting muscles (Celio & Heizmann 1982). The process of muscle relaxation occurs when Ca^{2+} is bound with troponin C and transported into the sarcoplasmic reticulum (SR). The role of calmodulin in Ca^{2+} signalling has been intensively studied. Calmodulin changes its conformation when Ca^{2+} binds with it, which allows calmodulin to transmit Ca^{2+} information to its downstream target proteins (Hudmon et al 2005; Rosenberg et al 2005). Calmodulin can serve as a separate subunit for some enzymes such as Ca^{2+}-dependent protein phosphatase, and calcineurin (Perrino et al 1995). Some enzymes can integrate "calmodulin" domains into their genomic sequence (Carafoli 2003). Another major source of intracellular Ca^{2+} storage is in the ER. The resting ER free Ca^{2+}

concentration is thought to be on the order of several hundreds of μM (Miyawaki et al 1997). There are some low affinity Ca^{2+} binding proteins such as calreticulin, calsequestrin, calnexin etc., that act in the sarco (endo)-plasmic reticulum (Carafoli 2003).

In addition to the Ca^{2+} binding proteins, Ca^{2+} pumps or exchanger proteins on different cellular membranes maintain homeostasis of intracellular Ca^{2+} storage. Ca^{2+} can be extruded by a high-affinity/low capacity plasma membrane Ca^{2+} ATPase (PMCA) pump and a low-affinity/high capacity Na^{+}/ Ca^{2+} exchanger (NCX) to the outside of the plasma membrane (Blaustein & Lederer 1999; Herchuelz 2007). Ca^{2+} pumps on the ER membrane are called SERCAs (sarcoplasmic-endoplamic type ATPase), which can balance the Ca^{2+} uptake and release through the ER to regulate the free-Ca^{2+} level within the ER (Carafoli & Brini 2000). The SERCAs play a dominant role of Ca^{2+} homeostasis in the insulin releasing β-cells of pancreas (Hughes et al., 2006).

There is another Na^{+}/Ca^{2+} exchanger on the plasma membrane of mitrochondria (MNCX, mitochodrial Na^{+}/Ca^{2+} exchanger) that transports Ca^{2+} out from the mitochondrial matrix (Hernandez-SanMiguel et al 2006). Mitochondria also express Ca^{2+} transporters that are physically close to the ER Ca^{2+} releasing port and move Ca^{2+} into the mitochondria by a uniporter (Rizzuto et al 1998). The mitochondrion is the

dominant regulatory intracellular organelle that regulates intracellular Ca^{2+} and therefore maintains the proper hormone release from corticotropes, the cells release adrenocorticotropic hormone (ACTH) in the anterior pituitary gland (Lee et al., 2005).

The cytoplasm or sarcoplasm of cells is not a free space where Ca^{2+} ion can diffuse, but is instead filled with Ca^{2+} binding proteins. Therefore, to effectively reach intracellular targets, a local Ca^{2+} releasing mechanism for signal transduction is needed. The ER is not only an important Ca^{2+} storage organelle, but also a local Ca^{2+} releasing organelle (Blaustein & Golovina 2001). Ca^{2+} is released from the ER in either a stimulated or passive way. Stimulated release is dependent on two receptors: the IP_3 receptors and the ryanodine receptors (RyR). These two receptors are among the largest ion channels with molecular weights around 1-2 million daltons (Fill & Copello 2002; Wu et al 2002). IP_3 receptors trigger Ca^{2+} release when they bind with IP_3, which is generated by phospholipase C enzymes upon activation of other receptors on the plasma membrane (Patterson et al 2004). The important functions of RyRs in muscular systems have been well reviewed (Fill & Copello 2002), where the VGCCs are distributed and coupled with the RyR channels throughout the T-tubule network. This spatial arrangement insures rapid and near simultaneous release of Ca^{2+} to bind adjacent troponin and enable myosin-actin contraction. Although multiple mechanisms related to intracellular storage and release may affect the exocytosis, in this thesis I will focus on Ca^{2+}-dependent exocytosis mediated by VGCCs.

As we introduced above, Ca^{2+} ions flowing through the cellular membrane is mediated by many different kinds of ion channels (Figure 1.1). The gradient of Ca^{2+} concentrations between outside and inside of the cell is so high ($[Ca^{2+}]_o$ is approximately 1.2mM and $[Ca^{2+}]_i$ is only about 10^{-7}M), that the VGCCs, the fastest Ca^{2+} signaling proteins, are widely used and can initiate dramatic changes of Ca^{2+} level within cells. It is estimated that each VGCC channel conducts roughly a million Ca^{2+} ions per second down the 20,000-fold gradient, and only a few thousand channels per cell can drive >10-fold changes in intracellular levels within milliseconds (Clapham 2007). I will introduce more about the Ca^{2+}-dependent exocytosis that is related to fundamental functions of neurons and neuroendocrine cells.

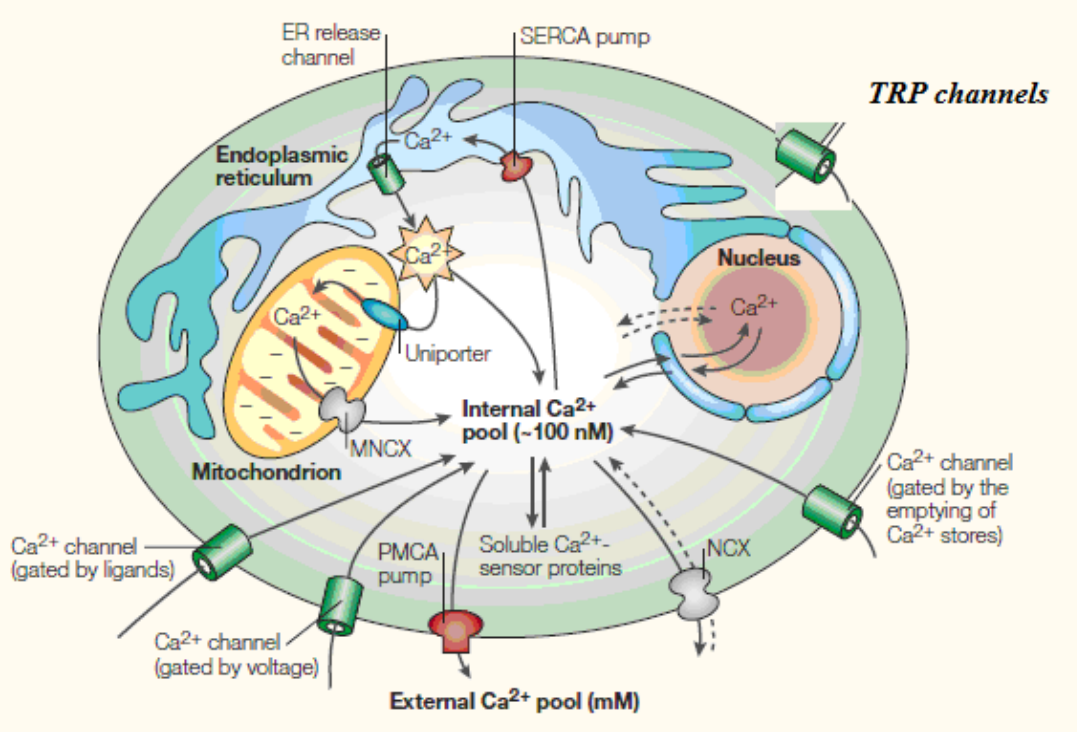

Figure 1.1 Calcium influx, storage, and release in a cell. Calcium influx can be mediated mainly by four types of ion channels on the plasma membrane: voltage-gated, ligand-gated, those activated by emptying of Ca^{2+} stores, and TRP channels. The intracellular Ca^{2+} pool is regulated by binding to Ca^{2+} sensors and by transport into organelles. Ca^{2+} can be stored in the sarco(endo)plasmic reticulum by SERCA (sarcoplasmic-endoplasmic type ATPase) pumps or released through IP_3 receptors or ryanodine receptors. Ca^{2+} can exit mitochondria through MNCX, the mitochodrial Na^{+}/ Ca^{2+} exchanger. There might be nuclear Ca^{2+} transporter(s) responsible for the trafficking of Ca^{2+} in and out of the nuclear ports (not identified yet). Ca^{2+} is expelled from the cell through PMCA (plasma membrane Ca^{2+} ATPase) and NCX (Na^{+}/ Ca^{2+} exchanger). This Figure is modified from the paper (Carafoli 2003) and reproduced with permission from Copyright Clearance Center.

1.2 Neuronal Ca^{2+} signaling and the SNAREs hypothesis

1.2.1 Ca^{2+}-dependent exocytosis mediated by VGCCs

The process of Ca^{2+}-dependent exocytosis is among the central events of neural function. The release of neurotransmitters from presynaptic terminals of neurons and of hormones from neuroendocrine cells are both controlled precisely by Ca^{2+} signals. In the following sections, I will discuss the vesicles that hold neurotransmitters/hormones, the soluble N-ethylmaleimide–sensitive factor attachment protein receptors (SNAREs) that regulate the membrane fusion of vesicles and the VGCCs that mediate the Ca^{2+} influx.

1.2.1.1 Vesicles holding eurotransmitters and hormones

Neurons are highly asymmetric (polarized) cells that have three major structures: a cell body (soma), a single long process called axon, and a variety of branches known as dendrites. The axon is a fine tubular process that conducts electrical impulses from the soma to the axon terminals that form the presynaptic component of the synapse. A synapse is a specialized structure involved in transmission of information from one neuron to another. The functions of the dendrites include reception, processing, and integration of incoming synaptic communications. Neurotransmitters (glutamate, γ-aminobutyric acid (GABA), acetylcholine etc.) are packed into small membranous compartments called synaptic vesicles (SVs, A small secretory vesicle (~50 nm in diameter) containing neurotransmitters that are released during Ca^{2+}-dependent exocytosis, Ludwig & Leng 2006, see Figure 1.2) within the synaptic specializations (Rizzoli & Betz 2005).

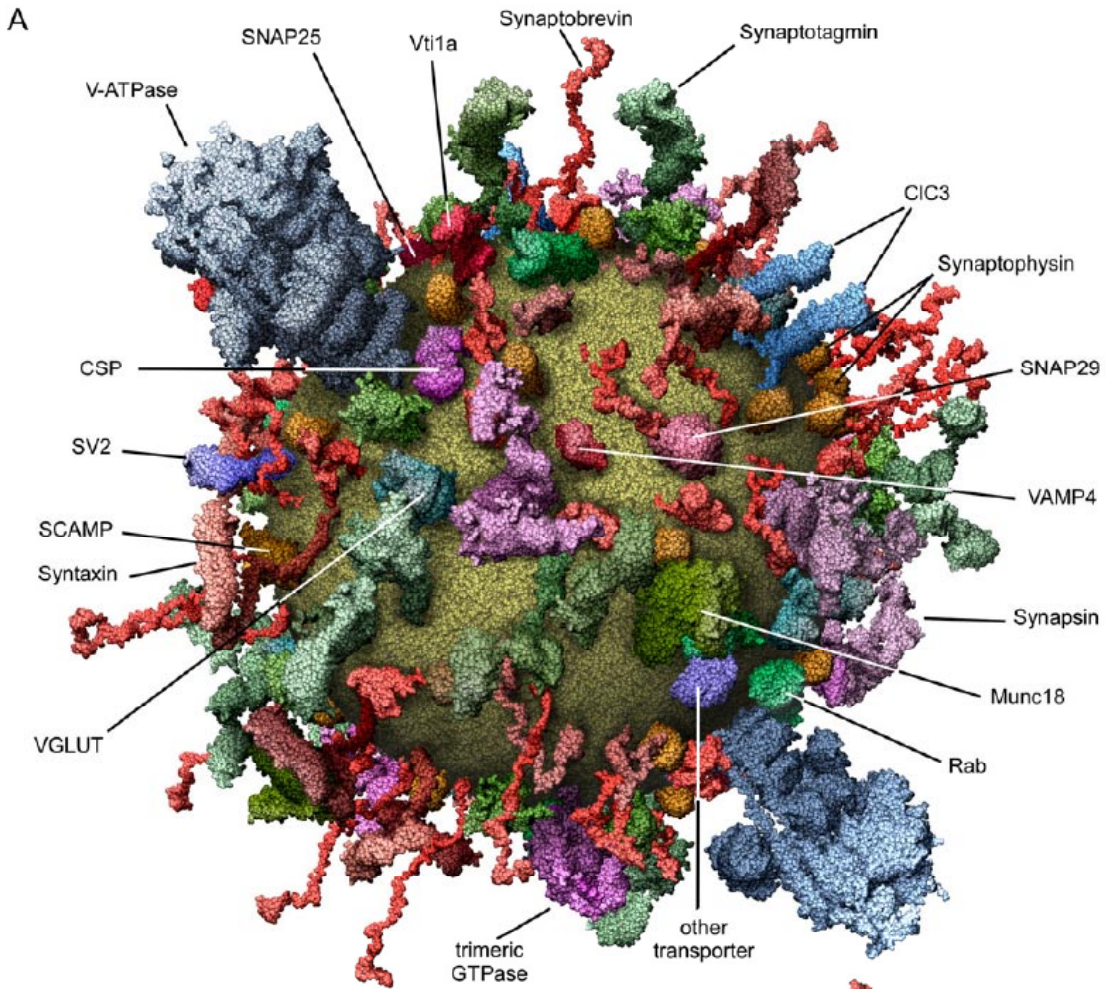

Figure 1.2 Molecular model of a typical synaptic vesicle. This figure shows important macromolecules such as **syntaxin**, **SNAP25, and VAMP** that are associated with a typical synaptic vesicle at near atomic resolution. **CSP** (cysteine string protein); **SCAMP** (Secretory carrier membrane proteins); **VGLUT** (vesicular glutamate transporter); **VAMP4** (vesicle-associated membrane protein 4); CIC3 (voltage-gated chloride channel 3); **SNAP29** (soluble NSF attachment protein 29); **V-ATPase** (vacuolar ATP synthase subunit H) (Takamori et al 2006) (Reproduced with permission from Copyright Clearance Center).

Most synapses rely on three vesicle pools: the readily releasable pool, the recycling pool, and the reserve pool. The reserve pool makes up ~ 80-90% of the total pool, and the recycling pool is significantly smaller (~10-15%). Both of them are highly movable in the presynaptic terminals. The readily releasable pool (RRP) consists of a few vesicles (~1%) that seem to be docked and primed for release (Rizzoli & Betz 2005). The RRP is important for fast neurotransmission because of its physical proximity to the releasing site. Vesicles in the RRP are docked to the presynaptic active zone, a region of membrane that faces the postsynaptic density where synaptic vesicles are clustered, docked and depleted. The RRP is depleted rapidly (Smith & Augustine 1988). This process is initiated by influx of Ca^{2+} through VGCCs and may occur in less than 1ms when the action potential arrives at the synaptic terminals (Catterall 1999; Zucker 1993).

Neuroendocrine cells are cells of neural origin that release hormones or neuropeptides into the circulatory system, such as the magnocellular neurosecretory cells of hypothalamus or the chromaffin cells of the adrenal gland. Hormones in neuroendocrine cells are packed into the large-dense core vesicles (LDCVs). LDCVs are large secretory vesicles (100 – 150 nm in diameter) that contain proteins or peptides, and can be released from all parts of a neuron **(**Kasai 1999; Robinson & Martin 1998)). A comparison of time courses needed for neurosecretion from

neuroendocrine cells and nerve terminals of neurons suggests the two types of vesicles may respond differently to action potential firing patterns (Neher 1998; Verhage et al 1994). SVs, being tightly coupled to VGCCs, would respond to both single action potential and to bursts, whereas LDCVs, located further away from channels, would require bursts of action potentials, which cause Ca^{2+} concentrations to build up slowly to reach the threshold of exocytosis (Klingauf & Neher 1997).

1.2.1.2 The SNARE proteins

Neurosecretion is mediated by a specialized membrane trafficking cycle that includes the assembly and filling of secretory vesicles, their transport to the active zone, docking, fusion, and recycling (Bajjalieh 1999). I will now describe the SNARE hypothesis, which attempts to explain the process underlying the docking and fusion of SVs and LDCVs with the plasma membranes of secretory cells (Sudhof & Rothman 2009).

SNARE proteins were identified as the receptors for N-ethylmaleimide–sensitive factor (NSF) and soluble NSF attachment protein (SNAP) which were purified on the basis of their functions in vesicular trafficking. Three proteins, syntaxin-1, SNAP25 and VAMP (vesicle-associated membrane protein, also called synaptobrevin), form the core of the SNARE complex that is proposed to bridge the exocytotic vesicle to

the plasma membrane (Bennett et al 1992; Sollner et al 1993). The SNARE hypothesis postulates that SNAREs fall into two broad categories, v-SNAREs (in transport vesicles) and t-SNAREs (in target membranes), which pair specifically to add compartmental specificity to membrane fusion. The evidence of the importance of SNARE complex in synaptic exocytosis was revealed when the atomic structure of a core domain of the SNARE complex was determined (Sutton et al 1998). Individual SNARE proteins can spontaneously assemble into a stable bundle of four helices (*trans*-conformation) that forms between membranes. These bundles can generate an inward force to pull the membranes together, forcing them to fuse. When the fusion is completed, the SNARE complex returns to the low-energy *cis*-position (Hua & Scheller 2001; Li et al 2007). The SNARE proteins function as general fusion machinery responsible for nearly all intracellular membrane fusion.

There are other important molecular elements that act as the Ca^{2+} sensor or as regulatory proteins in the processes of forming the SNARE complex and triggering exocytosis. Synaptotagmin is one of the most well investigated Ca^{2+} binding proteins and ensures that the exocytotic machinery is competent to undergo fusion upon an increase in Ca^{2+} concentration (Arac et al 2006; Fernandez-Chacon et al 2001; Voets et al 2001). Complexin acts as a grappling protein that elevates the zippered SNARE complex (Reim et al 2001; Tang et al 2006) and releases them when Ca^{2+} binds to synaptotagmin (Sudhof & Rothman 2009). Munc18 or Sec1 is a cytosolic protein that

binds to the N-terminal of syntaxin. Syntaxin must dissociate from Munc 18 before it can form the core complex with SNAP25 and VAMP (Dulubova et al 2003; Misura et al 2000). Therefore, the core SNARE complex (syntaxin, SNAP25, and VAMP) and synaptotagmin play important roles in Ca^{2+}-dependent exocytosis.

1.3 Voltage-gated Ca^{2+} channels (VGCCs)

1.3.1 VGCCs and Ca^{2+} domains

The Ca^{2+} influx mediated by VGCCs is essential for the exocytosis of neurons and neuroendocrine cells. Once Ca^{2+} ion enters the presynaptic terminals, the diffusion of Ca^{2+} will yield an immediate accumulation of Ca^{2+} ions within nanometers of the mouth of a VGCC (Augustine 2001; Augustine et al 2003). This area is called "nanodomain" (Kasai 1993). In a single nanodomain, Ca^{2+} concentration can go as high as 100μM. When VGCCs are clustered together in a membrane area of roughly $1\mu m^2$, a "microdomain" will be formed from the spatial summation of Ca^{2+} entering from multiple channels (Augustine et al 2003; Llinas et al 1992). Free Ca^{2+} concentration within microdomains can range from tens of micromolar to hundreds of micromolar, depending on the the numbers of nanodomains that are summated. A third type of Ca^{2+} signal is from an even bigger spatial domain when VGCCs are 1μm or further from target Ca^{2+} binding proteins. The radial gradients of $[Ca^{2+}]$ occur when

Ca^{2+} diffuses into the interior of the cell (Marengo & Monck 2000). These three models of Ca^{2+} domains are all useful to explain some exocytotic events in certain neuronal terminals or neuroendocrine cells, but not all (Figure 1.3). It appears that the Ca^{2+} concentration needed for exocytosis varies; rapid exocytosis triggered by physiological Ca^{2+} concentrations can be as low as 5-10 μM (Heidelberger et al 1994) or as high as 100-200 μM (Mennerick & Matthews 1996) . Because the VGCCs are important for triggering neurotransmitters and hormone release, in the following sections, I will give more details of the classification of VGCCs and why I am interested in studing the Ca_V2 channels.

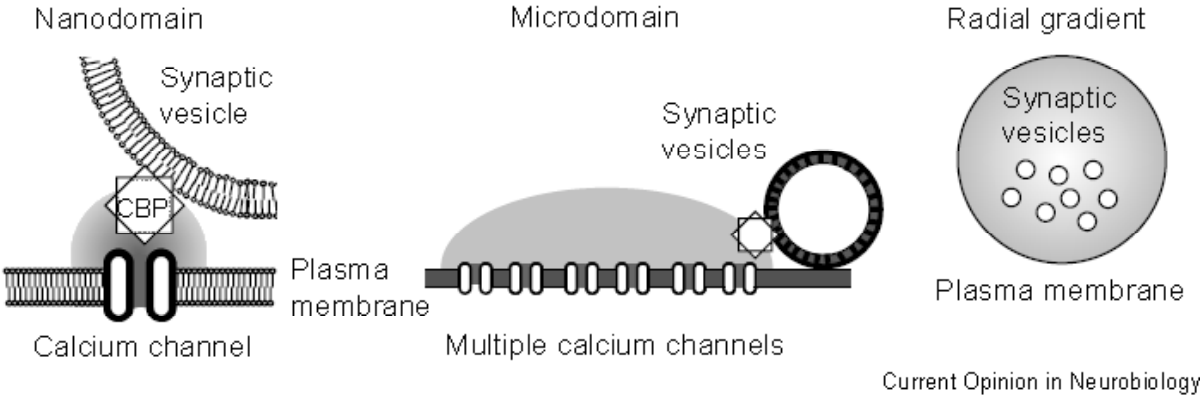

Figure 1.3 Types of presynaptic Ca^{2+} signals. 'Nanodomains' arise from local diffusion from single open Ca^{2+} channels, 'microdomains' from multiple open Ca^{2+} channels, and 'radial gradients' from long-distance movements of Ca^{2+} away from the channels. CBP indicates a Ca^{2+}-binding protein that translates Ca^{2+} entry into vesicle fusion (Augustine 2001) (Reproduced with permission from Copyright Clearance Center).

1.3.2 Classification of VGCCs

The establishment of the concept of voltage-gated Ca^{2+} channels was due to the early work done by Sir Bernard Katz, Susumu Hagiwara, Harald Reuter and their colleagues (Fatt & Katz 1953b; Hagiwara & Nakajima 1966; Reuter 1967). These early discoveries opened a new era of searching for VGCCs by biochemists and electrophysiologists. Electrophysiological recordings from neurons, muscle and endocrine cells revealed voltage-activated Ca^{2+} currents with distinct characteristics. Based on their biophysical properties, VGCCs can be classified into two categories: high-voltage activated (HVA) and low-voltage activated channels (LVA) (Ertel et al 2000). HVA currents generally have larger conductances (15-25 pS), are activated by stronger depolarization (about -10mV) and display variable inactivation kinetics. The HVA group includes L- , N-, P/Q- and R-type currents, whereas the LVA group only includes T-type currents which show a much lower voltage threshold of activation (about -60mV) and smaller channel conductance (8 pS).

L-type (long-lasting) currents are the major Ca^{2+} currents found in cardiac, skeletal and smooth muscles and are characterized by high voltage activation, large single channel conductance, and slow, voltage-dependent inactivation (Catterall 2000). Selective blockers are useful tools for identifing different subtyes of Ca^{2+} currents. For example, the L-type currents can be selectively inhibited by antagonists including

dihydropyridines (DHP), phenylalkylamines, and benzothiazepines. Drugs from these families are clinically useful antihypertensive drugs (Nowycky et al 1985; Triggle 1999).

N-type (non-classical, neither L- nor T-) currents were first identified in chicken dorsal root ganglion neurons (Carbone & Lux 1984). These currents usually have faster voltage dependent inactivation than L-type, but slower than that of T-type Ca^{2+} currents (Nowycky et al 1985), and they are insensitive to selective L-type blockers. Pharmacologically, N-type currents are sensitive to inhibition by a class of peptide toxins called ω-conotoxins, which are a family of small (13-29 amino acid) peptides found in the venom of marine snails (Olivera et al 1994).

Later, analysis of the effects of other peptide toxins revealed three additional Ca^{2+} current types: P-, Q-, and R- types. P-type currents were originally identified in Purkinje cells of cerebellum and distinguished by high sensitivity to spider toxin ω-agatoxin IVA (with a dissociation constant, or Kd of about 2nM) (Llinas et al 1989). Q-type currents were first described in cerebellar granule cells and differ in sensitivity to ω-agatoxin IVA (Kd> 100 nM). Their inactivation kinetics are also different; P-type currents show a non-inactivating waveform during prolonged membrane depolarization, whereas Q-type currents show a pronounced inactivation (Bourinet et al 1999). R-type (residual or resistant) currents comprise approximately 15% of the

HVA currents in cerebellar granule cells and were classified due to their lack of sensitivity to all Ca^{2+} subtype selective blockers mentioned above (Randall & Tsien 1995). A selective R-type channel blocker was not found until the molecular identity of this subtype was clear. A toxin extracted from the venom of the tarantula *Hysterocrates gigas* called SNX-482 blocks heterologously expressed R-type currents, but is only partially effective on native cerebellar R-type currents (Newcomb et al 1998; Tottene et al 2000).

T-type (transient, or tiny) currents was among the earliest Ca^{2+} currents discovered in various excitable cells due to their dramatic differences from HVA currents (Bean 1985; Hagiwara et al 1975). T-type currents can be reliably distinguished from other types of currents by relatively low threshold of activation and rapid inactivation at fairly negative voltages (Armstrong & Matteson 1985; Monteil et al 2000). The permeability of T-type channels for Ca^{2+} is equal to (Carbone & Lux 1984), or higher than Ba^{2+} (Friedman et al 1986). In contrast, other Ca^{2+} channels have significantly larger conductance for Ba^{2+} than Ca^{2+} (Fox et al 1987). T-type Ca^{2+} channels can be selectively blocked by a scorpion toxin called kurtoxin (Chuang et al 1998).

The development of techniques in molecular biology eventually led to a new nomenclature of all VGCCs subtypes based on their molecular entities (Figure 1.4). The genomic screening of primary and accessory subunits of VGCC had its

breakthrough by the sequencing of the first L-type gene from skeletal muscle (Tanabe et al 1987). The cDNA sequences of α1 subunits were carefully identified and the amino acid structures of different subtypes of channels were also predicted (Dubel et al 1992; Lee et al 1999; Mori et al 1991; Naylor et al 2000; Soong et al 1993; Starr et al 1991; Williams et al 1992). These cDNA sequences are very useful because researchers can construct heterologous expression vectors with mammalian promoters and other necessary protein translational information and then incorporate these vectors into experimental model cells to investigate specific properties of each subtype of Ca^{2+} channels. These tools provide platforms for studying the electrophysiology of VGCCs, systemically screening of new selective blockers, and imaging of channel distribution and targeting (Figure 1.4).

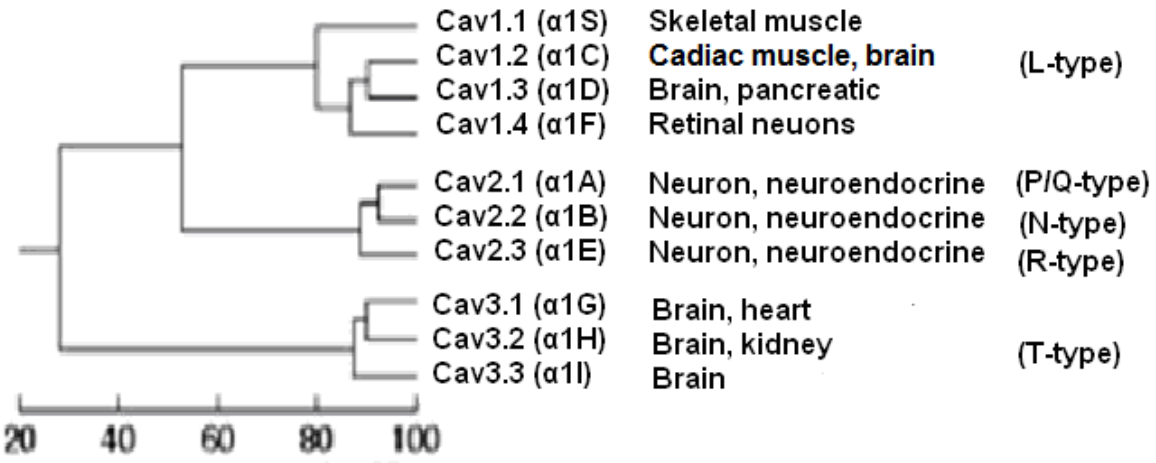

Figure 1.4 Sequence similarities of VGCCs α1 subunits and their major tissue distributions (Catterall et al 2005) (Reproduced with permission from Copyright Clearance Center).

Historically, a variety of names have been given to the corresponding VGCC genes, resulting in confusing nomenclature. A new nomenclature system therefore was adopted using the chemical symbol of the principal permeating ion (Ca^{2+}) with the principal physiological regulator (voltage) indicated as a subscript (Ca_V) (Catterall et al 2005). The numerical identifier corresponds to the Ca_V channel α1 subunit gene subfamily (1 to 3 at present) and the order of discovery of the α1 subunit within that subfamily (1 through n). According to this nomenclature, the Ca_V1 subfamily ($Ca_V1.1$–$Ca_V1.4$) includes channels containing α1S, α1C, α1D, and α1F, which mediate L-type Ca^{2+} currents (McRory et al 2004; Mori et al 1991; Tanabe et al 1987). The Ca_V2 subfamily ($Ca_V2.1$–$Ca_V2.3$) includes channels containing α1A, α1B, and α1E, which mediate P/Q-type, N-type, and R-type Ca^{2+} currents, respectively (Dubel et al 1992; Soong et al 1993; Starr et al 1991). The Ca_V3 subfamily ($Ca_V3.1$–$Ca_V3.3$) includes channels containing α1G, α1H, and α1I, which mediate T-type Ca^{2+} currents (Lee et al 1999; Naylor et al 2000; Soong et al 1993) (Table 1-1).

Table 1-1 The α1 subunits of VGCCs and corresponding Ca^{2+} currents

Family	α1 subunits	Former name	Ca^{2+} currents
Ca_V1	$Ca_V1.1$	α1S	L-type
	$Ca_V1.2$	α1C	
	$Ca_V1.3$	α1D	
	$Ca_V1.4$	α1F	
Ca_V2	$Ca_V2.1$	α1A	P/Q-type
	$Ca_V2.2$	α1B	N-type
	$Ca_V2.3$	α1E	R-type
Ca_V3	$Ca_V3.1$	α1G	T-type
	$Ca_V3.2$	α1H	
	$Ca_V3.3$	α1I	

1.3.3 The expression and function of subtypes of VGCCs in neural systems

As we can see in Figure 1.4, at least eight types of VGCCs have been identified in neurons, including $Ca_V1.2$, $Ca_V1.3$, $Ca_V2.1$, $Ca_V2.2$, $Ca_V2.3$, $Ca_V3.1$, $Ca_V3.2$ and $Ca_V3.3$ channels (Fisher & Bourque 2001). Different subtypes of VGCCs may have different functions in different cells and in different subcellular locations.

For example, the $Ca_V1.2$ and $Ca_V1.3$ channels are predominant forms of Ca_V1 Ca^{2+} channel family in the CNS. They are important for long-term adaptation of neuronal functions, such as dendritic development, synaptic plasticity, and neuronal survival

(Ahlijanian et al 1990; Bean 1989; Silver et al 1990). The $Ca_V1.2$ and $Ca_V1.3$ channels are mostly found in somatic and dendritic structures (Hell et al 1993; Westenbroek et al 1990; Westenbroek et al 1998b). Compared to $Ca_V1.2$ channels, which are activated at ~-10 mV, the biophysical properties of $Ca_V1.3$ channels are different because they are activated at relatively hyperpolarized potential (Koschak et al 2001; Xu & Lipscombe 2001).

Morgan and Curran hypothesized that Ca^{2+} influx through L-type Ca^{2+} channels activates expression of *c*-fos, an immediate early gene (IEG) (Morgan & Curran 1986; West et al 2001; Zhang et al 2006). They suggested that a calmodulin (CaM)-sensitive kinase would phosphorylate a transcription factor, initially located in the cytoplasm, causing it move into the nucleus to activate gene expression (Deisseroth et al 2003). This CaM nuclear translocation pathway is widely utilized by neuronal and non-neuronal cells to transduct Ca^{2+} signals from the plasma membrane into the nucleus (Deisseroth et al 1998; Mermelstein et al 2001).

Ca^{2+} signals mediated by L-type channels can preferentially activate the transcription factor cAMP-responsive element binding (CREB) protein (Deisseroth et al 1998; Dolmetsch et al 2001). CREB drives the expression of many genes, including IEGs, that are critical for neuronal survival and plasticity (Shaywitz & Greenberg 1999). CREB is activated by phosphorylation of Ser^{133}, which allows recruitment of

CREB binding protein (CBP) and initiation of transcription (Chrivia et al 1993). Phosphorylation of the CREB proteins can be activated by several pathways, including a Ca^{2+}/calmodulin kinase IV (CaMKIV) pathway (Kang et al 2001), a mitogen-activated protein kinase (MAPK/Erk) pathway (Dolmetsch et al 2001), a nuclear factor of activated T-cells family of transcription factors (NFATc4) pathway (Graef et al 1999), and an inhibition of the calcineurin/PP1 (protein phosphatase 1) pathway (Malleret et al 2001; Rajadhyaksha & Kosofsky 2005).

In addition, both $Ca_V1.2$ and $Ca_V1.3$ channels contain PDZ (postsynaptic density-95, PSD-95/Discs large/Zona occludens 1) (Sheng 1996) interaction sequences that bind with PDZ domain proteins (Craven & Bredt 1998). $Ca_V1.2$ contains the motif Val-Ser-Asn-Leu (VSNL), which is critical for binding to PDZ proteins and activating CREB phosphorylation (Weick et al 2003). $Ca_V1.3$ binds with the post-synaptic scaffold protein Shank (SH3 and ankyrin repeat-containing protein) via the motif Ile-Thr-Thr-Leu ITTL that is essential for CREB activation (Olson et al 2005; Zhang et al 2005). Shank proteins are thought to be key scaffold elements in the synaptic signaling complex (Sheng & Kim 2000).

The Ca_V3 family ($Ca_V3.1$-3.3) genes have been identified to encode the T-type currents (Mittman et al 1999a; Mittman et al 1999b; Monteil et al 2000). These channels are found mainly in the neuronal somata and dendrites. Because of their low

threshold and slow inactivation, they are often involved in regulating firing patterns of neurons. For example, in the thalamus, Ca_V3 channels are distributed in the somata and dendrites of neurons and contribute to thalamic oscillations (Perez-Reyes 2003). Mutations of the Ca_V3 channels cause altered channel activities and link to epilepsy in humans (Becker et al 2008; Khosravani et al 2004).

Among the VGCCs expressed in neurons, the Ca_V2 channel subfamily is of special interest because of their roles in mediating neurotransmission of neurons and hormone release of neuroendocrine cells.

The $Ca_V2.1$ and $Ca_V2.2$ channels are highly expressed in presynaptic terminals of neurons (Stea et al 1994; Westenbroek et al 1992). Mutations of $Ca_V2.1$ channels have been linked to multiple human genetic disorders, including familial hemiplegic migraine, ataxia and epilepsy (Fletcher et al 1996; Ophoff et al 1996; Zhuchenko et al 1997). Although $Ca_V2.2$ channels have a function that is similar to that of $Ca_V2.1$ in presynaptic neurotransmission, there appear to be fundamental differences between $Ca_V2.1$ and $Ca_V2.2$ channels. The $Ca_V2.1^{-/-}$ knockout mice suffer fatal consequences shortly after birth whereas the $Ca_V2.2^{-/-}$ knockout mice show a normal lifespan (Ino et al 2001). The $Ca_V2.2^{-/-}$ knockout mice, however, exhibit significant higher thresholds of pain sensation (Beuckmann et al 2003; Saegusa et al 2001). They are particularly important in mediating rapid neurotransmission (Catterall 2000; Jarvis & Zamponi

2007). The $Ca_V2.3$ channels are expressed preferentially within the somata and dendrites of many neurons in the rat brain (Fisher & Bourque 1996; Yokoyama et al 1995), and their roles in fast neurotransmission are obscure, but they do contribute to presynaptic long-term potentiation in the mossy fibers of hippocampal neurons (Dietrich et al 2003).

Neurosecretion of neuroendocrine cells, such as MNCs, also depends primarily on Ca^{2+} influx through $Ca_V2.1$ and $Ca_V2.2$ channels (Cazalis et al 1987; Wang et al 1997). Ca^{2+}-dependent increases in whole cell capacitance of patch clamped MNCs suggests that the rate of Ca^{2+} evoked release is slower from MNC terminals than from neurons (Giovannucci & Stuenkel 1997; Lim et al 1990). Why do the same subtypes of VGCCs result in significantly different exocytotic behaviors between neuronal and neuroendocrine terminals? The study of the main subunits of Ca_V2 channels may provide some hint to explain why the neuroendocrine cells have a much slower hormone release comparing to neurons.

In the following sections, I will dissect the molecular structures of VGCCs and elaborate how channel regulation may be involved with different segments of those structures, especially the synaptic protein interaction (synprint) site.

1.4 VGCC molecular structure and regulation

1.4.1 Molecular structure of VGCCs

VGCCs are heterogenous complexes consisting of a channel forming α1 subunit as well as accessory α2-δ, β, and γ subunits (Catterall 2000). To form a fully functional VGCC, the α1 subunit is essential, and the other subunits are considered as auxiliary components (Liu et al 1996; McEnery et al 1991; Witcher et al 1993). The combinations of different subunits vary in different tissues. The α1 subunit is the largest component (molecular weight MW~190 kDa). The α1 subunit is the pore-forming subunit, determines most channel biophysical properties, and has structural similarity with the Na^+ channel (Goldin 2001). Four different α2-δ subunits (α2-δ1, α2-δ2, α2-δ3, α2-δ4, MW~170kDa), four different β subunits (β1, β2, β3, and β4, MW~55kDa), and eight different γ subunits (γ1, γ2, γ3, γ4, γ5, γ6, γ7, and γ8, MW~33kDa) have been identified and characterized from a variety of tissues (Catterall et al 2005; Ertel et al 2000; Klugbauer et al 1999).

The amino acid sequence of the α1 subunit is organized in four repeated domains (I to IV), each of which contains six transmembrane segments (S1 to S6) and a membrane associated loop between S5 and S6. The S4 segments of each homologous domain serve as the voltage sensors for activation, which move according to voltage change and initiate a conformational switch that opens the pore (Catterall 2000). There are five major intracellular parts of the α1 subunit molecular structure,

including the N-terminus, carboxyl C-terminus, and 3 loops (or linkers) that connect domains (I-II, II-III, and III-IV loop; see Figure 1.5B). These are important regulatory regions that provide protein binding sites or phosphorylation sites and allow other intracellular or membrane components to modulate VGCC functions or anchor the channels in specific locations (Jarvis & Zamponi 2007; Randall & Benham 1999; Spafford & Zamponi 2003).

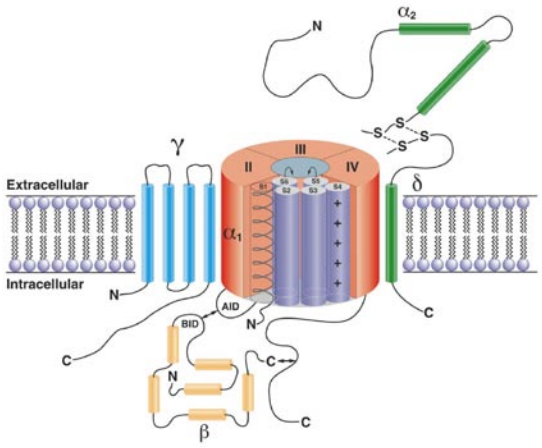

A

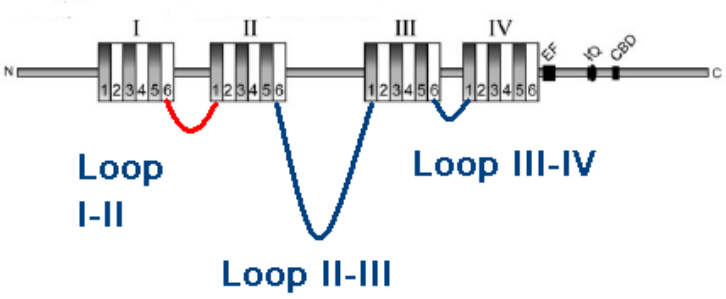

B

Figure 1.5 Primary and accessory subunits of VGCCs on the plasma membrane. A. Three dimensional demonstration of relationships between subunits of VGCCs. B. Major domains of the VGCC α1 subunit structure (Randall & Benham 1999;

Reproduced with permission from Copyright Clearance Center).

The β subunits are cytoplasmic proteins that bind to the I-II loop of the α1 subunits (Pragnell et al 1994). The β subunits have important regulatory effects on the level of expression and biophysical properties of VGCCs in both neuronal and cardiac tissues (Birnbaumer et al 1998; Dolphin 2003). The α2-δ subunit is transcribed and translated from one gene but post-translationally cleaved into α2 (extracellular) and δ (transmembrane) units that are linked by disulfide bonds (Klugbauer et al 1999; Takahashi et al 1987). Loss of the α2-δ subunits in cerebellum, for example, which naturally occur in the *ducky* (α2-δ2 mutant) mice (Barclay et al 2001), results in reduction of Ca^{2+} currents in Purkinje neurons (Donato et al 2006). Nevertheless, it has been revealed recently that the α2-δ subunits may play important roles in channel targeting at the presynaptic terminals (Dickman et al 2008; Taylor & Garrido 2008). The γ subunits were first discovered in the VGCCs of skeletal muscle and later in neurons (Letts et al 1998; Tanabe et al 1987). Unlike the α2-δ and β subunits, the functions of the γ subunits are less clear (Arikkath & Campbell 2003). No auxiliary subunits are necessary for functional Ca_V3 channels (Cribbs et al 1998; Perez-Reyes et al 1998). The γ2 subunit seems to have broader effects on neuronal membrane protein trafficking, such as on AMPA receptors (Chen et al 2000).

As I introduced above, the α1 subunits of VGCCs are the main determinants for the channel activities and functions. I will further explain the importance of the synprint site within the II-III loop of the Ca_V2 channels.

1.4.2 Neurotransmission and Ca_V2 channel activities regulated by SNARE proteins

The term “synprint site” is designated to describe the synaptic protein interaction sites of the α1 subunits of $Ca_V2.1$ and $Ca_V2.2$ channels (Catterall 1999). This protein interaction site was first identified as a segment of amino acid sequence (residues 718-963) within the II-III loop of the $Ca_V2.2$ channels. Immunochemical studies have indicated a tight association of the core SNARE proteins, such as syntaxin, SNAP25, and synaptotagmin, with the $Ca_V2.2$ channels in rat brains through the synprint site (Bennett et al 1992; Leveque et al 1992; Sheng et al 1996; Sheng et al 1994). A similar synprint site (residues 722-1036) has been identified in the II-III loop of the $Ca_V2.1$ channels (Rettig et al 1996).

The interaction between the Ca_V2 channels and SNARE proteins has been shown to have functional effects on neurotransmitter release. The biological function of this direct coupling of the SNARE proteins and $Ca_V2.2$ channels has been tested by injecting competing peptides containing synprint site into the the superior cervical

ganglion neurons (SCGN). The peptides representing segment (LII-III 718-963) disrupted the coupling of $Ca_V2.2$ channels and syntaxin *in vitro* and reduced synaptic transmission in SCGN by 42% (Mochida et al 1996). The corresponding peptides from L-type Ca^{2+} channels had no effect. These results provide direct evidence that binding of presynaptic Ca^{2+} channels to the SNARE proteins is required for rapid neurotransmitter release. Further tests of the effects on Ca^{2+} dependence of neurotransmitter release revealed that the competing peptides shifted the Ca^{2+} dependence of neurotransmission to a higher values, suggesting the interaction between syntaxin and $Ca_V2.2$ channels is important for docking synaptic vesicles to the Ca^{2+} entry sites (Rettig et al 1997). In a mouse chromaffin cell line that lacks endogenous $Ca_V2.2$ channels, exogenously expressing a recombinant plasmid encoding channels lacking the synprint site showed a significantly decreased total amount and rate of neurosecretion detected by capacitance measurements (Harkins et al 2004) compared to cells transfected with the WT channels.

The synprint site interaction might also modulate Ca^{2+} channel biophysical properties. Bezprozvanny and colleagues found that coexpression of syntaxin with $Ca_V2.1$ and $Ca_V2.2$ channels in *Xenopus* oocytes resulted in a change in the voltage-dependent inactivation of the channels (Bezprozvanny et al 1995; Bezprozvanny et al 2000). Another functional link between syntaxin and the Ca_V2 channels was suggested by the observation that proteolytic cleavage of syntaxin by

botulinum, a specific SNARE protein toxin (Rossetto et al 1994), prevented the normal G protein modulation of presynaptic terminal Ca_V2 channels in the calyx-type chicken ciliary ganglion synapse (Stanley & Mirotznik 1997). This G protein modulation normally shifts the channels to the reluctant state, from which the gating of channel is slow, which is reversible upon strong depolarization (Wickman & Clapham 1995). The G protein interaction site on $Ca_V2.2$ channels is within the I-II loop, which was proved by site-directed mutagenesis and expression experiments (Page et al 1997; Zamponi et al 1997); see Figure 1.6). It appears that co-expression of individual SNARE proteins (e.g. syntaxin 1A) with $Ca_V2.2$ channels causes decreased current amplitude, enhanced G protein inhibition, and increased voltage-dependent inactivation (Jarvis et al 2002; Jarvis et al 2000).

The synprint site may be involved in the Ca_V2 channel targeting. Mochida and colleagues showed that deletion of synprint site impaired the effective targeting of $Ca_V2.1$ channels into nerve terminals of the SCGNs (Mochida 2003). However, similar synprint site deletion isoforms of $Ca_V2.2$ did not affect the ability of channel targeting to the axonal compartments of cultured hippocampal neurons (Szabo 2006), and thus the role of the synprint site in Ca_V2 channel targeting is not clear. Because the channel targeting mechanism will determine the numbers of channels transported and anchored to the proper location(s) that will eventually affect the Ca^{2+}-dependent

exocytosis (Dolphin 2009), I will expand my introduction to some identified mechanisms that are related to Ca_V2 channel targeting.

1.4.3 Mechanisms of Ca_V2 channel targeting

1.4.3.1 β subunits regulation of the Ca_V2 channel targeting

The α1 subunits of VGCC contain endoplasmic reticulum retention motifs in the N-terminus and I-II loop, but when the α1 subunits are bound with by β subunit, the retention motifs are blocked, thus allowing for co-trafficking of the α1/β protein complex to the plasma membrane (Cornet et al 2002). It is believed that the α1 subunit binds β subunit by its beta-interaction domain (BID), and β subunit has its alpha-interaction domain (AID). Only recently, it has been revealed that the Src homology 3 (SH3) domain and the guanylate kinase (GK) domain within the β subunit contribute to this high affinity binding between the two subunits (Chen et al 2004).

The β subunits may have differential effects on targeting of Ca_V2 channels. Using Madin-Darby canine kidney (MDCK) cells, Brice and Dolphin found that $Ca_V2.2$ channels were expressed at the apical membrane with all accessory subunit combinations (β1, β2, β3 and β4). In contrast, $Ca_V2.1$ channels can only be targeted to the cell membrane with β1 or β4 but not with β2 or β3 (Brice & Dolphin 1999).

Although there has been no exclusive association between particular α1/β combinations in tissue, the β3 subunit has been found to associate mainly with $Ca_V2.2$ channels in rabbit brain (Scott et al 1996). Expression of GFP-β4 subunits in the hippocampal neurons revealed a synaptic staining pattern of β4 (Wittemann et al 2000), and endogenous expression of β4 subunits was detected in the presynaptic terminals of Purkinje and granule cells (Westenbroek et al 1995). However, there is no clear evidence showing which β subunits are mainly associated with presynaptic $Ca_V2.1$ channels.

1.4.3.2 CASK/Mint1 regulation of the Ca_V2 channel targeting

CASK (calcium, calmodulin associated serine kinase) is enriched in the brain at the synaptic membrane (Hata et al 1996), and it binds with neuronal junction proteins during neuronal development (Biederer & Sudhof 2001; Hsueh et al 1998). The ability to form macromolecular complexes beneath the synaptic membranes might involve a role for CASK in trafficking and anchoring ion channels on the plasma membrane (Schuh et al 2003). It has been reported that CASK is important for the targeting for ion channels such as potassium channels and NMDARs (Jeyifous et al 2009; Leonoudakis et al 2004).

More interestingly, CASK and Mint1 (Munc-18-interacting protein 1) are proposed to form macromolecular complex with VGCCs to anchor Ca^{2+} channels at presynaptic terminals (Maximov et al 1999). It has been observed that CASK binds to $Ca_V2.2$ at C-terminals between the amino acid 2020-2233 and Mint1 binds to $Ca_V2.2$ between the amino acids residues 2331-2336 (Maximov et al 1999). Blocking this interaction resulted in inhibited synaptic targeting of $Ca_V2.2$ channels in hippocampal neurons (Maximov & Bezprozvanny 2002). CASK can also be detected in peripheral tissues like adrenal gland and pituitary gland (Stevenson et al 2000), suggesting that it may interact with the exocytotic machinery in neuroendocrine cells, but whether CASK/Mint1 interaction is important for $Ca_V2.2$ channel targeting in neuroendocrine terminals is not known.

1.4.3.3 G protein regulation of the Ca_V2 channel targeting

Recently, a few studies have shown that G protein coupled receptors are involved in the distribution of $Ca_V2.2$ channels. The opioid receptor-like receptor 1 (ORL1) physically binds with $Ca_V2.2$ channels and triggers internalization and degradation of calcium channels upon prolonged agonist application. This may mediate inactivation of the involvement of the $Ca_V2.2$ channels in pain sensation (Altier et al 2006; Beedle et al 2004). $GABA_B$ receptor activation results in rapid internalization of $Ca_V2.2$ channels from the plasma membrane but this process may not include $Ca_V2.2$ channel

degradation (Richman et al 2004; Tombler et al 2006). It has been found that in prefrontal cortex, the interaction of dopamine D1 receptor with $Ca_V2.2$ channels are critical for the distribution of channels (Kisilevsky et al 2008). These mechanisms are not fully understood and I will not elaborate upon them in this thesis.

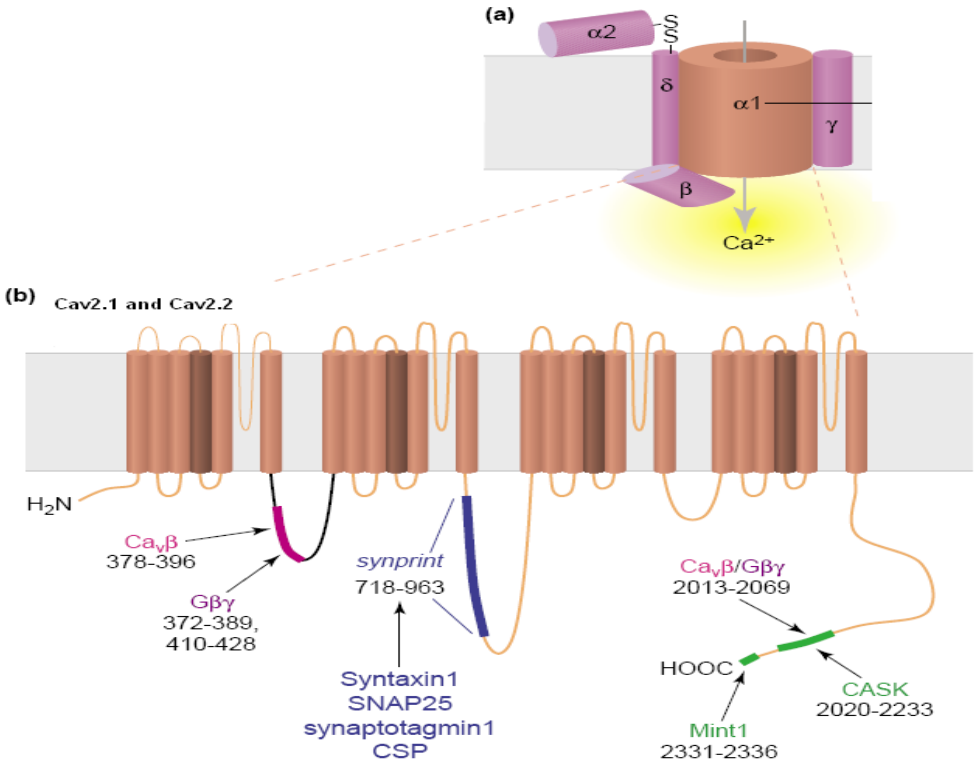

Figure 1.6 Possible regulatory regions that affect channel activity and targeting. (Modified from figure of the paper (Spafford & Zamponi 2003) and reproduced with permission from Copyright Clearance Center). The α1 subunit defines the channel subtype, and is comprised of four homologous transmembrane domains, which are connected by large cytoplasmic loops, and formed by six membrane-spanning helices. The domain I-II linker interacts with the calcium channel β subunit and G protein βγ subunits. In N-type ($Ca_V2.2$) and P/Q-type ($Ca_V2.1$) channels, the domain II-III linker

region contains a synaptic protein interaction site (synprint) which binds syntaxin1 isoforms, SNAP25, cysteine string protein (CSP) and synaptotagmin 1. The carboxy-terminus of $Ca_V2.2$ calcium channels binds the scaffolding proteins CASK and Mint1, and contains a binding site for calcium channel β subunits.

1.4.4 Alternative splicing of Ca_V2 α1 subunits

As we introduced above, Ca_V2 channel function is largely determined by the molecular structure of Ca_V2 α1 subunits. Systematic screening of cDNA of VGCCs has revealed that several regions are consistently subjected to alternative splicing, including the domain IV, the II-III loop, and the C-terminus of the α1 subunits (Lipscombe 2005).

Alternative splicing is a mechanism used extensively in the mammalian nervous system to increase the level of diversity of proteins (Lipscombe et al 2002). In humans, over 80% of genes are alternatively spliced (Matlin et al 2005). Genes are composed of multiple short (50-300 nucleotides in length) protein coding regions called exons, which are disrupted by larger non-coding introns (200- several thousands nucleotides). Messenger RNAs are transcribed as precursors (pre-mRNAs) containing products of both exons and introns. Exons need to be reshuffled into mature mRNA with a process to remove introns. This process is called alternative splicing. Some exons are always part of the mature mRNA (i.e. they are constitutively expressed), while others are

alternatively expressed in subset of mRNAs depending on cell-type, developmental stage, and activity (Black 2003; Cheung & Spielman 2009).

Systematic screens of splice variants of human $Ca_V2.1$ channels have indicated at least 9 known exon loci that could be alternatively spliced (Hans et al 1999a; Soong et al 2002). These sites contain exon 10 in the I-II loop, exon 16 and 17 in the II-III loop, exon 31a in the IVS3-IVS4 linker, and exon 37a/37b, 43, 44 and 47 in the carboxyl terminus (Figure 1.7).

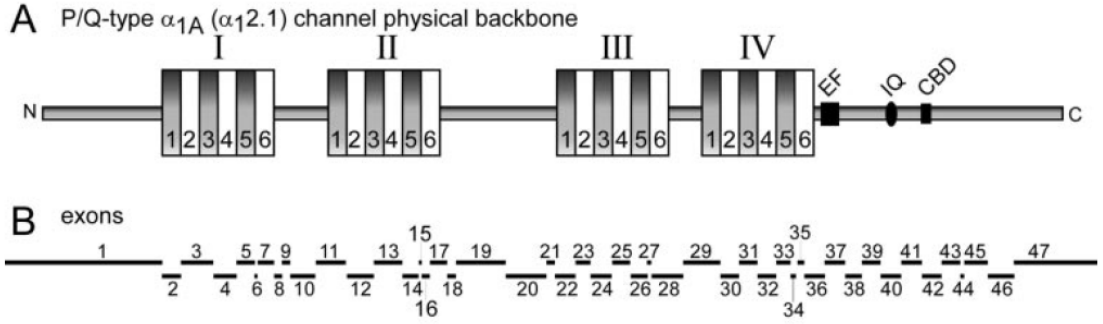

Figure 1.7 Schematic representation of human $Ca_V2.1$ molecular structure showing the loci of exons (Soong et al 2002); reproduced with permission from Copyright Clearance Center). A, Diagram of $Ca_V2.1$ channel backbone structure, showing four homologous domains (I–IV), each with six transmembrane spanning regions (1–6). The C-terminal tail contains structures postulated to be important for Ca^{2+} regulation of the channel. EF, EF-hand; IQ, IQ-like CaM interaction domain; CBD, CaM binding domain. B, Locations of exon transcripts corresponding to the backbone diagram in A.

I am particularly interested in the II-III loop, which is relatively long in the Ca_V2 channel subfamily in comparison to the Ca_V1 channel subfamily and also contains the synprint sites in $Ca_V2.1$ and $Ca_V2.2$ channels. Two isoforms of $Ca_V2.1$ in this loop were found to be present in presynaptic nerve terminals based on immunohistochemical studies (Rettig et al 1996; Sakurai et al 1995; Sakurai et al 1996; Wu et al 1999). Two other alternatively splicing sites have been identified as well that involve exons 16 and 17, although the functional significance is unclear (Soong et al 2002).

The C-terminus of $Ca_V2.1$ channels is another important region susceptive to alternative splicing and is related to CASK/Mint1 interaction with $Ca_V2.1$ channels. Exon 47 encodes >230 amino acids in the long isoform of channels, which has been found in human brain, spinal cord, and neuroblastoma cells (Hans et al 1999b; Krovetz et al 2000; Soong et al 2002). Notably, only isoforms that contain exon 47 express the SCA6 polyglutamine expansion that underlies spinocerebellar ataxia type 6 (Zhuchenko et al 1997). As I mentioned, this long C-terminus isoform is also involved in binding with modular adaptor proteins such as CASK and Mint1 (Maximov & Bezprozvanny 2002; Maximov et al 1999).

Lastly I would like to briefly mention another important exon of $Ca_V2.1$ channel,

exon 31, which can be alternatively spliced and alter the channel the sensitivity to selective blocker, ω-agatoxin IVA. Exon 31 has been identified in the S3-S4 extracellular linker of the domain IV. Bourinet and colleagues found relatively small alterations in the domain S3-S4 region (a two amino acid insertion, N_{1605}-P_{1606}). The splice variant containing this insertion causes an approximately +6 mV shift in the current-voltage relationship compared to the wild type $Ca_V2.1$ channel (Bourinet et al 1999; Hans et al 1999b). The second major change in channel properties associated with this splice variant is the altered affinity of ω-agatoxin IVA. The insertion of N_{1605}-P_{1606} causes about 11-fold decrease in toxin affinity of $Ca_V2.1$ channels (Bourinet et al 1999).

$Ca_V2.2$ channels have very similar molecular structure with $Ca_V2.1$ channels in terms of number of exons, cDNA size, and potential sites of alternative splicing (Fujita et al 1993; Lipscombe et al 2002); see Table 1-2 and 1-3). The II-III loop region of the $Ca_V2.2$ gene contains exons 18 to 21 and is dominated by exon 19, which encodes 266 amino acids. The majority of $Ca_V2.2$ mRNA in the adult sympathetic ganglia expresses exon 18a, which refers to an isoform with a 21 amino acid insertion in the exon 18 of wild type $Ca_V2.2$ gene. This splice variant is tissue specific, probably linked to monoaminergic neurons (Ghasemzadeh et al 1999; Pan & Lipscombe 2000), and its expression varies during development. During the first three weeks of postnatal life, for example, the expression of splice variant 18a continuously

increases in the rat superior cervical ganglia (Gray et al 2007; Thaler et al 2004). Surprisingly, isoforms that are missing all of exon 19 to 21 have been found in human brain tissue and cell lines (Kaneko et al 2002). These two splice variants lack 382 and 263 amino acids within the II-III loop, causing an alteration of channel inactivation properties and the loss of binding with syntaxin (Kaneko et al 2002). These results suggest that the synprint site could be alternatively spliced in normal rat brains.

Table 1-2 Comparison of the genome information between the human $Ca_V2.1$ and $Ca_V2.2$ channels

	Chromosome	Genome size	Number of exons	cDNA size
hCa2.1	19p13	400kb	49	~7800bp
hCav2.2	9q34	300kb	50	~7300bp

Table 1-3 Comparison of alternative splicing sites between the human $Ca_V2.1$ and $Ca_V2.2$ channels

	I-II loop	II-III Loop	IVS3-S4	C-terminus
hCa2.1	E10	E16, 17	E31a	E37a/37b, 43, 44, 47
hCav2.2	E10	E18a,19,20, 21	E31a	37a/37b, 46

However, whether the synprint site is essential for Ca_V2 channel targeting in neurons is not known, and there is even less knowledge available for the roles of the synprint site in the Ca_V2 channel functions in neuroendocrine cells. As the alternative splicing of channels is a common mechanism used for regulation of the channel

expression and targeting, it is possible that synprint site deletion isoforms of the Ca_V2 channels are expressed in neuroendocrine cells.

In the next few sections, I will focus on introducing the model system I used in my research, and why I used them to test my hypotheses.

1.5 VGCCs expression and function of neuroendocrine cells and pituicytes in the hypothalamo-neurohypophysial system (HNS)

1.5.1 Magnocellular neurosecretory cells (MNCs) in the HNS

Mammalian neurosecretion has been well investigated in the rat hypothalamo-neurohypophysial system (HNS) (Hatton 1988; 1997). The HNS is composed of hypothalamic magnocellular neurons and the neural lobe pituicytes that accommodate surround and regulate the nerve terminals. The magnocellular neurosecretory cells (MNCs) have their somata located in the paraventricular nucleus (PVN) and supraoptic nucleus (SON) of the hypothalamus and nerve terminals in the posterior ptuitary (Figure 1.8). Individual MNC axons frequently entwin around blood vessels and a short length of axon can form multiple “endings” (Tweedle 1989). In this thesis, nerve terminals of MNCs do not structurally resemble presynaptic terminals of neurons, but are described as “MNC terminals”. Oxytocin (OT) and vasopressin (VP) are synthesized and released from MNCs (Brownstein et al 1980). LDCVs filled with

OT or VP are assembled in the somata of MNCs and then transported to the terminals where they are exocytosed in response to the arrival of action potentials (Fisher & Bourque 2001).

A 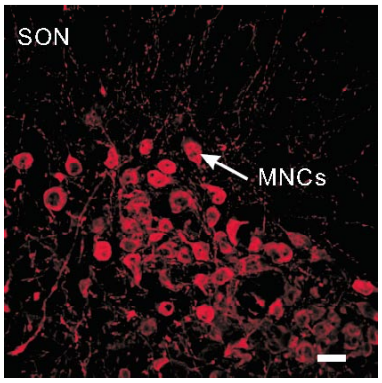

B 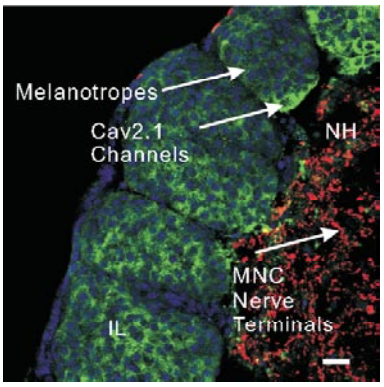

Figure 1.8 MNC soma in the SON of hypothalamus and terminals in the posterior pituitary (permission from Dr. Thomas Fisher's lab). A. MNC soma (red) labeled by neurophysin I and II antibodies in the SON of the rat brain. Scale bar =20 µm. B. MNC nerve terminals in the (red) labeled by neurophysin I and II antibodies in the posterior pituitary of the rats Scale bar = 40 µm.

MNCs synthesize and release oxytocin (OT) and vasopressin (VP; Brownstein et al 1980). Both OT and VP are 9 amino acid peptides, and their genes are closely related which consist of three exons (and two introns) with little variability in structure among species from rodents to humans (Gainer & Wray 1992). OT and VP are synthesized as portions of large carrier proteins, neurophysin I and neurophysin II, respectively. Although these two precursors are encoded by a pair of genes that share many similarities in structure and sequence, they are separately associated with OT and VP (Marini et al 1993; Mason et al 1986; Rose et al 1996).

OT has been known for its function in lactation and the initiation of labour. During labour, sensory signals from the uterus and birth canal stimulate MNCs, and the OT released into the bloodstream binds to uterine OT receptors to facilitate parturition by contracting the smooth muscle (Gainer & Wray 1992). OT also has central effects where it may act as a key mediator of complex emotional and social behaviours (Insel et al 1999; Insel & Young 2001).

VP is the main hormone involved in regulating water balance and the osmolality of body fluids. The physiologic regulation of VP synthesis and secretion involves the osmolality of body fluids and the pressure and volume of the plasma. VP acts in the collecting duct of the kidney to increase water permeability, thereby allowing osmotic equilibration by extracting water from the urine into the medullary interstitial blood vessels, resulting in increased urine concentration and decreased urine volume (antidiuresis). The epithelial principal cells of the collecting tubule in the kidney possess vasopressin V2 receptors that allow VP to produce antidiuretic effects (Park et al 1998; Petersen 2006; Spanakis et al 2008). There is some evidence showing the involvement of oxytocin in regulating salt appetite during hyperosmolality in some species (Blackburn et al 1993; 1995).

Biophysical and pharmacological experiments demonstrated the presence of T-type currents and several HVA currents (L-, N-, P/Q-, and R-) in isolated MNC somata (Fisher & Bourque 1995b; Foehring & Armstrong 1996; Joux et al 2001). These channels are involved with the regulation of firing patterns, gene expression, and somatodendritic release in MNCs. The somatodendritic regions of MNCs are responsible for regulation of the cell firing pattern and can release OT and VP. MNC somata can undergo plasticity following sustained dehydration involving gene expression and morphological changes. Oxytocin and vasopressin are released into the circulation from MNC terminals upon physiological stimulations such as dehydration and lactation (Bielefeldt et al 1993 (Fisher & Bourque 1996; Li & Hatton 1997; Renaud & Bourque 1991). Recording from isolated terminals from neurohypophysis demonstrated Ca^{2+} currents sensitive to channel blockers DHPs, ω-conotoxin GVIA, and ω-agatoxin IVA (Fisher & Bourque 1995b; Lemos & Nowycky 1989; Wang et al 1997), which suggested the importance of L-, N- and P/Q- type VGCCs for the release of OT and VP.

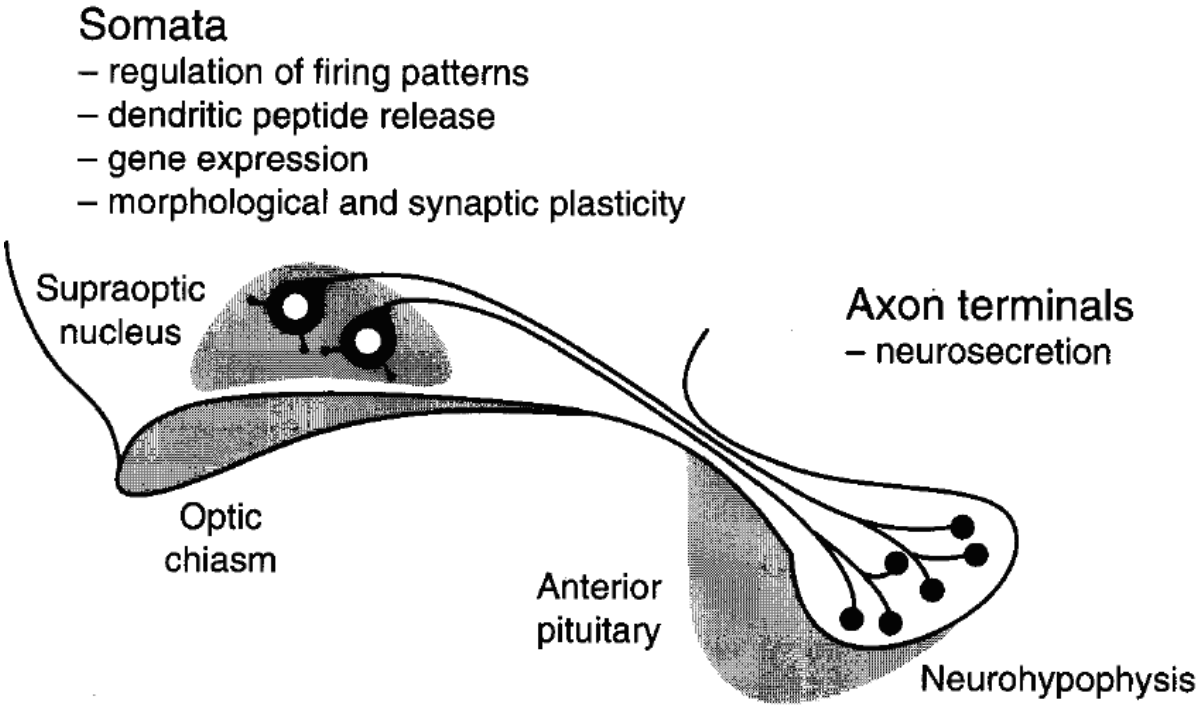

Figure 1.9 Possible functions for VGCCs in the MNCs (Fisher & Bourque 1996) (Reproduced with permission from Copyright Clearance Center).

MNCs can display different firing patterns upon osmotic changes. The intrinsic sensitivity to osmotic changes makes MNCs osmoreceptor cells that are able to detect differences between extracellular fluid osmolality and pre-established set-point (which represents normal or isotonic condition), and to encode this signal into persistent electrical information during acute and chronic perturbations (Bourque 2008). Plasma VP level is strongly correlated with the osmotic changes and feelings of "thirst" in animals (Baylis & Thompson 1988). Studies have revealed that VP-MNCs change their firing pattern when the external osmolality change (Bourque 1998); see Figure 1.9). The rate and pattern of the action potentials generated by the somata are

controlled by Ca^{2+}-dependent afterpotentials (activity dependent currents), endogenous membrane currents, and external synaptic inputs (Fisher & Bourque 1996; Li & Hatton 1997; Renaud & Bourque 1991). VP release increases when the osmolality increases within physiological range, accrodingly, the firing rate of VP-MNCs also increased (Figure 1.8 A and B). On the other hand, high frequencies of firing also results in neuronal fatigue and ultimately a decrease in VP release, thus, the VP release is therefore maximized by burst firing (Bicknell 1988).

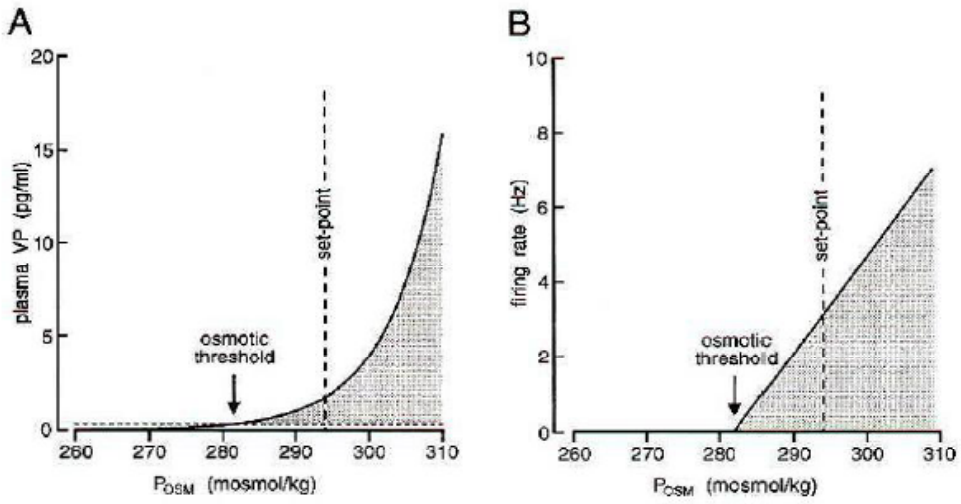

Figure 1.10 Effects of plasma osmolality on vasopressin secretion and firing rate in VP-MNCs (Bourque 1998) (Reproduced with permission from Copyright Clearance Center).

1.5.2 Pituicytes in the posterior lobe of the pituitary gland

I have introduced the neurosecretion of MNCs and the VGCCs expressed on them. As an important component of the entire HNS, the Ca^{2+} signaling of the neurohypophysis is critical for the proper MNC terminal hormone release. In the next and last section, I will briefly dissect the physiology of each part of the pituitary gland including the neurohypophysis, especially the Ca^{2+} signaling in the the pituicytes of the neurohypophysis.

The rat pituitary gland consists of three parts: the anterior lobe (adenohypophysis, AH), the intermediate lobe (IL), and the posterior lobe (neurohypophysis, NH). The AH has a special vascular connection with the brain through the portal hypophysial vessels. Five endocrine cell types have been identified by immunocytochemistry and electron microscopy: somatotrope, lactotrope, corticotrope, thyrotrope, and gonadotrope, which release growth hormone (GH), prolactin, adrenocorticotropic hormone (ACTH), thyroid- stimulating hormone (TSH), follicle-stimulating hormone (FSH) and luteinizing hormone (LH), respectively.

The NH is made up with neurosecretory axons, axonal swellings called Herring bodies, and axonal endings of the MNCs, all of which contain LDCVs (Hatton 1988; Hussy 2002). In addition to the tens of thousands of axonal structures, the NH

contains non-secretory axons, basal lamina, capillaries and pituicytes. The pituicytes are the only cell bodies of neural origin in the NH. They constitute a large percentage (30%) of the total volume of the NH (Tian et al 1991), and could contribute to the extracellular microenvironment of the NH. In rat tissues, they are relatively large. Under basal conditions, pituicytes processes often physically engulf the MNC axons and separate them from the basal lamina, occupying a high proportion of the vascular surface and therefore limiting the number of contacts between axons and vessels (Hussy 2002).

Pituicytes are characterized as glial cells (Salm et al 1982). By definition, the term glia (from the Greek word meaning “glue”) reflects the nineteenth-century presumption that these cells play a supportive role in the CNS. There are three major types of glial cells located in the mature CNS, including astrocytes, microglia and oligodendrocytes. Astrocytes communicate with neurons in a variety of ways to maintain and regulate neuronal signaling. One of the many functions of astrocytes is to buffer extracellular ion gradients of neurons to maintain the microenvironment (Walz 1989). Microglia function in a manner similar to macrophages in the immune system (Hatten et al 1991) and oligodendrocytes surround the axons of neurons with myelin, which is important for transmission of electrical signals (Purves et al 2004).

In contrast, pituicytes are glial cells located outside of the brain. Both OT and VP terminals and non-secretory axons make contacts with pituicytes. Physiological stimulations (lactation, parturition, and dehydration etc.) lead to retraction of the pituicyte processes, allowing increased occupation of the perivascular contact zone by MNC terminals (Beagley & Hatton 1992; Tweedle & Hatton 1980). This retraction is reversible following return to basal conditions (Tweedle & Hatton 1987).

Similar morphological changes are observed in astrocytes around MNC soma in the hypothalamus, where the withdrawal of the processes leads to the increased soma-somatic and dendro-dendritic membrane apposition (Hatton & Tweedle 1982; Theodosis et al 1981). This glial-neuron interaction is important for maintaining proper functions of MNCs in the hypothalamo-neurohypophsial system (Haydon 2001; Watkins et al 2001). For example, Gordon and colleauges found norepinephrine can trigger ATP release from astrocytes surrounding the MNCs in the PVN (Gordon et al 2005), and their ATP acts at postsynaptic P2X7 receptors on the MNCs to promote the insertion of AMPA receptors through a mechanism requiring the calcium-dependent activation of PI3K (phosphoinositide 3-kinase) to increases postsynaptic efficacy (Gordon et al 2005).

In addition, astrocytes surrounding MNC somata in the hypothalamus and pituicytes in the neurohypophysis can release an organic osmolyte, taurine. In the

hypothalamus, taurine is a potent opener of the strychnine-sensitive glycine receptors expressed on MNCs (Hussy et al 2001), and its release has been shown to contribute to the inhibitory effect of hypotonicity on the firing rate of MNCs *in vivo* (Deleuze et al 2005; Hussy et al 1997). Therefore, the tonic release of taurine under isotonic or hypotonic condition from glial cells is essential to keep MNC soma at a low excitatory level in SON. In the NH, the retraction of pituicytes from the basal lamina will not only increase the hormone secreted from MNC terminals to the blood circulation, the reduced presence of pituicytes should also diminish the influence of taurine by limiting its access to the glycine receptors (Hussy 2002; Rosso & Mienville 2009).

1.5.3 Ca^{2+} signalings in the pituicytes and glial cells in the CNS

For a long time, glial cells were regarded as electrically silent elements, lacking transmitter receptors and expressing a limited set of ion channels (Seifert et al 2006). The study of voltage-gated ion channels on the glial cells was ignored. Now we know that glial cells are not passive players in the CNS. They express many voltage-gated ion channels (Na^+, K^+ and Ca^{2+}) and actively participate in many Ca^{2+} signaling related pathophysiological processes such as pain, ischemic injury, and epilepsy (Fellin & Carmignoto 2004; Mulligan & MacVicar 2004; Watkins et al 2001).

Some evidence supports the idea that glial cells release gliotransmitters through Ca^{2+} -dependent exocytosis. Glial cells can release a variety of gliotransmitters, such as ATP, glutamate, and D-serine, into the extracellular space to communicate with neurons. Although other mechanisms are important for gliotransmitter release such as cell volume changes (Pasantes Morales & Schousboe 1988), opening of hemi-channels (Cotrina et al 1998) or activation of transporters (Szatkowski et al 1990), strong evidence suggests that gliotransmission may be linked to Ca^{2+}-dependent vesicular release (Parpura et al 1994; Zhang et al 2004).

First, the notion that increased $[Ca^{2+}]_i$ is necessary for glutamate release was proved by the high performance liquid chromatography measurement of glutamate release from cultured astrocytes (Parpura et al 1994). Adding the Ca^{2+} ionophore, ionomycin, in the presence of normal external Ca^{2+} (2.4 mM), caused increased release of glutamate from astrocytes, whereas depleting the external free Ca^{2+} inhibited the release (Parpura et al 1994). This notion was further proved by photolysis of caged Ca^{2+} (Parpura & Haydon 2000; Zhang et al 2004), which suggested that elevated intracellular Ca^{2+} is sufficient and necessary to trigger transmitter release from glial cells.

Second, the presence of SNARE proteins such as synaptobrevin II has been identified in glial cells (Maienschein et al 1999; Montana et al 2006). The glutamate

release from cultured astrocytes is inhibited by the neurotoxin Botulinum B that selectively cleaves synaptobrevin (Araque et al 2000). The use of tetanus toxin, which cleaves astrocytic synaptobrevin II and cellubrevin, leads to a reduction of exocytotic events recorded from astrocytes. The toxin abolished the increased plasma membrane capacitance or the number of amperometric spikes, which can be measured by amperometry and represent the release of single LDCVs (Chen et al 2005; Kreft et al 2004). Other evidence supporting the vesicular release mechanism is that astrocytes *in situ* in the hippocampus have been found to contain small vesicles resembling those at synapses (Bezzi et al 2004). Proteins used for sequestering glutamate into vesicles have also been found in astrocytes (Wilhelm et al 2004).

The identification of VGCCs expression in astrocytes further proved that Ca^{2+} signaling may serve multiple functions in glia. In 1984, MacVicar and colleagues found spontaneous Ca^{2+} action potentials possibly mediated by VGCCs in rat cortical astrocytes that were reminiscent of Ca^{2+} oscillation in some neurons (MacVicar 1984). This finding inspired a series of studies aiming to further identification of VGCCs in glial cells. The L- and T-type Ca^{2+} currents could be detected in cultured astrocytes, but only under certain circumstances (for instance, when co-cultured with neurons or exposed to increased intracellular cAMP levels (Barres et al 1989; MacVicar & Tse 1988)). Later, multiple subtypes of VGCCs were detected in cultured astrocytes (Latour et al 2003). Despite of all the observations metioned above, evidence of

VGCC expression in glial cells *in situ* is ambiguous. Some reseachers showed that both L- and T-type Ca^{2+} currents could be detected in subpopulations of immature astrocytes or progenitor glial cells of mouse brain slices (Akopian et al 1996; Berger et al 1992), but other groups failed to detect Ca^{2+} currents in astrocytes from postnatal rat preparations (Carmignoto et al 1998; Walz & MacVicar 1988). Another example is the observation that depolarization-evoked Ca^{2+} influx can be blocked by the selective L-type Ca^{2+} blocker in cultured astrocytes (MacVicar et al 1991), but not in the hippocampal slices (Duffy & MacVicar 1994). These evidences may suggest a differential expression of VGCCs in glial cells *in situ* compared to that in culture.

The expression of VGCCs has been reported in glial cells outside of the brain. For instance, the mRNAs of L-type and T-type Ca^{2+} channels have been detected in the Muller cells, the retinal glia (Bringmann et al 2000; Puro et al 1996). Whether there is any VGCC(s) expressed in the pituictyes *in situ* or in culture is however unknown. Ca^{2+} signaling has been reported in cultured pituicytes (Hatton et al 1992), which showed activation of VP receptors, but not OT receptors, caused a transient elevation of intracellular [Ca^{2+}]. Ca^{2+} signals were observed when the pituicytes were stimulated by other transmitters or nucleotides such as ATP, which mediated Ca^{2+} signals propagation in cultured pituicytes (Guthrie et al 1999; Nakai et al 1999). The consequences of Ca^{2+} signaling in pituicytes are largely unknown as well (Hussy 2002). The L-type Ca^{2+} channels has been found to be upregulated in reactive

astrocytes in many brain injury models (Westenbroek et al 1998a), and this increased expression level of VGCCs may allow enhanced uptake of extracellular Ca^{2+} to clear the excessive extracellular Ca^{2+} and initiate the release of cytokines and growth factors from glial cells that support neuronal survival (Rudge et al 1995; Vaca & Wendt 1992). Little is known about L-type Ca^{2+} channels regulation of pituicytes during dehydration in which situation the demand of hormone release is high.

1.5.4 Melanotropes of the intermediate lobe of pituitary gland

The melanotropes containing melanin granules in the IL are the main cell type in this area, and these cells have been used as a good model for neurosecretion research (Stanley & Russell 1988; Williams et al 1993). Melanotropes synthesize a large precursor protein, proopiomelanocortin (POMC), which is cleaved by proteolytic processing to generate melanocyte-stimulating hormone (MSH) in melanotropes and adrenocorticotropin (ACTH) in corticotropes (Mains & Eipper 1979). MSH regulates melatonin synthesis in the epidermis in some vertebrate species (Dasen & Rosenfeld 2001). α-MSH can inhibit the electrical activity of oxytocin cells by acting on their somata so that secretion from nerve terminals is inhibited (Sabatier et al 2003).

Rat melanotropes express a much broader repertoire of VGCCs than other anterior endocrine cells. Early studies only found T-type and L-type Ca^{2+} currents in the

melanotropes (Stanley & Russell 1988; Williams et al 1990; Williams et al 1991), but later using single electrode voltage clamp, Williams and colleagues found P-type currents using specific channel blockers (Williams et al 1993). A complete pharmacological identification was performed using whole cell patch-clamp demonstrating that melanotropes also express N- and Q-type currents (Mansvelder et al 1996). Surprisingly, the N- and P/Q-type currents in melanotropes are very sensitive to the L-type Ca^{2+} blocker, nimodipine (Mansvelder & Kits 2000; Mansvelder et al 1996). The exocytotic properties of melanotropes are similar to those of some neuroendocrine cells (Neher & Zucker 1993; Thomas et al 1990; Thomas et al 1993). In this thesis, I will therefore study the Ca_V2 channel expression in melanotropes.

2. RATIONALE, HYPOTHESES AND OBJECTIVES

Because both the $Ca_V2.1$ and $Ca_V2.2$ channels are important for the neurosecretion at the nerve terminals in neurons and neuroendocrine cells, one of the main focuses of this thesis is to study the molecular properties and locations of these channels in MNCs.

The locations and the molecular properties of VGCCs are the determinants for proper Ca^{2+} influx to trigger neurosecretion. The synprint site within the II-III loop of the $Ca_V2.1$ and $Ca_V2.2$ channels is important for the presynaptic regulation of

channels by SNARE proteins (An & Almers 2004; Bezprozvanny et al 1995; Chen & Scheller 2001). There has been some evidence showing that the synprint site of Ca_V2 channels could be missing in the brain (Kaneko et al 2002; Mori et al 1991). Deletion variants of human $Ca_V2.2$ have been identified that lack the synprint site. The early study on splice variants of $Ca_V2.1$ in rabbit brain also revealed an isoform lacking 348 amino acids in the II-III loop (Mori et al 1991). However, there have been no further characterizations of such deletion variants (Jurkat-Rott & Lehmann-Horn 2004; Lipscombe et al 2002), and whether they are expressed in neuroendocrine cells was unknown. Through this thesis work, I am trying to identify the locations of the splice variants of the $Ca_V2.1$ or/and $Ca_V2.2$ channels in the rat brain, especially in MNCs of the hypothalamo-neurohypophysial system.

The rate of Ca^{2+}-dependent hormone release from MNC terminals is slower than neurotransmitters release from the presynaptic terminals of neurons (Giovannucci & Stuenkel 1997; Lim et al 1990). Both pulsed laser Ca^{2+} imaging (Fisher & Fernandez 1999) and immunocytochemical studies of VGCCs expressed on the MNC terminal membranes (Fisher et al 2000) suggest that the MNC terminals lack specialized release sites. These observations suggest that the Ca^{2+} channels responsible for activating exocytosis in MNC terminals are not physically associated with synaptic proteins. To understand the hormone secretion process it is therefore important to understand the molecular architecture of release sites, the mechanism(s) by which

Ca^{2+} channels are targeted to them, and the significance of this architecture to the kinetics of secretion. I hypothesize here that the splice variants affecting the presence of the synprint site in the $Ca_V2.1$ or $Ca_V2.2$ channels may be expressed in neuroendocrine cells and these variants will lead to the alterations of SNARE protein regulations and channel activities of the Ca_V2 channels in neuroendocrine cells.

To study the terminal targeting of channels, I used differentiated PC12 cells as my cell model. PC12 cells are cell lines of a tumor of rat chromaffin cells, which are located in the adrenal medulla and originate from neural crest. They are neuroendocrine cells containing small synaptic vesicles and large dense core vesicles (LDCVs). Exocytotic release from PC12 cells depends on $Ca_V2.1$ and $Ca_V2.2$ channels (Chen & Scheller 2001; Fox et al 2008). PC12 cells can be transfected and efficiently express recombinant plasmids encoding proteins of interest. PC12 cells can also be experimentally stimulated to differentiate and grow neurite-like processes called growth cones or varicones (Adler et al 2006; Mingorance-Le Meur et al 2009). I therefore used PC12 cells as my model to study the Ca_V2 channel targeting in this neuroendocrine cells (Burgoyne 1997; Westerink & Ewing 2008).

The pituicytes are important glial cells regulating MNC terminal functions. Whether they express VGCCs or not is unclear. The Ca^{2+} oscillations and uptake have

been observed in pituicytes, I therefore hypothesize that pituicytes express VGCCs and these channels may have function(s) related to MNC hormone release.

In summary, our hypotheses are: 1) The neuroendocrine cells (MNCs) primarily express one or more Ca_V2 channels that lack the synprint site of the II-III loop; 2) Pituicytes express one or more VGCCs and the expression levels of channels can be regulated by dehydration.

I propose to perform experiments to test: 1. Expression and locations of alternative splicing of $Ca_V2.1$ and $Ca_V2.2$ channels in the rat brain and neuroendocrine cells. Further identification of the possible cell-type specific expression of those variants. Targeting mechanism(s) of channels will also be studied. 2. The expression of voltage-gated Ca^{2+} channels in the pituicytes both *in situ* and in culture. Identifying the colocalization of VGCCs and pituicytes and quantifying the expression level of certain subtypes of Ca^{2+} channels before and after dehydration.

3. MATERIALS AND METHODS

3.1 Animal and cell preparations

MNC cultures

Male Long-Evans rats (200-300g, 3-4 weeks old) were anesthetized with halothane and killed with a rodent guillotine following a protocol approved by the University of Saskatchewan Animal Care Committee. The supraoptic nucleus of the hypothalamus was dissected and MNCs were isolated. Coronal brain slices (~1 mm thick) were cut and blocks of tissue (~1 mm^3) containing part of the supraoptic nucleus were dissected and incubated for 90 min at 34 °C in 10 ml of an oxygenated (100% O_2) Pipes saline (mM: NaCl, 120; KCl, 5; MgCl2, 1; CaCl2, 1; Pipes, 20; D-glucose, 25; pH 7.1) containing trypsin (0.7 mg ml^{-1}: Sigma). Tissue blocks were then placed in trypsin-free oxygenated Pipes saline and kept (up to 8 h) until use. Tissue blocks were triturated with fire-polished pipettes (0.2-0.5 mm i.d.) and plated onto Petri dishes (Fisher & Bourque 1995b; Oliet & Bourque 1992; Zhang et al 2007). For isolation of axon terminals, the anterior lobe was separated from the pituitary gland; the intermediate lobe was cut off as much as possible to expose the posterior pituitary. The isolated posterior pituitary was incubated in trypsin solution and rinsed as above. Trituration was performed in a Pipes saline just before plating (Fisher & Bourque 1995a; Fisher et al 2000).

Pituicyte cultures

The pituicyte culture was performed using a slightly modified version of a method from previous studies (Beagley & Hatton 1992; Bicknell 1988). Briefly, adult male Long-Evans rats were anesthetized with halothane and killed by decapitation and the pituitary glands were immediately removed. The neurohypophysis was dissected free from the anterior and intermediate pituitaries in sterile culture medium (Dulbecco's modified Eagle Medium, Sigma, Oakville, ON) under a dissecting microscope. The neurohypophysis was then cut into four pieces and each piece was placed on a glass coverslip coated with collagen (BD, CA) in a 35-mm-diameter plastic Petri dish. The pieces of neurohypophysis were secured in place by covering them with a small piece of a glass cover slip. Cultures were maintained in culture medium for 10-14 days with 10% fetal calf serum (Invitrogen, San Jose, CA), penicillin (100 U/ml, Invitrogen) and streptomycin (100 mg/ml, Invitrogen) in a humidified atmosphere (37°C) containing 95% air and 5% CO_2. After 10-14 days in culture, the pituicytes will grow into a single cell layer with the purity >95% and all the MNC terminals die off and can be washed away.

Hippocampal neuron cultures

Hippocampi were isolated from embryonic day 18 (E18) rat embryos and dissociated by digestion with trypsin (Invitrogen) and DNase I (Sigma). Neurons were plated on glass coverslips coated with poly-L-lysine (Sigma) and cultured in Neurobasal-A

Media (Gibco) supplemented with B-27 (Gibco). Neurons were plated at a density of 50-60 neurons/mm^2. Immunocytochemistry was performed on day 4-7 after plating. For transfection experiments, a glial feeder layer was prepared one week before the hippocampal neurons were plated (Kaech & Banker 2006). Primary cultures of glia were prepared from the cortices of newborn rat pups (postnatal 2 days), and the glial cells were isolated and plated at density of 7.5 x 10^6 per 75 cm^2 flask. Gilal cells were maintained in the glial medium (Kaech & Banker 2006) for 7 days before they formed a thin glial layer. Neurons were co-cultured with ready-to use glial layer and transfected with expression constructs by the Lipofectamine 2000 methods following a commercial protocol from Invitrogen. Hippocampal neurons were fixed and observed 48h after transfection (Kaech & Banker 2006).

PC12 cell cultures

PC12 cells were obtained from American Type Culture Collection (ATCC) and cultured in Ham's F12K medium with 2 mM L-glutamine adjusted to contain 1.5 g/L sodium bicarbonate, 82.5%; horse serum, 15%; fetal bovine serum, 2.5% in a 5% CO2 air humidified atmosphere. For channel targeting research, PC12 cells were treated with NGF 7S (neural growth factor 7S, Invitrogen) at final concentration of 10 ng/ml for two days. When the cells differentiated and had growth cones, DNA transfection was performed.

3.2 RT-PCR and Molecular Cloning

Rats were sacrificed as described above. The brains were immediately removed and various parts dissected for total RNA extraction. RNA from these parts was isolated immediately or stored at –70°C after being frozen in liquid nitrogen. RNA was extracted using Trizole™ reagent (Invitrogen, Life Technologies). RNA was reversely transcribed using SuperScript First-Strand Synthesis System™ for RT-PCR (Invitrogen, Life Technologies).

1) $Ca_V2.1$

Variants with differences in the II-III loop were sought using nested RT-PCR. The sequence of the rat $Ca_V2.1$ II-III loop (accession number NM_012918) was used to design two sets of primers (P1 forward, 5'GGC ATG GTG TTC TCC ATC TA, corresponding to bases numbers 2065-2084 and P2 reverse, 5' GAG CCC TGG CTC TCT TTT CT, corresponding to base numbers 2959-2978) that were then synthesized by the University Core DNA Services, University of Calgary. Initial amplification was carried out by 20 cycles of 95°C for 35 seconds, 60°C for 45 seconds and 72°C for 3 minutes after initial denaturation of 95°C for 3 minutes and then the final elongation of 72°C for 10 minutes using primers P1 and P2 in 25 μl. A two microliter sample of these products was re-amplified with nested primers (P3 forward, 5'ACC CTC TTC GGG AAC TAC AC, corresponding to base numbers 2098-2117 and P4 reverse,

5’CTC CCC ATC ATC GCC TTC, corresponding to base numbers 2878-2895) using 23 cycles of 95°C for 35 seconds, 60°C for 45 seconds and 72°C for 3 minutes after initial denaturation of 3 minutes at 95°C and then a final elongation at 72°C for 10 minutes in 25 μl volume. Reactions were carried out in a solution containing 1.5 mM $MgCl_2$, Taq DNA polymerase 2 Units, 2 pmol each primers 10 μmol dNTP and 1× PCR buffer (Invitrogen, Life Technologies). A negative control without cDNA was run with each reaction. The PCR products were analyzed on 1.5 % agarose gel stained with ethidium bromide. Gels were visualized under UV light and documented with Polaroid film. Primers designed for the housekeeping gene GAPDH (P5 forward, 5’CAT GAC AAC TTT GGC ATC GT, corresponding to base numbers 1336-1355 and P6 reverse 5’ATG TAG GCC ATG AGG TCC AC corresponding to base numbers 1816-1835) were used as a positive control (31 cycle of 95°C for 30 sec, 60°C for 40 sec and 72°C for 1.5 minutes).

2) $Ca_V2.2$

For the first round primers (DFc01-DRc01, 2016-3427 base pair NM92905 rat $Ca_V2.2$, D is the alphabet used for laboratory storage purpose, F means forward, and R means reverse) were used to get template covering the II-III loop. For the second round, primers (DFc02-DRc02, 2072-2433 bp) were used to amplify a small region within II-III loop that cover the portion of synprint site (Dubel et al 1992; Ghasemzadeh et al 1999)

All PCR reagents were purchased from Invitrogen, Life Technologies, unless otherwise stated.

Gel bands were cut and DNA was eluted using Quantum Prep™ Freeze 'N Squeeze DNA gel extraction spin columns (BIO-RAD) and then DNA was precipitated with sodium acetate (pH 5.2) and ethanol. PCR products were cloned into pGEM-T easy vector and sequenced using an automated sequencer (Plant Biotechnology Institute, National Research Council, Saskatoon). For the study of expression of these splice variants in individual MNCs, single-cell RT-PCR was carried out. Healthy cells were picked up by glass micropipettes using a micromanipulator and transferred to lysis buffer (5 μl) containing RNAse inhibitors, random hexamers, RNA guard, $MgCl_2$, dNTP and reverse transcriptase buffer. Reverse transcription was carried out by addition 50 units of SuperScript First-Strand Synthesis System for RT-PCR (Invitrogen, Life Technologies) and incubated at 37°C for one hour (Glasgow et al 1999). The product (1μl) was amplified by 40 cycles.

3.3 Plasmid preparation

1. Plasmids for $Ca_V2.2$ channel targeting experiments. Green fluorescent protein (GFP) fusion constructs were generated on the basis of pEGFPC3 (Clontech, Palo Alto, CA)

vector, GFP-NC3 (2021–2339) of rat $Ca_V2.2$ gene (Gene bank Access Number: M92905). GFP and GFP-NC3 encoding plasmids were gifts from Dr. I. Bezprozvanny at the University of Texas Southwestern Medical Center, Dallas.

2. Plasmids for electrophysiology and imaging experiments of splice variants of $Ca_V2.1$ channels. Full length $Ca_V2.1$ was first subcloned into vector pMT2sx, and fragments covering II-III loop of the two deleted splice variants Δ1 and Δ2 were amplified by PCR and then sub- cloned back to full-length $Ca_V2.1$ constructs at restriction endonuclease sites BmgBI and SgrAI. Plasmids pMT2sx-$Ca_V2.1$, pMT2sx-$Ca_V2.1$Δ1, pMT2sx-$Ca_V2.1$Δ2, pEYFP-C-$Ca_V2.1$, pEYFP-C-$Ca_V2.1$ Δ 1 and pEYFP-C-$Ca_V2.1$Δ2 are all constructed in the laboratory of Dr. G. Zamponi at the Hotchkiss Brain Institute, University of Calgary and confirmed and sequenced by University Core DNA Services, University of Calgary. Plasmids pEGFP- $Ca_V2.1$, pEGFP -$Ca_V2.1$Δ1, pDsRed-$Ca_V2.1$, pDsRed-$Ca_V2.1$Δ1 and pDsRed-$Ca_V2.1$Δ2 were constructed at AgeI, XhoI, and SalI restriction endonuclease sites based on pEYFP-C encoding plasmids and sequenced at the Plant Biotechnology Institute Sequencing Center, National Research Council, Saskatoon, SK.

Maximum preparation of plasmid

Methods were modified from the protocol (Preparation of plasmid DNA by alkaline lysis with SDS: maxipreparation, see appendix I (Sambrook et al 2001).

3.4 Western-blot

All procedures were performed on ice to prevent proteolysis of the Ca^{2+} channel subunits. Whole brains were removed from decapitated adult male Long-Evans rats and 1/2 of the brain was transferred into 4.5 ml of homogenization buffer that contained 50 mM Tris pH 7.4 (Sigma), 0.3 M sucrose, 0.1 M NaCl, 1 tablet of complete mini (Roche), 100 μg/ml benzamidine (Sigma), 1 μg/ml pepstatin (Sigma), 10 μg/ml calpain inhibitor I (Sigma), and 10 μg/ml calpain inhibitor (Sigma), the tissues were homogenized three for 30 second each, centrifuged for 15 min at 17,000 rpm, and the supernatant was collected for Western-blot analysis. For cultured pituicytes, the cells were harvested on day 10-14 of culturing, rinsed by ice-cold PBS briefly, and collected with a plastic cell scraper in 1 ml of lysis buffer (homogenization buffer with 1% Triton X-100 and 0.5M NaCl). The solution was centrifuged at 10,000 g for 10 min at 4°C. The supernatant was removed and kept on ice or frozen until loading on the gel. After separation by sodium dodecyl sulfate–polyacrylamide gel electrophoresis (SDS-PAGE), proteins were transferred from the gels to nitrocellulose membranes (Amersham Biosciences). The membranes were then blocked by 5% nonfat milk in PBST for 1 h, followed by overnight incubation of different antibodies against α1 subunits of Ca^{2+} channels as described previously at 4°C in the blocking solution (dilutions were made according to the recommendations of the manufacturer). Horseradish peroxidase-coupled secondary

antibodies and ECL™ Western blotting reagents (Amersham Biosciences) were used according to the manufacturer's protocol.

3.5 Immunohistochemistry and Immunocytochemistry

Immunohistochemistry

All procedures used in these experiments were in accordance with the guidelines of the University of Saskatchewan Animal Care Committee. Adult male Long-Evans rats were anesthetized with a ketamine (125 mg/kg) and xylazine (7 mg/kg) mixture and intra- cardially perfused with ice-cold PBS, followed by cold, freshly prepared 4% paraformaldehyde (PFA) in PBS (pH 7.4). The rats were decapitated and the brains removed. Brains and pituitary glands were taken out immediately and transferred into 4% PFA for postfixation overnight, then moved into 30% sucrose solution for cryoprotection. Samples were stored at 4°C until sectioning. The tissues were frozen on dry ice, and sectioned at 30 μm on a sliding microtome. The sections were incubated with 4% donkey serum and 0.3% Triton X-100 in 0.1M PBS, and then incubated with primary antibody overnight at 4 °C with constant rotation. The following antibodies were used: mouse anti-S100β (1:1,000, Sigma, Oakville, ON), rabbit anti-$Ca_V2.1$ (1:1,000, Alomone Labs, Israel), $Ca_V2.2$ (1:1,000, Alomone Labs), $Ca_V1.2$ (1:1,000, Alomone Labs), $Ca_V1.3$ (1:1,000, Alomone Labs), $Ca_V2.3$ (1:1,500 Alomone Labs), $Ca_V3.1$ (1:1,500 Alomone Labs), rabbit anti-synapsin I (1:1,500,

Millipore), goat anti-neurophysin I (1:1500, Santa Cruz, CA), and goat anti-neurophysin II (1:1500 Santa Cruz, CA); rabbit anti-oxytocin (1:500 Genway, CA), rabbit anti-neurophysin II (1:1000 Novus Biologicals); mouse anti-synaptophysin (1:1000 Sigma), rabbit anti-α-MSH (Melanocyte Stimulating Hormone, 1:500 Sigma). After incubation of primary antibodies, sections were washed 3 times with PBS and incubated with secondary antibody for 2h. The secondary antibodies used were: Alexa Fluor 555 donkey anti-rabbit IgG (1:500 Invitrogen), Alexa Fluor 488 donkey anti-mouse IgG (1:500; Invitrogen), and Alexa Fluor 555 donkey anti-goat IgG (1:500; Invitrogen). After washing sections by PBS 3 times, the samples were then air dried for 1 h at 37°C, dipped in xylene, and mounted on a microscope slide with Citifluor (Marivac, Lakefield QC) before confocal microscopy. Two types of negative control experiments were carried out for each of the Ca^{2+} channel antibodies. When the primary antibody was not added, or when the primary antibody was pre-incubated with the peptide antigen (supplied by the manufacturer).

Immunocytochemistry

General immunocytochemical methods were used for different types of cultured or acutely isolated cells except specifically described otherwise.

For isolated MNCs and hippocampal neurons, a goat polyclonal antibody directed against the carboxy-terminus of human $Ca_V2.1$ (Santa Cruz) and a rabbit polyclonal antibody directed against peptide residues 865-881 in rat $Ca_V2.1$ II-III loop (Alomone Labs) were used for immunofluorescence experiments on cultured cells. Cells were fixed in 4% paraformaldehyde (PFA, Sigma) and permeabilized and blocked for 1h with digitonin 100µg/mL, bovine serum albumin 4%, normal donkey serum 4%, and sodium azide 0.02% in PBS. Primary antibodies (range from 1:50 to 1:400) were incubated overnight at 4°C, followed by incubation for 1h with secondary antibodies Alexa Fluor 488 donkey anti-goat (1:400, Molecular Probes) or Alexa Fluor 555 donkey anti-rabbit goat (1:200, Molecular Probes). Immunofluorescence was visualized using a Zeiss Axiovert 200 microscope with a 40× objective and appropriate filter sets and images were captured using a cooled CCD camera.

Pituicytes were fixed in 4% PFA for 15 min at 4°C. The coverslips were then washed 5 times with cold PBS for 5 min and incubated for 30 min at room temperature in a fresh solution of PBS containing 10% normal donkey serum (Jackson ImmunoResearch). Cultures were incubated overnight at 4°C in antibodies diluted in a solution containing 1% BSA (Sigma), 0.05% sodium azide (Sigma) and 0.04% sodium EDTA (Sigma) in PBS. Pituicytes were co-labeled with an antibody directed against S100β (1:1,000, Sigma), and one of the following Ca^{2+} channel antibodies (all of which are from Alomone Labs, Israel): anti-$Ca_V2.1$ (1:400), $Ca_V2.2$ (1:400), $Ca_V1.2$

(1:400), $Ca_V1.3$ (1:400), $Ca_V2.3$ (1:400), and $Ca_V3.1$ (1:1000). The next day, cultured pituicytes were rinsed three times in cold PBS for 5 min and transferred in fresh PBS containing Alexa Fluor 555 donkey anti-rabbit IgG (1:200, Invitrogen) and Alexa Fluor 488 donkey anti-mouse IgG (1:200, Invitrogen) and incubated for 1h at room temperature. Cells were washed again 3 times with cold PBS for 5 min each time and mounted with mounting solution. Samples were observed under fluorescent microscopy with appropriate filters.

3.6 Epifluorescent and Confocal Microscopy

Acutely isolated cells and cultured cells were examined with an epifluorescent microscope after immunostaining. Immunofluorescence was visualized using a Zeiss Axiovert 200 microscope with a 40× objective and appropriate filter sets and images were captured using a cooled CCD camera. Immunofluorescence of fixed brain slices were observed with a Zeiss LSM 700 confocal microscope using a 20x objective and appropriate filters (in Dr. F. Cayabyab's lab). The confocal imaging results presented here are the representative of three independent experiments performed on twenty different rats. The quantitative measurements of samples between treatment and control groups in one specific experiment were performed using the same fluorescent or confocal settings.

3.7 Statistics

Intensity analysis for immunohistochemistry

For the study of VGCCs expression in MNC somata, brain slices containing most of the SON area were chosen from 10-12 rats. For the study of VGCC expression in pituicytes, the pituitary slices containing most of the neurohypophysial area were chosen. The intensity of immunoreactivity to the indicated calcium channel antibodies and S100β were measured as follows: images stained with S100β (usually green) showing the location of pituicytes were converted to binary images in which each pixel valued either “0” or “1” representing background or pituicyte respectively. Images showing indicated calcium channels (red) were obtained at same standardized confocal settings that distinguished control slices from positive staining. Red images were converted into 8-bit monochromatic images and overlaid with binary ones as described previously. New overlaid images will only show immunoreactivity of indicated calcium channels on pituicytes after each pixel multiplied from corresponding images. Fluorescent intensity was quantified in matched ROIs (region of interest) for each overlaid image. Three measurements from each slice were averaged and analyzed using imageJ (NIH). Values were presented as mean ± SEM and were compared using the Student’s t test, with $p<0.05$ being deemed as indicating a significant difference.

Intensity analysis for immunocytochemistry

For the fluorescence of channels in PC12 growth cones, fluorescent intensity was quantified in regions of interest (ROIs) within the terminals of the growth cones. A ROI with about 1 μm^2 was used to measure the intensity within this area. Three measurements from each growth cone were averaged and analyzed. Values were presented as mean ± SEM and were compared using the Student's t test, with $p<0.05$ being deemed as indication of a significant difference.

DNA gel analysis

PCR products were semi-quantified by using the ratio of $Ca_V2.1$ channel product: GAPDH. Two sets of independent RT-PCR were performed to amplify housekeeping gene GAPDH and a portion of the II-III loop of $Ca_V2.1$ channels in different brain and peripheral tissues. The DNA gel was imaged using a KODAK GEL LOGIC 200 imaging system and the intensities of DNA bands were measured by Image J software (NIH).

Colocalization analysis

The standard test for the colocalization of two proteins by immunocytochemistry generally involve tagging the first, protein A, one colour (usually green), and the second, protein B, a different and contrasting colour (usually red). Each colour is imaged separately, and proteins are deemed to be colocalized in areas stained with the

combined colour when the two images are overlaid (in this case, red plus green = yellow). Image J software was used to analyze the percentage of yellow colour within matched ROIs. If the ratio >50% then the colocalization analysis was considered as positive, in other words, the two proteins I am interested in are colocalized. For distribution analysis, if the yellow area is under 10% of the ROI, then the result will be considered as not colocalized.

4. RESULTS

4.1 Expression and distribution of VGCCs on pituicytes

4.1.1 $Ca_V2.2$ and $Ca_V2.3$ channels are expressed on pituicytes of the NH

4.1.1.1 Identification of pituicytes

I labeled pituicytes in slices of the pituitary gland using antibodies directed against the astrocytic marker S100 β, which has been shown to label these cells (Cocchia & Miani 1980; Fujiwara et al 2002). Figure 4.1A shows immunoreactivity to S100 β in a pituitary slice. There is much stronger fluorescence in the neurohypophysis (NH) than that in the adenohypophysis (AH) or the intermediate lobe (IL). There was however a clear band of immunoreactivity between the intermediate lobe and the anterior pituitary (Figure 4.1A S100β) that corresponds to the S100 β-positive cells in the marginal cell layer of the hypophysial cleft (Cocchia & Miani 1980; Fujiwara et al 2002). To ensure that the antibody to S100β was not labeling neuronal elements I also stained with an antibody directed towards the synaptic vesicle associated protein synapsin I (Navone et al 1984). There was intense immunoreactivity to synapsin I in the neurohypophysis (Figure 4.1A Synapsin I), which is consistent with the high density of synaptic terminals, and less so in the adenohypophysis and the intermediate lobe. Control experiments were performed without adding the primary antibodies for S100β and synapsin I, and there was no immunostaining detected at the same

microscope settings (Figure 4.1B). Table 4-1 describes the antibody labeling I used for identifying different components within NH. The immunostaining for GFAP in pituicytes was not observed in pituitary slices, but immunostaining of GFAP in cultured pituicytes was positive. The immunofluorescence of S100β was consistently stronger than that of GFAP for cultured pituicytes, which suggests that S100β is a better glial marker for labeling the pituicytes.

Table 4-1 Immunohistochemistry in the neurohypophysis (single labeling of MNC nerve terminals, synaptic inputs and S100β positive pituicytes).

(This table is shown to demonstrate how I identified different components within the neurohypophysis using different markers)

Target	Marker	Fluorescence	Staining
OT-MNCs	Neurophysin I	Alexa Fluor 488	Posterior ++, Intermediary -, Anterior lobe -
OT- and VP-MNCs	Neurophysin I &II	Alexa Fluor 488	Posterior ++, Intermediary-, Anterior lobe -
Glia-like cells	S100β	Alexa Fluor 488	Posterior ++, Intermediary ++, Anterior lobe++
Glia-like cells	GFAP (Glial fibrillary acidic protein)	Alexa Fluor 488	Posterior –, Intermediary +
Synaptic inputs	Synapsin I	Alexa Fluor 555	Posterior +++, Intermediary + Anterior lobe -
Synaptic inputs	Synaptophysin	Alexa Fluor 488	Posterior +++ , Intermediary + Anterior lobe -

+++ strong immunofluorescence (>10 marker positive spots/400 μm^2) ; ++ moderate immunofuorescence (range from 3-10 marker positive spots/400 μm^2); + weak

immunofluorescence (range from 1-3 marker positive spots/400 μm^2); - no immunofluorescence (0 marker positive spots/in any area of 400 μm^2).

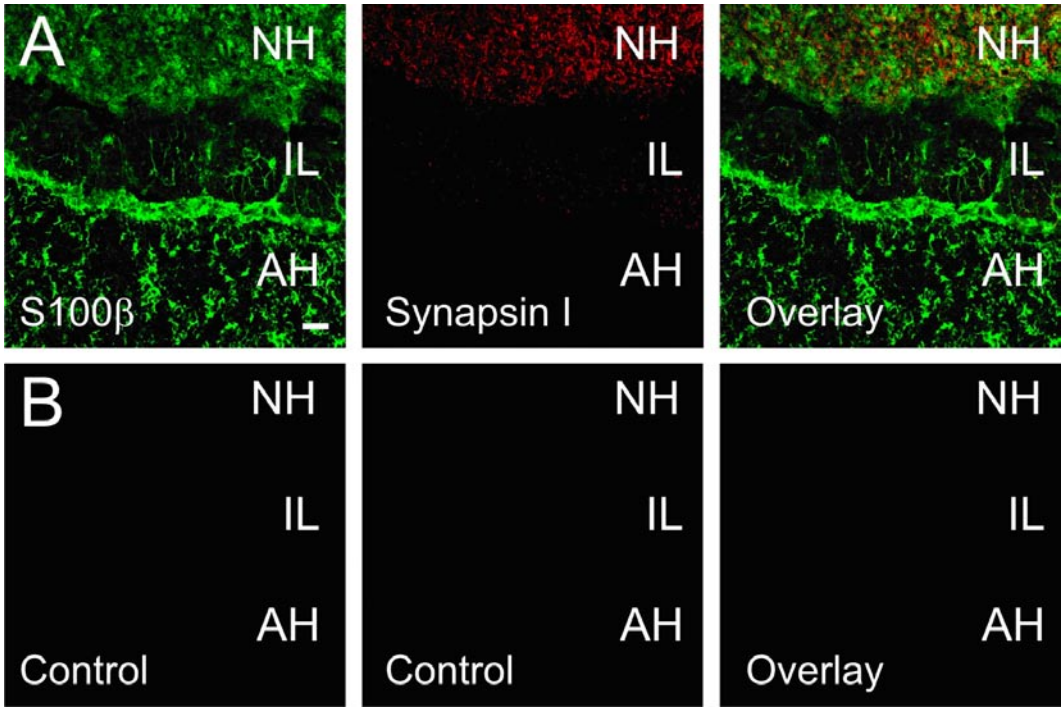

Figure 4.1 Distribution of immunoreactivity to S100 β and synapsin I in the pituitary gland. The panels show confocal fluorescent images of slices of rat pituitary glands. The labels show the location of the neurohypophysis (NH), the adenohypophysis (AH), and the intermediate lobe (IL). A. The image on the left shows immunoreactivity to S100β, the image in the center shows immunoreactivity to synapsin I, and the image on the right shows the overlay of the two images. B. These images show the negative controls for the images in part A, in which slices were incubated with the secondary but not the primary antibodies. Scale bars =40 μm.

4.1.1.2 Identification of different subcellular components in the NH

To better define the cellular elements of the neurohypophysis, I compared the

immunoreactivity to S100 β and synapsin I to that of the neurophysins, which are carrier proteins for VP and OT that are expressed only in the MNCs. Neurophysin I is selectively expressed in oxytocin-releasing MNCs and neurophysin II is selectively expressed in vasopressin-releasing MNCs. The combination of antibodies to the two neurophysins should therefore stain all of the MNC terminals, but not the pituicytes or synaptic terminals. The double staining studies illustrated in Figure 4.2 show that there is no colocalization between S100 β immunoreactivity and that of either neurophysins (Figure 4.2A) or synapsin I (Figure 4.2B). A comparison of immunoreactivity to synapsin I and the neurophysins shows some overlap (Figure 4.2C), which is consistent with the observation that some MNC terminals do express small vesicles containing synapsin I (Navone et al 1986). There are also many small objects that appear to be positive for synapsin I but not the neurophysins, which likely correspond to synaptic terminals abutting onto either MNC terminals or pituicytes. Table 4-2 describes the colocalization analysis results for combinations of antibodies that recognized different components within the NH. These studies confirm that I can use immunoreactivity to S100 β to selectively label pituicytes in the neurohypophysis.

Table 4-2 Immunohistochemistry in the neurohypophysis (double staining of the combinations among MNC terminals, synaptic inputs and pituicytes).

Target	Marker	Fluorescence	Colocalization
MNC terminals and synaptic inputs	Neurophysin I & II and Synapsin I	Alexa Fluor 488 Alexa Fluor 555	<50%
MNC terminals and synaptic inputs	Neurophysin I & II and Synaptophysin	Alexa Fluor 555 Alexa Fluor 488	<50%
MNC terminals and pituicytes	Neurophysin I & II and S100β	Alexa Fluor 555 Alexa Fluor 488	<10%
Synaptic inputs and pituicytes	S100β and Synapsin I	Alexa Fluor 488 Alexa Fluor 555	<10%

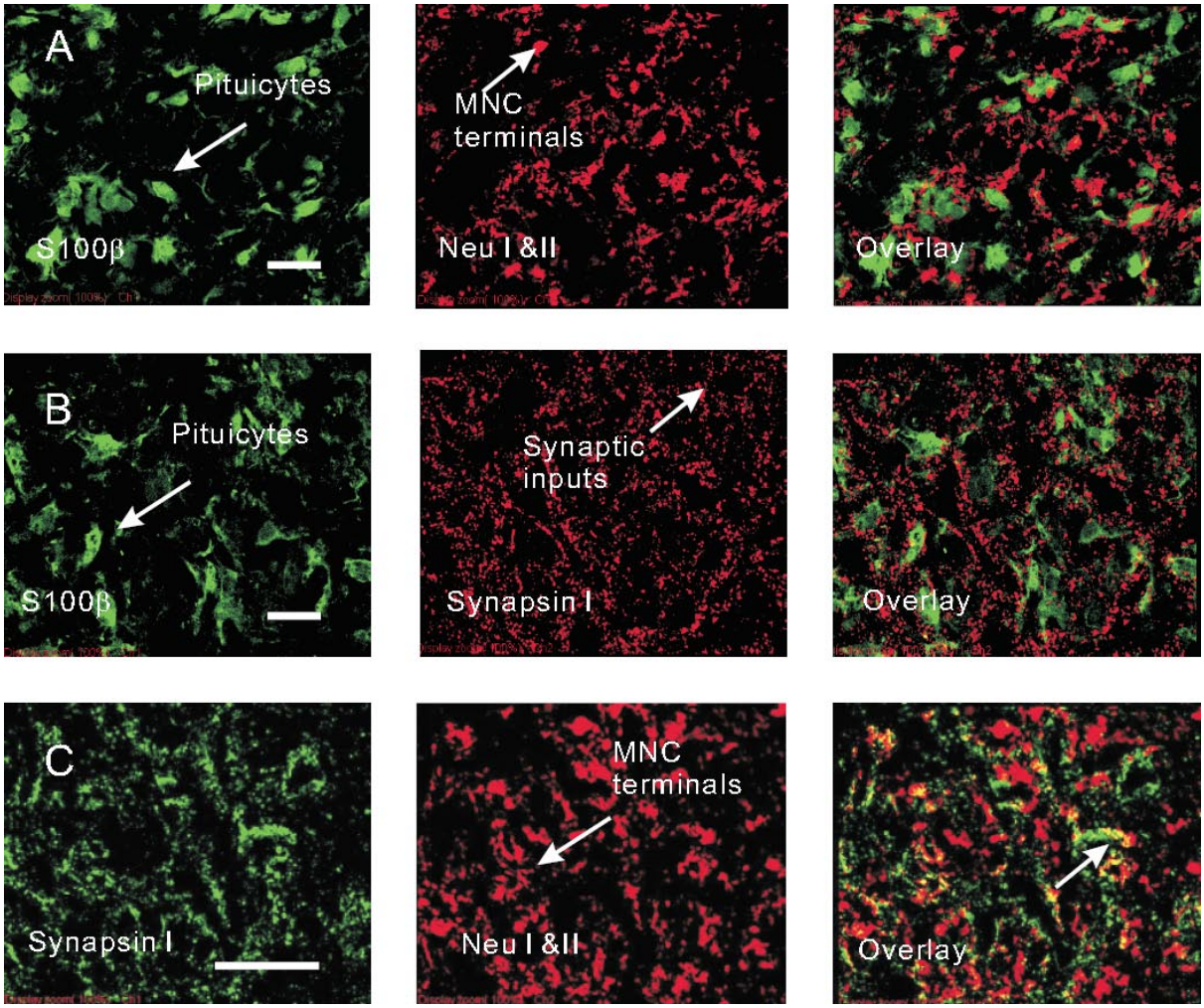

Figure 4.2 Distribution of immunoreactivity to S100 β, the neurophysins, and synapsin I in the neurohypophysis. The panels show confocal fluorescent images of slices of rat pituitary glands. A. The image on the left shows immunoreactivity to S100 β, the image in the center shows immunoreactivity to the neurophysins (i.e. a combination of neurophysin I and neurophysin II), and the image on the right shows the overlay of the two images. B. The image on the left shows immunoreactivity to S100 β, the image in the center shows immunoreactivity to synapsin I, and the image on the right shows the overlay of the two images. C. The image on the left shows immunoreactivity to the synapsin I, the image in the center shows immunoreactivity to neurophysin I and II, and the image on the right shows the overlay of the two images. Scale bars =20 μm.

4.1.1.3 Identifying VGCCs on the pituicytes

I therefore undertook studies to co-label neurohypophysial slices with S100β and antibodies directed against a variety of Ca^{2+} channel α1 subunits. Figure 4.3 shows the immunostaining results obtained from a set of rabbit polyclonal antibodies directed against the α1 subunits of different VGCCs (Alomone Labs). Immunoreactivity in neurohypophysial slices was detected for $Ca_V2.1$ (Figure 4.3A), $Ca_V2.2$ (Figure 4.3B), $Ca_V1.2$ (Figure 4.3C), $Ca_V2.3$ (Figure 4.3E), and $Ca_V3.1$ (Figure 4.3F), but not for $Ca_V1.3$ (Figure 4.3D, despite the identification of staining for $Ca_V1.3$ in the AH). The double staining experiments show clear colocalization with S100β immunoreactivity for two types of Ca^{2+} channel α1 subunits, $Ca_V2.2$ and $Ca_V2.3$. Table 4-3 describes the details of each double staining for detecting the colocalization of pituicytes marker and VGCC marker. To further comfirm the colocalization results, I used another set of goat polyclonal antibodies directed against each VGCC subtype I am interested in. The Table 4-4 demonstrates colocalization results showing both the $Ca_V2.2$ and $Ca_V2.3$ markers are overlaid with pituicytes, whereas $Ca_V1.3$ and $Ca_V2.1$ are not (the immunostaining obtained from the goat polyclonal antibodies are similar to that from the rabbit polyconal antibodies, images are thus not shown here). These two groups of results confirm that only the $Ca_V2.2$ and $Ca_V2.3$ antibodies are colocalized with S100β, respectively. These results support the hypothesis that pituicytes in the NH express the $Ca_V2.2$ and $Ca_V2.3$ Ca^{2+} channels.

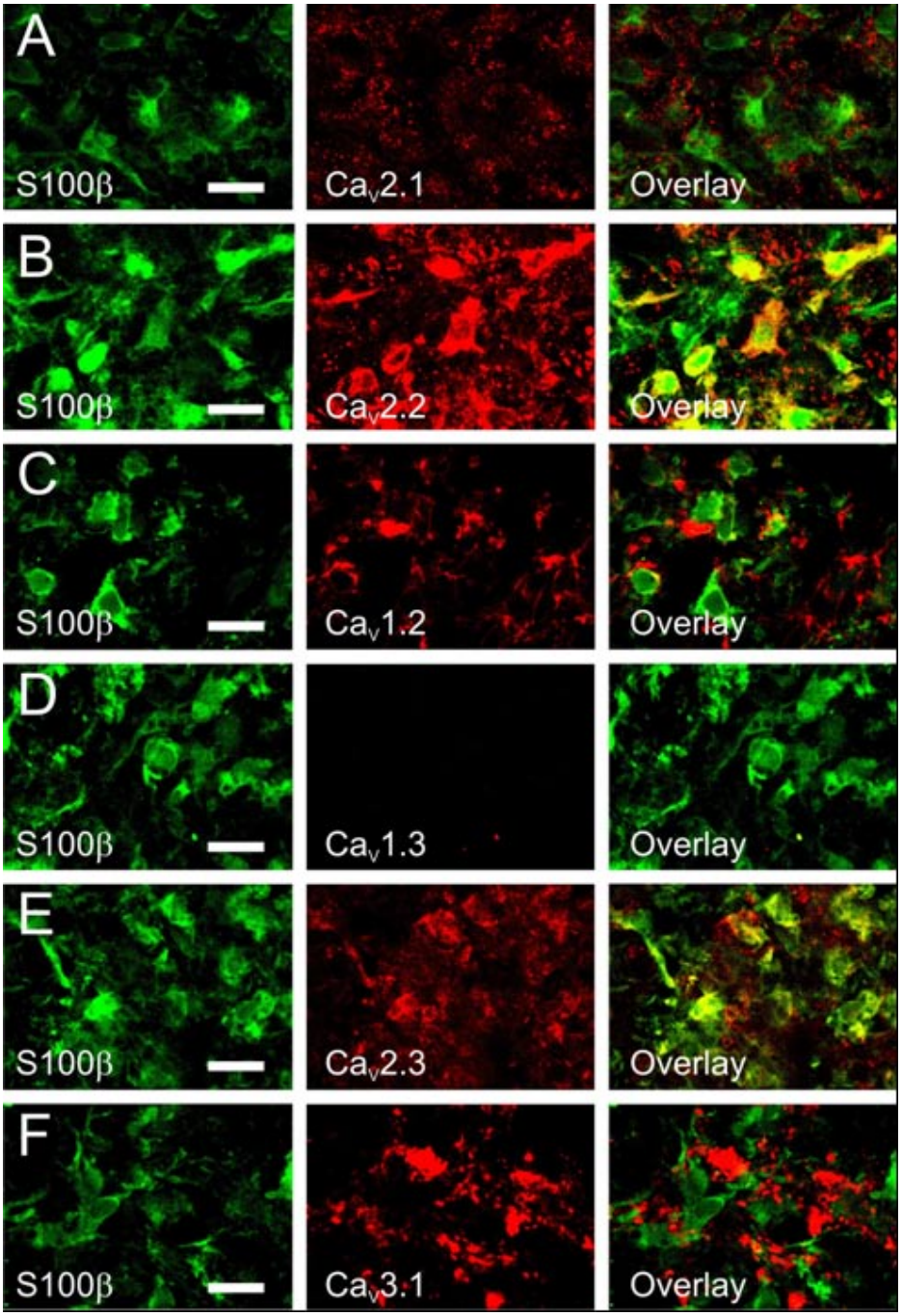

Figure 4.3 Distribution of immunoreactivity to Ca^{2+} channels in the NH. The panels show confocal fluorescent images of slices of rat pituitary glands. A-F show the results of double staining of the pituitary marker, S100β, and different Ca^{2+} channels antibodies in the rat NH. The images on the left show immunoreactivity to S100β, the images in the center show immunoreactivity to the indicated Ca^{2+} channel type, and the images on the right show the overlay of the two images. Double staining

of S100β and $Ca_V2.1$ (A), Double staining of S100β and $Ca_V2.2$ (B), Double staining of S100β and $Ca_V1.2$ (C), Double staining of S100β and $Ca_V1.3$ (D), Double staining of S100β and $Ca_V2.3$ (E), and Double staining of S100β and $Ca_V3.1$ (F). Scale bars =20 μm.

Table 4-3 Immunohistochemistry in the neurohypophysis. Double staining of VGCC α1 subunits and pituicytes by rabbit polyclonal α1 subunit antibodies (Alomones laboratories) and S100β.

Target	**Marker**	**Fluorescence**	**Colocalization**
pituicytes and $Ca_V2.1$ α1 subunit	S100β and $Ca_V2.1$ antibodies	Alexa Fluor 488 Alexa Fluor 555	<10% (the staining pattern of $Ca_V2.1$ is dot-like)
pituicytes and $Ca_V2.2$ α1 subunit	S100β and $Ca_V2.2$ antibodies	Alexa Fluor 488 Alexa Fluor 555	>90% ($Ca_V2.2$ antibody strongly stains in the NH and colocalized with pituicytes in the NH)
pituicytes and $Ca_V1.2$ α1 subunit	S100β and $Ca_V1.2$ antibodies	Alexa Fluor 488 Alexa Fluor 555	<50% (the staining pattern of $Ca_V1.2$ antibody is along the periphery of pituicytes, which may represents the L-type channels expressed in basal lamina)
pituicytes and $Ca_V1.3$ α1 subunit	S100β and $Ca_V1.3$ antibodies	Alexa Fluor 488 Alexa Fluor 555	No significant positive staining has been found for $Ca_V1.3$

pituicytes and $Ca_V2.3$ α1 subunit	S100β and $Ca_V2.3$ antibodies	Alexa Fluor 488 Alexa Fluor 555	>90% (Clear colocalization has been found between α 1E and pituicytes)
pituicytes and $Ca_V3.1$ α1 subunit	S100β and $Ca_V3.1$ antibodies	Alexa Fluor 488 Alexa Fluor 555	<10% (Not colocalized)

Table 4-4 Immunohistochemistry in the neurohypophysis
Double staining of VGCC α1 subunits and pituicytes by goat polyclonal α1 subunit antibodies (Santa Cruz Biotechnology) and S100β.

Target	**Marker**	**Fluorescence**	**Colocalization**
pituicytes and $Ca_V2.1$	S100β and $Ca_V2.1$ antibodies (Santa Cruz)	Alexa Fluor 488 Alexa Fluor 555	<10%
pituicytes and $Ca_V2.2$	S100β and $Ca_V2.2$ antibodies (Santa Cruz)	Alexa Fluor 488 Alexa Fluor 555	>90% ($Ca_V2.2$ subunits is colocalized with pituicytes
pituicytes and $Ca_V1.3$	S100β and $Ca_V1.3$ antibodies (Santa Cruz)	Alexa Fluor 488 Alexa Fluor 555	<10% (no immunofluorescence)
pituicytes and $Ca_V2.3$	S100β and $Ca_V2.3$ antibodies (Santa Cruz)	Alexa Fluor 488 Alexa Fluor 555	>90% (α 1E subunit is colocalized with pituicytes)

4.1.2 The $Ca_V1.2$ channels can be selectively up-regulated in the pituicytes after dehydration.

Glia-neuron interactions in the hypothalamo-neurohypophsial system play an important role during dehydration. The interactions constitute a physiologically controlled system that intervenes in the regulation of several vital neuroendocrine processes such as hormone release during dehydration or lactation (Burbach et al 2001; Theodosis et al 2008). The regulation of L-type Ca^{2+} channels are involved in adaptation of both neurons and astrocytes (Deisseroth et al 2003; Westenbroek et al 1998a), I therefore tested whether L-type Ca^{2+} channel expression changes in the NH during dehydration. Neurohypophysial slices from rats that had been deprived of water for 24 hours were compared with those obtained from normally hydrated rats. There was a significantly increase in the immunoreactivity to $Ca_V1.2$ on the pituicytes of dehydrated rats comparing to that of control rats, indicating a specific up-regulation of $Ca_V1.2$ L-type Ca^{2+} channels. Figure 4.4A-C show immunostaining of $Ca_V1.2$ channels in the NH of normal rats, and the $Ca_V1.2$ fluorescence was along the periphery of the pituicytes. Figure 4.4D-F show the results of staining in representative slices obtained from dehydrated rats. The $Ca_V1.2$ expression was found relatively low on pituicytes from control rats as indicated by the staining of S100β (see overlaid images in Figure 4.4G-I), whereas the $Ca_V1.2$ expression on the S100β positive components was increased in the NH of the dehydrated rats (Figure 4.4 J-L).

Quantification of the staining in the slices is shown in the bar graph in Figure 4.5. There was a significant increase in the mean immunofluorescence for $Ca_V1.2$ in the pituicytes from water deprived rats (>50% increase when the immunofluorescence was normalized, 12.17 ±1.79 normal *vs* 16.8 ± 1.2 dehydrated, n=15). Negative control experiments were performed using a pre-absorption approach (primary antibodies were pre-incubated with specific antigens provided by manufacturer; Figure 4.6D and 4.6H) and using omission of antibodies (Figure 4.6C and 4.6G). There was no significant immunostaining found in the negative control slices. Figure 4.6A, B, E, and F show the location of pituicytes on the same slices with Figure 4.6C, D, G, and H, respectively.

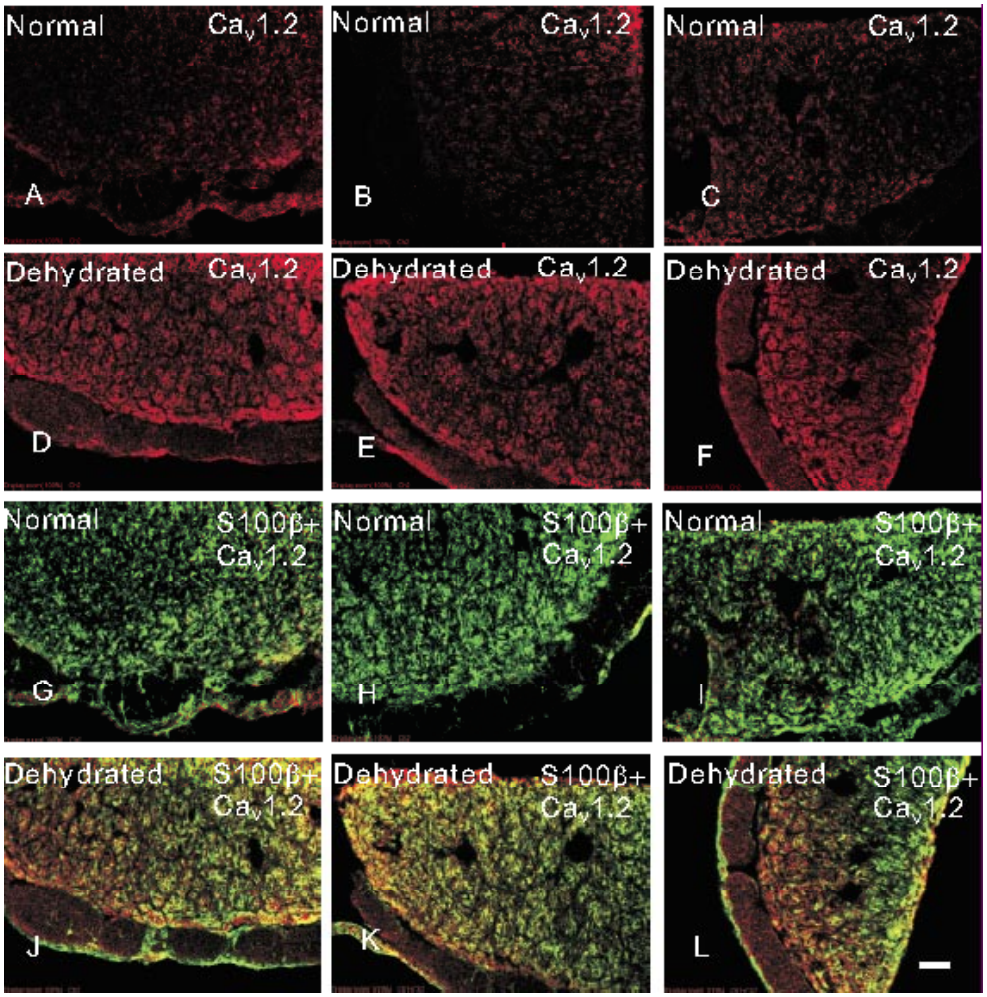

Figure 4.4 Increased expression of $Ca_V1.2$ in the pituicytes after 24h dehydration. A-C) Representative images show immunofluorescence of $Ca_V1.2$ in slices of the normal rats; D-F) Representative images show immunofluorescence of $Ca_V1.2$ in slices of the dehydrated rats; G-I) Representative overlaid images show double staining of $Ca_V1.2$ and S100β in the slices from normal rats; J-L) Representative overlaid images show double staining of $Ca_V1.2$ and S100β in the slices from dehydrated rats. Scale bar =40 μm.

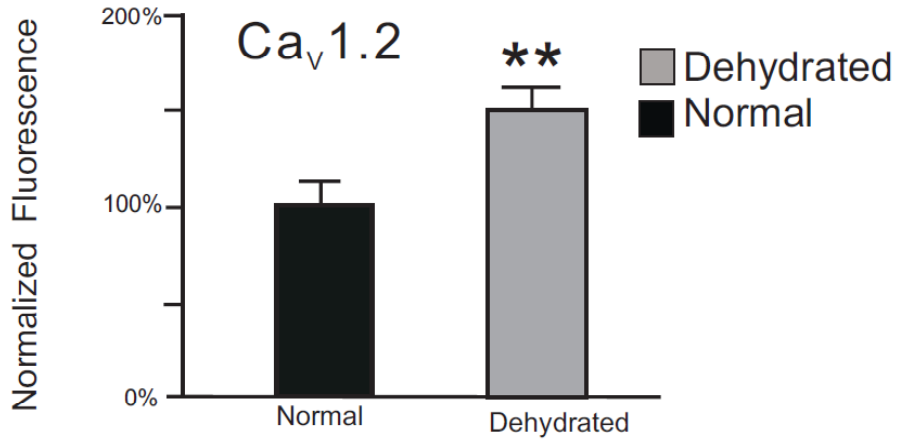

Figure 4.5 Quantitative measurement of immunofluorescence of the $Ca_V1.2$ channels in the pituicytes of control and dehydrated rats.

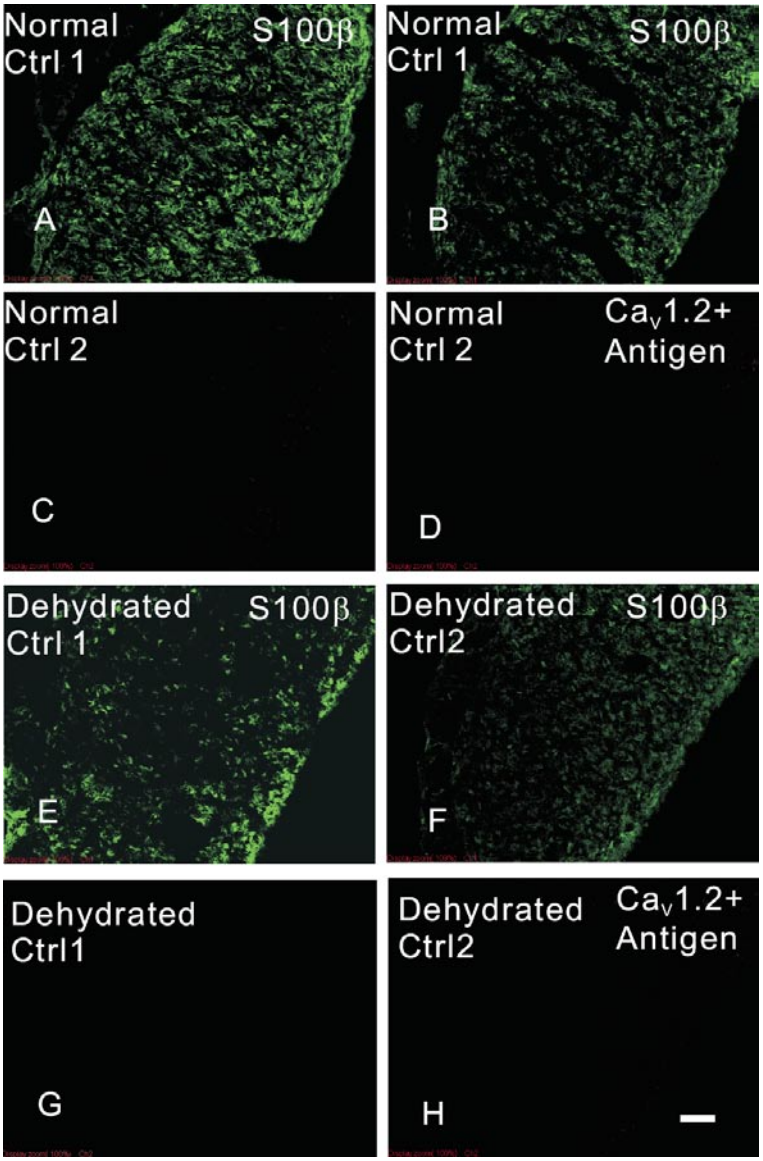

Figure 4.6 Negative control of immunostaining of the $Ca_V1.2$ antibody. A) and B) Representative FITC images of S100β immunostaining in the slices from normal rats. C) Representative CY3 image of control 1 showing immunostaining in the slices from normal rats without adding primary anti-$Ca_V1.2$ antibody. D) Representative CY3 image of control 2 showing immunostaining in the slices from normal rats with the pre-absorption approach. E) and F) Representative FITC images of S100β immunostaining in the slices from dehydrated rats. G) Representative CY3 image of control 1 showing immunostaining in the slices from dehydrated rats without adding primary anti-$Ca_V1.2$ antibody. H) Representative CY3 image of control 2 showing

immunostaining in the slices from dehydrated rats with the pre-absorption approach. Scale bar =40μm.

I also compared immunofluorescence of several different subtypes of Ca^{2+} channels on pituicytes from both normal and dehydrated rats including $Ca_V1.3$, $Ca_V2.2$ and $Ca_V2.3$ using the similar methods, and I found that there was no significant increase of $Ca_V1.3$ channels during dehydration (Figure 4.7 and Figure 4.8). For $Ca_V2.3$ channels, although the basal expression level of channels was very strong (Figure 4.3), there were no significant changes that could be observed during dehydration (Figure 4.9 and Figure 4.10 42.12 ±1.68 normal *vs* 47.72 ± 5.18 dehydrated, n=15). The expression of $Ca_V2.2$ channels, which had strong basal expression in the pituicytes of normal rats, was unchanged after 24 hours dehydration (Figure 4.11 and 4.12, 100 ± 12.43 *vs* 97.83 ± 11.43, n=15).

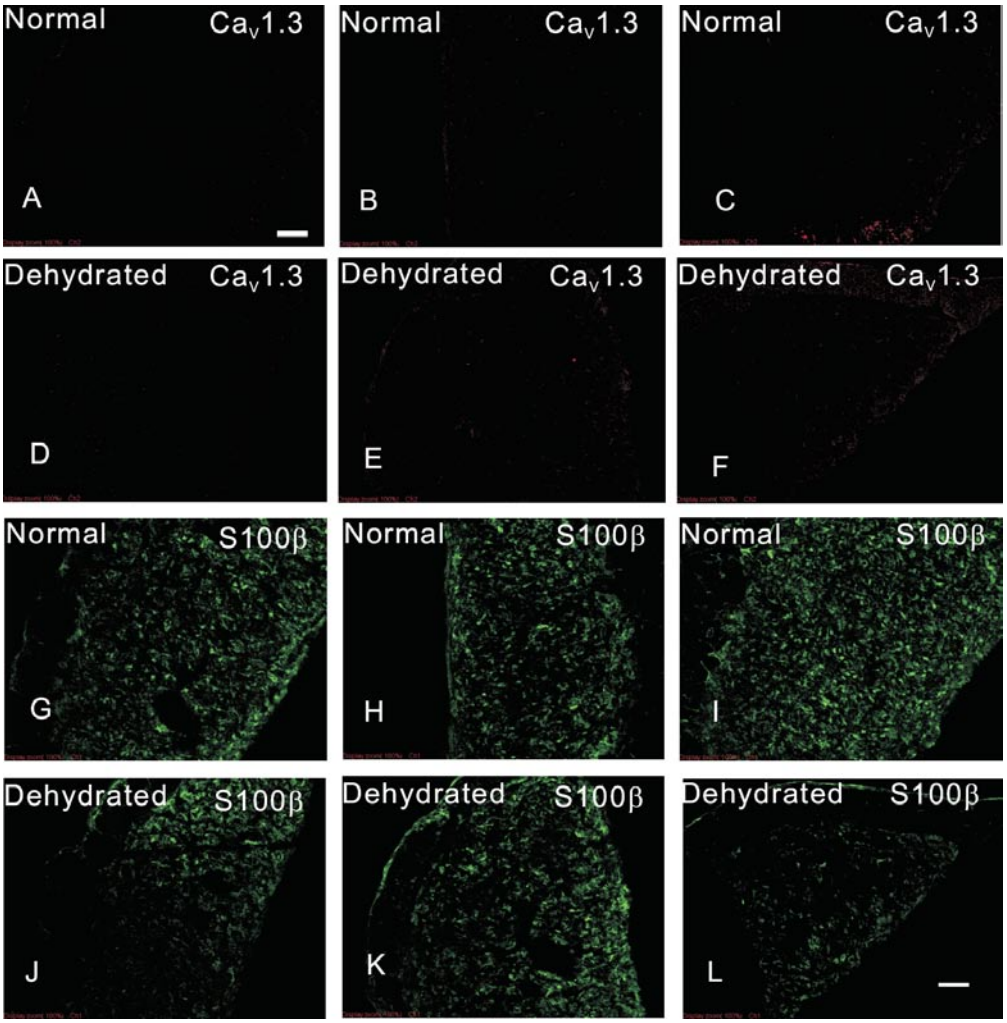

Figure 4.7 Expression level of the $Ca_V1.3$ channels in the pituicytes was unchanged during dehydration in comparison with normal condition. A-C) Representative images show immunofluorescence of $Ca_V1.3$ in slices of the normal rats. D-F) Representative images show immunofluorescence of $Ca_V1.3$ in slices of the dehydrated rats. G-I) Representative overlaid images show double staining of $Ca_V1.3$ and S100β in the slices from normal rats. J-L) representative overlaid images show double staining of $Ca_V1.3$ and S100β in the slices from dehydrated rats. Scale bar =40 μm.

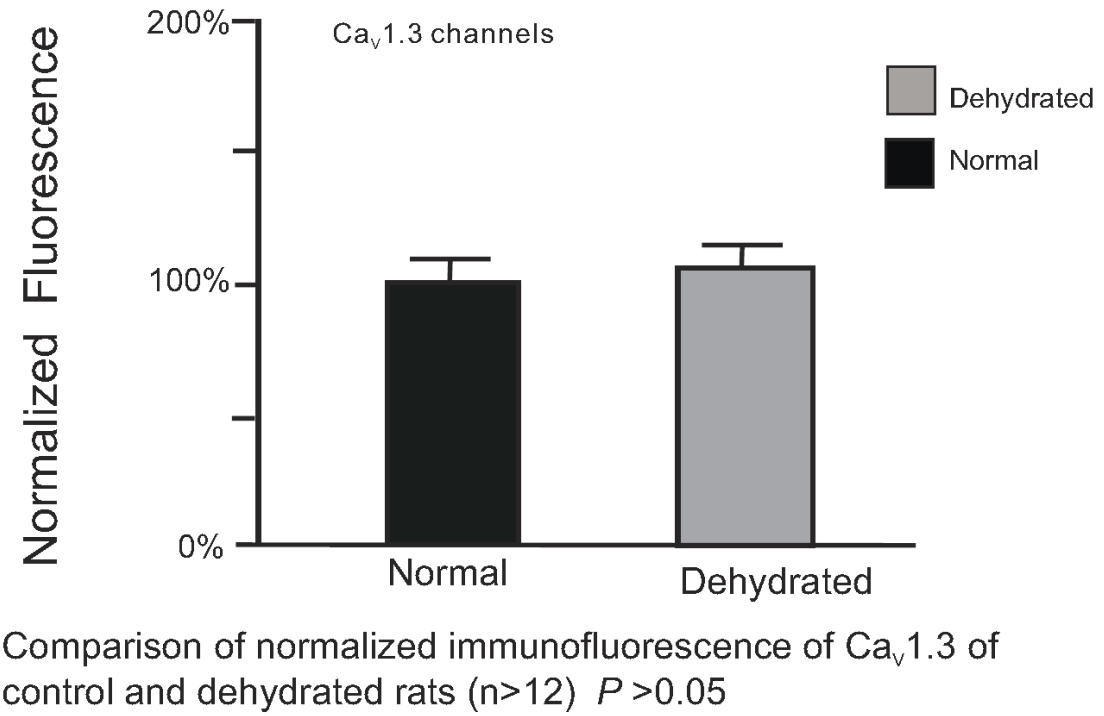

Figure 4.8 Normalized immunofluorescence of $Ca_V1.3$ channels in the pituicytes of control and dehydrated rats.

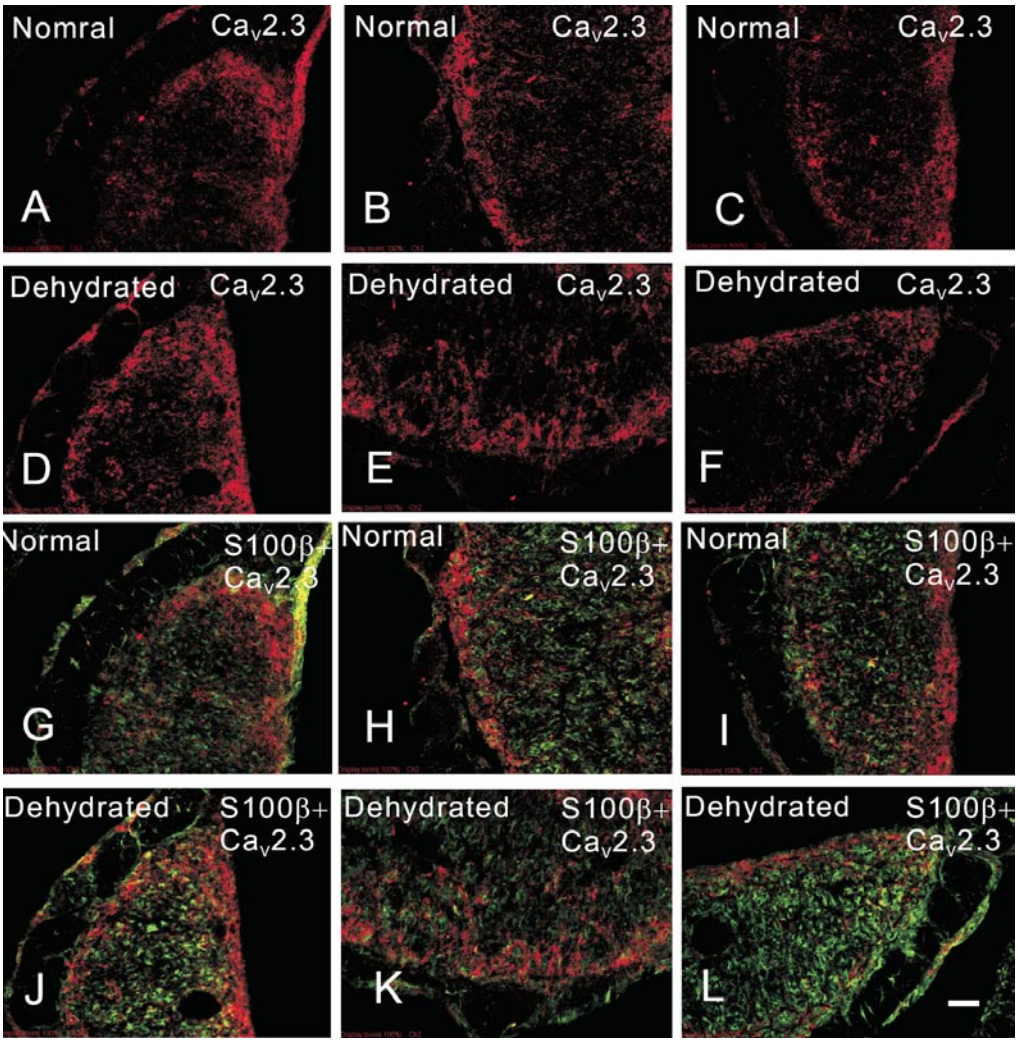

Figure 4.9 Expression level of $Ca_V2.3$ in the pituicytes was unchanged during dehydration in comparison with normal condition. A-C) Representative images show immunofluorescence of $Ca_V2.3$ in slices of the normal rats. D-F) Representative images show immunofluorescence of $Ca_V2.3$ in slices of the dehydrated rats. G-I) Representative overlaid images show double staining of $Ca_V2.3$ and S100β in the slices from normal rats. J-L) Representative overlaid images show double staining of $Ca_V2.3$ and S100β in the slices from dehydrated rats. Scale bar =40 μm.

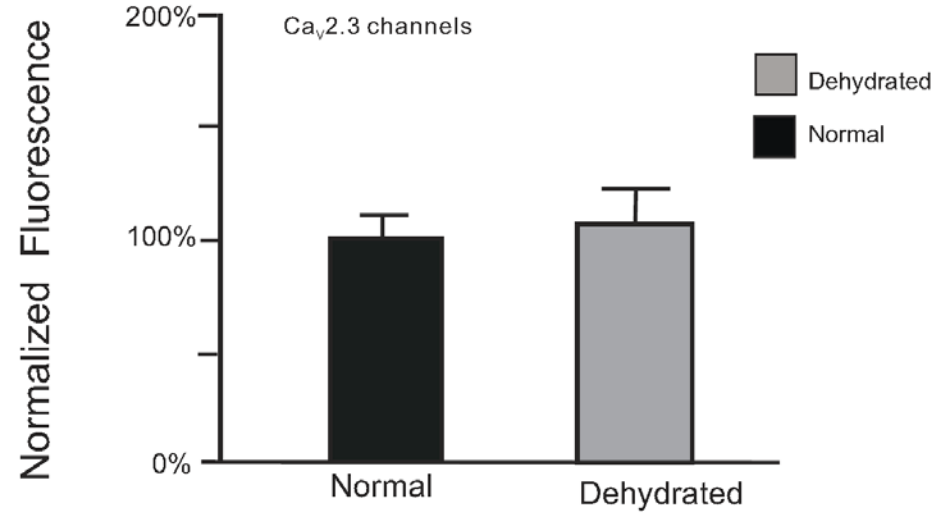

Figure 4.10 Normalized immunofluorescence of the $Ca_V2.3$ channels in the pituicytes of control and dehydrated rats.

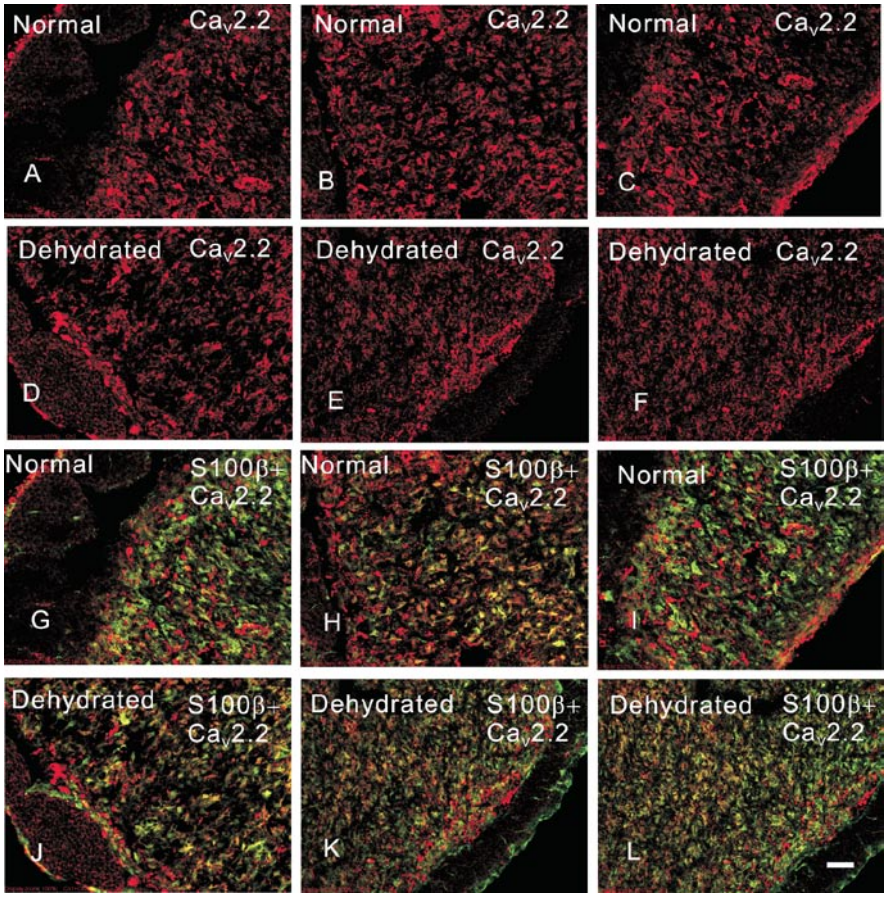

Figure 4.11 Expression levels of the $Ca_V2.2$ channels in the pituicytes was not changed during dehydration in comparison with normal condition. A-C) Representative images show immunofluorescence of $Ca_V2.2$ in slices of the normal rats; D-F) Representative images show immunofluorescence of $Ca_V2.2$ in slices of the dehydrated rats; G-I) Representative overlaid images show double staining of $Ca_V2.2$ and S100β in the slices from normal rats; J-L) Representative overlaid images show double staining of $Ca_V2.2$ and S100β in the slices from dehydrated rats. Scale bar =40 μm.

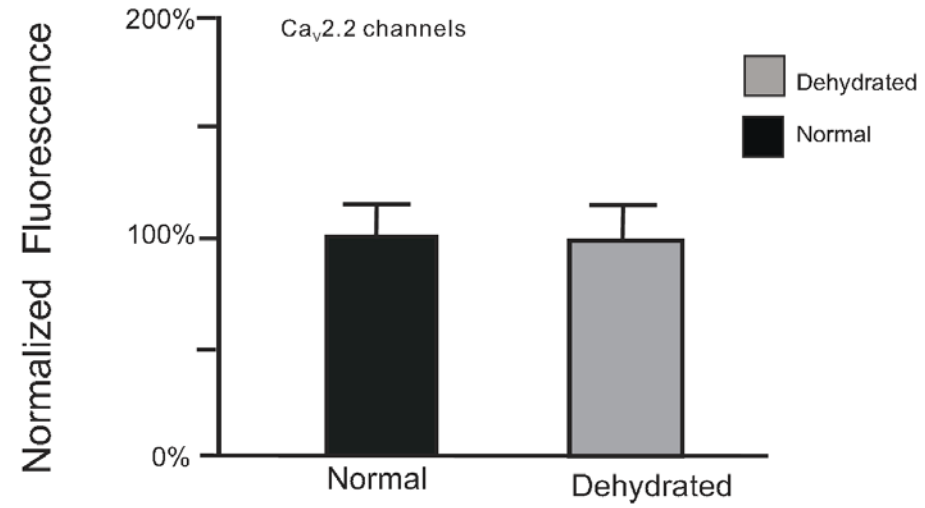

Figure 4.12 Quantitative measurement of immunofluorescence of the $Ca_V2.2$ channels in the pituicytes of control and dehydrated rats.

4.1.3 Multiple subtypes of VGCCs expressed on cultured pituicytes.

It has been reported that in primary cultured cortical astrocytes, multiple VGCCs are expressed including $Ca_V1.2$, $Ca_V1.3$, $Ca_V2.2$, $Ca_V2.3$, and $Ca_V3.1$ (Latour et al 2003). I therefore tested whether there are more subtypes of VGCCs expressed in primary cultures of pituicytes. The pituicytes can be made to grow and expand from neurohypophysial explant using glial favoured cell culture medium, and after 14 days, >95% of total cellular population is S100β positive cells (i.e. pituicytes). I have tested and counted cell numbers after performing immunocytochemistry to identify the percentage of pituicytes in the primary culture .The purity of our cultures was also tested by using RT-PCR for the neuronal marker SNAP25. The purity of the cultures was assured when the PCR results of SNAP25 was negative, which meant the neuronal inputs or MNC terminals were elminated after culturing. I then performed immunocytochemistry and Western blot analysis on the cultures to test the expression of VGCCs. I confirmed expression of these types of Ca^{2+} channels by Western-blot using homogenates of whole brain and pituicyte cultures. Whole brain membrane protein extracts were used as positive controls, and in some cases, cultured cortical astrocytes were used as specific positive controls. Generally, in the protein homogenates multiple VGCCs can be detected using Western-blot as we can see in Figures 4.13-4.18. Namely, $Ca_V1.2$ (Figure 4.13A), $Ca_V2.1$ (Figure 4.13C), $Ca_V2.2$ (Figure 4.13D), $Ca_V2.3$ (Figure 4.13E), and $Ca_V3.1$ (Figure 4.13F), but not $Ca_V1.3$

(Figure 4.13B). Normally, in the whole brain, more than three bands can be detected in each independent immunoblot of Ca^{2+} channels except for $Ca_V2.2$ (Figure 4.1D), which may indicate differences in mRNA splicing or post-translational modification. The band for each subtype of VGCCs in the whole brain was determined by comparing to the standard molecular weight provided from the antibody manufacturer. Most detectable VGCC proteins labeled by specific antibodies were similar in size with the corresponding bands detected from the whole brain except for $Ca_V2.3$, which were slightly larger. A larger size for $Ca_V2.3$ was also noted in cultures of hippocampal astrocytes (Latour et al 2003). The expression of VGCCs was confirmed by immunocytochemistry which showed immunoreactivity of S100β positive pituicytes in culture to antibodies directed against the types of Ca^{2+} channels mentioned above (Figure 4.14A-F).

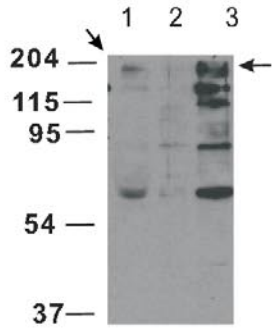

(A) $Ca_V1.2$

1. Pituicytes
2. Cortical astrocytes
3. Whole brain

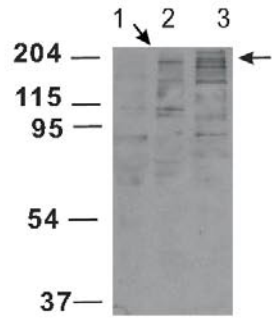

(B) $Ca_V1.3$

1.Pituicytes
2.Cortical astrocytes
3. Whole brain

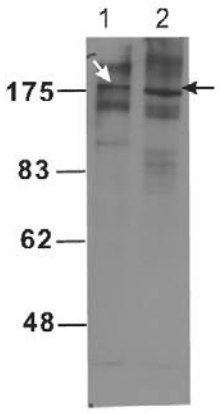

(C) $Ca_V2.1$

1. Pituicytes
2. Whole brain

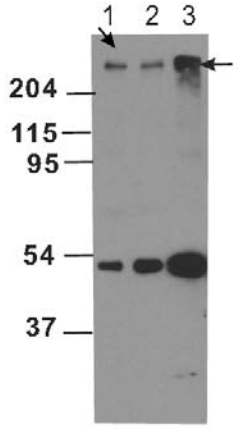

(D) $Ca_V2.2$

1. Pituicytes
2. SON
3. Whole brain

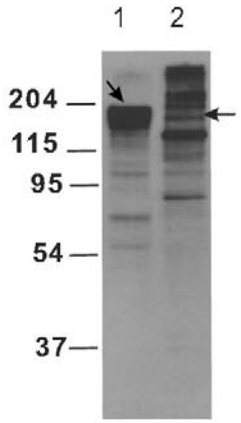

(E) $Ca_V2.3$

1.Pituicytes
2. Whole brain

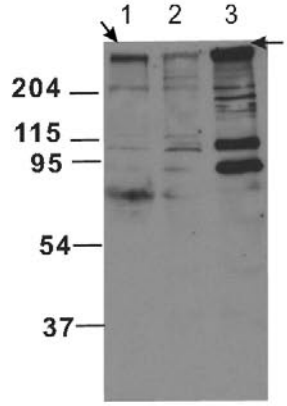

(F) $Ca_V3.1$

1. Pituicytes
2. Cortical astrocytes
3. Whole brain

Figure 4.13 Western-blot of VGCC expression in cultured pituicytes. Whole brain cortical astrocytes preparation was used as control in some cases. A) $Ca_V1.2$ channles are detected using anti-$Ca_V1.2\alpha1$ subunit antibody in the protein homogenates extracted from cultured pituicytes (~ 204 KDa), the same band is shown in the whole brain preparation. B) $Ca_V1.3$ channels are not expressed in cultured pituicytes. No band was detected at the position representing $Ca_V1.3\alpha1$ subunit in cultured pituicytes, whereas a band (black arrow) with molecular weight ~ 204 kDa was detected using anti-$Ca_V1.3\alpha1$ subunit antibody in the cultured cortical astrocytes and the whole brain. C) $Ca_V2.1$ channels are expressed in cultured pituicytes. A band (black arrow) with molecular weight ~ 175 kDa was detected which is at the same position which demonstrated the expression of $Ca_V2.1$ channels in the whole brain. D) $Ca_V2.2$ channels are expressed in cultured pituicytes. A band (black arrow) with molecular weight ~ 204 kDa was detected using anti-$Ca_V2.2$ $\alpha1$ subunit antibody in cultured pituicytes which is at the same position with the $Ca_V2.2$ channels in the SON and whole brain. E) $Ca_V2.3$ channels are expressed in cultured pituicytes. High level of $Ca_V2.3$ expression was observed and a band lower than 204 kDa (black arrow) showed the presence of one isoform of $Ca_V2.3$ $\alpha1$ subunits in the pituicytes. Multiple bands were detected in the whole brain which may suggest a diverse expression of isoforms of $Ca_V2.3$ in the rat brain. F) $Ca_V3.1$ channels are expressed in cultured pituicytes. Similar bands were detected at the same position in the cultured cortical astrocytes and the whole brain.

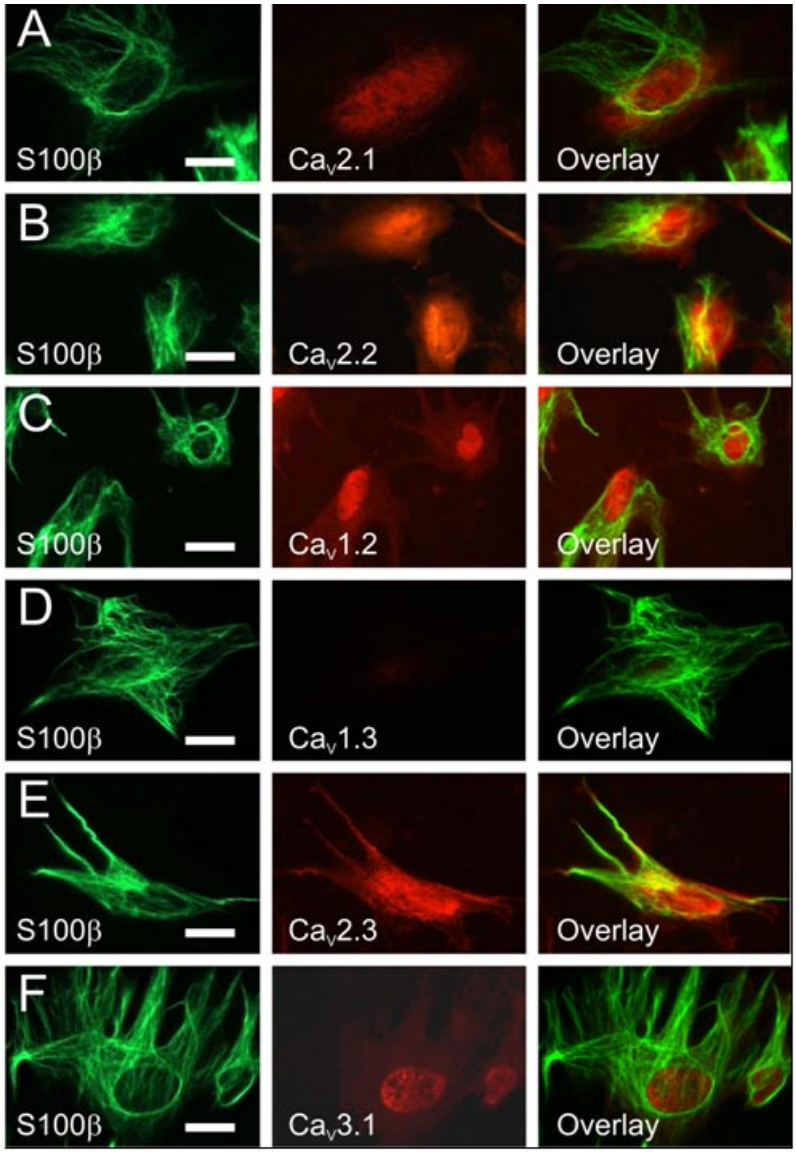

Figure 4.14 Expression of multiple VGCCs in cultured pituicytes. Images show pituicytes double-labelled with antibodies directed against S100β and α1 subunits in immunocytochemistry. FITC images showing green colour were obtained using the pituicytes marker, S100β; CY3 images showing red colour were obtained using antibodies directed against α1 subunits of VGCCs; and overlaid images demonstrate the expression of VGCCs on pituicytes. A) $Ca_V2.1$; B) $Ca_V2.2$; C) $Ca_V1.2$; D) $Ca_V1.3$; E) $Ca_V2.3$; and F) $Ca_V3.1$. Scale bar = 20 μm.

Summary and brief discussion for Section 4.1

The immunohistochemical evidence shows that the glial cells (pituicytes) in the neurohypophysis express at least two subtypes of VGCCs ($Ca_V2.2$ and $Ca_V2.3$) in tissue, and during dehydration, the expression level of $Ca_V1.2$ channels is selectively up-regulated. More subtypes of VGCCs expression could be detected when the pituicytes are cultured, including $Ca_V1.2$, $Ca_V2.1$ and $Ca_V3.1$ which suggests the expression of these channels is driven buy cultured condition. The immunocytochemical results showed that some of the VGCCs were expressed in the perinuclear regions of the cultured pituicytes, such as $Ca_V1.2$, $Ca_V2.2$, $Ca_V2.3$, and $Ca_V3.1$, which may demonstrate an upregulated protein synthesis for VGCCs in cultured pituicytes. It is however unknown whether these VGCCs are expressed on the plasma membranes or in the cytoskeletal networks of the pituicytes. The immunofluorescence of $Ca_V2.2$ and $Ca_V2.3$ channels showed clear staining on processes of the pituicytes.

Under physiological condition, cortical astrocytes express an array of mRNA of VGCCs, including $Ca_V1.2$, $Ca_V1.3$, $Ca_V2.2$, $Ca_V2.3$, and $Ca_V3.1$ (Latour et al 2003), and only L-, N- and R- type currents could be detected electrophysiologically (D'Ascenzo et al 2004). In our results, pituicytes express substantial level of $Ca_V2.2$ and $Ca_V2.3$ Ca^{2+} channels which may suggest the similarity of pituicytes with

astrocytes. The $Ca_V2.2$ channels interact with proteins in the core of SNARE complex; it is thus possible that the $Ca_V2.2$ channels in glial cells are involved with the process of docking vesicles filled with gliotransmitters at release site.

In our results, only the expression of $Ca_V1.2$ channels was up-regulated, but not that of $Ca_V1.3$ channels, which is consistent with the earlier observation of L-type channels of the astrocytes in several brain injury models (Westenbroek 1998). It has been reported that acutely isolated astrocytes from hippocampus do not express L-type channels. The high $[K^+]$-induced Ca^{2+} influx is not sensitive to L-type channel blockers (dihydropyridines, BAYK8644, or nifedipine) suggested that astrocytes might not express L-type channels in normal condition (Duffy & MacVicar 1994). However, L-type channels are needed when the demand of new protein synthesis is high, and to specifically activate CREB signal pathway (Ghosh and Greenberg 1995), or when the glial cells are under stress. Therefore, Ca^{2+} influx through voltage-gated Ca^{2+} channels may play a role in pituicytes function during periods of high hormone demand such as dehydration.

4.2 Targeting properties of the $Ca_V2.1$ and $Ca_V2.2$ channels in neuroendocrine cells

The role of the synprint site in the II-III loop in Ca_V2 channel targeting is controversial. The $Ca_V2.1$ and $Ca_V2.2$ channels have physical associations with synaptic proteins that may be essential for fast neurotransmission and axonal targeting in neurons (Bezprozvanny et al 1995; Mochida et al 2003). Our objectives are to determine whether these variants are expressed in neuroendocrine cells, and to determine their targeting properties.

4.2.1 RT-PCR results revealed the presence of $Ca_V2.1$ channel splice variants in rats

Firstly, I dissected different brain areas and several peripheral tissues from Long-Evans rats (including whole brain, spinal cord, pons/medulla, midbrain, thalamus, amygdala, hypothalamus, hippocampus, cerebellum, cortex and adrenal gland). Total RNAs were extracted from tissues separately and further reversely transcribed into cDNA for PCR amplification. One of the housekeeping genes (typically constitutive genes that is required for the maintenance of basic cellular function, and are found in all cells, and their expression are kept at relatively constant

level), glyceraldehyde 3-phosphate dehydrogenase (GAPDH), was used to test the cDNA preparation.

Secondly, several pairs of primers were designed to specifically amplify the II-III loop region of $Ca_V2.1$ (as shown Figure 1.8). Previously, Dr. Rajapaksha in our lab had performed wide range screening for splice variants of $Ca_V2.1$ gene within different regions including synprint site. He found it would be more effective if nested PCR was used to encompass the cDNA sequence coding for much of the $Ca_V2.1$ subunit II-III loop. Nested RT-PCR is a two step PCR strategy by using multiple pairs of primers covering interested regions. It normally contains two or multiple PCR aiming at amplifying genes that have low copies of initial template(s). Having designed primers that should generate a PCR product with the size of about 797bp, he identified three bands of smaller size in multiple brain tissues (such as the whole brain, cortex, thalamus etc). These three bands were isolated and the DNA was sequenced. These sequences, which correspond to lengths of 330, 260, and 221 base pairs, were used to predict the amino acid sequences that would result from the deletions. Although the intermediate band would result in an mRNA containing a stop codon, and would thus be unlikely to be physiologically relevant, the smallest and largest bands would result in unchanged reading frames with expected deletions of 194 and 155 amino acids.

I will refer to these two deletion mutants as $Ca_V2.1\Delta1$ and $Ca_V2.1\Delta2$. The predicted structures and sequences of the two variants are shown in Figure 4.15. The diagram in Figure 4.15A shows the structure of the $Ca_V2.1\Delta1$ subunit. The II-III loop is the intracellular loop between domains II and III. The synprint site is shown by the thicker line and the sites of the deletions in the identified mutants are shown by the arrows. The sequence coded for by $Ca_V2.1\Delta1$ would correspond to a deletion beginning at amino acid 754 and ending at amino acid 948 (Pro754-Arg948, 194 aa deletion), whereas $Ca_V2.1\Delta2$ would predict a deletion between amino acids 793 and 948 (Ser793-Arg948, 155 aa deletion). The amino acid sequences of the two deletion variants are compared to the sequence of the WT $Ca_V2.1$ in Figure 4.15B. The upper sequence is that of the full length protein with the synprint site underlined, the second sequence is that of Δ1, and the bottom sequence is that of Δ2. Neither variant was seen in tissues from peripheral tissues (such as spleen and adrenal gland). To analyze the relative abundance of these two isoforms of $Ca_V2.1$ channels in different brain tissues, I quantified the intensity of DNA bands for each isoform using GAPDH as internal control. Most of the brain regions express relatively high level of Δ1 isoform in comparison with that of Δ2 isoform. For example, in hypothalamus and cortex, the abundance of Δ1 is more than twice as much as that of Δ2 (Figure 4.16).

A.

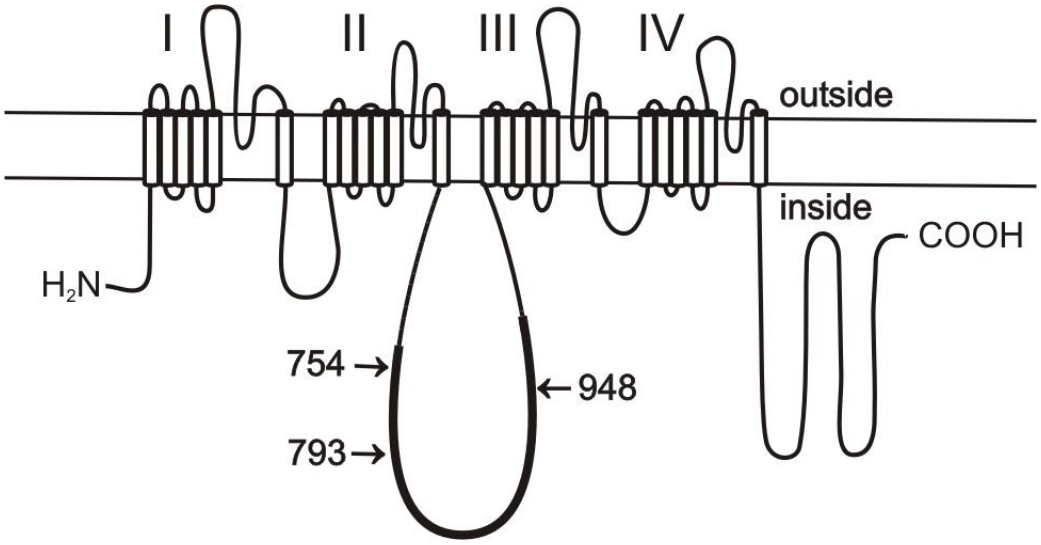

B

FL QGGVQGGMVFSIYFIVLTLFGNYTLLNVFLAIAVDNLANAQELTKDEQEEEEAANQKL 741
Δ 1 QGGVQGGMVFSIYFIVLTLFGNYTLLNVFLAIAVDNLANAQELTKDEQEEEEAANQKL
Δ 2 QGGVQGGMVFSIYFIVLTLFGNYTLLNVFLAIAVDNLANAQELTKDEQEEEEAANQKL

FL ALQKAKEVAEVSPLSAANMSIAVKEQQKNQKPAKSVWEQRTSEMRKQNLLASREALYG 799
Δ 1 ALQKAKEVAEVSP----------
Δ 2 ALQKAKEVAEVSPLSAANMSIAVKEQQKNQKPAKSVWEQRTSEMRKQNLLAS----------

FL DAAERWPTTYARPLRPDVKTHLDRPLVVDPQENRNNNTNKSRAPEALRQTARPRESAR 857
Δ 1 ----------
Δ 2 ----------

FL DPDARRAWPSSPERAPGREGPYGRESEPQQREHAPPREHVPWDADPERAKAGDAPRRH 915
Δ 1 ----------
Δ 2 ----------

FL THRPVAEGEPRRHRARRRPGDEPDDRPERRPRPRDATRPARAADGEGDDGERKRRHRH 973
Δ 1 ----------RDATRPARAADGEGDDGERKRRHRH
Δ 2 ----------RDATRPARAADGEGDDGERKRRHRH

FL GPPAHDDRERRHRRRKESQGSGVPMSGPNLSTTRPIQQDLGRQDLPLAEDLDNMKNNK 1031
Δ 1 GPPAHDDRERRHRRRKESQGSGVPMSGPNLSTTRPIQQDLGRQDLPLAEDLDNMKNNK
Δ 2 GPPAHDDRERRHRRRKESQGSGVPMSGPNLSTTRPIQQDLGRQDLPLAEDLDNMKNNK

FL LATGEPASPHDSLGHSGLPPSPAKIGNSTNPGPALATNPQNAASRRTPNNPGNPSNPG 1089
Δ 1 LATGEPASPHDSLGHSGLPPSPAKIGNSTNPGPALATNPQNAASRRTPNNPGNPSNPG
Δ 2 LATGEPASPHDSLGHSGLPPSPAKIGNSTNPGPALATNPQNAASRRTPNNPGNPSNPG

Figure 4.15 Amino acid sequences of the splice variants of $Ca_V2.1$ channels. The diagram in part A shows the structure of the $Ca_V2.1\Delta1$ subunit. The synprint region of the II-III linker is shown in bold and the location of the amino acids that mark the barriers of the sequences deleted in the alternatively spliced variants are shown. Part B shows the sequences of the variants. The upper sequence is that of the full-length version of rat $Ca_V2.1$ with the synprint region underlined. The second and third sequences are those of $Ca_V2.1$ Δ1 and Δ2, respectively. Numbers on the right refer to the number of the amino acid at the end of row in the full length sequence of $Ca_V2.1$.

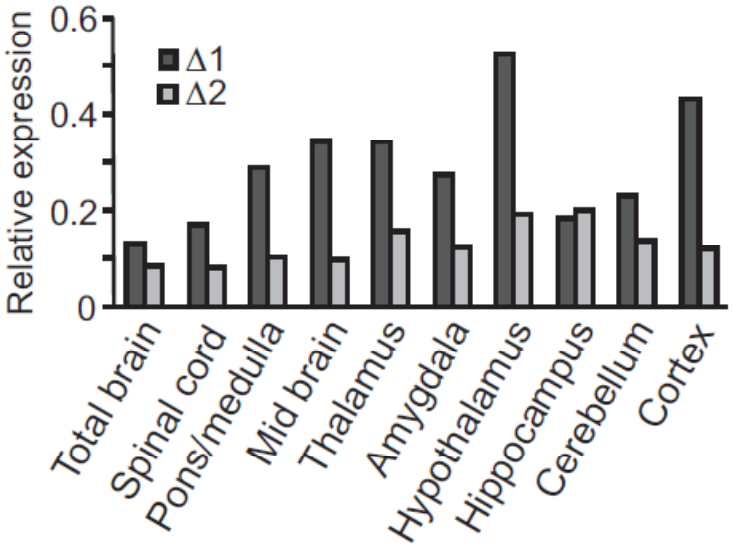

Figure 4.16. Splice variants of $Ca_V2.1$ observed in RNA isolated from rat brains tissues. The graph below shows the relative expression of $Ca_V2.1$ Δ1 and Δ2 (compared to that of GAPDH), in the indicated brain areas. The bars indicate the mean results obtained from the quantification of two sets of gels, those shown above and those from a similar experiment. The unit for relative expression is the ratio of the intensities representing DNA bands for isoform and GAPDH.

Thirdly, further tests were conducted to detect the presence of these splice variants in a variety of cells, especially neuroendocrine cells. I therefore probed for expression of the variants in PC12 cells. Previously, single cell RT-PCR experiments demonstrated that MNCs express $Ca_V2.1$, as well as $Ca_V1.2$, $Ca_V1.3$ and $Ca_V2.2$ (Glasgow et al 1999), and currents mediated by $Ca_V2.1$ have been characterized in both MNC somata (Fisher & Bourque 1995b; Foehring & Armstrong 1996) and axon terminals (Fisher & Bourque 1995b). Studies of evoked secretion from isolated MNC terminals suggested that currents mediated by $Ca_V2.1$ are important in mediating VP release (Wang et al 1997). Dr. K. Rajapaksha and I used single cell PCR to look at the expression of the variants in acutely isolated MNCs and PC12 cells. The result of one such experiment is illustrated in Figure 4.17. The cDNA corresponding to $Ca_V2.1$ Δ1 and Δ2 were observed in each of the three cells tested. These data demonstrate that individual MNCs can express splice variants of $Ca_V2.1$ lacking the synprint site. The splice variants were also detected in the PC12 cells where $Ca_V2.1$ Δ1 is the predominant form of channels.

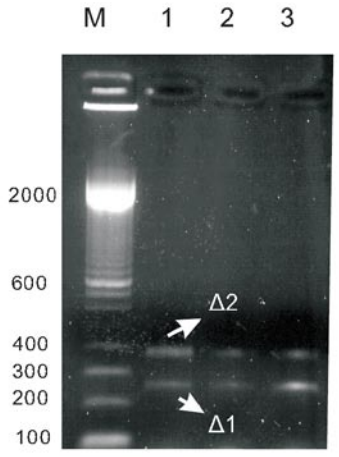

Figure 4.17. A representative RT-PCR image demonstrating that the $Ca_V2.1$ splice variants are found in isolated neuroendocrine cells. $Ca_V2.1$ Δ1 and Δ2 were detected in the isolated MNCs and PC12 cells. M. molecular marker, Lane 1 the splice variants in the whole brain; Lane 2. the splice variants in single MNCs; Lane 3, the splice variants in single PC12 cells.

4.2.2 Immunohistochemical and immunocytochemical evidence showing the expression of the $Ca_V2.1$ splice variants.

I used immunocytochemistry to test whether the splice variants are expressed as proteins. An antibody directed against a sequence in the II-III loop, which binds only to channels contain the full synprint site, is therefore referred to as the "selective antibody" (see the illustration in Figure 4.18A). An antibody directed against the C-terminus, which binds with any isoforms possessing the C-terminus of wild type $Ca_V2.1$ channels, is therefore referred to as the "inclusive antibody" (see the illustration in Figure 4.18B). Both the selective and inclusive antibodies were used to probe cultured neonatal hippocampal neurons, PC12 cells, and acutely isolated MNCs. I reasoned that immunoreactivity to the inclusive antibody, in the absence of immunoreactivity to the selective antibody, would suggest the presence of II-III loop deletion variants of $Ca_V2.1$, whereas overlapping immunoreactivity would suggest the presence of channels with or without the synprint site.

Immunoreactivity to the two antibodies in hippocampal neurons is compared. The

two antibodies clearly stain both the somatic membrane and the axon terminals of hippocampal neurons, suggesting that $Ca_V2.1$ channels in both areas include the synprint site (Figure 4.19A-D). Our data do not, therefore, provide evidence for expression of $Ca_V2.1$ II-III loop deletion variants in hippocampal neurons. The patterns of staining for the two antibodies were clearly different, however, in PC12 cells. Although there was robust membrane staining for the inclusive antibody, there was little or no staining observed on the membrane for the selective antibody (Figure 4.19 E-H). This suggests that a variant lacking a portion of the II-III loop is the predominant form in PC12 cells. Similar results were obtained for isolated MNCs. I compared the staining of the two antibodies both in the MNC somata isolated from the hypothalamus and the large MNC axon terminals isolated from the neurohypophysis (Fisher & Bourque 1995b; Fisher et al 2000). The inclusive antibody showed clear staining in both locations, while the selective antibody showed little membrane staining (Figure 4.19 I-L). The lack of clear immunoreactivity on the MNC terminal membrane using the selective antibody is consistent with a previous report (Fisher et al 2000) and while punctuate staining near the plasma membrane of MNC somata has been observed in a tissue slice preparation, the authors of the report noted that they could not distinguish between membrane staining and staining of synaptic inputs onto the MNC somata (Joux et al 2001). Our data support the conclusion that the dominant form of $Ca_V2.1$ in both neuroendocrine cell types is not immunoreactive to the selective antibody and therefore may lack a portion of the II-III loop. Furthermore,

these data suggest that an intact II-III loop is not necessary for the targeting of $Ca_V2.1$ to MNC axon terminals.

A

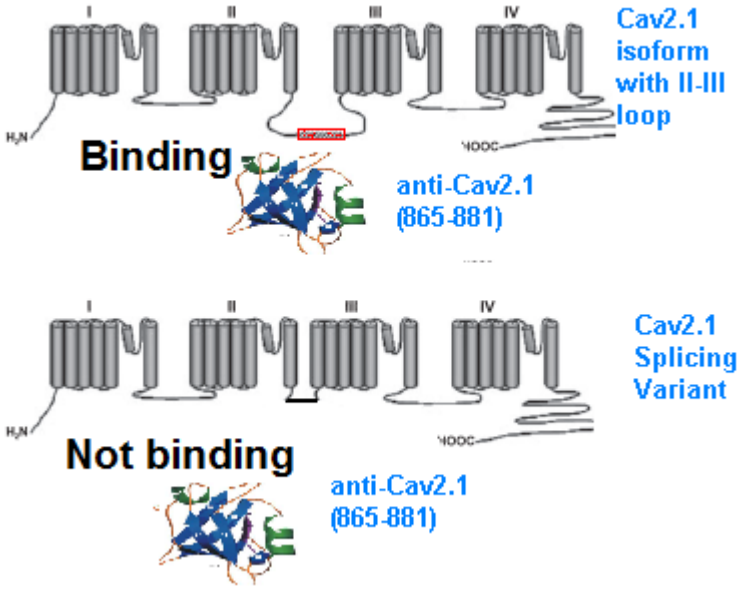

B

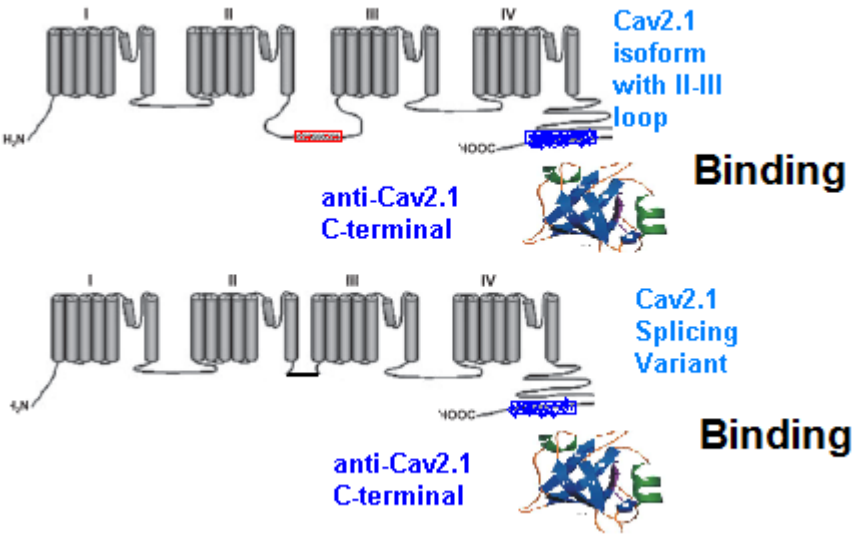

Figure 4.18. Working mechanism of the inclusive and selective antibodies directed against different parts of the $Ca_V2.1$ channels. A) The selective antibody is a rabbit polyclonal antibody directed against peptide residues 865-881 in rat $Ca_V2.1$ II-III loop (Alomone Labs). It only binds with full-length $Ca_V2.1$ with intact synprint site. B) The inclusive antibody is a goat polyclonal antibody directed against the carboxy-terminus of human $Ca_V2.1$ (Santa Cruz). It binds with both the full-length and the splice variants of $Ca_V2.1$ channels. If the predominant form(s) of channels are splice variants, then this antibody could be used to label deleted forms of $Ca_V2.1$ channels.

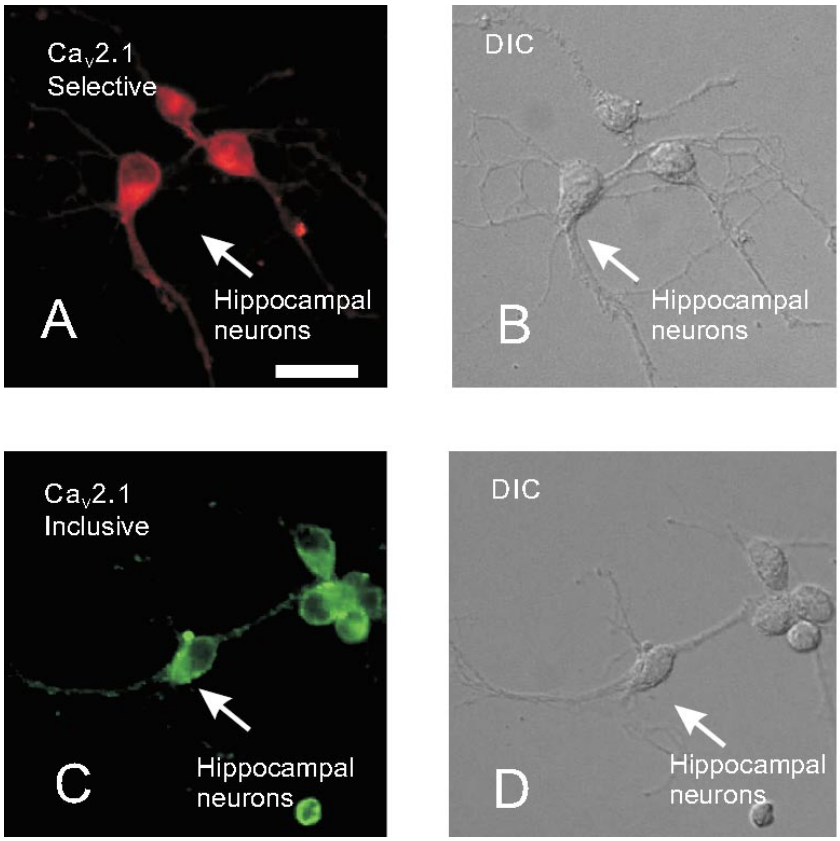

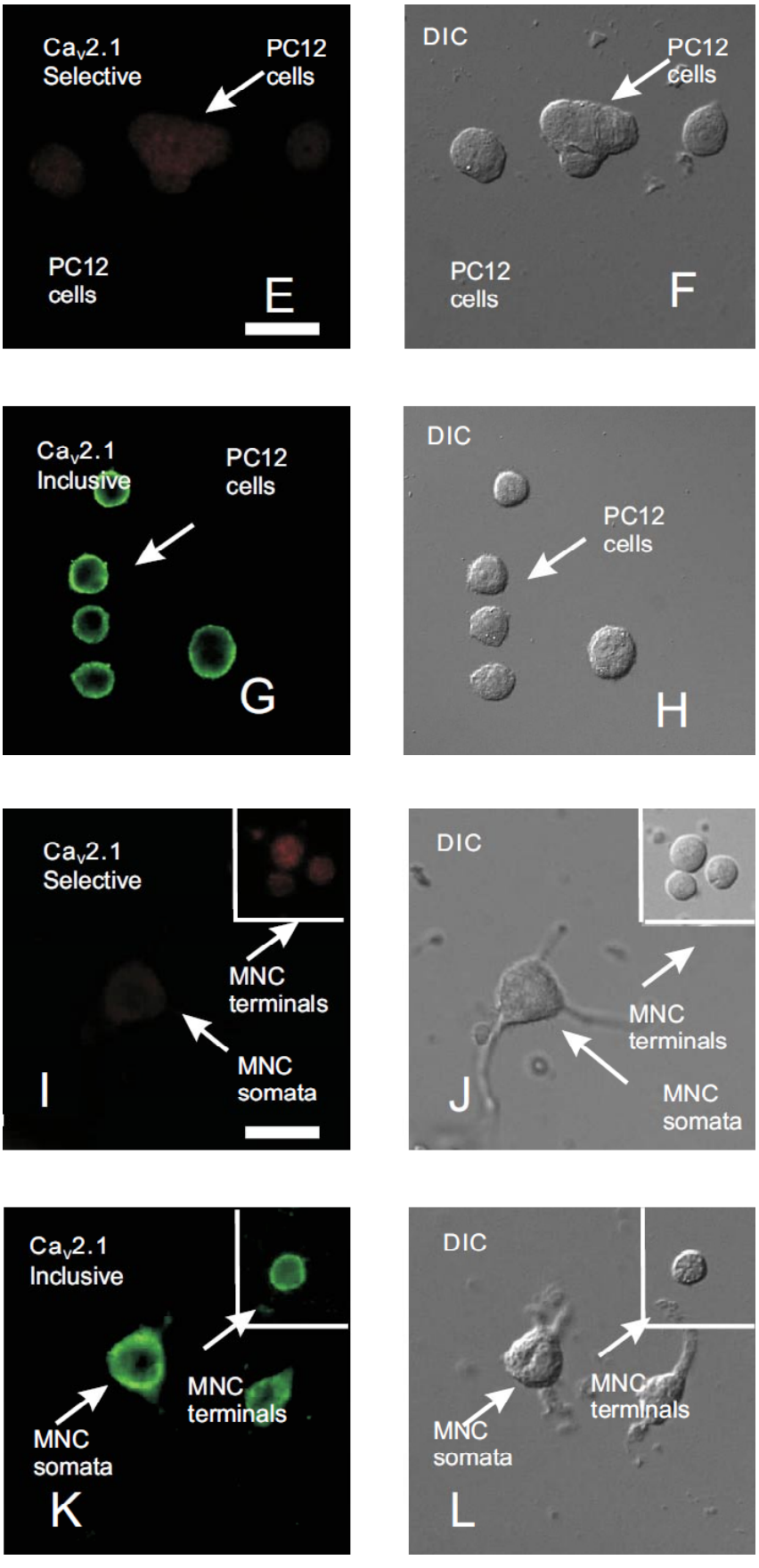
$Ca_V2.1$ Selective
PC12 cells
PC12 cells
E
DIC
PC12 cells
PC12 cells
F
$Ca_V2.1$ Inclusive
PC12 cells
G
DIC
PC12 cells
H
$Ca_V2.1$ Selective
MNC terminals
MNC somata
I
DIC
MNC terminals
MNC somata
J
$Ca_V2.1$ Inclusive
MNC terminals
MNC somata
K
DIC
MNC terminals
MNC somata
L

Figure 4.19 Immunofluorescence in three different cell types using two antibodies directed against different portions of the $Ca_V2.1$ α1 subunit. Images in the left column show results for an antibody (the selective antibody) that recognizes a sequence within the $Ca_V2.1$ synprint site. Images in the right column show immunoreactivity for an antibody (the inclusive antibody) that recognizes a sequence in the $Ca_V2.1$ carboxyl terminus. A-D) Results for cultured hippocampal neurons. Note that both antibodies clearly label the somatic membrane as well as the processes. E-G) Results for cultured PC12 cells. I-L) Results for acutely isolated MNCs. The insets show immunoreactivity for the two antibodies on MNC terminals isolated from the neurohypophysis. The colour images on the left are epifluorescence images, and the ones on the right are differential interference contrast (DIC) images. Note that for PC12 cells, MNC somata, and MNC terminals, the inclusive antibody displayed clear plasma membrane staining, while the selective antibody did not. The scale bar in each case represents 20 μm.

4.2.2.1 Differential distribution of the $Ca_V2.1$ splice variants in OT-MNCs and VP-MNCs.

To test whether these synprint site deletion forms of $Ca_V2.1$ are also expressed in SON, I performed a series of immunohistochemistry using high resolution confocal microscopy. I was expecting to identify the location of immunostaining of different isoforms of channels at single cell level *in situ*.

Firstly, I performed immunostaining with two MNC markers (neurophysin I and neurophysin II) and each of the $Ca_V2.1$ channel antibodies. The patterns of staining for

the selective and inclusive antibodies are very different in SON. Immunostaining of neurophysin I and II with the selective $Ca_V2.1$ antibody showed no colocalization of MNC somata and full-length $Ca_V2.1$ channels (Figure 4.20A-F). Immunostaining of the selective antibody showed a punctate pattern suggesting synaptic input staining (Figure 4.20A and 4.20D). The neuophysin I and II labeled all the OT and VP-MNCs (Figure 4.20 B and 4.20E). In addition, most of the dot-like staining is outside of somata of MNCs. In contrast, the inclusive antibody showed immunoreactivity that labeled at least some of the somata of the MNCs (Figure 4.20G and 4.20J). These results are consistent with the interpretation that full-length $Ca_V2.1$ channels are not the predominant form in MNCs. Interestingly, I noticed that the immunofluorescence of the inclusive antibody only colocalized with a portion of neurophysin I and II positive cells (Figure 4.20I and L), which suggested there might be a selectivity of distribution for splice variants on different subtypes of MNCs (Figure 4.20H and 4.20K showing the somata of all the OT and VP-MNCs).

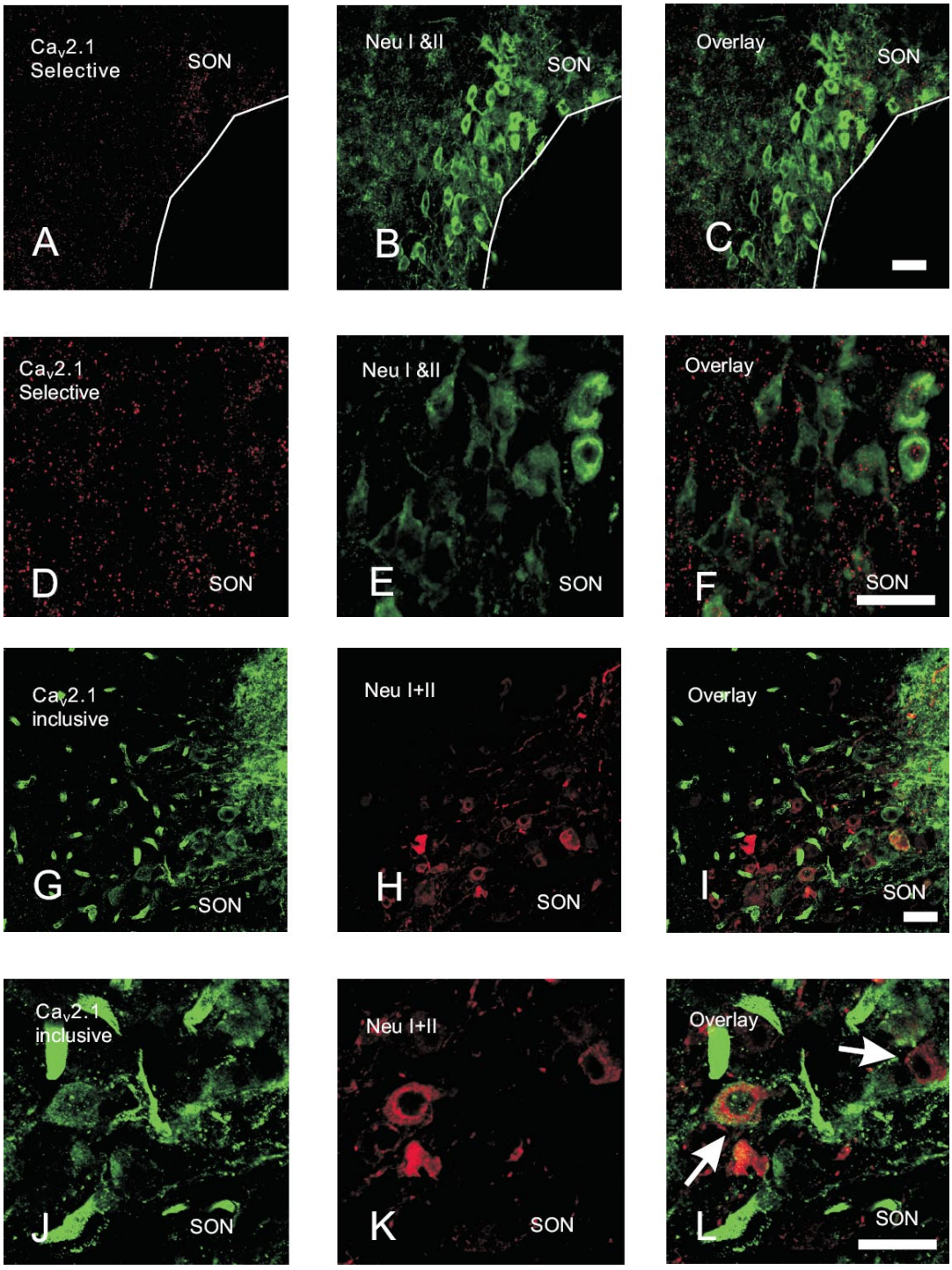

Figure 4.20 Expression patterns of different isoforms of $Ca_V2.1$ channels in the rat SON. Images (A) and (D, enlarged) reveal the distribution pattern of full-length $Ca_V2.1$ subunits (immunostained by $Ca_V2.1$ selective) are punctuate. (B) and (E, enlarged) show soma and projections of MNCs in SON using goat anti-neurophysin I and II antibodies. (C) and (F, enlarged) show that the full-length $Ca_V2.1$ α1 subunit

does not colocalize with MNCs. (G) and (J, enlarged) reveal the somatic distribution of splice variants of $Ca_V2.1$ subunits (immunostained by inclusive antibody) in MNCs. (H) and (K, enlarged) show soma and projections of MNCs in SON using rabbit anti-neurophysin I and II antibodies. (I) and (L, enlarged) reveal colocalization between variants of $Ca_V2.1$ subunits and soma of MNCs (original images are from 20x confocal objective lens and the enlarged images are all 3x digitally zoomed). Scale bar = 40 μm.

I then performed double staining with either only neurophysin I or neurophysin II with the inclusive $Ca_V2.1$ antibody to test whether splice variants are differentially expressed on OT and VP-MNCs. Double staining of neurophysin I and inclusive $Ca_V2.1$ antibody showed that neurophysin I positive cells were not colocalized with $Ca_V2.1$ channel positive cells (Figure 4.21C and 4.21F). Figure 4.21A and 4.21D show components that express $Ca_V2.1$ channels in the SON. Figure 4.21B and 4.21E show the locations of OT-MNCs in the SON. The lack of staining for inclusive $Ca_V2.1$ antibody suggests that the OT-MNCs do not express any $Ca_V2.1$ channels that can be stained by the inclusive antibody. Figure 4.21 G and 4.22J show the location of components that express either splice variants or full-length $Ca_V2.1$ channels. Double staining of neurophysin II and the inclusive $Ca_V2.1$ antibody demonstrate that the neurophysin II positive cells are largely colocalized with $Ca_V2.1$ channels, suggesting the splice variants of $Ca_V2.1$ are mainly distributed on VP-MNCs (Figure 4.21I and 4.21L).

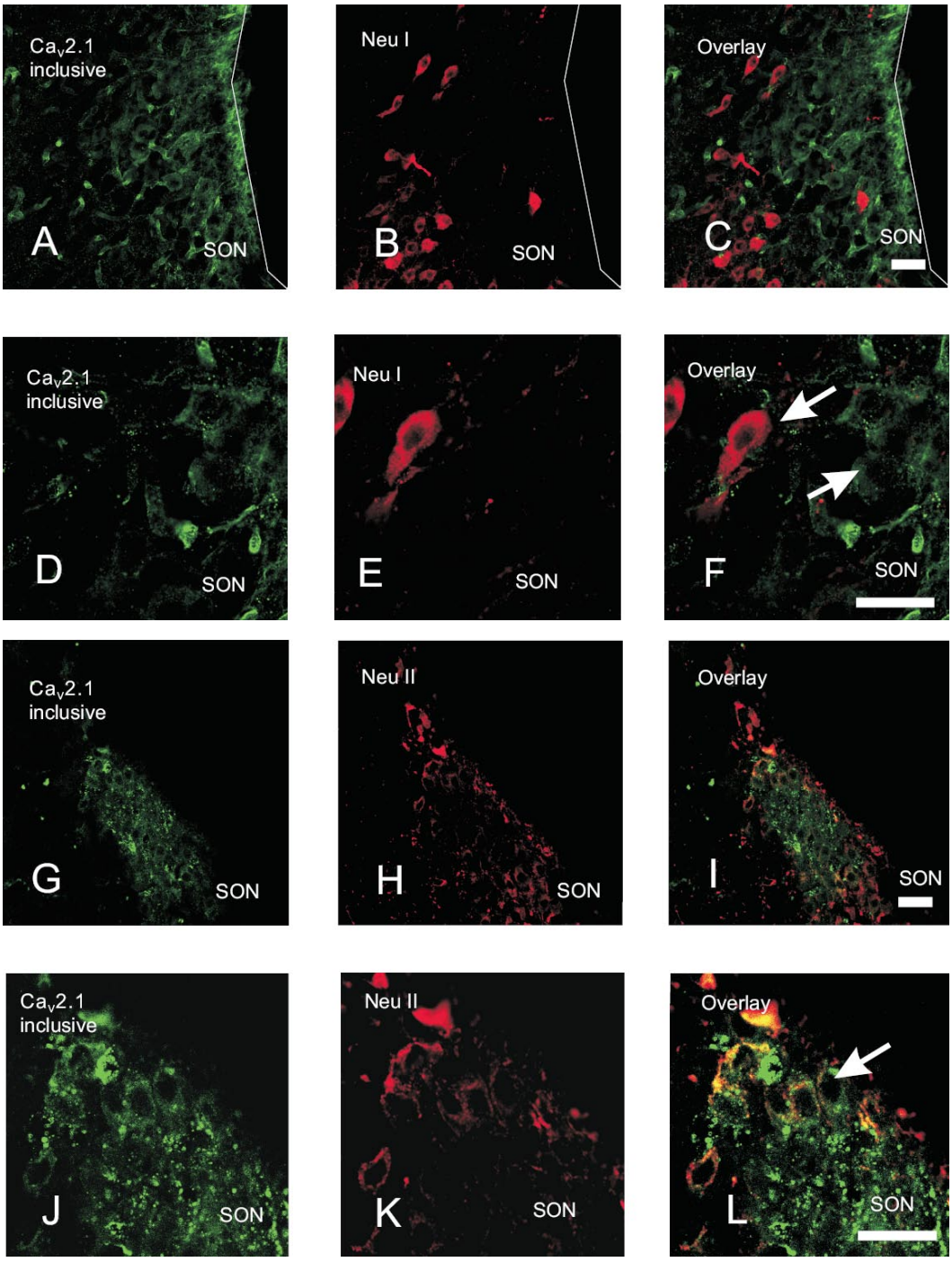

Figure 4.21 Distribution of the splice variants of $Ca_V2.1$ channels in OT-MNCs and VP-MNCs. Images (A, D, G, and J) show distribution of the $Ca_V2.1$ splice variants in soma of MNCs; (B) and (E, enlarged) show neurophysin I expressed on oxytocin-releasing MNCs; (C) and (F, enlarged) reveal splice variants of $Ca_V2.1$ are not colocalized with OT-MNCs; (H) and (K) show neurophysin II expressed on

vasopressin-releasing MNCs; (I) and (L) demonstrate the colocalization between splice variants of $Ca_V2.1$ channels and vasopressin-releasing MNCs. Scale bar = 40 μm.

To test the distribution of full-length and splice variants of $Ca_V2.1$ channels on the nerve terminals of MNCs in hypothalamic slices, I performed colocalization analysis of the inclusive $Ca_V2.1$ antibody with neurophysin I and II to determine whether MNC terminals express $Ca_V2.1$ channels. The green spots shown in Figure 4.22A are all elements expressing $Ca_V2.1$ channels in the NH; the red spots shown in Figure 4.22B are all MNC terminals in the NH. Figure 4.22C is the overlaid image of Figure 4.22A and 4.22B, which shows that only a portion of MNC terminals are colocalized with the inclusive $Ca_V2.1$ antibody. The yellow regions show the MNC terminals that express $Ca_V2.1$ channels, and the red regions in the Figure 4.22C represent the MNC terminals that do not express $Ca_V2.1$ channels. Using double staining of the selective $Ca_V2.1$ antibody and neurophysin I and II, I found that the selective $Ca_V2.1$ antibody only labeled the non-MNC terminal components of the NH. Figure 4.22D shows the location of components labeled by the selective $Ca_V2.1$ antibody (red), which has the same punctate staining pattern as is seen in SON (Figure 4.20D). Figure 4.22E shows the all the MNC terminals (green). Figure 4.22F is the overlaid image of Figure 4.22D and Figure 4.22E. As the red spots are not colocalized with green spots, these data suggest that MNC terminals do not express full-length $Ca_V2.1$ channels. Double staining of the inclusive $Ca_V2.1$ antibody (Figure 4.22G) and neurophysin II (Figure

4.22H) shows the colocalization of these two components (Figure 4.22I), suggesting that VP-MNC-terminals express $Ca_V2.1$ channels, which is consistent with the previous observation that VP-MNC somata may express the splice variants of $Ca_V2.1$ channels (Figure 4.21G-L). To further confirm the selective $Ca_V2.1$ antibody positive components in the NH are neuronal inputs, I used synaptic vesicle marker, synaptophysin, to test whether the red spots seen in Figure 4.22D are colocalized with synaptophysin. As we can see in Figure 4.22J-L, the immunoreactivity to the selective $Ca_V2.1$ antibody is colocalized with that of the synaptophysin antibody, suggesting these full-length $Ca_V2.1$ channels are located in the synaptic inputs (Figure 4.22L, the yellow regions show that most of the selective $Ca_V2.1$ antibody positive spots label the same components that are synaptophysin positive). Figure 4.22M-O demonstrate the locations of synaptophysin and MNC-terminals. The red regions are synaptic terminals with synaptic-like vesicles (Figure 4.22M), the green regions are MNC terminals (Figure 4.22N), and the yellow regions are probably due to the presence of a small portion of the synaptic-like vesicles in the MNC terminals. Figure 4.22O shows that most of the immunoreactivity to synaptophysin is located outside of the MNC terminals, which confirms the synaptophysin positive components are mostly synaptic inputs.

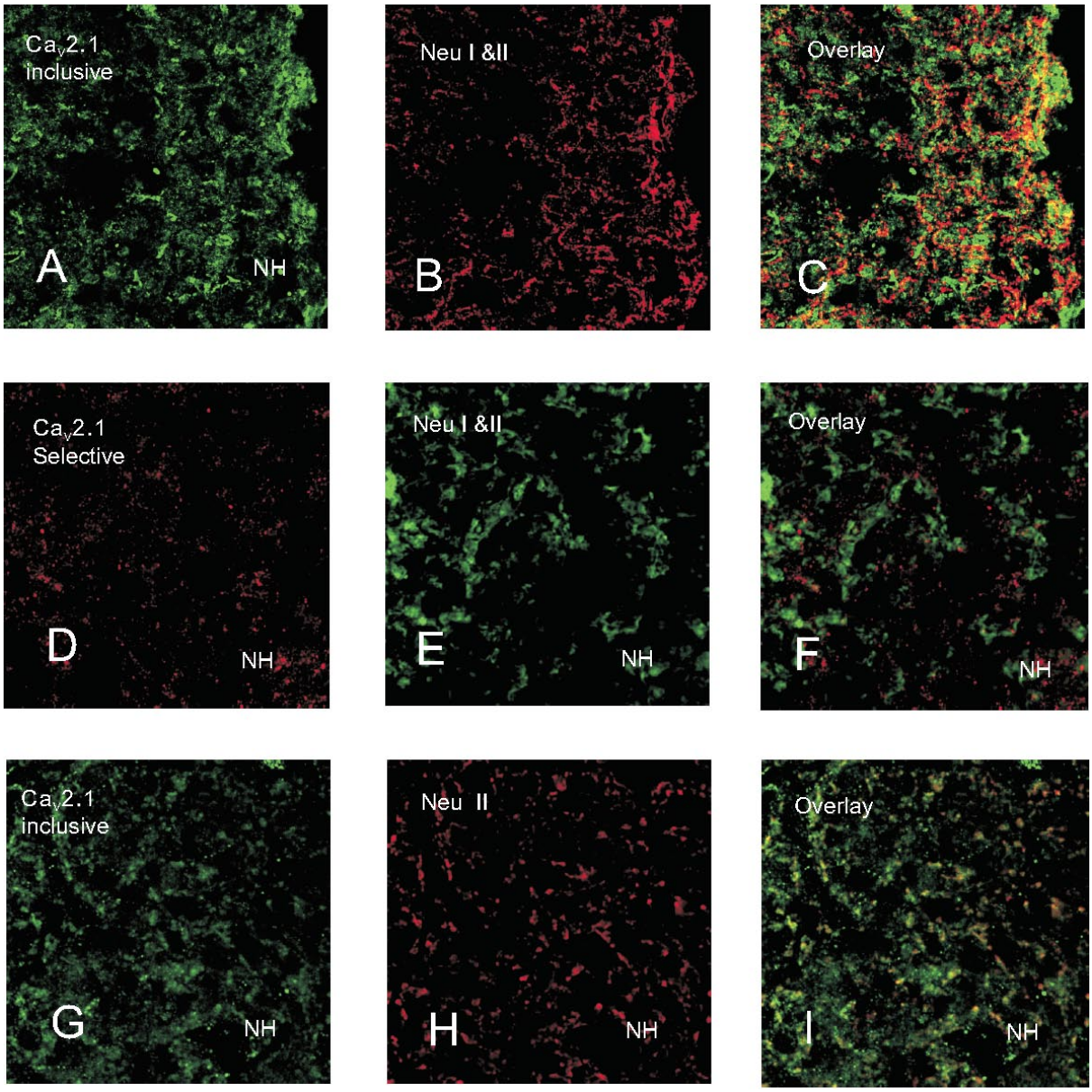
$Ca_v2.1$ inclusive
A
NH
Neu I &II
B
Overlay
C
$Ca_v2.1$ Selective
D
NH
Neu I &II
E
NH
Overlay
F
NH
$Ca_v2.1$ inclusive
G
NH
Neu II
H
NH
Overlay
I
NH

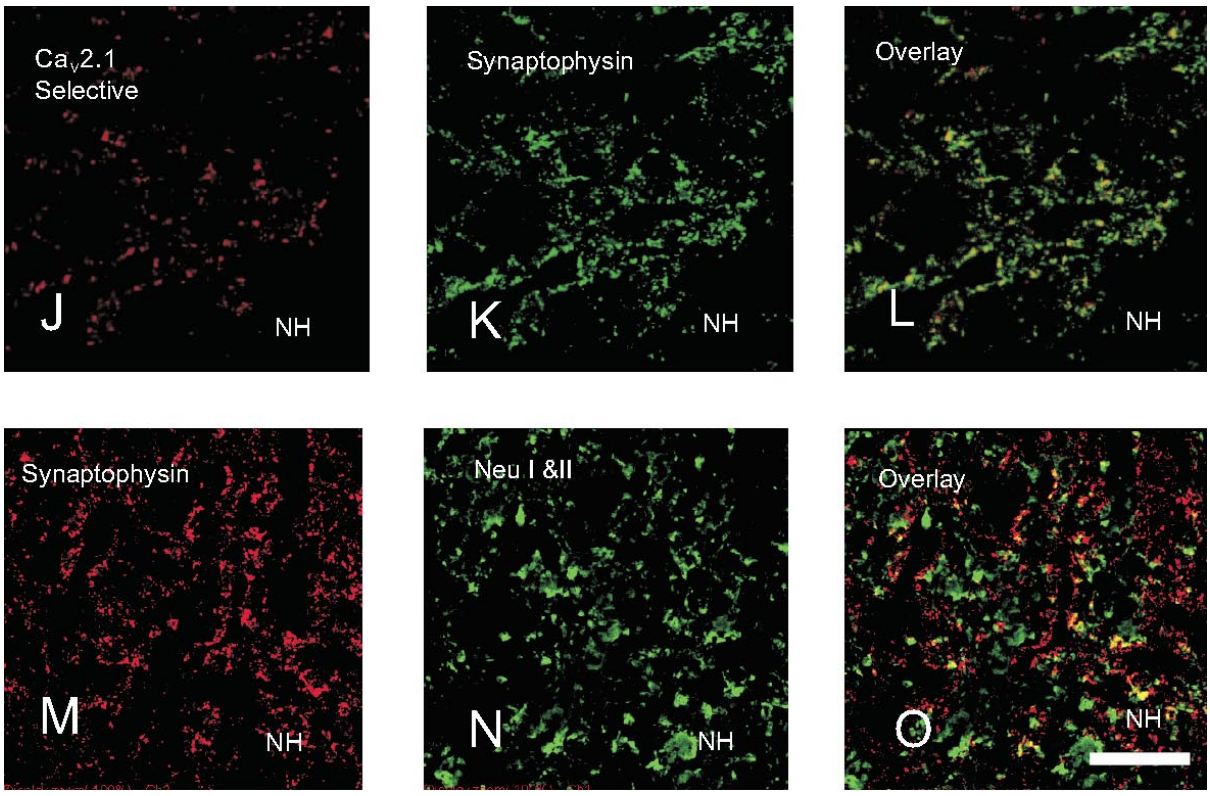

Figure 4.22 Localizations of the full-length and splice variants of Ca$_V$2.1 channels on MNC terminals. Slices from isolated rat pituitary glands were stained with inclusive Ca$_V$2.1 antibody and anti-neurophysin I and II. Image (A) All Ca$_V$2.1 channels in the NH. (B) All the MNC terminals labeled by neurophysin I and II (C) Colocalization between Ca$_V$2.1 channels and the MNC terminals. (D) The selective Ca$_V$2.1 antibody positive components in the NH. (E) All the MNC terminals. (F) The full-length Ca$_V$2.1 channels are not colocalized with any MNC terminals. Pituitary slices were double stained with synaptophysin (synaptic marker) and the inclusive Ca$_V$2.1 antibody. (G) The inclusive antibody positive components in the NH. (H) The location of VP-MNC terminals. (I) Overlaid image showing the colocalization of the inclusive Ca$_V$2.1 antibody and the VP-MNC terminals. Double staining of the selective Ca$_V$2.1 antibody and synaptophysin were performed. (J) The selective Ca$_V$2.1 antibody positive components in the NH. (K) Locations of the synaptophysin positive components in the NH labeled with Alexa Fluor 488 (green). (L) Colocalization between the selective Ca$_V$2.1 and synaptophysin antibodies in the NH,

showing the selective $Ca_V2.1$ antibody labels synaptic inputs. (M) Synaptophysin positive components in the NH labeled with Alexa Fluor 555 (red). (N) MNC terminals labeled by neurophysins. (O) Synaptophysin is not mainly colocalized with MNC terminals. Scale bar = 40 μm.

4.2.2.2 Expression of the $Ca_V2.1$ splice variants in the melanotropes of the IL

The melanotropes in the intermediate lobe (IL) of the pituitary gland also showed evidence for expression of $Ca_V2.1$ splice variants that lack the synprint site. However, the neuroendocrine cells in the AH showed no similarity. Double staining of melanotrope marker, α-MSH, and the $Ca_V2.1$ inclusive antibody was performed using pituitary slices.The $Ca_V2.1$ inclusive antibody positive cells in the IL (Figure 4.23A and 4.23D) is colocalized with α-MSH positive cells in the IL (Figure 4.23B and 4.23E), and in the same set of experiments, the selective $Ca_V2.1$ antibody showed no immunoreactivity to components within IL region (Figure 4.23G). These data suggest that the melanotropes may also express synprint site deletion splice variants of $Ca_V2.1$ channels (Figure 4.23C and 4.23F). Because the α-MSH antibody is from the same species as the selective $Ca_V2.1$ antibody, and most of the cells in the IL region are melanotropes (Figure 4.23E), in the Figure 4.23H and 4.23K, I used nuclear marker Hoechst 33342 to show the location of melanotropes. As Figure 4.23I and 4.23L show, the overlaid images demonstrate that there is no immunostaining of the selective $Ca_V2.1$ antibody in the melanotropes. Using the synaptic marker, synapsin I, I showed

that in the IL there are few or no neuronal inputs (Figure 4.1). The positive staining of the selective $Ca_V2.1$ antibody in the IL (part of the NH Figure 4.23G) likely represents neuronal inputs expressing full-length $Ca_V2.1$ channels.

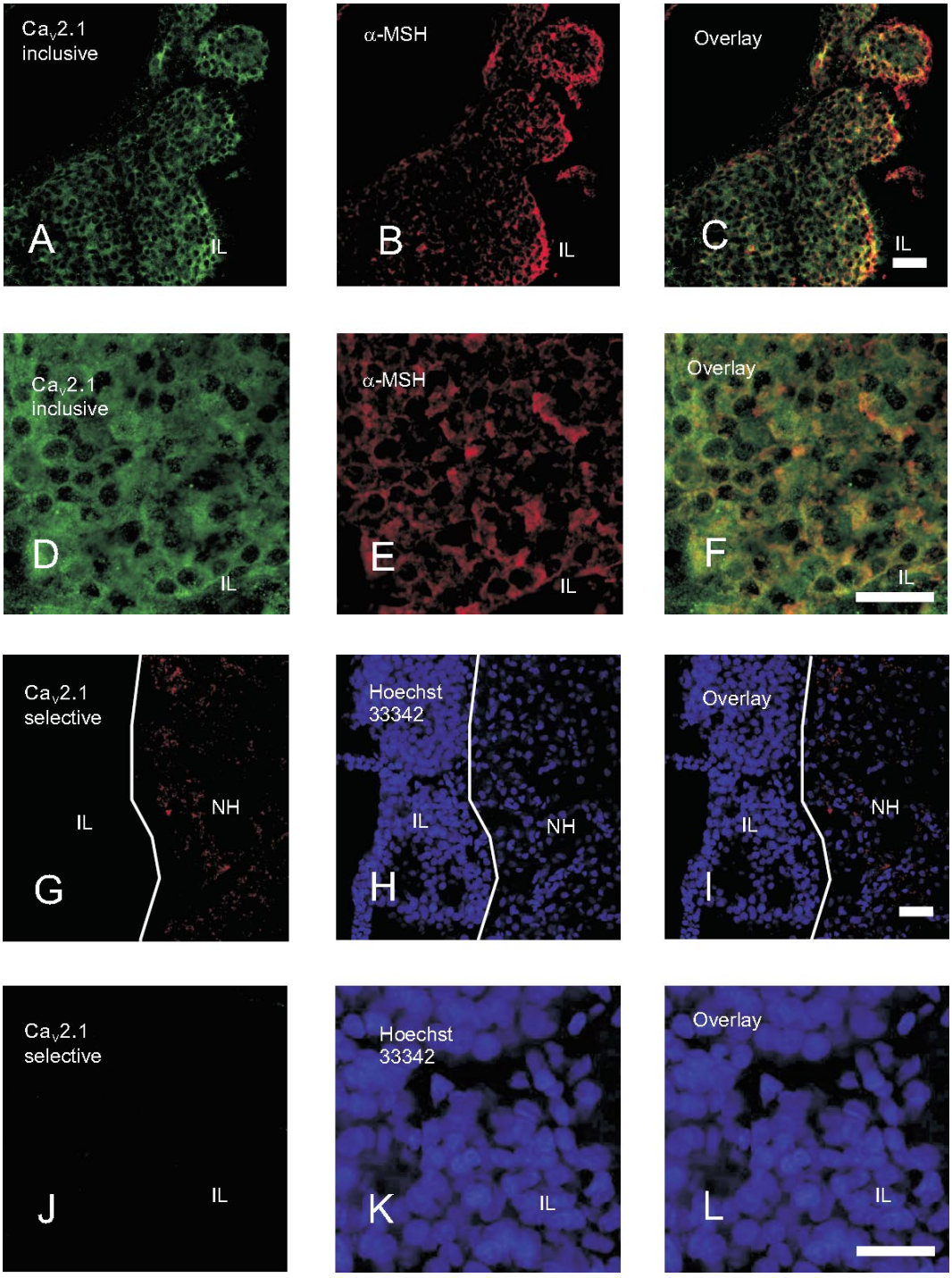

Figure 4.23 Localization of the splice variants of $Ca_V2.1$ channels on melanotropes in IL. Double staining of anti- α-MSH and inclusive $Ca_V2.1$ antibodies reveals the localization of splice variants of $Ca_V2.1$ channels in melanotropes. (A) demonstrates localization of splice variants of $Ca_V2.1$ channels in the IL of pituitary gland; (B) shows immunostaining of melanotropes in the IL; (C) colocalization between splice variants of $Ca_V2.1$ channels and melanotropes. (D, E and F) Representative region of interest showing enlarged images for image A, B and C, respectively. (G) Immunostaining of the selective $Ca_V2.1$ antibody in the IL and NH. (H) Nuclear staining of melanotropes in the IL. (I) Overlaid images of (G) and (H) showing that there is no positive staining of the selective $Ca_V2.1$ antibody in the IL. (J, K, and L) Enlarged image of (G), (H), and (I) in the IL area, respectively. Scale bar = 40 μm.

-

4.2.3 Expression of the $Ca_V2.2$ splice variants in the SON and NH

Splice variants of the $Ca_V2.2$ (N-type) Ca^{2+} channel lacking portions of the II-III loop have not been identified in rat, and I therefore used the nested RT-PCR strategy described above (Rajapaksha et al 2008) to determine whether such variants are expressed in rat tissues. In addition, antibodies directed against the synprint site and the C-terminus of the $Ca_V2.2$ channel are commercially available, which enables us to employ the immunological strategy described above for the $Ca_V2.1$ channel variants to test for the expression of splice variants of $Ca_V2.2$ channels.

As Figure 4.24A shows, the synprint site is a fragment covering 2319-2577bp (773-859 amino acid) of cDNA of the $Ca_V2.2$ channels (Rettig et al 1996; Sheng et al 1994). I firstly ran PCR to confirm the validity of cDNA template by testing GAPDH, and all the cDNA samples used in the following experiments were housekeeping gene positive. Then, nested PCR was performed using primers DFc02 and DRc02. Two amplified fragments of 362 and 425 bp were detected and separated by gel electrophoresis (Figure 4.24B). The PCR products were isolated, purified, and sequenced. This 362 bp PCR product is the fragment of the wild type $Ca_V2.2$ channels within the synprint site, and the 425 bp fragment represents an isoform containing a 21-amino acid cassette (e[18a+]) insertion in the synprint site between domains IIS6 and IIIS1 (e[18a+]), which is consistent with the $Ca_V2.2$ channel isoforms expressed

in the monoaminergic neurons of the rat brain (Ghasemzadeh et al 1999). In our case, I tested different brain areas, and this splice variant is observed in the SON and pituitary gland (Figure 4.24B).

Then, I used another pair of primers (DFc02-DRc03, 2072-2836) that were designed for amplifying the whole synprint site. Two bands of 765bp and 828 bp were detected, suggesting an isoform containing the entire synprint site might be the predominant form of the $Ca_V2.2$ channels present in the rat brain (Figure 4.24C). The full-length $Ca_V2.2$ channels were also detected in SON, pituitary glands and PC12 cell lines. Although it is still possible that other splice variants within II-III loop exist, for example, if the alternative splicing starts beyond the sequence of the II-III loop, then the primers I chose could not identify the deletion**.** I only focused on a very narrow segment that is closely related to the synprint site, and did not find any evidence for the II-III loop deletion vatiants of $Ca_V2.2$ channels.

A. Illustration of RT-PCR primer locations for amplification of the synprint site of $Ca_V2.2$ channels.

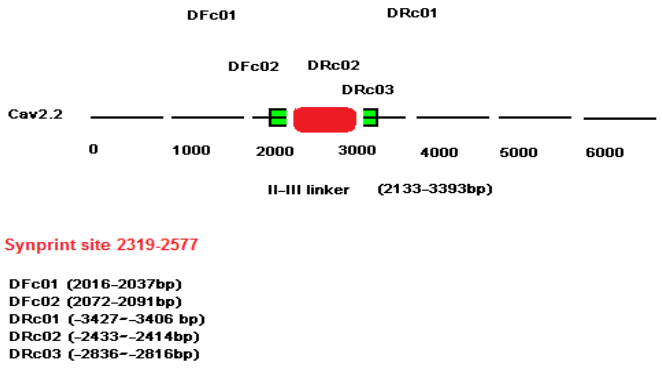

B. PCR results for a fragment of the synprint site of $Ca_V2.2$ channel.

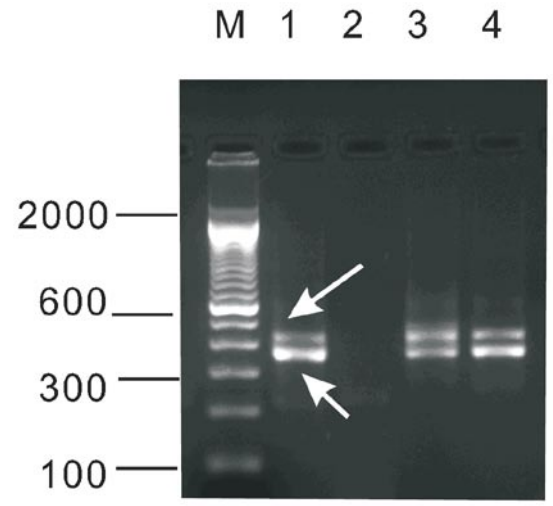

C. PCR results for full sequence of synprint site of $Ca_V2.2$ channel.

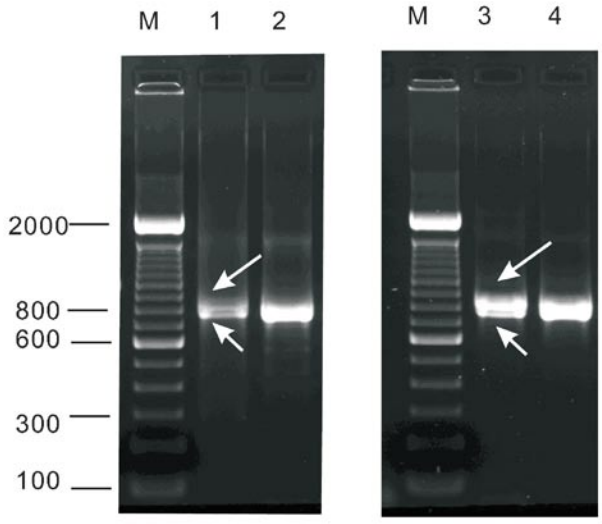

Figure 4.24 RT-PCR results of screening synprint site deletion isoform(s) of $Ca_V2.2$ channels. A) Illustration of primer design for amplifying regions contain synprint site within II-III loop of $Ca_V2.2$ channels. B) Representative PCR results for segment of synprint site of $Ca_V2.2$ channels) representative DNA gel image showing that PCR product of $Ca_V2.2$ channels contain full-length synprint site. Lane 1, whole brain; lane 2, pituitary gland; lane 3, PC12 cells; Lane 4, SON.

Further, I also performed immunocytochemistry using the selective and inclusive $Ca_V2.2$ antibodies to study channel expression at the protein level. Acutely isolated MNCs showed clear plasma membrane staining by both selective and inclusive antibodies of $Ca_V2.2$ channels. This is different from what we saw in $Ca_V2.1$ channels, suggesting the antibodies directed against different portion of the channels recognized an isoform that contains synprint site (Figure 4.25 A-D). I also did immunocytochemistry for hippocampal neurons, here as positive control because this model has been investigated intensively and reported that hippocampal neurons express $Ca_V2.2$ channels that contain the full-length synprint site. As we can see in Figure 4.25 E-H, two antibodies for $Ca_V2.2$ had same pattern of immunostaining on the plasma membrane of these cells. PC12 cells were used as a neuroendocrine cell model to test whether deletion variants of $Ca_V2.2$ channels are expressed. Not surprisingly, the similar pattern of staining observed in the Figure 4.25I-L further proved that the $Ca_V2.2$ channels in neuroendocrine cells contain full-length $Ca_V2.2$ channels.

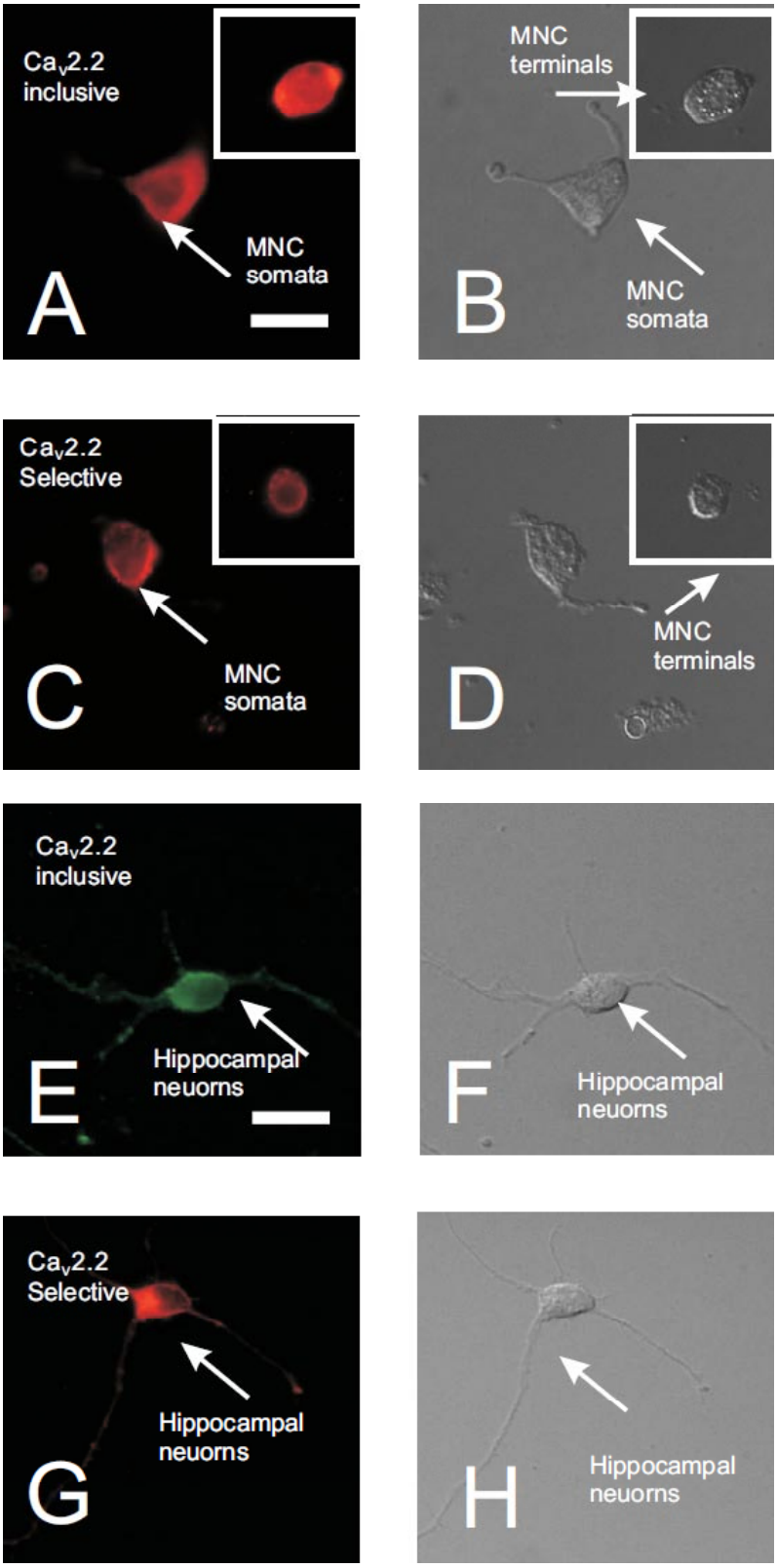
Cav2.2
inclusive
MNC
somata
A
MNC
terminals
MNC
somata
B
Cav2.2
Selective
MNC
somata
C
MNC
terminals
D
Cav2.2
inclusive
Hippocampal
neuorns
E
Hippocampal
neuorns
F
Cav2.2
Selective
Hippocampal
neuorns
G
Hippocampal
neuorns
H

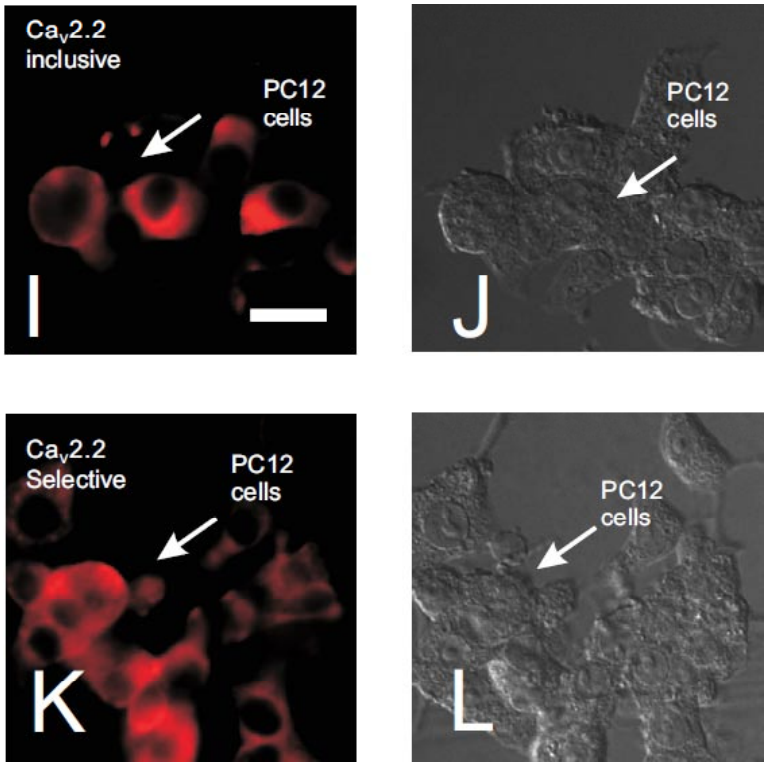

Figure 4.25 Localization of $Ca_V2.2$ channels in soma and nerve terminals of acutely isolated MNCs, and cultured hippocampal neurons and PC12 cell lines. Three sets of immunocytochemistry were done using both selective and inclusive $Ca_V2.2$ antibodies to test the localization of $Ca_V2.2$ channels in soma and terminals of isolated MNCs, hippocampal neurons and PC12 cells. (A) Plasma membrane distribution of $Ca_V2.2$ channels stained by inclusive $Ca_V2.2$ antibody in isolated MNCs (isolated nerve ending of MNCs from the NH were also stained with the same antibody, shown at the upper right corner) (B) DIC images showing an isolated MNC and one of the nerve endings. (C) Similar plasma membrane distribution $Ca_V2.2$ channels stained by selective antibody. (D) DIC images of single MNC. (E) $Ca_V2.2$ channels recognized by inclusive $Ca_V2.2$ antibody expressed on the plasma membrane of hippocampal neurons. (F) DIC images for hippocampal neurons labeled by the inclusive $Ca_V2.2$ antibody. (G) Membrane staining of the $Ca_V2.2$ selective antibody showed similar pattern as that of the inclusive antibody. H) DIC image for hippocampal neurons labeled by the selective antibody. (I) $Ca_V2.2$ channels stained in

PC12 cells by the inclusive antibody. (J) A DIC image of PC12 cells labeled in (I); (K) Similar membrane staining was observed in PC12 cells by the inclusive $Ca_V2.2$ antibody. (L) A DIC image of PC12 cells labeled in (K); Scale bar =20 μm.

Immunohistochemistry was also performed on rat brain and pituitary slices to test the expression of splice variants distribution of $Ca_V2.2$ channels *in situ*. Immunostaining of the inclusive $Ca_V2.2$ antibody and neurophysin I and II antibodies were perfomed using brain slices containing SON. Figure 4.26A and 4.26D show the locations of $Ca_V2.2$ channels labeled by the inclusive antibody, and Figure 4.26B and 4.26E show the location of MNCs in the SON. I found that the inclusive $Ca_V2.2$ antibody is colocalized with neurophysin I and II antibodies. Alternatively, I did another immunostaining using the selective $Ca_V2.2$ antibody and the neurophysin I and II antibodies. As the Figure 4.26G and 4.26J show, the selective antibody labels the cellular components within the SON. Figure 4.26H and 4.26K show the MNCs that are labeled by neurophysin I and II. I found that the immunostaining of selective $Ca_V2.2$ antibody is colocalized with those of neurophysin I and II antibodies, suggesting that the two types of MNCs express the same isoform of $Ca_V2.2$ channels. These data also supports the hypothesis that $Ca_V2.2$ channels on MNCs have the full-length synprint site.

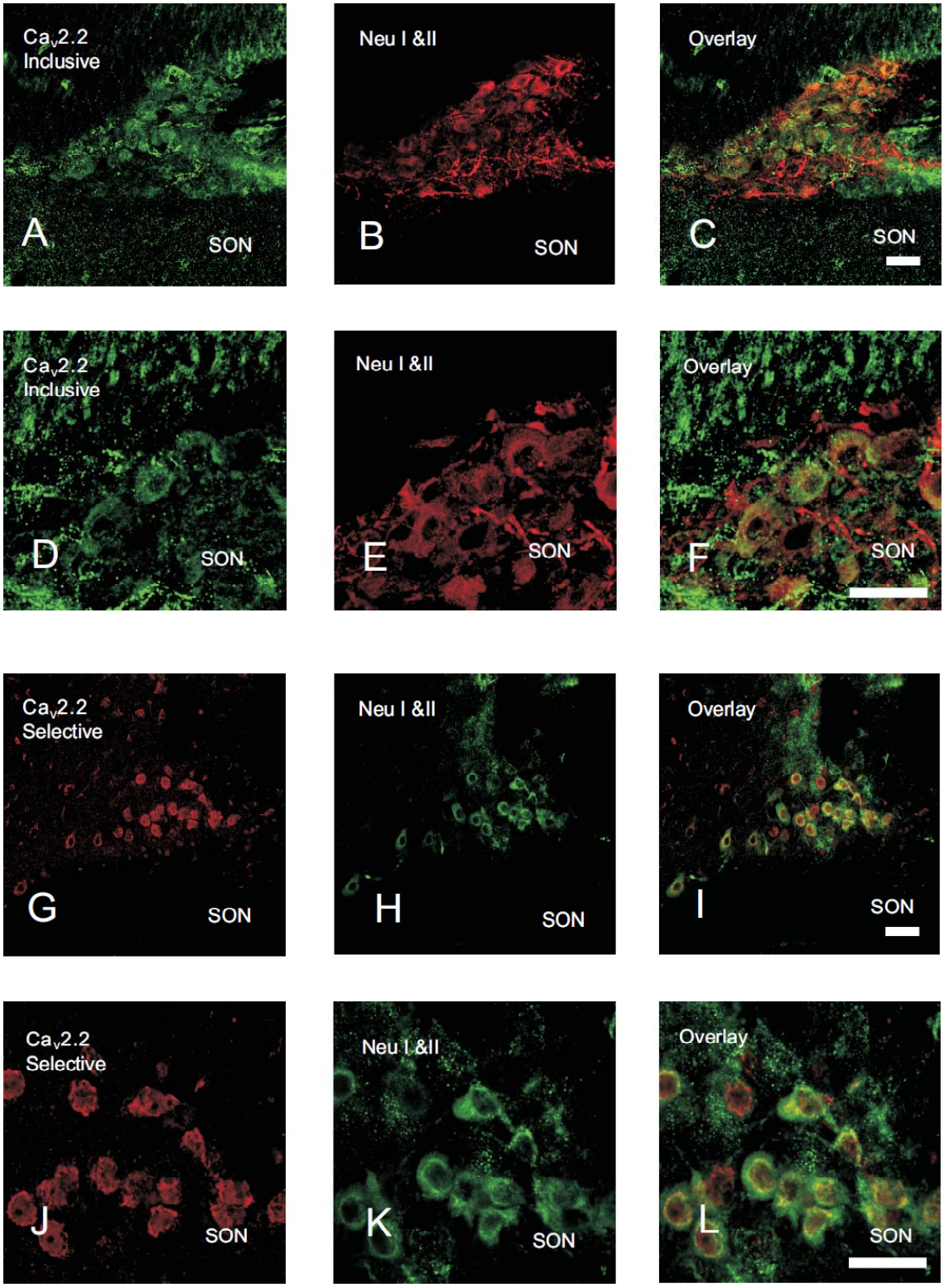

Figure 4.26 Distribution of $Ca_V2.2$ channels in the SON. Immunostaining of inclusive $Ca_V2.2$ antibody and neurophysin I and II was performed using brain slices.

(A and D) $Ca_V2.2$ channels revealed by inclusive antibody have somatic staining and synaptic staining in the SON. (B and E) MNCs stained by neurophysin I and II in the SON. (C and F) coloalization of $Ca_V2.2$ channels and MNCs. Immunostaining of selective $Ca_V2.2$ antibody with neurophysin I and II was performed using brain slices. (G and J) Expression of $Ca_V2.2$ channels revealed by the selective antibody shows a similar pattern of immunofluorescence in the SON. (H and K) MNCs stained by neurophysin I and II. (I and J) colocalization between $Ca_V2.2$ channels and MNCs, and some $Ca_V2.2$ positive cells other than MNCs. Scale bar = 40 μm

Finally, a comparison of immunofluorescence between the selective and inclusive $Ca_V2.2$ antibodies was conducted using pituitary slices containing the IL. As Figure 4.27A and D show, the two antibodies both label the periphery of melanotropes residing in the IL. Figure 4.27B and 4.27E show the nuclear staining of IL slices. Selective and inclusive antibodies have similar patterns of immunostaining on the melanotropes (Figure 4.27C and 4.27F), which suggests that melanotropes express $Ca_V2.2$ channels with the synprint site.

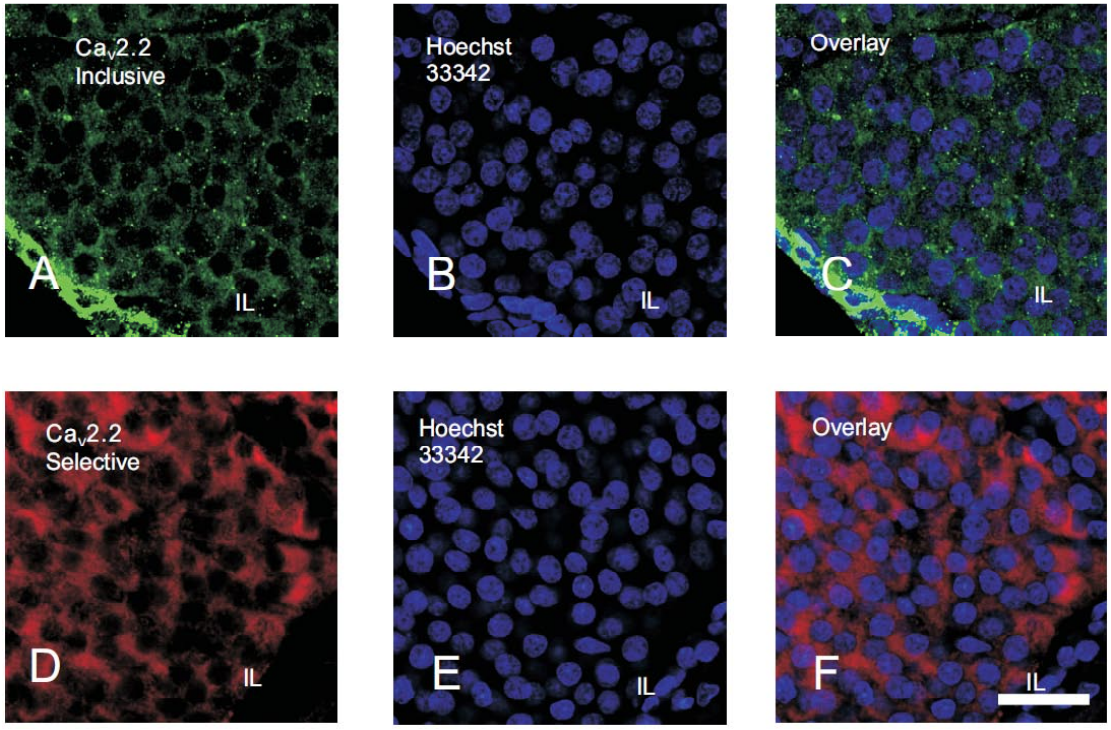

Figure 4.27 α-MSH releasing melanotrophs in the IL of the pituitary express the full-length $Ca_V2.2$ channel. (A) $Ca_V2.2$ channels revealed by the inclusive antibody have somatic staining in the IL. (B) Nuclear staining of cells in the IL, which demonstrates the location of melanotropes. (C) An overlaid image from image (A) and (B), showing the melanotropes can be stained by the inclusive $Ca_V2.2$ antibody. (D) Expression of $Ca_V2.2$ channels revealed by the selective antibody shows a similar pattern of immunofluorescence in the IL. (E) Nuclear staining of melanotropes by Hoechst 33342. (F) Overlaid images of (D) and (E), showing that the selective $Ca_V2.2$ antibody labels the same membrane structures of the melanotropes as the inclusive antibody does; Scale bar = 40 μm.

In brief summary, the systemic screening of the synprint site could not find an evidence for the existence of deletion variants of $Ca_V2.2$ channels in MNCs and

melanotropes, as we have detected for $Ca_V2.1$ channels. These data suggests that the alternative splicing of the II-III loop that occurs in $Ca_V2.1$ may not occur in $Ca_V2.2$.

4.2.4 Terminal targeting of the $Ca_V2.2$ channels in differentiated PC12 cells.

To test possible targeting mechanism of $Ca_V2.2$ channels in neuroendocrine cells, I chose a molecular event that is important for forming the exocytotic machinery and terminal structure, and then try to interrupt or inhibit this process to see if the channel targeting or distribution could be altered. Adaptor modular proteins CASK and Mint1 have been found to bind with $Ca_V2.2$ channels *in vitro* (Maximov et al 1999). I therefore aimed to test the role of CASK in $Ca_V2.2$ targeting in PC12 cells. Previously, Xiaoyu Xu in our lab tested the expression of CASK in primary cell culture of bovine chromaffin cells. Co-immunoprecipitation also proved the interaction between CASK and $Ca_V2.2$ using endogenous membrane protein extracts from chromaffin cells. I then used green fluorescent protein (GFP) tagged constructs encoding partial sequences of carboxy-terminus of $Ca_V2.2$, namely, GFP-NC3 to competitively interrupt this interaction. To develop a model that can make possible the observation of neuroendocrine terminal targeting using DNA transfection, I used differentiated PC12 cell lines that can effectively express these constructs to test our hypothesis. As Figure 4.28A and 4.28B show, I hypothesize that by blocking the interaction between CASK

and $Ca_V2.2$ channels, the targeting of channels to the growth cones of PC12 cells will be inhibited.

A

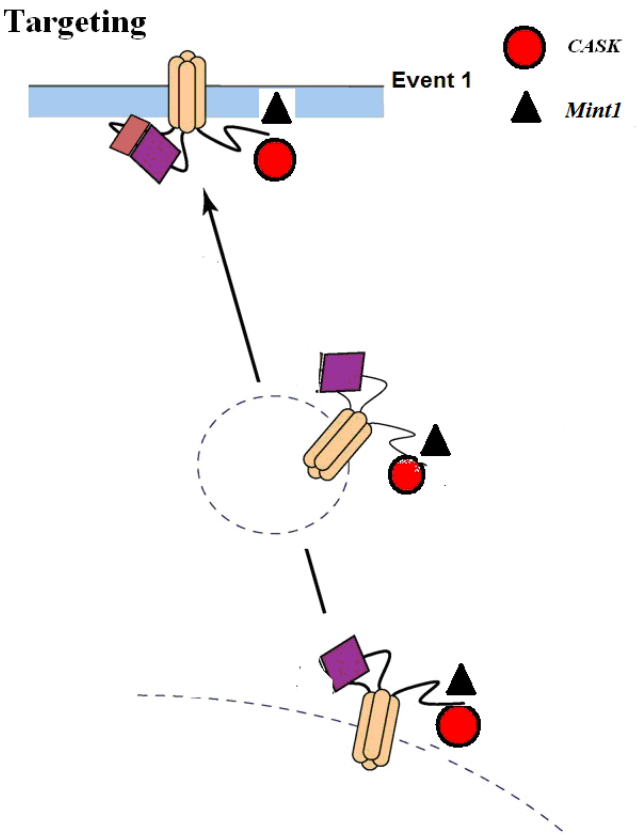

B

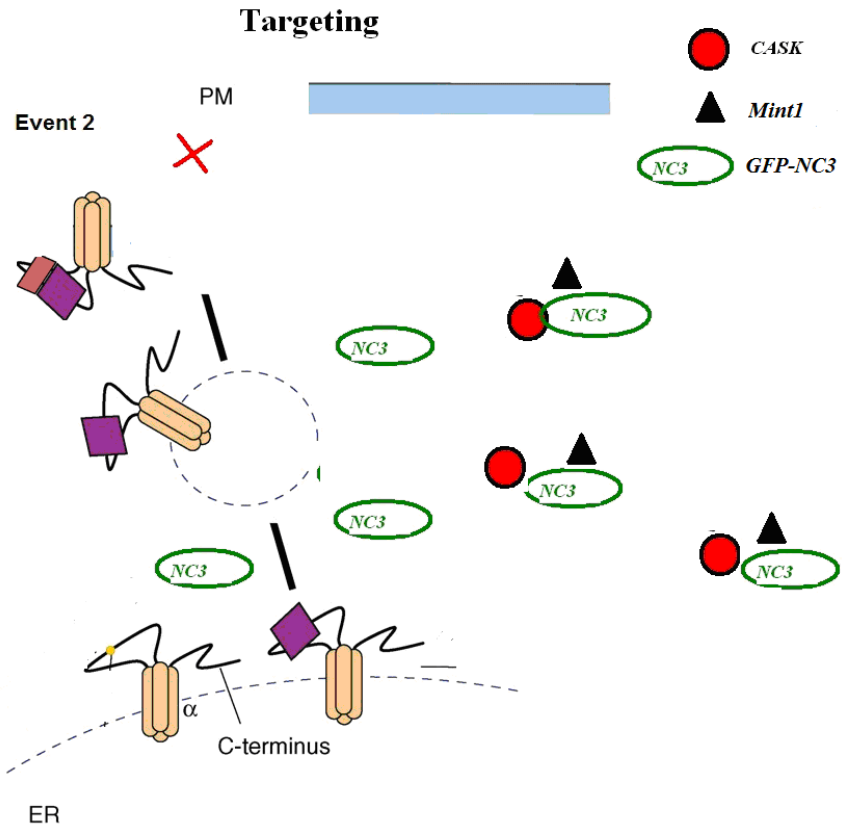

Figure 4.28 Illustration of interaction between CASK and the $Ca_V2.2$ channel. A) $Ca_V2.2$ channels can be successfully targeted to the plasma membrane of PC12 cells when CASK/Mint1 is bound with $Ca_V2.2$ channels. B) When the NC3 peptide is overexpressed, the NC3 peptide binds with CASK/Mint1 and prevents the binding of CASK/Mint1 to the $Ca_V2.2$ channels, and prevents channel targeting to the plasma membrane.

Previously, Xiaoyu Xu and I performed transfection of GFP-NC3 into undifferentiated bovine chromaffin cells (BCCs), the plasma membrane clustering of $Ca_V2.2$ channels was altered, and channels formed a dispersed pattern of distribution (some data have been shown in Xiaoyu Xu's thesis). This data suggested the function of CASK as a protein to anchor $Ca_V2.2$ channels. However, the BCCs are difficult to

transfect with exogenous expression plasmids, they tend to not display long processes, and have relatively short lifespans in culture. PC12 cell lines have several advantages to improve those conditions for terminal targeting research. Figure 4.29A shows a GFP-NC3 expression PC12 cell, and $Ca_V2.2$ expression in the growth cones of this cell can be quantified (Figure 4.29B-D). Consistently, the distribution of $Ca_V2.2$ channels was significantly decreased (>40% in comparison with controlled cells, $p<0.01$) in the growth cones of PC12 cells after transfection of GFP-NC3 (Figure 4.29B). In contrast, transfection of the GFP plasmid without the NC3 coding segment did not change the $Ca_V2.2$ channel distribution (<10% decrease for the GFP-NC3 positive group, and not statistically significant, $p>0.05$; Figure 4.29C).

A

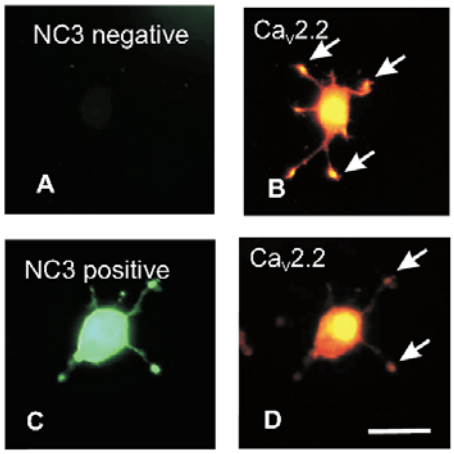

B

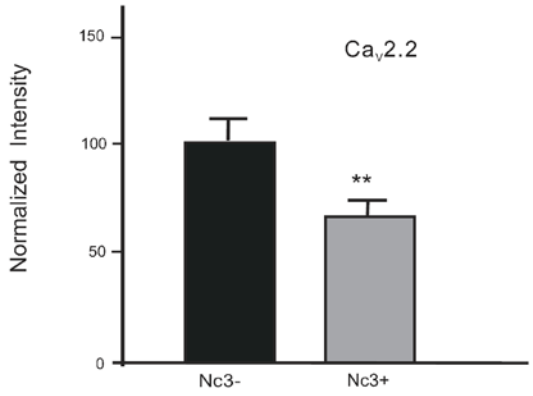
Normalized Intensity
150
100
50
0
$Ca_V2.2$
**
Nc3-
Nc3+

C

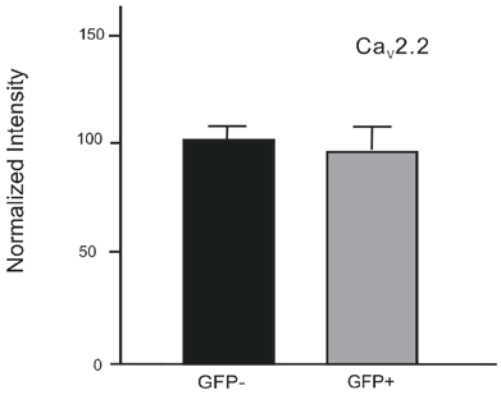
Normalized Intensity
150
100
50
0
$Ca_V2.2$
GFP-
GFP+

D

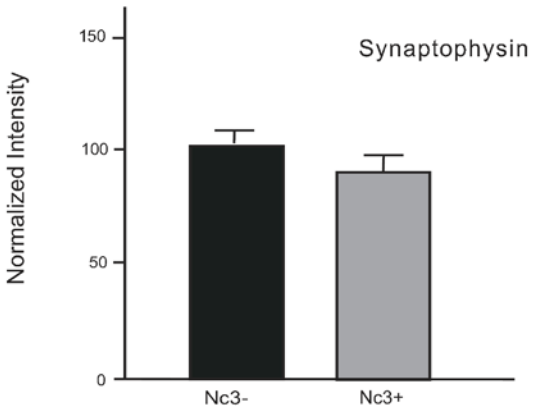
Normalized Intensity
150
100
50
0
Synaptophysin
Nc3-
Nc3+

Figure 4.29 GFP-NC3 inhibitory peptides significantly decreased the terminal targeting of $Ca_V2.2$ channels in differentiated PC12 cells. A) Representative images showing the immunofluorescence of $Ca_V2.2$ channels on the growth cones of GFP-NC3 positive and GFP-NC3 negative PC12 cells. B) $Ca_V2.2$ targeting in the neurite-like terminal was significantly decreased by expressing GFP-NC3 (black bar n=20 for NC3 negative control; grey bar n=27 for NC3 positive PC12 cells, >40% decrease $p<0.01$). C) GFP control plasmid has no effect on $Ca_V2.2$ targeting (black bar GFP negative control n=18; grey bar GFP positive PC12 cells n=12, $p>0.05$). D) GFP-NC3 does not affect granule biosynthesis in the terminals (black bar NC3 negative n=15; grey bar n=12 NC3 positive PC12 cells, $p>0.05$). Scale bar = 20 μm.

To test whether this decreased distribution of channel was due to the inhibited secretory vesicle biosynthesis, I used the synaptophysin antibodies to label the secretory vesicle (Takamori et al 2006). Neither plasma membrane nor terminals of growth cones showed significant changes of synaptophysin immunostaining in the GFP-NC3 positively transfected cells in comparison with control cells (Figure 4.29D). These results suggested that overall protein expression level of the granules was not changed by overexpressing blocking peptide, and the inhibitory effects of NC3 peptide is selective to $Ca_V2.2$ channels. These results suggest CASK may not only anchor $Ca_V2.2$ channel at hormone releasing sites (Maximov et al 1999), but exert a regulatory role in sorting the channel into nerve terminals of neuroendocrine cells.

Summary and brief discussion for Section 4.2

In this study, I tested the expression and distribution of $Ca_V2.1$ and $Ca_V2.2$ channels in neuroendocrine cellular models, and studied the alternative splicing of these channels within the II-III loop that have important roles in channel targeting and function.

First, two splice variants that lack large portion of II-III loop of $Ca_V2.1$ channels have been detected by RT-PCR ($Ca_V2.1$-Δ1 and $Ca_V2.1$-Δ2 that have 155 and 194 amino acid deletions, respectively) in different brain tissues of the rat. Single cell RT-PCR also detected the presence of these two splice variants in the MNCs. Immunocytochemistry was performed to study the distribution of channels in isolated MNCs. I found the splice variants expressed on the plasma membrane of the MNCs and PC12 cells, whereas the isolated hippocampal neurons appear to express only the wild type channels. The observation of nerve terminal distribution of the splice variants in MNCs suggested that the synprint site may not be necessary for the axonal targeting of $Ca_V2.1$ channels in these neuroendocrine cells.

Second, I performed immunohistochemistry to test the tissue distribution of splice variants within the hypothalamus and neurohypophysis of rats. In the SON of hypothalamus, I found the immunostaining of $Ca_V2.1$ channels in the somata of MNCs showed cell-type specificity. The OT-MNCs express few or no $Ca_V2.1$

channels whereas VP-MNCs do express $Ca_V2.1$ channels. The immunostaining of the $Ca_V2.1$ inclusive antibody shows the splice variants of $Ca_V2.1$ lacking the synprint site may be expressed solely on the VP-MNCs.

In the neurohypophysis, the immunostaining of wild type $Ca_V2.1$ channels was largely colocalized with the synaptic vesicle marker, synaptophysin, which suggested that the $Ca_V2.1$ channels may be predominantly expressed in synaptic terminals (Hatton 1988; Hussy 2002). Colocalization of OT and VP markers and inclusive antibody of $Ca_V2.1$ for splice variants suggested the main forms of $Ca_V2.1$ expressed on the nerve terminals of MNCs were the synprint site deleted form. The expression of the splice variants of $Ca_V2.1$ channels in melanotropes of the intermediate lobe was also detected, suggesting that this type of $Ca_V2.1$ alternative splicing may be present in other endocrine cells (Mansvelder et al 1996; Williams et al 1993).

Third, I tested whether the synprint site deletion variants of $Ca_V2.2$ channels are expressed on MNCs using the same RT-PCR and immunohistochemical methods. RT-PCR results showed that all the detectable isoforms ($Ca_V2.2$ e[18a+] and $Ca_V2.2$ e[Δ18a]) of $Ca_V2.2$ channels expressed full-length synprint site in the rat brain tissues. I also found that both the selective and inclusive antibodies for $Ca_V2.2$ channels had similar staining in the somata of MNCs and melanotropes, suggesting the deleted splice variants are not expressed in these neuroendocrine cells. These data also

suggest that alternative splicing of the synprint site in Ca_V2 channels is specific for only $Ca_V2.1$ channels in these neuroendocrine cells.

Fourth, I studied targeting properties of full length Cav2.2 channels in an *in vitro* chromaffin cell model. I found that the terminal targeting of $Ca_V2.2$ channels are regulated by the interaction of CASK and the C-terminus of $Ca_V2.2$ channels.

5. GENERAL DISCUSSION

5.1 VGCCs expressed in the glial cells of the neurohypophysis

5.1.1 Ca^{2+} signaling in pituicytes and cortical astrocytes

It is clear that the elevation of intracellular $[Ca^{2+}]_i$ of glial cells is important for glial–neuronal interactions. Early studies showed that glutamate could trigger elevation of $[Ca^{2+}]_i$ in cultured astrocytes, which could propagate through individual and even between glial cells (Cornell-Bell et al 1990). Further evidence demonstrated that the increased $[Ca^{2+}]_i$ could evoke a $[Ca^{2+}]_i$ rise in surrounding neurons (Attwell 1994; Parpura et al 1994). These findings suggest a new model of functional synapse consisting of glial cells, presynaptic and postsynaptic neuronal elements (Hamilton & Attwell 2010; Perea et al 2009).

Elevations of intracellular Ca^{2+} could result from release from intracellular stores or from influx through Ca^{2+} channels of the plasma membrane. It was thought that the Ca^{2+} release from intracellular stores was the only mechanism. Thapsigargin, which depletes the internal Ca^{2+} store of ER, potently reduces Ca^{2+} dependent glutamate release (Hua et al 2004). Diphenylboric acid 2-aminoethyl ester (2-APB), a cell-permeant IP_3 receptor antagonist, greatly reduced exocytotic glutamate release from astrocytes, suggesting the importance of internal Ca^{2+} stores in gliotransmission (Hua et al 2004).

Elevation of the $[Ca^{2+}]_i$ in pituicytes has been observed when pituicytes are stimulated by VP (Hatton et al 1992). Hatton and colleagues found that VP (10-20 nM) could cause a reliable $[Ca^{2+}]_i$ oscillation in cultured pituicytes, whereas isotonic addition of K^+ (25-50 mM) was not able to activate $[Ca^{2+}]_i$ oscillations. Their results suggested that VP but not OT receptor activation in pituicytes can trigger an intracellular $[Ca^{2+}]$ release from intracellular Ca^{2+} stores. This phenomenon has been observed in other cell types that express V_1 receptors such as hepatocytes and fibroblasts (Harootunian et al 1991; Kawanishi et al 1989). The sensitivity of VP concentrations for $[Ca^{2+}]_i$ were quite different though (0.1 nM in hepatocytes and 50 nM in fibroblasts, respectively). Although cultured pituicytes express V_1 receptors, the expression of V_1 receptors in pituicytes *in vivo* is controversial. It has been reported that $[^3H]$ VP binding in the NL is not specific (Freund-Mercier et al 1991; Tribollet et al 1988; Phillips et al 1990; van Leeuwen et al 1987), which may rule out a role for VP in triggering the $[Ca^{2+}]_i$ oscillations in pituicytes *in vivo*.

Some recent observations from astrocytes contradicted the notion that intracellular stores are the sole sources responsible for intracellular $[Ca^{2+}]$ increase. If the intracellular release of Ca^{2+} plays a major role in the process of gliotransmitter release, inhibiting the IP_3 or RyR receptors should affect synaptic function. A recent study using IP_3 receptor knockout mice, however, failed to see an impaired synaptic

plasticity of hippocampal neurons (Agulhon et al 2010). The researchers used IP_3R2 knockout mice to specifically inhibit Gq G-protein coupled receptor (GPCR) Ca^{2+} signaling of astrocytes (Fiacco et al 2007). $MrgA1^+$ transgenic mice were also used, which express the MrgA1 gene only in astrocytes to enable an astrocytic-specific activation of Gq GPCR Ca^{2+} signals. Both activation and inactivation of intracellular Ca^{2+} signaling pathways showed no significant effects on synaptic function, thus challenging the role of Ca^{2+} elevation induced by IP_3 receptors for gliotransmission (Kirchhoff 2010). Additionally, there is also a lack of evidence showing the functionality of RyR receptors mediating intracellular Ca^{2+} release in astrocytic activity *in vivo* (Beck et al 2004). These observations suggest that other channels such as VGCCs or transient receptor protential (TRP) channels may be responsible for Ca^{2+}-dependent gliotransmission (Kirchhoff 2010).

Some evidence suggests that elevations of the $[Ca^{2+}]_i$ in glial cells can be mediated by VGCCs. MacVicar and colleagues found that a 3-4 fold increase of $[Ca^{2+}]_i$ was evoked by extracellularly adding 50mM of K^+ in cultured cortical astrocytes, and this increase could be blocked by a selective L-type Ca^{2+} channel blocker (MacVicar et al 1991). Electrophysiological evidence of L-, N- and R-type Ca^{2+} currents has been recorded in cultured cortical astrocytes using whole-cell patch-clamp and single channel recording (D'Ascenzo et al 2004). In these experiments, the L-type Ca^{2+} channel blocker nifedipine (5 μM) reduced HVA Ba^{2+} current amplitude by 28%, the

N-type selective blocker ω-conotoxin-GVIA (3μM) produced a further 32% decrease and the R-type blocker SNX-482 (100 nM) contributed to 34% reduction (D'Ascenzo et al 2004). These results indicate that cultured cortical astrocytes may express VGCCs with properties resembling those in neurons.

My data demonstrate that VGCCs are expressed in pituicytes in culture. Many subtypes of VGCCs were detected using immunocytochemistry, namely $Ca_V2.1$ (P/Q-type), $Ca_V2.2$ (N-type), $Ca_V1.2$ (L-type), $Ca_V2.3$ (R-type) and $Ca_V3.1$ (T-type), but not $Ca_V1.3$ (L-type). Differential expression of the two types of L-type Ca^{2+} channels may reflect a functional difference between $Ca_V1.2$ and $Ca_V1.3$ channels. The expression of Ca^{2+} channel α1 subunits in cultured pituicytes was different than that seen in cultured cortical astrocytes (Latour et al 2003), which were reported to express $Ca_V2.2$, $Ca_V1.2$, $Ca_V1.3$, $Ca_V2.3$ and $Ca_V3.1$, but not $Ca_V2.1$.This difference may reflect a difference between glial cells obtained from neonatal and adult rats, or a difference between cortical astrocytes and pituicytes.

My observation that pituicytes express the $Ca_V2.2$ and $Ca_V2.3$ Ca^{2+} channels *in situ* provide evidence of VGCC expression in glial cells in the pituitary gland (Wang et al 2009). Immunoreactivity for $Ca_V2.2$ Ca^{2+} channels has been observed in astrocytes in the SON (Joux et al 2001). The $Ca_V2.2$ channels in astrocytes in the SON are predominantly located in astrocytic processes (Joux et al 2001). The immunostaining

of $Ca_V2.2$ channels in pituicytes show no preference for either the processes or somata (Figure 4.3B), whereas the $Ca_V2.3$ channels are mainly expressed in the somata of the pituicytes (Figure 4.3E). The relatively high expression level of $Ca_V2.3$ channels may represent the unique properties of pituicytes, for example, the $Ca_V2.3$ channels may be important to maintain a low basal release probability of gliotransmitters from glial cells. It is not known whether the $Ca_V2.2$ and $Ca_V2.3$ channels play a role in the osmotically-evoked morphological changes of pituicytes or whether they are involved in the osmotically regulated taurine release from pituicytes.

5.1.2 L-type Ca^{2+} channels are up-regulated in the pituicytes during dehydration

To test the hypothesis that the L-type Ca^{2+} channels are related to MNC functions, I measured the changes of expression levels of different VGCCs (including the $Ca_V1.2$ and $Ca_V1.3$ channels) in pituicytes after dehydration. Our data showed that the expression of the $Ca_V1.2$ Ca^{2+} channels was selectively increased in the pituicytes *in vivo* after 24 hour dehydration in rats.

The $Ca_V1.2$ channel regulation could be important in initiating $[Ca^{2+}]$ oscillations in glial cells (Fiacco & McCarthy 2006). If Ca^{2+} influx is involved in the activation of exocytotic release from glia, increased L-type Ca^{2+} channels expression could contribute to the activation of the release of excitatory gliotransmitters or modulators such as glutamate (Montana et al 2006) and D-serine (Mothet et al 2005). There is

some other evidence supporting that L-type Ca^{2+} channels may contribute to astrocytic $[Ca^{2+}]_i$ oscillation *in vivo* (Parri et al 2001). Parri and colleagues found nifedipine (1 μM) causes a marked reduction in astrocytic activity in the thalamus and the $[Ca^{2+}]_i$ oscillation was virtually abolished by the non-specific Ca^{2+} channel blocker, Co^{2+} (1 mM). In addition, the Ca^{2+} oscillation could be abolished by removing extracellular Ca^{2+}, or using thapsigargin (1 μM), to deplete the intracellular store, suggesting the underlying mechanism of Ca^{2+} oscillation observed in astrocytes *in vivo* involves $[Ca^{2+}]_i$ release with a possible dependence on plasma membrane L-type Ca^{2+} channels (Parri & Crunelli 2003; Parri et al 2001).

Increased L-type Ca^{2+} channel expression has been observed during various forms of neural damages, including ischemia (Westenbroek et al 1998a), hypoxia (Hirenallur et al 2008), or chronic stress (Zhao et al 2009). The L-type Ca^{2+} channel regulation may also be involved with adaptation of neuroendocrine system during dehydration. Previously, an increase in the density of L-type Ca^{2+} currents in the acutely isolated MNC somata of dehydrated rats has been observed in our lab using electrophysiology (Zhang et al 2007). Pituicytes undergo a remarkable structural and function reorganization during periods in which the need for VP or OT release is high (Hussy 2002; Rosso & Mienville 2009). The increased expression of the $Ca_V1.2$ Ca^{2+} channels in pituicytes might be part of a broader functional adaptation that involves changes in the MNCs themselves (Hatton 1997; Theodosis & MacVicar 1996).

An increase in Ca^{2+} influx through $Ca_V1.2$ could have other functions such as gene transcription. In neurons, $Ca_V1.2$ has a privileged function in the activation of the CREB signal pathway that triggers gene transcription and translation (Deisseroth et al 2003). The proliferation of pituicytes has been reported in adult rats after 72h of water deprivaton (Murugaiyan & Salm 1995), and it is possible that the activation of $Ca_V1.2$ signaling could occur in pituicytes, leading to an increase in expression of specific proteins during dehydration.

In conclusion, the data obtained in this study shows that pituicytes *in situ* express $Ca_V2.2$ and $Ca_V2.3$ Ca^{2+} channels and that there is an increase in the expression of $Ca_V1.2$ during water deprivation. These data suggest that Ca^{2+} influx through VGCCs plays a role in pituicyte function and in particular during periods of high hormone demand. The increase in $Ca_V1.2$ may be involved in the adaptation of the neurohypophysis to allow a sustained facilitation of hormone release.

5.2 Splice variants of the $Ca_V2.1$ channels lacking the synprint site are expressed in neuroendocrine cells

5.2.1 The regulation of the synprint site in fast neurotransmission and hormone release

The identification of the splice variants that lack large portion of the synprint site of the $Ca_V2.1$ channels may help us understand some aspects of Ca^{2+}-dependent exocytosis in neuroendocrine cells.

First, the proteins that interact with the synprint site, such as syntaxins, SNAP, and synaptotagmins, are important for the spatial arrangement of the exocytotic machinery and the dynamics of neurotransmitter release upon Ca^{2+} influx (Chapman 2002; Chen & Scheller 2001). In typical presynaptic terminals, VGCCs and releasable SVs are likely to be within tens of nanometers (Meinrenken et al 2002). In neuroendocrine cells, the distance between the LDCVs and VGCCs is estimated to be hundreds of nanometers. If the physical interaction between the $Ca_V2.1$ channels and synaptic proteins in the LDCVs is lacking, LDCVs may be located further from Ca^{2+} channels and thus may result in lower release probabilities of the LDCVs compare to the SVs in neurons (McNeil & Wu 2009).

Second, the $Ca_V2.1$ channel properties of mediating Ca^{2+} will be altered due to the lack of binding with syntaxin and SNAP25. Syntaxin 1A (35KDa) binds with WT Ca_V2 channels via its C-terminus at the active zone of the nerve terminals (Bennett et al 1992; Leveque et al 1994; Sheng et al 1994). The WT Ca_V2 channels bind with syntaxin via the synprint site (which is between amino acid residues 722 and 1036 in $Ca_V2.1$; and amino acid residues 773 and 859 in $Ca_V2.2$). Syntaxin has functional impact on the gating properties of Ca_V2 channels. Co-expression of syntaxin 1A with the $Ca_V2.2$ channels in *Xenopus* oocytes sharply decreases the availability of these channels at a neuronal resting membrane potential near -75mV. For both the $Ca_V2.2$ and the $Ca_V2.1$ WT isoforms, overexpressing syntaxin 1A leads to a shift of the voltage-dependence of inactivation by -20 mV (Bezprozvanny et al 1995; Bezprozvanny et al 2000). This increasing inactivation is due to the stabilization of inactivation rather than inhibiting the expression of channels, because it can be reversed by strong hyperpolarization (Bezprozvanny et al 1995). The syntaxin binding only affects the $Ca_V2.1$ and $Ca_V2.2$ channels without changing the gating of Ca_V1 channels, and thus the syntaxin regulation of Ca_V2 channels is channel-specific and may be critical for precisely control of the fast neurotransmission at neuronal terminals (Bezprozvanny et al 1995; Wiser et al 1996). Co-expression of syntaxin did not shift the voltage-dependence of inactivation in either of the deletion isoforms of $Ca_V2.1$ channels we identified in the rat brain (Rajapaksha et al 2008), indicating a lack of syntaxin regulation in these two splice variants. These results may suggest that

the splice variants identified in my study may result in altered channel properties of $Ca_V2.1$.

Lack of the SNAP25 binding site of these $Ca_V2.1$ splice variants may also give rise to the change of channel activities. SNAP25 has been shown to bind to a motif of $Ca_V2.2$ between residues 781 and 789 (LRASCEALY) (Yokoyama et al 1995) and a highly homologous motif of $Ca_V2.1$ at residues 790-798 (LLASREALY). Interestingly, Snutch and colleagues have previously identified one $Ca_V2.1$ isoform (called rbA, rat brain class A, which is the old name of $Ca_V2.1$ channels, Snutch et al 1990; Starr et al 1991) that has a partial deletion of the synprint site. The rbA isoform could only bind with SNAP25 but not syntaxin *in vitro* by immunoprecipitation (Rettig et al 1996). In addition, the voltage-dependence of inactivation of the rbA isoform of $Ca_V2.1$ channels is shifted by SNAP25 but not by syntaxin (Zhong et al 1999), which is consistent with the *in vitro* binding results showing only the interaction between SNAP25 and the rbA isoform (Rettig et al 1996). SNAP25 binding causes a -10 mV negative shift in the voltage-dependence of inactivation of rbA, and it can be completely restored by co-expression of syntaxin, SNAP25 and synaptotagmin together (Zhong et al 1999). These data suggest a possible mechanism of this restoration of the negative shifted inactivation of $Ca_V2.1$ channels include other exocytotic components that interact directly with syntaxin (Bezprozvanny et al 1995; Zhong et al 1999).

Neither of the splice variants of the $Ca_V2.1$ channels found in this thesis, namely $Ca_V2.1$-Δ1 and Δ2, is the same with the rbA isoform. The synprint site is completely absent in $Ca_V2.1$-Δ1 and is severely truncated in $Ca_V2.1$-Δ2, making it unlikely that these variants interact with any of those synaptic proteins mentioned above *in vivo.* The electrophysiological properties of the splice variants were further investigated in Dr. Zamponi's lab at the University of Calgary. Both splice variants of $Ca_V2.1$ resulted in a positive shift in the voltage dependence of inactivation (Figure 5.1). Although the $Ca_V2.1$-Δ2 isoform resulted in currents that were similar in amplitude and biophysical properties to the full length channel, the $Ca_V2.1$-Δ1 variant yielded currents that were of much smaller amplitude, and displayed a much larger positive shift (~40 mV) compared with the ~6 mV positive shift in $Ca_V2.1$-Δ2 (Rajapaksha et al 2008).

A.

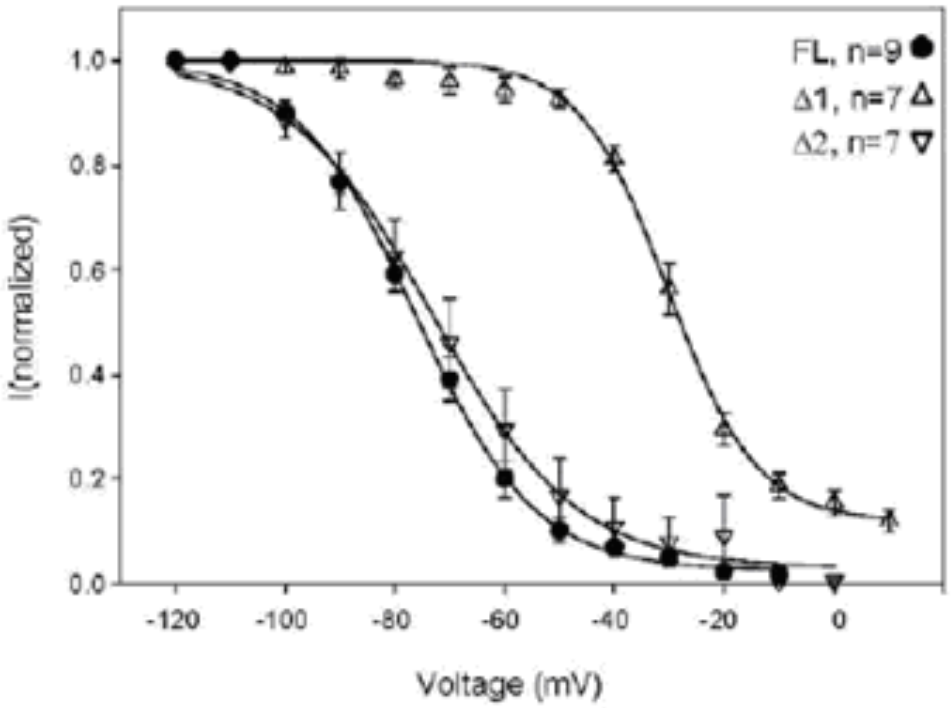
FL, n=9
Δ1, n=7
Δ2, n=7
I (normalized)
1.0
0.8
0.6
0.4
0.2
0.0
-120
-100
-80
-60
-40
-20
0
Voltage (mV)

B.

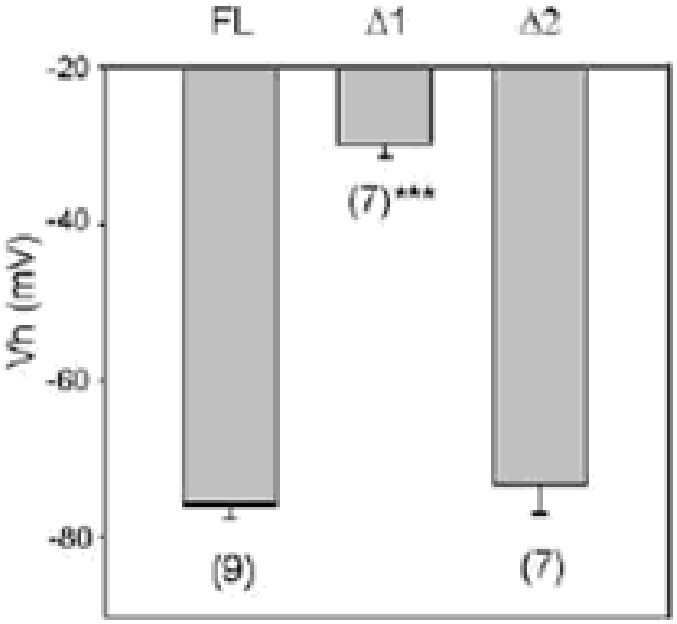
FL
Δ1
Δ2
-20
-40
-60
-80
Vh (mV)
(7)***
(9)
(7)

Figure 5.1 Steady-state inactivation curves obtained from the WT $Ca_V2.1$ channels and the splice variants. A. The steady-state inactivation curve of the $Ca_V2.1$-Δ1, $Ca_V2.1$-Δ2 and WT $Ca_V2.1$. The curve of the $Ca_V2.1$-Δ1 isoform was shifted toward a more depolarized voltage, whereas the $Ca_V2.1$-Δ2 isoform showed steady-state inactivation properties that were similar to those observed with WT $Ca_V2.1$. B. The bar graph illustrates half inactivation potentials determined from fits to individual steady-state inactivation curves. Numbers in parentheses reflect numbers of experiments (Electrophysiological recording was performed by Dr. Zamponi's lab at the Hotchkiss Brain Institute, University of Calgary; Reproduced with permission from Copyright Clearance Center).

The lack of synprint site of these two splice variants may also be implicated in the spatial arrangement between $Ca_V2.1$ channels and syntaptotagmin proteins. Synaptotagmins bind with the synprint site of Ca_V2 channels directly (Leveque et al 1994; Leveque et al 1992; Sheng et al 1997), and have been found to express abundantly on both SVs of neurons and LDCVs of neuroendocrine cells (Matthew et al 1981). Synaptotagmin binds with Ca^{2+} through its two functional C_2 domains (Chapman 2002; Sudhof 2006).

Neurons have both highly synchronous release (the fast form of neurotransmitter release that predominates in synapses during low-frequency action-potential firing, Schneggenburger and Neher 2005) and slower asynchronous release (a slower form of release that mediates synaptic transmission in some synapses during high-frequency action potential trains, Sun et al 2007). Neuroendocrine and endocrine cells, in

contrast, release hormone in a more asynchronous fashion. Different synaptotagmins may serve as Ca^{2+} sensors to trigger synchronous and asynchronous release (Gustavsson & Han 2009). Synaptotagmin-1 knockout mice showed a complete absence of synchronous neurotransmission (Geppert et al 1994; Maximov & Sudhof 2005). Similar to the hormone release in neuroendocrine cells, the deletion of synaptotagmin-1 specifically abolished the fast burst of LDCVs exocytosis in chromaffin cells, which suggests that the synaptotagmin-1 may be important for switching the slowly releasable state to a readily releasable state of the exocytotic machinery (Voets et al 2001).

Synchronous release is determined by proper positioning of the SVs (Forsythe et al 1998; Wadel et al 2007). Wadel and colleagues found that during short depolarization the slowly releasing vesicles experience $[Ca^{2+}]_i$ lower than 10 μM (at which level a normal fast release will be triggered during action potentials; Bollmann & Sakmann 2005; Bollmann et al 2000), suggesting the time-limiting process of synchronous fast release is the recruitment of releasable vesicles to the VGCCs. Regulation of vesicle positioning was proposed as a mechanism underlying the decrease of release probability (Wu et al 1999), which is not due to a decreased sensitivity of the Ca^{2+} sensors, but by an increased distance between releasable vesicles and VGCCs (Wadel et al 2007).

In addition to the role of a Ca^{2+} sensor, synaptotagmin proteins may be also important for positioning the releasable vesicle pool near the VGCCs (Gustavsson & Han 2009). Young and Neher found that the mutation in synaptotagmin-2 at the calyx of Held causes an increase of synaptic delay and a slowing of the kinetics of synchronous release induced by depolarization (Young & Neher 2009) These data suggest that the mutant synaptotagmin-2 leads to defective vesicle positioning, and uncoupled primed vesicles with VGCCs (McNeil & Wu 2009; Young & Neher 2009). In this thesis work, the lack of synaptagmin binding site in the splice variants of the $Ca_V2.1$ channels may shift the hormone releasing pattern in neuroendocrine cells to a slower and more asynchronous pattern. If the physical link between vesicles and VGCCs is missing or blocked, it will result in a lower accessibility of vesicles to the Ca^{2+} entry site or a removal of predocked vesicles away from VGCCs, which would decrease the efficiency by shifting Ca^{2+} dependence to higher values for triggering a typical synchronous synaptic transmission. This has been proven by the synprint site blocking experiments of $Ca_V2.2$ channels (Mochida et al 1996; Rettig et al 1997). By injecting competing peptides into the presynaptic cells of both sympathetic ganglion neuron synapses and *Xenopus* embryonic neuromuscular junctions in culture where only the $Ca_V2.2$ channels are involved with acetylcholine release, the rapid, synchronous transmission is inhibited, while late, asynchronous excitatory postsynaptic potential and paired-pulse facilitation are increased, consistent with the

conclusion that the vesicles are shifted from a pool primed for synchronous release to a pool that is not optimally positioned for synchronous release (Catterall 1999).

Using a similar competing synprint site peptide that disrupts the interaction between synaptic proteins and $Ca_V2.1$ channels, Rettig and colleaugues observed a 25% reduction in synaptic transmission which corresponds to uncoupling of about 70% of the predocked vesicles from Ca^{2+} channels (Rettig et al 1997). This study suggests that the synprint site interaction may not be necessary for normal synaptic transmission but rather serves as a regulatory mechanism to shift the Ca^{2+}-dependence to relatively higher values.

Interestingly, the lack of synprint site regulation has been reported in the neuronal systems of different species. The splice variants of $Ca_V2.2$ channels lacking large portion of synprint site are distributed all over the human brain, including thalamus and cerebellum (Kaneko et al 2002). In addition, Kaneko and colleagues found the deletion isoforms of $Ca_V2.2$ channels showed relatively higher level of expression in the fetal brain than that in the adult brain (Kaneko et al 2002), suggesting the expression of the splice variants may change during development (Gray et al 2007). Other members of the Ca_V2 channel family such as $Ca_V2.3$ channels have been found to lack the synprint site as well. They are located in presynaptic nerve terminals but do not express the synprint site (Kamp et al 2005). In some inverbrate species, such as

Lymnaea stagnalis, Ca_V2 channels lack the synprint site yet still keep proper presynaptic neurotransmission (Spafford et al 2003). The synprint site deletion isoforms of the $Ca_V2.1$ variants we found in this thesis are not only distributed in the hypothalamus, but also other brain tissues such as cortex and thalamus, suggesting that the variants are widely distributed. Although our immunohistochemical data suggest that the dominant form of $Ca_V2.1$ in the MNCs lacks the synprint site, our approach could not differentiate the proportion of either of the splice variants at the MNC terminals. I therefore do not know which isoform is the predominant form of the $Ca_V2.1$ channels in MNCs. The exact physiological function of these splice variants is still not clear, but the positive shifted voltage-dependence of inactivation of channels suggest that the isoforms of P/Q-type channel observed in the MNCs may support more sustained Ca^{2+} entry during trains of action potentials arriving to the MNC terminals.

5.2.2 Targeting properties of the $Ca_V2.1$ channels and splice variants

The role of the synprint site in synaptic targeting is not clear. By creating recombinantly expressed $Ca_V2.1$ channels in which the synprint site was artificially deleted, Mochida and colleagues found the channel targeting to the nerve terminals of the superior cervical ganglion neurons (SCGNs) was significantly inhibited (Mochida et al 2003). The WT $Ca_V2.1$ channels were efficiently distributed in the terminal

structures, whereas the $Ca_V2.1$ deleted mutants (793–878) were less efficiently localized and another deleted mutant (864–934) could hardly be detected in nerve terminals of SCGNs (Mochida et al 2003). In contrast, similar splice variants of $Ca_V2.2$ channels that lack large portions of the synprint site (Kaneko et al 2002) can be properly targeted into the axons of hippocampal neurons (Szabo et al 2006). Szabo and colleagues found two distinct targeting features shown for the WT $Ca_V2.2$ channels: axonal targeting and presynaptic clustering in the transfected hippocampal neurons. The axonal targeting of the splice variants of the $Ca_V2.2$ channels was not changed compared to the WT $Ca_V2.2$ channels, but their presynaptic clustering was significantly decreased. These data suggest that the protein-protein interactions at the synprint site of the $Ca_V2.2$ channels are neither necessary nor sufficient for axonal targeting (Szabo et al 2006), and also suggest that other mechanism(s) may be involved in the axonal targeting of $Ca_V2.2$. However, the inhibition of presynaptic clustering of the splice variants may still suggest a role of the synprint site in the incorporation of presynaptic $Ca_V2.2$ channels into the active zones of hippocampal neurons (Szabo et al 2006).

Our data demonstrate that the synprint site deletion isoforms of $Ca_V2.1$ channels were targeted to the plasma membranes of MNC somata and terminals, suggesting the synprint site interaction is not necessary for targeting of $Ca_V2.1$ to the plasma membrane of MNCs (Rajapaksha et al 2008). The precise subcellular distributions of

$Ca_V2.1$ Δ1 and $Ca_V2.1$ Δ2 are still unknown in MNCs, but our data suggest that the targeting of $Ca_V2.1$ channels may be determined by mechanism(s) other than the synaptic protein interactions observed in some neurons.

One possibility is that the channel targeting of the splice variants is determined by the interaction between the C-terminus of $Ca_V2.1$ channels and the modular adaptor proteins CASK and Mint1 (Maximov et al 1999). Our previous data have shown the expression of mRNA and protein of CASK in chromaffin cells. Interactions between CASK and $Ca_V2.1$ and $Ca_V2.2$ channels have been detected by co-immunoprecipitation (Xiaoyu Xu's thesis). Experiments in cultured hippocampal neurons demonstrated that this interaction is necessary and sufficient for axonal targeting of $Ca_V2.2$ in hippocampal neurons (Maximov & Bezprozvanny 2002; Maximov et al 1999). When expressed, GFP-Mint1 and GFP-CASK clustered at synapses and colocalized in presynaptic locations with recombinant $Ca_V2.2$ channels. In contrast, the C-terminal GFP-NC3 construct disrupts the synaptic clustering of the recombinant $Ca_V2.2$ channels by blocking the interaction between CASK and Ca^{2+} channels (Maximov & Bezprozvanny 2002; Maximov et al 1999). Using RNA interference knockdown, Spafford and colleagues found that when the expression of CASK homolog (LCASK) is knocked down in the neurons of sea snail *Lymnaea stagnalis*, the presynaptic transmission of LCa_V2 channels (which are homologs to $Ca_V2.1$ and $Ca_V2.2$, but lack the syprint site) was significantly decreased (Spafford et

al 2003). These data suggest that the inhibition of CASK to the C-terminus of Ca_V2 channels is important for synaptic targeting.

My results demonstrate that the CASK can regulate the $Ca_V2.2$ channel targeting to the plasma membrane in neuroendocrine cells. Co-expression of the blocking peptide GFP-NC3 results in a significantly decreased terminal distribution of $Ca_V2.2$ channels in differentiated PC12 cells. The clustering of $Ca_V2.2$ channels on the plasma membrane of undifferentiated bovine chromaffin cells was abolished as well (Xiaoyu Xu's thesis, data not shown here)**,** indicating that CASK may be important for both axonal targeting and anchoring at the releasing site of neuroendocrine cells.

However, recent evidence raises questions about the importance of CASK in both targeting and anchoring Ca^{2+} channels. Genetic studies showed that CASK knockout mice suffer premature death one day after birth, but surprisingly, Ca^{2+}-dependent presynaptic neurotransmission in the knockout mice was generally unchanged in primarily isolated neurons, except a decrease in spontaneous release events of GABAergic neurons (Atasoy et al 2007). Using immunocytochemistry, Khanna and colleagues found that the long C-terminus isoform of $Ca_V2.2$ channels is not colocalized with CASK and Mint1 at the specialized presynatic interface of chicken ciliary ganglion calyx terminal (Khanna et al 2006). These data suggest that CASK is not necessary to form a functional synapse as an anchoring protein for Ca^{2+} channels.

Notably, expressing an isoform of the $Ca_V2.1$ channel lacking the CASK binding site in hippocampal neurons showed no significant difference in their subcellular distribution compared to that of the WT $Ca_V2.1$ channels, which suggests that the CASK is not essential in synaptic targeting of $Ca_V2.1$ channels (Hu et al 2005). We still do not know whether the $Ca_V2.1$ and $Ca_V2.2$ channels share a similar targeting mechanism in terms of CASK binding or whether there are other determinant(s) that determine their trafficking from ER to the presynaptic site.

The interaction between the α1 and their β subunits may also contribute to the targeting of $Ca_V2.1$ splice variants in MNCs. Ca^{2+} channel targeting experiments in a polarized epithelial cell lines suggest that association with different β subunits can be an important determinant of axonal targeting for $Ca_V2.1$, but not $Ca_V2.2$ (Brice & Dolphin 1999). Using MDCK cells, which are considered to be a model of axonal dendritic targeting in neurons (the basolateral targeting of channels in MDCK is believed to be equivalent to the somatodendritic targeting of channels in neurons; while the apical targeting in MDCK is equivalent to the axonal targeting of neurons; Dotti et al 1991; Jareb & Banker 1998), Brice and Dolphin found the targeting of $Ca_V2.1$ into the apical membranes of MDCK when co-expressed with the β1 or β4 subunits (Herlitze et al 2003), whereas the $Ca_V2.1$ channels can only be targeted into the basolateral membranes of MDCK when co-expressed with the β2 subunit (Brice & Dolphin 1999). In contrast, no any specific β subunit effect on channel targeting was

observed for $Ca_V2.2$.

The preferential interaction between the β4 subunit and the $Ca_V2.1$ channel has been observed in hippocampal neurons (Mich & Horne 2008; Wittemann et al 2000). Wittermann and colleagues found GFP-β4 colocalized with $Ca_V2.1$ channels and synaptic protein VAMP 2, and GFP-β4 co-expression with $Ca_V2.1$ channels significantly increased the excitatory post-synaptic current amplitude and paired pulse facilitation ratio, suggesting the role of β4 subunit in enhancing the $Ca_V2.1$ channel allocation into the presynaptic terminals (Wittemann et al 2000). Mich and colleagues further identified that the trafficking of $Ca_V2.1$ channels is highly dependent on the concentration of β4 subunits in the *Xenopus* oocytes, and the gabapentin inhibition of channel targeting is particularly related to only one of the isoform of β4 subunit, β4a (Mich & Horne 2008). Moreover, the binding of β4 might be also specialized for $Ca_V2.1$ channel to adopt a slow mode of single channel activity, which may be functionally linked to slow hormone release (Luvisetto et al 2004; Walker & De Waard 1998). Co-expression of β4 with the $Ca_V2.1$ channel has been found to cause slower inactivation and decreased current decay compared with $Ca_V2.1$ channels co-expressed with β1b or β3 (Brody & Yue 2000; Stea et al 1994). Therefore, the future studies on the β subunit regulation of the channel targeting of the $Ca_V2.1$ splice variants identified in my work would be of interest.

5.2.3 $Ca_V2.2$ channels expressed in neuroendocrine cells contain the synprint site and exon 18a

The II-III loop of $Ca_V2.2$ channels regulates cumulative inactivation of channels in response to stimulus trains (Catterall 1999; Degtiar et al 2000; Thaler et al 2004). One of the distinct alternative splicing cassettes found in $Ca_V2.2$ and $Ca_V2.3$ channels is the inserted exon 18a, a 21 amino acid insertion in $Ca_V2.2$ and a 19 amino acid insertion in $Ca_V2.3$ channels between the exons 18 and 19 within the II-III loop of channels (Ghasemzadeh et al 1999; Gray et al 2007; Pan & Lipscombe 2000). The exon 18a is found evolutionarily conserved in $Ca_V2.2$ and $Ca_V2.3$ channels (Figure 5.2).

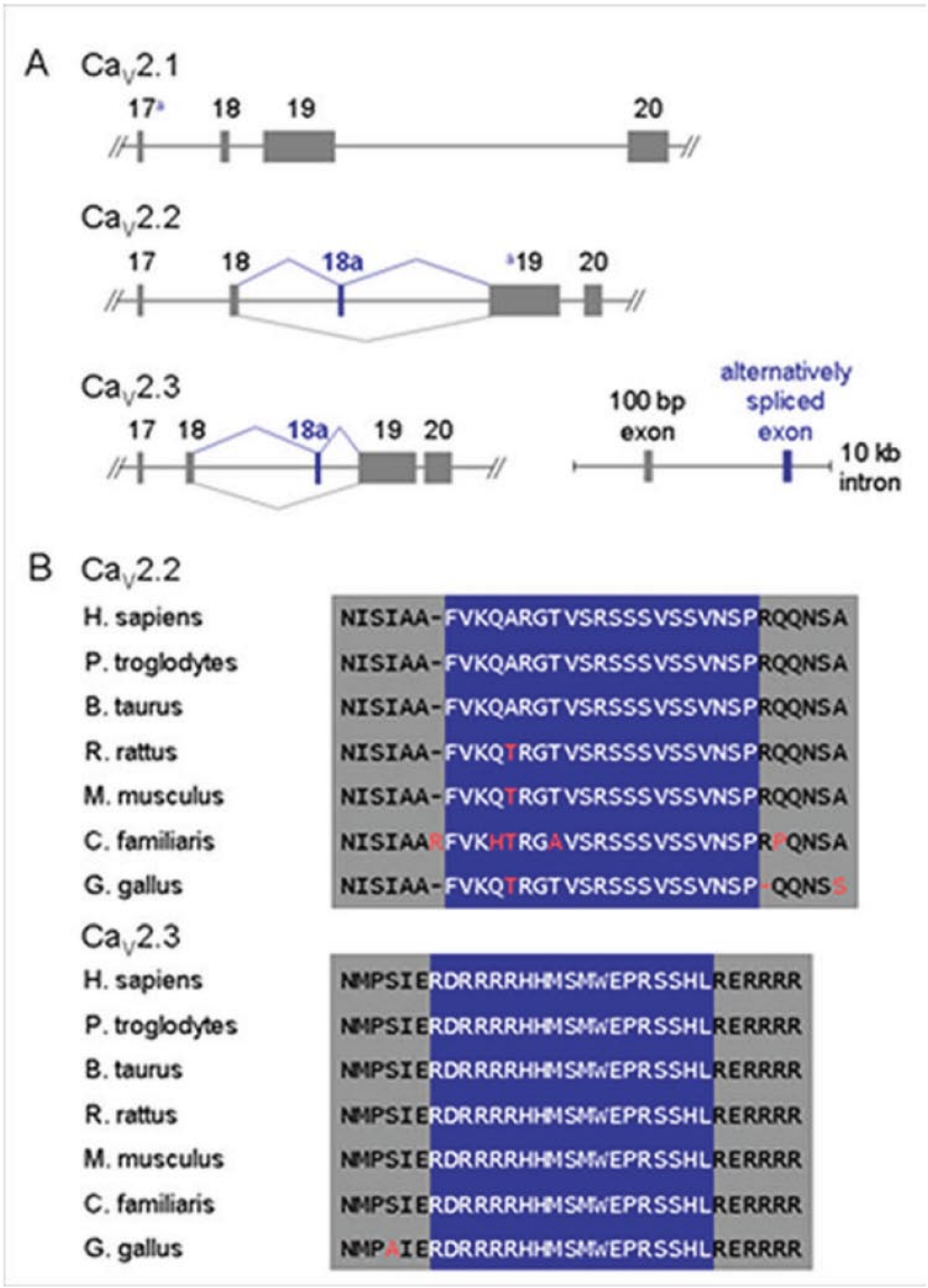

Figure 5.2 Exon 18a alternative splicing within the II-III loop of Ca$_V$2.2 and Ca$_V$2.3 Ca^{2+} channels. A) Alternatively spliced cassette exons, e18a, are found within human Ca$_V$2.2 and Ca$_V$2.3 genes. Partial gene structures, spanning e17 through e20, of human Ca$_V$2.1, Ca$_V$2.2, and Ca$_V$2.3 are illustrated. Exons are illustrated as gray (constitutive exons) or blue (alternatively spliced exons, e18a of Ca$_V$2.2 and Ca$_V$2.3)

boxes, and introns are depicted as lines. Sequences for $Ca_V2.1$ (PubMed Accession #X99897), $Ca_V2.2$ (#M94172, #AF222338), and $Ca_V2.3$ (#L27745). B) Partial alignments of the deduced amino acid sequence of the exon 18a (blue highlighted) in $Ca_V2.2$ (top) and $Ca_V2.3$ (bottom) from different species (Permission from Copyright Clearance Center; (Gray et al 2007)

Our results are consistent with the earlier observation that both wild type $Ca_V2.2$ e[Δ18a] and the splice variant containing exon 18a of $Ca_V2.2$ channels, $Ca_V2.2$ e[18a+], are expressed in the rat brain. The mRNAs of $Ca_V2.2$ e[18a+] are abundant in peripheral ganglia, spinal cord, and caudal regions of the brain, but less prevalent in the neocortex, cerebellum, and hippocampus (Ghasemzadeh et al 1999; Pan & Lipscombe 2000). I found clear DNA bands representing the 18a splice variant in the SON, which has not been reported previously. Our data also show relatively abundant expression of $Ca_V2.2$ e[18a+] in the pituitary gland, suggesting that the neuroendocrine cells in the pituitary gland might have prevalent expression of $Ca_V2.2$ e[18a+]. Thaler and colleagues found that exon 18a insertion in $Ca_V2.2$ channels protected the channel from inactivation (Thaler et al 2004). The $Ca_V2.2$e [18a+] is less sensitive to close-state inactivation compared to $Ca_V2.2$ e[Δ18a], which is inactivated at voltages ≈10 mV more depolarized than $Ca_V2.2$ e[Δ18a]. Close-state inactivation is a mechanism thought to underlie cumulative inactivation of HVA Ca^{2+} channels when stimulated by trains of action potentials waveforms (Patil et al 1998). The presence of $Ca_V2.2$ e[18a+] in neuroendocrine cells may provide a protective mechanism for

$Ca_V2.2$ channels when the demand of hormone release is high in the neuroendocrine cells that fire bursts like MNCs.

The antibodies I used for $Ca_V2.2$ channels were unable to distinguish the $Ca_V2.2$ e[18a+] and $Ca_V2.2$ e[Δ18a] in MNCs, but the results suggested that all isoforms of $Ca_V2.2$ channels I detected contained the synprint site. There were no differences in the immunostaining between selective and inclusive antibodies in all cells tested, including hippocampal neurons, MNC, PC12 cells, and melanotropes.

5.2.4 Functions of $Ca_V2.1$ and $Ca_V2.2$ channels in MNCs

Our data in this thesis demonstrate the synprint site alternative splicing of $Ca_V2.1$ and $Ca_V2.2$ channel in neuroendocrine cells. This is of special interest because it may provide comparable information to understand Ca^{2+}-dependent exocytosis during hormone release *vs* presynaptic neurotransmitter release.

Whether the $Ca_V2.1$ and $Ca_V2.2$ channels function the same way in neuroendocrine cells as they do in neurons is an important question to answer. In isolated MNC somata, multiple HVA Ca^{2+} currents could be detected by electrophysiology including the P/Q-, N-, L-, and R-type currents (Fisher & Bourque 1995a; Foehring & Armstrong 1996). Electrically stimulated VP release from MNC terminals can be

blocked by N-type and P/Q-type Ca^{2+} channel blockers, and by L-type Ca^{2+} channel blockers under certain conditions (Fisher & Bourque 2001; Jorgensen et al 1994). Using electrically evoked hormone release measurements, Jorgensen et al., found that a selective L-type channel blocker decreased the vasopressin release only at lowest frequency they used experimentally (6.5 Hz), suggesting the L-type channels may be involved in MNC terminal release only at certain firing rate.

A detailed comparison between the ω-Aga-IVA sensitive currents in terminals and somata of MNCs showed marked differences in inactivation kinetics and sensitivity to toxin (Fisher & Bourque 1995a). Although the current in the somata is non-inactivating and highly sensitive to ω-agatoxin IVA (IC_{50}≈3 nM), the current in the terminals inactivates (τ≈450 ms) and is much less sensitive to toxin (IC_{50}≈270 nM). These properties support the conclusion that the current in the somata is a P-type current (Foehring & Armstrong 1996), while that in the terminals is more similar to identified Q-type currents (Randall & Tsien 1995; Sather et al 1993).

We now know that P- and Q- type Ca^{2+} channels are not two distinct subtype of VGCC in terms of molecular identities, but rather that their differences may originate from the alternative splicing of $Ca_V2.1$ channels. For example, in the cerebellar granule neurons, a single amino acid insertion, valine at V421 within I-II loop of $Ca_V2.1$ cDNA sequence, which falls into the regular mechanism of alternative splicing

(with 5' donor and 3' acceptor sites), is implicated in slowing dramatically the inactivation of P-type currents (Bourinet et al 1999; Jimenez et al 2000). The synprint site deletion isoforms of $Ca_V2.1$ found in this thesis may provide another explanation of the different electrophysiological properties found in soma and terminals of MNCs. The possibly different distribution between the $Ca_V2.1$-Δ1 and $Ca_V2.1$-Δ2 variants on somata *vs* terminals of the MNCs could result in different rates of voltage-dependent inactivation.

Functional studies using peptide-specific radioimmunoassay to measure the effects of different VGCCs blockers on K^+ induced VP and OT release revealed that the Q-type component found in MNC terminals was specifically associated with VP but not OT release (Wang et al 1997). Using the same model, Wang and colleagues found that OT release was specifically sensitive to block of the R-type currents (Wang et al 1999), which explained the resistance of the OT release inhibition to block of Q-type Ca^{2+} channel. In this thesis, I found that the $Ca_V2.1$ channels are preferentially expressed in the VP-MNCs but not OT-MNCs, which explains why the $Ca_V2.1$ channels have a role in regulating VP but not OT release.

A difference in inactivation of N-type Ca^{2+} channels has also been reported between the somata and terminals of MNCs. In the somata the N-type currents are slowly or non-inactivating (Fisher & Bourque 1995b), while the currents in the terminals

inactivate rapidly (Lemos & Nowycky 1989). It is not known whether the $Ca_V2.2$ e[18a+] variant, which is inactivated at voltages ≈10 mV more depolarized than the WT $Ca_V2.2$ channels (Thaler et al 2004), contributes to the different N-type currents displayed in MNC somata and terminals.

In conclusion, although isoforms of alternative splicing in $Ca_V2.1$ channels that are involved with different binding properties with syntaxin and SNAP25 (Rettig et al 1996) have been found in rat brain using immunoblot analysis (Sakurai et al 1995; Sakurai et al 1996), our observations represent the first identification of splice variants of rat $Ca_V2.1$ that lack large portions of the II-III loop (Jurkat-Rott & Lehmann-Horn 2004; Lipscombe et al 2002). These variants appear to be analogous to two alternatively spliced variants that have deletions within the synprint site in human $Ca_V2.2$ (Kaneko et al 2002). Using a combination of molecular, imaging and electrophysiological methods, we identified that the deletion of the synprint site of $Ca_V2.1$ may have multiple consequences including altered coupling to the synaptic release machinery and altered channel function. The predominance of these deletion variants in neuroendocrine cells suggests that they may have a role in triggering non-synaptic exocytotic release. The shift to more depolarized steady-state inactivation of $Ca_V2.1$-Δ1 may suggest an enhanced Ca^{2+} influx during multiple action potential firing of MNCs to sustain hormone release.

5.3 Future direction

1. Our findings provide clues to address other questions related to the functional significance of splice variants of $Ca_V2.1$ Ca^{2+} channels in hormone release. Further investigation on the role of the splice variants in different phases of exocytosis in the neuroendocrine cells is expected. **One way to approach this study is to measure the membrane expression of channels in the neuroendocrine cells that are transfected with fluorescently tagged isoforms of the $Ca_V2.1$ channels. The targeting properties of the $Ca_V2.1$ splice variants could be further identified in neuroendocrine cells. Capacitance measurements or amperometry could also be used to study the effect(s) of synprint site deleted $Ca_V2.1$ isoform on exocytosis compared to that of WT $Ca_V2.1$ isoform.**

2. The second direction will be further investigating the distributions of different β subunits or the distributions of small GTP-binding proteins (RGK family) that regulate β subunits to see if there is any specific combination of β and $Ca_V2.1$ α1 subunits or combination of RGK proteins and α1 subunits that will be important for the distribution of splice variants in the neuroendocrine cells. Co-immunoprecipitation can be used to test which β subunit or which small GTP-binding protein is bound with the $Ca_V2.1$ splice variants *in vitro*. Immunohistochemistry can be used to study the colocalization of different β subunits and the $Ca_V2.1$ splice variants.

3. Our finding that the $Ca_V1.2$ channels are selectively up-regulated in rat pituicytes after dehydration could lead to a series of experiments testing the downstream pathway(s) involved in the alterations of pituicytes. These experiments can be conducted both *in vivo* and *in vitro* using the selective L-type Ca^{2+} blockers in dehydrated rats. It would also be interesting to test whether $Ca_V1.2$ channels are regulated during other physiological changes related to the MNC functions such as lactation. Further immunohistochemical experiments aiming to measure the $Ca_V1.2$ expression in the MNC somata and their terminals would also help to understand this specific regulation of L-type Ca^{2+} signaling.

4. The study of Ca^{2+}-dependent mechanism of gliotransmission is still in the early stage. The hurdles apparently include the difficulties to define a releasing site for glial cells, regardless of their even more irregular morphologies under normal or stimulated conditions in comparison to presynaptic terminals. Finding out where glial Ca^{2+} comes from and how it supports gliotransmission is an important issue because it will provide more integrative information describing the dynamics between neurons and glial cells within the central nervous and neuroendocrine system. More sensitive imaging (e.g. two photon microscopy) that operates at submicrometer resolution would allow recording of Ca^{2+} signals from astrocyte processes just outside the synapse (Kirchhoff 2010; Svoboda & Yasuda 2006).

6. CONCLUSIONS

This thesis work mainly describes the expression and targeting of VGCCs in the neuroendocrine system, especially the typical neurosecretory cells in the SON of hypothalamus and glial cells in the neurohypophysis.

Our major findings are as follows:

1. Pituicytes express $Ca_V2.2$ and $Ca_V2.3$ Ca^{2+} channels in the neurohypophysis that belong to HVA VGCCs. When the rats are dehydrated, the $Ca_V1.2$ Ca^{2+} channels are selectively up-regulated in the pituicytes.
2. Two novel splice variants of rat $Ca_V2.1$ that lack large portion of synprint site within the II-III loop of channel have been identified. Such deletion variants appear to be expressed in different regions of the brain and two types of neuroendocrine cells, including somata and terminals of VP-MNCs. These data suggested that synprint site might not be indispensible for channel targeting in the MNCs. Both deletions in $Ca_V2.1$ resulted in a rightward shift in the voltage dependence of inactivation (more depolarized direction), suggesting these variants of $Ca_V2.1$ channels may play a role for the process of Ca^{2+}-dependent exocytosis of neuroendocrine cells. Our data also

indicate that alternative splicing of synprint site of $Ca_V2.1$ channels may be a general mechanism of VGCC regulation in neuroendocrine cells.

3. $Ca_V2.2$ channel distribution in the plasma membranes of MNCs and other type of neuroendocrine cells were tested, where all detectable $Ca_V2.2$ channels contain the synprint site. The targeting of channels was measured by transfection and immunocytochemistry. Our data suggested the interaction of CASK and the C-terminus of $Ca_V2.2$ channels are important for the distribution of channels on the nerve terminals of differentiated PC12 cells. This may suggest that the targeting signal of the $Ca_V2.2$ channels through the interaction of CASK protein is conservative between neuroendocrine cells and neurons.

This research provides insights into alternative splicing of the $Ca_V2.1$ and $Ca_V2.2$ channels in the neuroendocrine cells and their significance in terms of channel activity and targeting. It also sheds light on VGCC expression and regulation in glial cells in the neurohypophysis and contributes to our understanding of the physiology of Ca^{2+} signaling in both neuronal and neuroendocrine systems.

7. REFERENCES

Adler EM, Gough NR, Blundon JA. 2006. Differentiation of PC12 cells. Sci STKE 2006:9

Agulhon C, Fiacco TA, McCarthy KD. 2010. Hippocampal short- and long-term plasticity are not modulated by astrocyte Ca2+ signaling. Science 327:1250-4

Ahlijanian MK, Westenbroek RE, Catterall WA. 1990. Subunit structure and localization of dihydropyridine-sensitive calcium channels in mammalian brain, spinal cord, and retina. Neuron 4:819-32

Akopian G, Kressin K, Derouiche A, Steinhauser C. 1996. Identified glial cells in the early postnatal mouse hippocampus display different types of Ca2+ currents. Glia 17:181-94

Altier C, Khosravani H, Evans RM, Hameed S, Peloquin JB, et al. 2006. ORL1 receptor-mediated internalization of N-type calcium channels. Nat Neurosci 9:31-40

An SJ, Almers W. 2004. Tracking SNARE complex formation in live endocrine cells. Science 306:1042-6

Arac D, Chen X, Khant HA, Ubach J, Ludtke SJ, et al. 2006. Close membrane-membrane proximity induced by Ca(2+)-dependent multivalent binding of synaptotagmin-1 to phospholipids. Nat Struct Mol Biol 13:209-17

Araque A, Li N, Doyle RT, Haydon PG. 2000. SNARE protein-dependent glutamate release from astrocytes. J Neurosci 20:666-73

Arikkath J, Campbell KP. 2003. Auxiliary subunits: essential components of the voltage-gated calcium channel complex. Curr Opin Neurobiol 13:298-307

Armstrong CM, Matteson DR. 1985. Two distinct populations of calcium channels in a clonal line of pituitary cells. Science 227:65-7

Atasoy D, Schoch S, Ho A, Nadasy KA, Liu X, et al. 2007. Deletion of CASK in mice is lethal and impairs synaptic function. Proc Natl Acad Sci U S A 104:2525-30

Attwell D. 1994. Glia and neurons in dialogue. Nature 369:707-8

Augustine GJ. 2001. How does calcium trigger neurotransmitter release? Curr Opin Neurobiol 11:320-6

Augustine GJ, Santamaria F, Tanaka K. 2003. Local calcium signaling in neurons. Neuron 40:331-46

Bailey K. 1942. Myosin and adenosinetriphosphatase. Biochem J 36:121-39

Bajjalieh SM. 1999. Synaptic vesicle docking and fusion. Curr Opin Neurobiol 9:321-8

Barclay J, Balaguero N, Mione M, Ackerman SL, Letts VA, et al. 2001. Ducky mouse phenotype of epilepsy and ataxia is associated with mutations in the Cacna2d2 gene and decreased calcium channel current in cerebellar Purkinje cells. J Neurosci 21:6095-104

Barres BA, Chun LL, Corey DP. 1989. Calcium current in cortical astrocytes: induction by cAMP and neurotransmitters and permissive effect of serum factors. J Neurosci 9:3169-75

Baylis PH, Thompson CJ. 1988. Osmoregulation of vasopressin secretion and thirst in health and disease. Clin Endocrinol (Oxf) 29:549-76

Beagley GH, Hatton GI. 1992. Rapid morphological changes in supraoptic nucleus and posterior pituitary induced by a single hypertonic saline injection. Brain Res Bull 28:613-8

Bean BP. 1985. Two kinds of calcium channels in canine atrial cells. Differences in kinetics, selectivity, and pharmacology. J Gen Physiol 86:1-30

Bean BP. 1989. Classes of calcium channels in vertebrate cells. Annu Rev Physiol 51:367-84

Bear MF, Malenka RC. 1994. Synaptic plasticity: LTP and LTD. Curr Opin Neurobiol 4:389-99

Beck A, Nieden RZ, Schneider HP, Deitmer JW. 2004. Calcium release from intracellular stores in rodent astrocytes and neurons in situ. Cell Calcium 35:47-58

Becker AJ, Pitsch J, Sochivko D, Opitz T, Staniek M, et al. 2008. Transcriptional upregulation of Cav3.2 mediates epileptogenesis in the pilocarpine model of epilepsy. J Neurosci 28:13341-53

Beedle AM, McRory JE, Poirot O, Doering CJ, Altier C, et al. 2004. Agonist-independent modulation of N-type calcium channels by ORL1 receptors. Nat Neurosci 7:118-25

Bennett MK, Calakos N, Scheller RH. 1992. Syntaxin: a synaptic protein implicated in docking of synaptic vesicles at presynaptic active zones. Science 257:255-9

Berger T, Schnitzer J, Orkand PM, Kettenmann H. 1992. Sodium and Calcium Currents in Glial Cells of the Mouse Corpus Callosum Slice. Eur J Neurosci 4:1271-84

Beuckmann CT, Sinton CM, Miyamoto N, Ino M, Yanagisawa M. 2003. N-type calcium channel alpha1B subunit (Cav2.2) knock-out mice display hyperactivity and vigilance state differences. J Neurosci 23:6793-7

Bezprozvanny I, Scheller RH, Tsien RW. 1995. Functional impact of syntaxin on gating of N-type and Q-type calcium channels. Nature 378:623-6

Bezprozvanny I, Zhong P, Scheller RH, Tsien RW. 2000. Molecular determinants of the functional interaction between syntaxin and N-type Ca2+ channel gating. Proc Natl Acad Sci U S A 97:13943-8

Bezzi P, Gundersen V, Galbete JL, Seifert G, Steinhauser C, et al. 2004. Astrocytes contain a vesicular compartment that is competent for regulated exocytosis of glutamate. Nat Neurosci 7:613-20

Bicknell RJ. 1988. Optimizing release from peptide hormone secretory nerve terminals. J Exp Biol 139:51-65

Biederer T, Sudhof TC. 2001. CASK and protein 4.1 support F-actin nucleation on neurexins. J Biol Chem 276:47869-76

Birnbaumer L, Qin N, Olcese R, Tareilus E, Platano D, et al. 1998. Structures and functions of calcium channel beta subunits. J Bioenerg Biomembr 30:357-75

Black DL. 2003. Mechanisms of alternative pre-messenger RNA splicing. Annu Rev Biochem 72:291-336

Blackburn RE, Samson WK, Fulton RJ, Stricker EM, Verbalis JG. 1993. Central oxytocin inhibition of salt appetite in rats: evidence for differential sensing of plasma sodium and osmolality. Proc Natl Acad Sci U S A 90:10380-4

Blackburn RE, Samson WK, Fulton RJ, Stricker EM, Verbalis JG. 1995. Central oxytocin and ANP receptors mediate osmotic inhibition of salt appetite in rats. Am J Physiol 269:R245-51

Blaustein MP, Golovina VA. 2001. Structural complexity and functional diversity of endoplasmic reticulum Ca(2+) stores. Trends Neurosci 24:602-8

Blaustein MP, Lederer WJ. 1999. Sodium/calcium exchange: its physiological implications. Physiol Rev 79:763-854

Bliss TV, Collingridge GL. 1993. A synaptic model of memory: long-term potentiation in the hippocampus. Nature 361:31-9

Bollmann JH, Sakmann B. 2005. Control of synaptic strength and timing by the release-site Ca2+ signal. Nat Neurosci 8:426-34

Bollmann JH, Sakmann B, Borst JG. 2000. Calcium sensitivity of glutamate release in a calyx-type terminal. Science 289:953-7

Boron WF, Boulpaep EL. 2005. Medical Physiology. Philadelphia: Sauders Elevier 334-340

Bourinet E, Soong TW, Sutton K, Slaymaker S, Mathews E, et al. 1999. Splicing of alpha 1A subunit gene generates phenotypic variants of P- and Q-type calcium channels. Nat Neurosci 2:407-15

Bourque CW. 1998. Osmoregulation of vasopressin neurons: a synergy of intrinsic and synaptic processes. Prog Brain Res 119:59-76

Bourque CW. 2008. Central mechanisms of osmosensation and systemic osmoregulation. Nat Rev Neurosci 9:519-31

Brice NL, Dolphin AC. 1999. Differential plasma membrane targeting of voltage-dependent calcium channel subunits expressed in a polarized epithelial cell line. J Physiol 515 (Pt 3):685-94

Bringmann A, Schopf S, Reichenbach A. 2000. Developmental regulation of calcium channel-mediated currents in retinal glial (Muller) cells. J Neurophysiol 84:2975-83

Brody DL, Yue DT. 2000. Relief of G-protein inhibition of calcium channels and short-term synaptic facilitation in cultured hippocampal neurons. J Neurosci 20:889-98

Brownstein MJ, Russell JT, Gainer H. 1980. Synthesis, transport, and release of posterior pituitary hormones. Science 207:373-8

Burbach JP, Luckman SM, Murphy D, Gainer H. 2001. Gene regulation in the magnocellular hypothalamo-neurohypophysial system. Physiol Rev 81:1197-267

Burgoyne RD. 1997. Introduction: the chromaffin cell. Semin Cell Dev Biol 8:99-100

Burgoyne RD. 2007. Neuronal calcium sensor proteins: generating diversity in neuronal Ca2+ signalling. Nat Rev Neurosci 8:182-93

Carafoli E. 2003. The calcium-signalling saga: tap water and protein crystals. Nat Rev Mol Cell Biol 4:326-32

Carafoli E, Brini M. 2000. Calcium pumps: structural basis for and mechanism of calcium transmembrane transport. Curr Opin Chem Biol 4:152-61

Carbone E, Lux HD. 1984. A low voltage-activated, fully inactivating Ca channel in vertebrate sensory neurones. Nature 310:501-2

Carmignoto G, Pasti L, Pozzan T. 1998. On the role of voltage-dependent calcium channels in calcium signaling of astrocytes in situ. J Neurosci 18:4637-45

Cates MS, Berry MB, Ho EL, Li Q, Potter JD, Phillips GN, Jr. 1999. Metal-ion affinity and specificity in EF-hand proteins: coordination geometry and domain plasticity in parvalbumin. Structure 7:1269-78

Catterall WA. 1999. Interactions of presynaptic Ca2+ channels and snare proteins in neurotransmitter release. Ann N Y Acad Sci 868:144-59

Catterall WA. 2000. Structure and regulation of voltage-gated Ca2+ channels. In Annu Rev Cell Dev Biol, pp. 521-55

Catterall WA, Perez-Reyes E, Snutch TP, Striessnig J. 2005. International Union of Pharmacology. XLVIII. Nomenclature and structure-function relationships of voltage-gated calcium channels. Pharmacol Rev 57:411-25

Cazalis M, Dayanithi G, Nordmann JJ. 1987. Hormone release from isolated nerve endings of the rat neurohypophysis. J Physiol 390:55-70

Celio MR, Heizmann CW. 1982. Calcium-binding protein parvalbumin is associated with fast contracting muscle fibres. Nature 297:504-6

Chapman ER. 2002. Synaptotagmin: a Ca(2+) sensor that triggers exocytosis? Nat Rev Mol Cell Biol 3:498-508

Chen L, Chetkovich DM, Petralia RS, Sweeney NT, Kawasaki Y, et al. 2000. Stargazin regulates synaptic targeting of AMPA receptors by two distinct mechanisms. Nature 408:936-43

Chen X, Wang L, Zhou Y, Zheng LH, Zhou Z. 2005. "Kiss-and-run" glutamate secretion in cultured and freshly isolated rat hippocampal astrocytes. J Neurosci 25:9236-43

Chen YA, Scheller RH. 2001. SNARE-mediated membrane fusion. Nat Rev Mol Cell Biol 2:98-106

Chen YH, Li MH, Zhang Y, He LL, Yamada Y, et al. 2004. Structural basis of the alpha1-beta subunit interaction of voltage-gated Ca2+ channels. Nature 429:675-80

Cheung VG, Spielman RS. 2009. Genetics of human gene expression: mapping DNA variants that influence gene expression. Nat Rev Genet 10:595-604
Choi DW, Koh JY, Peters S. 1988. Pharmacology of glutamate neurotoxicity in cortical cell culture: attenuation by NMDA antagonists. J Neurosci 8:185-96
Chrivia JC, Kwok RP, Lamb N, Hagiwara M, Montminy MR, Goodman RH. 1993. Phosphorylated CREB binds specifically to the nuclear protein CBP. Nature 365:855-9
Chuang RS, Jaffe H, Cribbs L, Perez-Reyes E, Swartz KJ. 1998. Inhibition of T-type voltage-gated calcium channels by a new scorpion toxin. Nat Neurosci 1:668-74
Clapham DE. 2007. Calcium signaling. Cell 131:1047-58
Clapham DE, Runnels LW, Strubing C. 2001. The TRP ion channel family. Nat Rev Neurosci 2:387-96
Cocchia D, Miani N. 1980. Immunocytochemical localization of the brain-specific S-100 protein in the pituitary gland of adult rat. J Neurocytol 9:771-82
Collingridge GL, Isaac JT, Wang YT. 2004. Receptor trafficking and synaptic plasticity. Nat Rev Neurosci 5:952-62
Cornell-Bell AH, Finkbeiner SM, Cooper MS, Smith SJ. 1990. Glutamate induces calcium waves in cultured astrocytes: long-range glial signaling. Science 247:470-3
Cornet V, Bichet D, Sandoz G, Marty I, Brocard J, et al. 2002. Multiple determinants in voltage-dependent P/Q calcium channels control their retention in the endoplasmic reticulum. Eur J Neurosci 16:883-95
Cotrina ML, Lin JH, Alves-Rodrigues A, Liu S, Li J, et al. 1998. Connexins regulate calcium signaling by controlling ATP release. Proc Natl Acad Sci U S A 95:15735-40
Craven SE, Bredt DS. 1998. PDZ proteins organize synaptic signaling pathways. Cell 93:495-8
Cribbs LL, Lee JH, Yang J, Satin J, Zhang Y, et al. 1998. Cloning and characterization of alpha1H from human heart, a member of the T-type Ca2+ channel gene family. Circ Res 83:103-9
D'Ascenzo M, Vairano M, Andreassi C, Navarra P, Azzena GB, Grassi C. 2004. Electrophysiological and molecular evidence of L-(Cav1), N- (Cav2.2), and R-(Cav2.3) type Ca2+ channels in rat cortical astrocytes. Glia 45:354-63
Dasen JS, Rosenfeld MG. 2001. Signaling and transcriptional mechanisms in pituitary development. Annu Rev Neurosci 24:327-55
Degtiar VE, Scheller RH, Tsien RW. 2000. Syntaxin modulation of slow inactivation of N-type calcium channels. J Neurosci 20:4355-67
Deisseroth K, Heist EK, Tsien RW. 1998. Translocation of calmodulin to the nucleus supports CREB phosphorylation in hippocampal neurons. Nature 392:198-202
Deisseroth K, Mermelstein PG, Xia H, Tsien RW. 2003. Signaling from synapse to nucleus: the logic behind the mechanisms. Curr Opin Neurobiol 13:354-65

Deleuze C, Alonso G, Lefevre IA, Duvoid-Guillou A, Hussy N. 2005. Extrasynaptic localization of glycine receptors in the rat supraoptic nucleus: further evidence for their involvement in glia-to-neuron communication. Neuroscience 133:175-83

Dellis O, Dedos SG, Tovey SC, Taufiq Ur R, Dubel SJ, Taylor CW. 2006. Ca2+ entry through plasma membrane IP3 receptors. Science 313:229-33

Dickman DK, Kurshan PT, Schwarz TL. 2008. Mutations in a Drosophila alpha2delta voltage-gated calcium channel subunit reveal a crucial synaptic function. J Neurosci 28:31-8

Dietrich D, Kirschstein T, Kukley M, Pereverzev A, von der Brelie C, et al. 2003. Functional specialization of presynaptic Cav2.3 Ca2+ channels. Neuron 39:483-96

Dolmetsch RE, Pajvani U, Fife K, Spotts JM, Greenberg ME. 2001. Signaling to the nucleus by an L-type calcium channel-calmodulin complex through the MAP kinase pathway. Science 294:333-9

Dolphin AC. 2003. Beta subunits of voltage-gated calcium channels. J Bioenerg Biomembr 35:599-620

Dolphin AC. 2009. Calcium channel diversity: multiple roles of calcium channel subunits. Curr Opin Neurobiol 19:237-44

Donato R, Page KM, Koch D, Nieto-Rostro M, Foucault I, et al. 2006. The ducky(2J) mutation in Cacna2d2 results in reduced spontaneous Purkinje cell activity and altered gene expression. J Neurosci 26:12576-86

Dotti CG, Parton RG, Simons K. 1991. Polarized sorting of glypiated proteins in hippocampal neurons. Nature 349:158-61

Dubel SJ, Starr TV, Hell J, Ahlijanian MK, Enyeart JJ, et al. 1992. Molecular cloning of the alpha-1 subunit of an omega-conotoxin-sensitive calcium channel. Proc Natl Acad Sci U S A 89:5058-62

Duffy S, MacVicar BA. 1994. Potassium-dependent calcium influx in acutely isolated hippocampal astrocytes. Neuroscience 61:51-61

Dulubova I, Yamaguchi T, Arac D, Li H, Huryeva I, et al. 2003. Convergence and divergence in the mechanism of SNARE binding by Sec1/Munc18-like proteins. Proc Natl Acad Sci U S A 100:32-7

Ertel EA, Campbell KP, Harpold MM, Hofmann F, Mori Y, et al. 2000. Nomenclature of voltage-gated calcium channels. Neuron 25:533-5

Fatt P, Katz B. 1953a. The effect of inhibitory nerve impulses on a crustacean muscle fibre. J Physiol 121:374-89

Fatt P, Katz B. 1953b. The electrical properties of crustacean muscle fibres. J Physiol 120:171-204

Fellin T, Carmignoto G. 2004. Neurone-to-astrocyte signalling in the brain represents a distinct multifunctional unit. J Physiol 559:3-15

Fernandez-Chacon R, Konigstorfer A, Gerber SH, Garcia J, Matos MF, et al. 2001. Synaptotagmin I functions as a calcium regulator of release probability. Nature 410:41-9

Feske S, Gwack Y, Prakriya M, Srikanth S, Puppel SH, et al. 2006. A mutation in Orai1 causes immune deficiency by abrogating CRAC channel function. Nature 441:179-85

Fiacco TA, Agulhon C, Taves SR, Petravicz J, Casper KB, et al. 2007. Selective stimulation of astrocyte calcium in situ does not affect neuronal excitatory synaptic activity. Neuron 54:611-26

Fiacco TA, McCarthy KD. 2006. Astrocyte calcium elevations: properties, propagation, and effects on brain signaling. Glia 54:676-90

Fill M, Copello JA. 2002. Ryanodine receptor calcium release channels. Physiol Rev 82:893-922

Fisher TE, Bourque CW. 1995a. Distinct omega-agatoxin-sensitive calcium currents in somata and axon terminals of rat supraoptic neurones. J Physiol 489 (Pt 2):383-8

Fisher TE, Bourque CW. 1995b. Voltage-gated calcium currents in the magnocellular neurosecretory cells of the rat supraoptic nucleus. J Physiol 486 (Pt 3):571-80

Fisher TE, Bourque CW. 1996. Calcium-channel subtypes in the somata and axon terminals of magnocellular neurosecretory cells. Trends Neurosci 19:440-4

Fisher TE, Bourque CW. 2001. The function of Ca(2+) channel subtypes in exocytotic secretion: new perspectives from synaptic and non-synaptic release. Prog Biophys Mol Biol 77:269-303

Fisher TE, Carrion-Vazquez M, Fernandez JM. 2000. Intracellular Ca(2+) channel immunoreactivity in neuroendocrine axon terminals. FEBS Lett 482:131-8

Fisher TE, Fernandez JM. 1999. Pulsed laser imaging of Ca(2+) influx in a neuroendocrine terminal. J Neurosci 19:7450-7

Fletcher CF, Lutz CM, O'Sullivan TN, Shaughnessy JD, Jr., Hawkes R, et al. 1996. Absence epilepsy in tottering mutant mice is associated with calcium channel defects. Cell 87:607-17

Foehring RC, Armstrong WE. 1996. Pharmacological dissection of high-voltage-activated Ca2+ current types in acutely dissociated rat supraoptic magnocellular neurons. J Neurophysiol 76:977-83

Forsythe ID, Tsujimoto T, Barnes-Davies M, Cuttle MF, Takahashi T. 1998. Inactivation of presynaptic calcium current contributes to synaptic depression at a fast central synapse. Neuron 20:797-807

Fox AP, Cahill AL, Currie KP, Grabner C, Harkins AB, et al. 2008. N- and P/Q-type Ca2+ channels in adrenal chromaffin cells. Acta Physiol (Oxf) 192:247-61

Fox AP, Nowycky MC, Tsien RW. 1987. Kinetic and pharmacological properties distinguishing three types of calcium currents in chick sensory neurones. J Physiol 394:149-72

Franklin JL, Johnson EM, Jr. 1992. Suppression of programmed neuronal death by sustained elevation of cytoplasmic calcium. Trends Neurosci 15:501-8

Freund-Mercier MJ, Stoeckel ME, Waeber C, Kremarik P, Palacios JM, Richard P. 1991. Neurophysins, rather than Receptors, are Involved in [H]Oxytocin and [H]Vasopressin Binding Detected by Autoradiography in the Hypothalamo-Neurohypophyseal System. J Neuroendocrinol 3:285-95

Friedman ME, Suarez-Kurtz G, Kaczorowski GJ, Katz GM, Reuben JP. 1986. Two calcium currents in a smooth muscle cell line. Am J Physiol 250:H699-703

Fujita Y, Mynlieff M, Dirksen RT, Kim MS, Niidome T, et al. 1993. Primary structure and functional expression of the omega-conotoxin-sensitive N-type calcium channel from rabbit brain. Neuron 10:585-98

Fujiwara K, Adachi S, Usui K, Maruyama M, Matsumoto H, et al. 2002. Immunocytochemical localization of a galanin-like peptide (GALP) in pituicytes of the rat posterior pituitary gland. Neurosci Lett 317:65-8

Gainer H, Wray S. 1992. Oxytocin and vasopressin. From genes to peptides. Ann N Y Acad Sci 652:14-28

Geppert M, Goda Y, Hammer RE, Li C, Rosahl TW, et al. 1994. Synaptotagmin I: a major Ca2+ sensor for transmitter release at a central synapse. Cell 79:717-27

Ghasemzadeh MB, Pierce RC, Kalivas PW. 1999. The monoamine neurons of the rat brain preferentially express a splice variant of alpha1B subunit of the N-type calcium channel. J Neurochem 73:1718-23

Ghosh A, Greenberg ME. 1995. Calcium signaling in neurons: molecular mechanisms and cellular consequences. Science 268:239-47

Gill DL, Spassova MA, Soboloff J. 2006. Signal transduction. Calcium entry signals--trickles and torrents. Science 313:183-4

Giovannucci DR, Stuenkel EL. 1997. Regulation of secretory granule recruitment and exocytosis at rat neurohypophysial nerve endings. J Physiol 498 (Pt 3):735-51

Glasgow E, Kusano K, Chin H, Mezey E, Young WS, 3rd, Gainer H. 1999. Single cell reverse transcription-polymerase chain reaction analysis of rat supraoptic magnocellular neurons: neuropeptide phenotypes and high voltage-gated calcium channel subtypes. Endocrinology 140:5391-401

Goldin AL. 2001. Resurgence of sodium channel research. Annu Rev Physiol 63:871-94

Gordon GR, Baimoukhametova DV, Hewitt SA, Rajapaksha WR, Fisher TE, Bains JS. 2005. Norepinephrine triggers release of glial ATP to increase postsynaptic efficacy. Nat Neurosci 8:1078-86

Graef IA, Mermelstein PG, Stankunas K, Neilson JR, Deisseroth K, et al. 1999. L-type calcium channels and GSK-3 regulate the activity of NF-ATc4 in hippocampal neurons. Nature 401:703-8

Gray AC, Raingo J, Lipscombe D. 2007. Neuronal calcium channels: splicing for optimal performance. Cell Calcium 42:409-17

Gustavsson N, Han W. 2009. Calcium-sensing beyond neurotransmitters: functions of synaptotagmins in neuroendocrine and endocrine secretion. Biosci Rep 29:245-59

Guthrie PB, Knappenberger J, Segal M, Bennett MV, Charles AC, Kater SB. 1999. ATP released from astrocytes mediates glial calcium waves. J Neurosci 19:520-8

Hagiwara S, Nakajima S. 1966. Differences in Na and Ca spikes as examined by application of tetrodotoxin, procaine, and manganese ions. J Gen Physiol 49:793-806

Hagiwara S, Ozawa S, Sand O. 1975. Voltage clamp analysis of two inward current mechanisms in the egg cell membrane of a starfish. J Gen Physiol 65:617-44

Hamilton NB, Attwell D. 2010. Do astrocytes really exocytose neurotransmitters? Nat Rev Neurosci 11:227-38

Hans M, Luvisetto S, Williams ME, Spagnolo M, Urrutia A, et al. 1999a. Functional consequences of mutations in the human alpha1A calcium channel subunit linked to familial hemiplegic migraine. J Neurosci 19:1610-9

Hans M, Urrutia A, Deal C, Brust PF, Stauderman K, et al. 1999b. Structural elements in domain IV that influence biophysical and pharmacological properties of human alpha1A-containing high-voltage-activated calcium channels. Biophys J 76:1384-400

Harkins AB, Cahill AL, Powers JF, Tischler AS, Fox AP. 2004. Deletion of the synaptic protein interaction site of the N-type (CaV2.2) calcium channel inhibits secretion in mouse pheochromocytoma cells. Proc Natl Acad Sci U S A 101:15219-24

Harootunian AT, Kao JP, Paranjape S, Tsien RY. 1991. Generation of calcium oscillations in fibroblasts by positive feedback between calcium and IP3. Science 251:75-8

Hata Y, Butz S, Sudhof TC. 1996. CASK: a novel dlg/PSD95 homolog with an N-terminal calmodulin-dependent protein kinase domain identified by interaction with neurexins. J Neurosci 16:2488-94

Hatten ME, Liem RK, Shelanski ML, Mason CA. 1991. Astroglia in CNS injury. Glia 4:233-43

Hatton GI. 1988. Pituicytes, glia and control of terminal secretion. J Exp Biol 139:67-79

Hatton GI. 1997. Function-related plasticity in hypothalamus Annu Rev Neurosci 20:375-97

Hatton GI, Bicknell RJ, Hoyland J, Bunting R, Mason WT. 1992. Arginine vasopressin mobilises intracellular calcium via V1-receptor activation in astrocytes (pituicytes) cultured from adult rat neural lobes. Brain Res 588:75-83

Hatton GI, Tweedle CD. 1982. Magnocellular neuropeptidergic neurons in hypothalamus: increases in membrane apposition and number of specialized synapses from pregnancy to lactation. Brain Res Bull 8:197-204

Haydon PG. 2001. GLIA: listening and talking to the synapse. Nat Rev Neurosci 2:185-93

Heidelberger R, Heinemann C, Neher E, Matthews G. 1994. Calcium dependence of the rate of exocytosis in a synaptic terminal. Nature 371:513-5

Hell JW, Westenbroek RE, Warner C, Ahlijanian MK, Prystay W, et al. 1993. Identification and differential subcellular localization of the neuronal class C and class D L-type calcium channel alpha 1 subunits. J Cell Biol 123:949-62

Herchuelz A. 2007. Historical note regarding the discovery of the Na/Ca exchanger and the PMCA. Ann N Y Acad Sci 1099:xvii-xviii

Herlitze S, Xie M, Han J, Hummer A, Melnik-Martinez KV, et al. 2003. Targeting mechanisms of high voltage-activated Ca2+ channels. J Bioenerg Biomembr 35:621-37

Hernandez-SanMiguel E, Vay L, Santo-Domingo J, Lobaton CD, Moreno A, et al. 2006. The mitochondrial Na+/Ca2+ exchanger plays a key role in the control of cytosolic Ca2+ oscillations. Cell Calcium 40:53-61

Hirenallur SD, Haworth ST, Leming JT, Chang J, Hernandez G, et al. 2008. Upregulation of vascular calcium channels in neonatal piglets with hypoxia-induced pulmonary hypertension. Am J Physiol Lung Cell Mol Physiol 295:L915-24

Hsueh YP, Yang FC, Kharazia V, Naisbitt S, Cohen AR, et al. 1998. Direct interaction of CASK/LIN-2 and syndecan heparan sulfate proteoglycan and their overlapping distribution in neuronal synapses. J Cell Biol 142:139-51

Hu Q, Saegusa H, Hayashi Y, Tanabe T. 2005. The carboxy-terminal tail region of human Cav2.1 (P/Q-type) channel is not an essential determinant for its subcellular localization in cultured neurones. Genes Cells 10:87-96

Hua X, Malarkey EB, Sunjara V, Rosenwald SE, Li WH, Parpura V. 2004. C(a2+)-dependent glutamate release involves two classes of endoplasmic reticulum Ca(2+) stores in astrocytes. J Neurosci Res 76:86-97

Hua Y, Scheller RH. 2001. Three SNARE complexes cooperate to mediate membrane fusion. Proc Natl Acad Sci U S A 98:8065-70

Hudmon A, Schulman H, Kim J, Maltez JM, Tsien RW, Pitt GS. 2005. CaMKII tethers to L-type Ca2+ channels, establishing a local and dedicated integrator of Ca2+ signals for facilitation. J Cell Biol 171:537-47

Hussy N. 2002. Glial cells in the hypothalamo-neurohypophysial system: key elements of the regulation of neuronal electrical and secretory activity. Prog Brain Res 139:95-112

Hussy N, Bres V, Rochette M, Duvoid A, Alonso G, et al. 2001. Osmoregulation of vasopressin secretion via activation of neurohypophysial nerve terminals glycine receptors by glial taurine. J Neurosci 21:7110-6

Hussy N, Deleuze C, Pantaloni A, Desarmenien MG, Moos F. 1997. Agonist action of taurine on glycine receptors in rat supraoptic magnocellular neurones: possible role in osmoregulation. J Physiol 502 (Pt 3):609-21

Ino M, Yoshinaga T, Wakamori M, Miyamoto N, Takahashi E, et al. 2001. Functional disorders of the sympathetic nervous system in mice lacking the alpha 1B subunit (Cav 2.2) of N-type calcium channels. Proc Natl Acad Sci U S A 98:5323-8

Insel TR, O'Brien DJ, Leckman JF. 1999. Oxytocin, vasopressin, and autism: is there a connection? Biol Psychiatry 45:145-57

Insel TR, Young LJ. 2001. The neurobiology of attachment. Nat Rev Neurosci 2:129-36

Jareb M, Banker G. 1998. The polarized sorting of membrane proteins expressed in cultured hippocampal neurons using viral vectors. Neuron 20:855-67

Jarvis SE, Barr W, Feng ZP, Hamid J, Zamponi GW. 2002. Molecular determinants of syntaxin 1 modulation of N-type calcium channels. J Biol Chem 277:44399-407

Jarvis SE, Magga JM, Beedle AM, Braun JE, Zamponi GW. 2000. G protein modulation of N-type calcium channels is facilitated by physical interactions between syntaxin 1A and Gbetagamma. J Biol Chem 275:6388-94

Jarvis SE, Zamponi GW. 2007. Trafficking and regulation of neuronal voltage-gated calcium channels. Curr Opin Cell Biol 19:474-82

Jeyifous O, Waites CL, Specht CG, Fujisawa S, Schubert M, et al. 2009. SAP97 and CASK mediate sorting of NMDA receptors through a previously unknown secretory pathway. Nat Neurosci 12:1011-9

Jimenez C, Bourinet E, Leuranguer V, Richard S, Snutch TP, Nargeot J. 2000. Determinants of voltage-dependent inactivation affect Mibefradil block of calcium channels. Neuropharmacology 39:1-10

Jorgensen A, Fjalland B, Christensen JD, Treiman M. 1994. Dihydropyridine ligands influence the evoked release of oxytocin and vasopressin dependent on stimulation conditions. Eur J Pharmacol 259:157-63

Joux N, Chevaleyre V, Alonso G, Boissin-Agasse L, Moos FC, et al. 2001. High voltage-activated Ca2+ currents in rat supraoptic neurones: biophysical properties and expression of the various channel alpha1 subunits. J Neuroendocrinol 13:638-49

Jurkat-Rott K, Lehmann-Horn F. 2004. The impact of splice isoforms on voltage-gated calcium channel alpha1 subunits. J Physiol 554:609-19

Kaech S, Banker G. 2006. Culturing hippocampal neurons. Nat Protoc 1:2406-15

Kamp MA, Krieger A, Henry M, Hescheler J, Weiergraber M, Schneider T. 2005. Presynaptic 'Ca2.3-containing' E-type Ca channels share dual roles during neurotransmitter release. Eur J Neurosci 21:1617-25

Kaneko S, Cooper CB, Nishioka N, Yamasaki H, Suzuki A, et al. 2002. Identification and characterization of novel human Ca(v)2.2 (alpha 1B) calcium channel variants lacking the synaptic protein interaction site. J Neurosci 22:82-92

Kang H, Sun LD, Atkins CM, Soderling TR, Wilson MA, Tonegawa S. 2001. An important role of neural activity-dependent CaMKIV signaling in the consolidation of long-term memory. Cell 106:771-83

Kasai H. 1993. Cytosolic Ca2+ gradients, Ca2+ binding proteins and synaptic plasticity. Neurosci Res 16:1-7

Kasai H. 1999. Comparative biology of Ca2+-dependent exocytosis: implications of kinetic diversity for secretory function. Trends Neurosci 22:88-93

Kaupp UB, Seifert R. 2002. Cyclic nucleotide-gated ion channels. Physiol Rev 82:769-824

Kawanishi T, Blank LM, Harootunian AT, Smith MT, Tsien RY. 1989. Ca2+ oscillations induced by hormonal stimulation of individual fura-2-loaded hepatocytes. J Biol Chem 264:12859-66

Khanna R, Sun L, Li Q, Guo L, Stanley EF. 2006. Long splice variant N type calcium channels are clustered at presynaptic transmitter release sites without modular adaptor proteins. Neuroscience 138:1115-25

Khosravani H, Altier C, Simms B, Hamming KS, Snutch TP, et al. 2004. Gating effects of mutations in the Cav3.2 T-type calcium channel associated with childhood absence epilepsy. J Biol Chem 279:9681-4

Kirchhoff F. 2010. Neuroscience. Questionable calcium. Science 327:1212-3

Kisilevsky AE, Mulligan SJ, Altier C, Iftinca MC, Varela D, et al. 2008. D1 receptors physically interact with N-type calcium channels to regulate channel distribution and dendritic calcium entry. Neuron 58:557-70

Klingauf J, Neher E. 1997. Modeling buffered Ca2+ diffusion near the membrane: implications for secretion in neuroendocrine cells. Biophys J 72:674-90

Klugbauer N, Lacinova L, Marais E, Hobom M, Hofmann F. 1999. Molecular diversity of the calcium channel alpha2delta subunit. J Neurosci 19:684-91

Koschak A, Reimer D, Huber I, Grabner M, Glossmann H, et al. 2001. alpha 1D (Cav1.3) subunits can form l-type Ca2+ channels activating at negative voltages. J Biol Chem 276:22100-6

Kreft M, Stenovec M, Rupnik M, Grilc S, Krzan M, et al. 2004. Properties of Ca(2+)-dependent exocytosis in cultured astrocytes. Glia 46:437-45

Krovetz HS, Helton TD, Crews AL, Horne WA. 2000. C-Terminal alternative splicing changes the gating properties of a human spinal cord calcium channel alpha 1A subunit. J Neurosci 20:7564-70

Latour I, Hamid J, Beedle AM, Zamponi GW, Macvicar BA. 2003. Expression of voltage-gated Ca2+ channel subtypes in cultured astrocytes. Glia 41:347-53

Lee JH, Daud AN, Cribbs LL, Lacerda AE, Pereverzev A, et al. 1999. Cloning and expression of a novel member of the low voltage-activated T-type calcium channel family. J Neurosci 19:1912-21

Lemos JR, Nowycky MC. 1989. Two types of calcium channels coexist in peptide-releasing vertebrate nerve terminals. Neuron 2:1419-26

Leonoudakis D, Conti LR, Radeke CM, McGuire LM, Vandenberg CA. 2004. A multiprotein trafficking complex composed of SAP97, CASK, Veli, and Mint1 is associated with inward rectifier Kir2 potassium channels. J Biol Chem 279:19051-63

Letts VA, Felix R, Biddlecome GH, Arikkath J, Mahaffey CL, et al. 1998. The mouse stargazer gene encodes a neuronal Ca2+-channel gamma subunit. Nat Genet 19:340-7

Leveque C, el Far O, Martin-Moutot N, Sato K, Kato R, et al. 1994. Purification of the N-type calcium channel associated with syntaxin and synaptotagmin. A complex implicated in synaptic vesicle exocytosis. J Biol Chem 269:6306-12

Leveque C, Hoshino T, David P, Shoji-Kasai Y, Leys K, et al. 1992. The synaptic vesicle protein synaptotagmin associates with calcium channels and is a putative Lambert-Eaton myasthenic syndrome antigen. Proc Natl Acad Sci U S A 89:3625-9

Li F, Pincet F, Perez E, Eng WS, Melia TJ, et al. 2007. Energetics and dynamics of SNAREpin folding across lipid bilayers. Nat Struct Mol Biol 14:890-6

Li Z, Hatton GI. 1997. Ca2+ release from internal stores: role in generating depolarizing after-potentials in rat supraoptic neurones. J Physiol 498 (Pt 2):339-50

Lim NF, Nowycky MC, Bookman RJ. 1990. Direct measurement of exocytosis and calcium currents in single vertebrate nerve terminals. Nature 344:449-51

Lipscombe D. 2005. Neuronal proteins custom designed by alternative splicing. Curr Opin Neurobiol 15:358-63

Lipscombe D, Pan JQ, Gray AC. 2002. Functional diversity in neuronal voltage-gated calcium channels by alternative splicing of Ca(v)alpha1. Mol Neurobiol 26:21-44

Liu H, De Waard M, Scott VE, Gurnett CA, Lennon VA, Campbell KP. 1996. Identification of three subunits of the high affinity omega-conotoxin MVIIC-sensitive Ca2+ channel. J Biol Chem 271:13804-10

Llinas R, Sugimori M, Lin JW, Cherksey B. 1989. Blocking and isolation of a calcium channel from neurons in mammals and cephalopods utilizing a toxin fraction (FTX) from funnel-web spider poison. Proc Natl Acad Sci U S A 86:1689-93

Llinas R, Sugimori M, Silver RB. 1992. Microdomains of high calcium concentration in a presynaptic terminal. Science 256:677-9

Luvisetto S, Fellin T, Spagnolo M, Hivert B, Brust PF, et al. 2004. Modal gating of human CaV2.1 (P/Q-type) calcium channels: I. The slow and the fast gating modes and their modulation by beta subunits. J Gen Physiol 124:445-61

MacVicar BA. 1984. Voltage-dependent calcium channels in glial cells. Science 226:1345-7

MacVicar BA, Hochman D, Delay MJ, Weiss S. 1991. Modulation of intracellular Ca++ in cultured astrocytes by influx through voltage-activated Ca++ channels. Glia 4:448-55

MacVicar BA, Tse FW. 1988. Norepinephrine and cyclic adenosine 3':5'-cyclic monophosphate enhance a nifedipine-sensitive calcium current in cultured rat astrocytes. Glia 1:359-65

Maienschein V, Marxen M, Volknandt W, Zimmermann H. 1999. A plethora of presynaptic proteins associated with ATP-storing organelles in cultured astrocytes. Glia 26:233-44

Mains RE, Eipper BA. 1979. Synthesis and secretion of corticotropins, melanotropins, and endorphins by rat intermediate pituitary cells. J Biol Chem 254:7885-94

Malenka RC, Bear MF. 2004. LTP and LTD: an embarrassment of riches. Neuron 44:5-21

Malleret G, Haditsch U, Genoux D, Jones MW, Bliss TV, et al. 2001. Inducible and reversible enhancement of learning, memory, and long-term potentiation by genetic inhibition of calcineurin. Cell 104:675-86

Mansvelder HD, Kits KS. 2000. Calcium channels and the release of large dense core vesicles from neuroendocrine cells: spatial organization and functional coupling. Prog Neurobiol 62:427-41

Mansvelder HD, Stoof JC, Kits KS. 1996. Dihydropyridine block of omega-agatoxin IVA- and omega-conotoxin GVIA-sensitive Ca2+ channels in rat pituitary melanotropic cells. Eur J Pharmacol 311:293-304

Marengo FD, Monck JR. 2000. Development and dissipation of Ca(2+) gradients in adrenal chromaffin cells. Biophys J 79:1800-20

Marini JC, Nelson KK, Battey J, Siracusa LD. 1993. The pituitary hormones arginine vasopressin-neurophysin II and oxytocin-neurophysin I show close linkage with interleukin-1 on mouse chromosome 2. Genomics 15:200-2

Mason WT, Hatton GI, Ho YW, Chapman C, Robinson IC. 1986. Central release of oxytocin, vasopressin and neurophysin by magnocellular neurone depolarization: evidence in slices of guinea pig and rat hypothalamus. Neuroendocrinology 42:311-22

Matlin AJ, Clark F, Smith CW. 2005. Understanding alternative splicing: towards a cellular code. Nat Rev Mol Cell Biol 6:386-98

Matthew WD, Tsavaler L, Reichardt LF. 1981. Identification of a synaptic vesicle-specific membrane protein with a wide distribution in neuronal and neurosecretory tissue. J Cell Biol 91:257-69

Maximov A, Bezprozvanny I. 2002. Synaptic targeting of N-type calcium channels in hippocampal neurons. J Neurosci 22:6939-52

Maximov A, Sudhof TC. 2005. Autonomous function of synaptotagmin 1 in triggering synchronous release independent of asynchronous release. Neuron 48:547-54

Maximov A, Sudhof TC, Bezprozvanny I. 1999. Association of neuronal calcium channels with modular adaptor proteins. J Biol Chem 274:24453-6

McEnery MW, Snowman AM, Snyder SH. 1991. Evidence for subtypes of the omega-conotoxin GVIA receptor. Identification of the properties intrinsic to the high-affinity receptor. Ann N Y Acad Sci 635:435-7

McNeil BD, Wu LG. 2009. Location matters: synaptotagmin helps place vesicles near calcium channels. Neuron 63:419-21

McRory JE, Hamid J, Doering CJ, Garcia E, Parker R, et al. 2004. The CACNA1F gene encodes an L-type calcium channel with unique biophysical properties and tissue distribution. J Neurosci 24:1707-18

Meinrenken CJ, Borst JG, Sakmann B. 2002. Calcium secretion coupling at calyx of held governed by nonuniform channel-vesicle topography. J Neurosci 22:1648-67

Mennerick S, Matthews G. 1996. Ultrafast exocytosis elicited by calcium current in synaptic terminals of retinal bipolar neurons. Neuron 17:1241-9

Mermelstein PG, Deisseroth K, Dasgupta N, Isaksen AL, Tsien RW. 2001. Calmodulin priming: nuclear translocation of a calmodulin complex and the memory of prior neuronal activity. Proc Natl Acad Sci U S A 98:15342-7

Mich PM, Horne WA. 2008. Alternative splicing of the Ca2+ channel beta4 subunit confers specificity for gabapentin inhibition of Cav2.1 trafficking. Mol Pharmacol 74:904-12

Mingorance-Le Meur A, Mohebiany AN, O'Connor TP. 2009. Varicones and growth cones: two neurite terminals in PC12 cells. PLoS One 4:e4334

Misura KM, Scheller RH, Weis WI. 2000. Three-dimensional structure of the neuronal-Sec1-syntaxin 1a complex. Nature 404:355-62

Mittman S, Guo J, Agnew WS. 1999a. Structure and alternative splicing of the gene encoding alpha1G, a human brain T calcium channel alpha1 subunit. Neurosci Lett 274:143-6

Mittman S, Guo J, Emerick MC, Agnew WS. 1999b. Structure and alternative splicing of the gene encoding alpha1I, a human brain T calcium channel alpha1 subunit. Neurosci Lett 269:121-4

Miyawaki A, Llopis J, Heim R, McCaffery JM, Adams JA, et al. 1997. Fluorescent indicators for Ca2+ based on green fluorescent proteins and calmodulin. Nature 388:882-7

Mochida S, Sheng ZH, Baker C, Kobayashi H, Catterall WA. 1996. Inhibition of neurotransmission by peptides containing the synaptic protein interaction site of N-type Ca2+ channels. Neuron 17:781-8

Mochida S, Westenbroek RE, Yokoyama CT, Zhong H, Myers SJ, et al. 2003. Requirement for the synaptic protein interaction site for reconstitution of synaptic transmission by P/Q-type calcium channels. Proc Natl Acad Sci U S A 100:2819-24

Montana V, Malarkey EB, Verderio C, Matteoli M, Parpura V. 2006. Vesicular transmitter release from astrocytes. Glia 54:700-15

Monteil A, Chemin J, Bourinet E, Mennessier G, Lory P, Nargeot J. 2000. Molecular and functional properties of the human alpha(1G) subunit that forms T-type calcium channels. J Biol Chem 275:6090-100

Morgan JI, Curran T. 1986. Role of ion flux in the control of c-fos expression. Nature 322:552-5

Mori Y, Friedrich T, Kim MS, Mikami A, Nakai J, et al. 1991. Primary structure and functional expression from complementary DNA of a brain calcium channel. Nature 350:398-402

Mothet JP, Pollegioni L, Ouanounou G, Martineau M, Fossier P, Baux G. 2005. Glutamate receptor activation triggers a calcium-dependent and SNARE protein-dependent release of the gliotransmitter D-serine. Proc Natl Acad Sci U S A 102:5606-11

Mulligan SJ, MacVicar BA. 2004. Calcium transients in astrocyte endfeet cause cerebrovascular constrictions. Nature 431:195-9

Murugaiyan P, Salm AK. 1995. Dehydration-induced proliferation of identified pituicytes in fully adult rats. Glia 15:65-76

Nakai S, Furuya K, Miyata S, Kiyohara T. 1999. Intracellular Ca2+ responses to nucleotides, peptides, amines, amino acids and prostaglandins in cultured pituicytes from adult rat neurohypophysis. Neurosci Lett 266:185-8

Navone F, Greengard P, De Camilli P. 1984. Synapsin I in nerve terminals: selective association with small synaptic vesicles. Science 226:1209-11

Navone F, Jahn R, Di Gioia G, Stukenbrok H, Greengard P, De Camilli P. 1986. Protein p38: an integral membrane protein specific for small vesicles of neurons and neuroendocrine cells. J Cell Biol 103:2511-27

Naylor MJ, Rancourt DE, Bech-Hansen NT. 2000. Isolation and characterization of a calcium channel gene, Cacna1f, the murine orthologue of the gene for incomplete X-linked congenital stationary night blindness. Genomics 66:324-7

Neher E. 1992. Cell physiology. Controls on calcium influx. Nature 355:298-9

Neher E. 1998. Vesicle pools and Ca2+ microdomains: new tools for understanding their roles in neurotransmitter release. Neuron 20:389-99

Neher E, Zucker RS. 1993. Multiple calcium-dependent processes related to secretion in bovine chromaffin cells. Neuron 10:21-30

Nestler E, Hyman S, Malenka R. 2008. Molecular Neuropharmacology: A Foundation for Clinical Neuroscience, Second Edition McGraw-Hill Medical,16-54

Newcomb R, Szoke B, Palma A, Wang G, Chen X, et al. 1998. Selective peptide antagonist of the class E calcium channel from the venom of the tarantula Hysterocrates gigas. Biochemistry 37:15353-62

North RA. 2002. Molecular physiology of P2X receptors. Physiol Rev 82:1013-67

Nowycky MC, Fox AP, Tsien RW. 1985. Three types of neuronal calcium channel with different calcium agonist sensitivity. Nature 316:440-3

Oliet SH, Bourque CW. 1992. Properties of supraoptic magnocellular neurones isolated from the adult rat. J Physiol 455:291-306

Olivera BM, Miljanich GP, Ramachandran J, Adams ME. 1994. Calcium channel diversity and neurotransmitter release: the omega-conotoxins and omega-agatoxins. Annu Rev Biochem 63:823-67

Olson PA, Tkatch T, Hernandez-Lopez S, Ulrich S, Ilijic E, et al. 2005. G-protein-coupled receptor modulation of striatal CaV1.3 L-type Ca2+ channels is dependent on a Shank-binding domain. J Neurosci 25:1050-62

Ophoff RA, Terwindt GM, Vergouwe MN, van Eijk R, Oefner PJ, et al. 1996. Familial hemiplegic migraine and episodic ataxia type-2 are caused by mutations in the Ca2+ channel gene CACNL1A4. Cell 87:543-52

Page KM, Stephens GJ, Berrow NS, Dolphin AC. 1997. The intracellular loop between domains I and II of the B-type calcium channel confers aspects of G-protein sensitivity to the E-type calcium channel. J Neurosci 17:1330-8

Pan JQ, Lipscombe D. 2000. Alternative splicing in the cytoplasmic II-III loop of the N-type Ca channel alpha 1B subunit: functional differences are beta subunit-specific. J Neurosci 20:4769-75

Parekh AB. 2006. Cell biology: cracking the calcium entry code. Nature 441:163-5

Parekh AB, Putney JW, Jr. 2005. Store-operated calcium channels. Physiol Rev 85:757-810

Park F, Koike G, Cowley AW, Jr. 1998. Regional time-dependent changes in vasopressin V2 receptor expression in the rat kidney during water restriction. Am J Physiol 274:F906-13

Parpura V, Basarsky TA, Liu F, Jeftinija K, Jeftinija S, Haydon PG. 1994. Glutamate-mediated astrocyte-neuron signalling. Nature 369:744-7

Parpura V, Haydon PG. 2000. Physiological astrocytic calcium levels stimulate glutamate release to modulate adjacent neurons. Proc Natl Acad Sci U S A 97:8629-34

Parri HR, Crunelli V. 2003. The role of Ca2+ in the generation of spontaneous astrocytic Ca2+ oscillations. Neuroscience 120:979-92

Parri HR, Gould TM, Crunelli V. 2001. Spontaneous astrocytic Ca2+ oscillations in situ drive NMDAR-mediated neuronal excitation. Nat Neurosci 4:803-12

Pasantes Morales H, Schousboe A. 1988. Volume regulation in astrocytes: a role for taurine as an osmoeffector. J Neurosci Res 20:503-9

Patil PG, Brody DL, Yue DT. 1998. Preferential closed-state inactivation of neuronal calcium channels. Neuron 20:1027-38

Patterson RL, Boehning D, Snyder SH. 2004. Inositol 1,4,5-trisphosphate receptors as signal integrators. Annu Rev Biochem 73:437-65

Perea G, Navarrete M, Araque A. 2009. Tripartite synapses: astrocytes process and control synaptic information. Trends Neurosci 32:421-31

Perez-Reyes E. 2003. Molecular physiology of low-voltage-activated t-type calcium channels. Physiol Rev 83:117-61

Perez-Reyes E, Cribbs LL, Daud A, Lacerda AE, Barclay J, et al. 1998. Molecular characterization of a neuronal low-voltage-activated T-type calcium channel. Nature 391:896-900

Perrino BA, Ng LY, Soderling TR. 1995. Calcium regulation of calcineurin phosphatase activity by its B subunit and calmodulin. Role of the autoinhibitory domain. J Biol Chem 270:340-6

Petersen MB. 2006. The effect of vasopressin and related compounds at V1a and V2 receptors in animal models relevant to human disease. Basic Clin Pharmacol Toxicol 99:96-103

Phillips PA, Abrahams JM, Kelly JM, Mooser V, Trinder D, Johnston CI. 1990. Localization of vasopressin binding sites in rat tissues using specific V1 and V2 selective ligands. Endocrinology 126:1478-84

Pragnell M, De Waard M, Mori Y, Tanabe T, Snutch TP, Campbell KP. 1994. Calcium channel beta-subunit binds to a conserved motif in the I-II cytoplasmic linker of the alpha 1-subunit. Nature 368:67-70

Puro DG, Hwang JJ, Kwon OJ, Chin H. 1996. Characterization of an L-type calcium channel expressed by human retinal Muller (glial) cells. Brain Res Mol Brain Res 37:41-8

Purves D, Augustine G, Fizpatrick D, Hall WC, Lamantia A, et al. 2004. Neuroscience. Sunderland, Massachusetts U.S.A.: Sinauer Associates, Inc., 8-9

Rajadhyaksha AM, Kosofsky BE. 2005. Psychostimulants, L-type calcium channels, kinases, and phosphatases. Neuroscientist 11:494-502

Rajapaksha WR, Wang D, Davies JN, Chen L, Zamponi GW, Fisher TE. 2008. Novel splice variants of rat CaV2.1 that lack much of the synaptic protein interaction site are expressed in neuroendocrine cells. J Biol Chem 283:15997-6003

Ramsey IS, Delling M, Clapham DE. 2006. An introduction to TRP channels. Annu Rev Physiol 68:619-47

Randall A, Benham CD. 1999. Recent advances in the molecular understanding of voltage-gated Ca2+ channels. Mol Cell Neurosci 14:255-72

Randall A, Tsien RW. 1995. Pharmacological dissection of multiple types of Ca2+ channel currents in rat cerebellar granule neurons. J Neurosci 15:2995-3012

Reim K, Mansour M, Varoqueaux F, McMahon HT, Sudhof TC, et al. 2001. Complexins regulate a late step in Ca2+-dependent neurotransmitter release. Cell 104:71-81

Renaud LP, Bourque CW. 1991. Neurophysiology and neuropharmacology of hypothalamic magnocellular neurons secreting vasopressin and oxytocin. Prog Neurobiol 36:131-69

Rettig J, Heinemann C, Ashery U, Sheng ZH, Yokoyama CT, et al. 1997. Alteration of Ca2+ dependence of neurotransmitter release by disruption of Ca2+ channel/syntaxin interaction. J Neurosci 17:6647-56

Rettig J, Sheng ZH, Kim DK, Hodson CD, Snutch TP, Catterall WA. 1996. Isoform-specific interaction of the alpha1A subunits of brain Ca2+ channels

with the presynaptic proteins syntaxin and SNAP-25. Proc Natl Acad Sci U S A 93:7363-8

Reuter H. 1967. The dependence of slow inward current in Purkinje fibres on the extracellular calcium-concentration. J Physiol 192:479-92

Richman RW, Tombler E, Lau KK, Anantharam A, Rodriguez J, et al. 2004. N-type Ca2+ channels as scaffold proteins in the assembly of signaling molecules for GABAB receptor effects. J Biol Chem 279:24649-58

Ringer S. 1883. A further Contribution regarding the influence of the different Constituents of the Blood on the Contraction of the Heart. J Physiol 4:29-42 3

Rizzoli SO, Betz WJ. 2005. Synaptic vesicle pools. Nat Rev Neurosci 6:57-69

Rizzuto R, Pinton P, Carrington W, Fay FS, Fogarty KE, et al. 1998. Close contacts with the endoplasmic reticulum as determinants of mitochondrial Ca2+ responses. Science 280:1763-6

Robinson LJ, Martin TF. 1998. Docking and fusion in neurosecretion. Curr Opin Cell Biol 10:483-92

Roos J, DiGregorio PJ, Yeromin AV, Ohlsen K, Lioudyno M, et al. 2005. STIM1, an essential and conserved component of store-operated Ca2+ channel function. J Cell Biol 169:435-45

Rose JP, Wu CK, Hsiao CD, Breslow E, Wang BC. 1996. Crystal structure of the neurophysin-oxytocin complex. Nat Struct Biol 3:163-9

Rosenberg OS, Deindl S, Sung RJ, Nairn AC, Kuriyan J. 2005. Structure of the autoinhibited kinase domain of CaMKII and SAXS analysis of the holoenzyme. Cell 123:849-60

Rossetto O, Schiavo G, Montecucco C, Poulain B, Deloye F, et al. 1994. SNARE motif and neurotoxins. Nature 372:415-6

Rosso L, Mienville JM. 2009. Pituicyte modulation of neurohormone output. Glia 57:235-43

Rudge JS, Pasnikowski EM, Holst P, Lindsay RM. 1995. Changes in neurotrophic factor expression and receptor activation following exposure of hippocampal neuron/astrocyte cocultures to kainic acid. J Neurosci 15:6856-67

Sabatier N, Caquineau C, Dayanithi G, Bull P, Douglas AJ, et al. 2003. Alpha-melanocyte-stimulating hormone stimulates oxytocin release from the dendrites of hypothalamic neurons while inhibiting oxytocin release from their terminals in the neurohypophysis. J Neurosci 23:10351-8

Saegusa H, Kurihara T, Zong S, Kazuno A, Matsuda Y, et al. 2001. Suppression of inflammatory and neuropathic pain symptoms in mice lacking the N-type Ca2+ channel. EMBO J 20:2349-56

Sakurai T, Hell JW, Woppmann A, Miljanich GP, Catterall WA. 1995. Immunochemical identification and differential phosphorylation of alternatively spliced forms of the alpha 1A subunit of brain calcium channels. J Biol Chem 270:21234-42

Sakurai T, Westenbroek RE, Rettig J, Hell J, Catterall WA. 1996. Biochemical properties and subcellular distribution of the BI and rbA isoforms of alpha 1A subunits of brain calcium channels. J Cell Biol 134:511-28

Salm AK, Hatton GI, Nilaver G. 1982. Immunoreactive glial fibrillary acidic protein in pituicytes of the rat neurohypophysis. Brain Res 236:471-6

Sambrook, MacCallum, Russell. 2001. Molecular Cloning: A Laboratory Manual (Third Edition)
CSHL Press: 38-45

Sather WA, Tanabe T, Zhang JF, Mori Y, Adams ME, Tsien RW. 1993. Distinctive biophysical and pharmacological properties of class A (BI) calcium channel alpha 1 subunits. Neuron 11:291-303

Schuh K, Uldrijan S, Gambaryan S, Roethlein N, Neyses L. 2003. Interaction of the plasma membrane Ca2+ pump 4b/CI with the Ca2+/calmodulin-dependent membrane-associated kinase CASK. J Biol Chem 278:9778-83

Scott VE, De Waard M, Liu H, Gurnett CA, Venzke DP, et al. 1996. Beta subunit heterogeneity in N-type Ca2+ channels. J Biol Chem 271:3207-12

Seifert G, Schilling K, Steinhauser C. 2006. Astrocyte dysfunction in neurological disorders: a molecular perspective. Nat Rev Neurosci 7:194-206

Shaywitz AJ, Greenberg ME. 1999. CREB: a stimulus-induced transcription factor activated by a diverse array of extracellular signals. Annu Rev Biochem 68:821-61

Sheng M. 1996. PDZs and receptor/channel clustering: rounding up the latest suspects. Neuron 17:575-8

Sheng M, Kim E. 2000. The Shank family of scaffold proteins. J Cell Sci 113 (Pt 11):1851-6

Sheng ZH, Rettig J, Cook T, Catterall WA. 1996. Calcium-dependent interaction of N-type calcium channels with the synaptic core complex. Nature 379:451-4

Sheng ZH, Rettig J, Takahashi M, Catterall WA. 1994. Identification of a syntaxin-binding site on N-type calcium channels. Neuron 13:1303-13

Sheng ZH, Yokoyama CT, Catterall WA. 1997. Interaction of the synprint site of N-type Ca2+ channels with the C2B domain of synaptotagmin I. Proc Natl Acad Sci U S A 94:5405-10

Silver RA, Lamb AG, Bolsover SR. 1990. Calcium hotspots caused by L-channel clustering promote morphological changes in neuronal growth cones. Nature 343:751-4

Smith SJ, Augustine GJ. 1988. Calcium ions, active zones and synaptic transmitter release. Trends Neurosci 11:458-64

Snutch TP, Leonard JP, Gilbert MM, Lester HA, Davidson N. 1990. Rat brain expresses a heterogeneous family of calcium channels. Proc Natl Acad Sci U S A 87:3391-5

Sollner T, Whiteheart SW, Brunner M, Erdjument-Bromage H, Geromanos S, et al. 1993. SNAP receptors implicated in vesicle targeting and fusion. Nature 362:318-24

Soong TW, DeMaria CD, Alvania RS, Zweifel LS, Liang MC, et al. 2002. Systematic identification of splice variants in human P/Q-type channel alpha1(2.1) subunits: implications for current density and Ca2+-dependent inactivation. J Neurosci 22:10142-52

Soong TW, Stea A, Hodson CD, Dubel SJ, Vincent SR, Snutch TP. 1993. Structure and functional expression of a member of the low voltage-activated calcium channel family. Science 260:1133-6

Spafford JD, Munno DW, Van Nierop P, Feng ZP, Jarvis SE, et al. 2003. Calcium channel structural determinants of synaptic transmission between identified invertebrate neurons. J Biol Chem 278:4258-67

Spafford JD, Zamponi GW. 2003. Functional interactions between presynaptic calcium channels and the neurotransmitter release machinery. Curr Opin Neurobiol 13:308-14

Spanakis E, Milord E, Gragnoli C. 2008. AVPR2 variants and mutations in nephrogenic diabetes insipidus: review and missense mutation significance. J Cell Physiol 217:605-17

Stanley EF, Mirotznik RR. 1997. Cleavage of syntaxin prevents G-protein regulation of presynaptic calcium channels. Nature 385:340-3

Stanley EF, Russell JT. 1988. Inactivation of calcium channels in rat pituitary intermediate lobe cells. Brain Res 475:64-72

Starr TV, Prystay W, Snutch TP. 1991. Primary structure of a calcium channel that is highly expressed in the rat cerebellum. Proc Natl Acad Sci U S A 88:5621-5

Stea A, Tomlinson WJ, Soong TW, Bourinet E, Dubel SJ, et al. 1994. Localization and functional properties of a rat brain alpha 1A calcium channel reflect similarities to neuronal Q- and P-type channels. Proc Natl Acad Sci U S A 91:10576-80

Stevenson D, Laverty HG, Wenwieser S, Douglas M, Wilson JB. 2000. Mapping and expression analysis of the human CASK gene. Mamm Genome 11:934-7

Sudhof TC. 2006. Synaptic vesicles: an organelle comes of age. Cell 127:671-3

Sudhof TC, Rothman JE. 2009. Membrane fusion: grappling with SNARE and SM proteins. Science 323:474-7

Sutton RB, Fasshauer D, Jahn R, Brunger AT. 1998. Crystal structure of a SNARE complex involved in synaptic exocytosis at 2.4 A resolution. Nature 395:347-53

Svoboda K, Yasuda R. 2006. Principles of two-photon excitation microscopy and its applications to neuroscience. Neuron 50:823-39

Szabo Z, Obermair GJ, Cooper CB, Zamponi GW, Flucher BE. 2006. Role of the synprint site in presynaptic targeting of the calcium channel CaV2.2 in hippocampal neurons. Eur J Neurosci 24:709-18

Szatkowski M, Barbour B, Attwell D. 1990. Non-vesicular release of glutamate from glial cells by reversed electrogenic glutamate uptake. Nature 348:443-6

Takahashi M, Seagar MJ, Jones JF, Reber BF, Catterall WA. 1987. Subunit structure of dihydropyridine-sensitive calcium channels from skeletal muscle. Proc Natl Acad Sci U S A 84:5478-82

Takamori S, Holt M, Stenius K, Lemke EA, Gronborg M, et al. 2006. Molecular anatomy of a trafficking organelle. Cell 127:831-46

Tanabe T, Takeshima H, Mikami A, Flockerzi V, Takahashi H, et al. 1987. Primary structure of the receptor for calcium channel blockers from skeletal muscle. Nature 328:313-8

Tang J, Maximov A, Shin OH, Dai H, Rizo J, Sudhof TC. 2006. A complexin/synaptotagmin 1 switch controls fast synaptic vesicle exocytosis. Cell 126:1175-87

Taylor CP, Garrido R. 2008. Immunostaining of rat brain, spinal cord, sensory neurons and skeletal muscle for calcium channel alpha2-delta (alpha2-delta) type 1 protein. Neuroscience 155:510-21

Thaler C, Gray AC, Lipscombe D. 2004. Cumulative inactivation of N-type CaV2.2 calcium channels modified by alternative splicing. Proc Natl Acad Sci U S A 101:5675-9

Theodosis DT, MacVicar B. 1996. Neurone-glia interactions in the hypothalamus and pituitary. Trends Neurosci 19:363-7

Theodosis DT, Poulain DA, Oliet SH. 2008. Activity-dependent structural and functional plasticity of astrocyte-neuron interactions. Physiol Rev 88:983-1008

Theodosis DT, Poulain DA, Vincent JD. 1981. Possible morphological bases for synchronisation of neuronal firing in the rat supraoptic nucleus during lactation. Neuroscience 6:919-29

Thomas P, Surprenant A, Almers W. 1990. Cytosolic Ca2+, exocytosis, and endocytosis in single melanotrophs of the rat pituitary. Neuron 5:723-33

Thomas P, Wong JG, Lee AK, Almers W. 1993. A low affinity Ca2+ receptor controls the final steps in peptide secretion from pituitary melanotrophs. Neuron 11:93-104

Tian M, Reger JF, Armstrong WE. 1991. Electron microscopic and immunocytochemical study of rapidly frozen, freeze-substituted neural lobes of rats. J Neurocytol 20:79-96

Tombler E, Cabanilla NJ, Carman P, Permaul N, Hall JJ, et al. 2006. G protein-induced trafficking of voltage-dependent calcium channels. J Biol Chem 281:1827-39

Tottene A, Volsen S, Pietrobon D. 2000. alpha(1E) subunits form the pore of three cerebellar R-type calcium channels with different pharmacological and permeation properties. J Neurosci 20:171-8

Tribollet E, Barberis C, Jard S, Dubois-Dauphin M, Dreifuss JJ. 1988. Localization and pharmacological characterization of high affinity binding sites for

vasopressin and oxytocin in the rat brain by light microscopic autoradiography. Brain Res 442:105-18

Triggle DJ. 1999. The pharmacology of ion channels: with particular reference to voltage-gated Ca2+ channels. Eur J Pharmacol 375:311-25

Tweedle CD, Hatton GI. 1980. Evidence for dynamic interactions between pituicytes and neurosecretory axons in the rat. Neuroscience 5:661-71

Tweedle CD, Hatton GI. 1987. Morphological adaptability at neurosecretory axonal endings on the neurovascular contact zone of the rat neurohypophysis. Neuroscience 20:241-6

Vaca K, Wendt E. 1992. Divergent effects of astroglial and microglial secretions on neuron growth and survival. Exp Neurol 118:62-72

van Leeuwen FW, van der Beek EM, van Heerikhuize JJ, Wolters P, van der Meulen G, Wan YP. 1987. Quantitative light microscopic autoradiographic localization of binding sites labelled with [3H]vasopressin antagonist d(CH2)5Tyr(Me)VP in the rat brain, pituitary and kidney. Neurosci Lett 80:121-6

Verhage M, Ghijsen WE, Lopes da Silva FH. 1994. Presynaptic plasticity: the regulation of Ca(2+)-dependent transmitter release. Prog Neurobiol 42:539-74

Voets T, Moser T, Lund PE, Chow RH, Geppert M, et al. 2001. Intracellular calcium dependence of large dense-core vesicle exocytosis in the absence of synaptotagmin I. Proc Natl Acad Sci U S A 98:11680-5

Wadel K, Neher E, Sakaba T. 2007. The coupling between synaptic vesicles and Ca2+ channels determines fast neurotransmitter release. Neuron 53:563-75

Walker D, De Waard M. 1998. Subunit interaction sites in voltage-dependent Ca2+ channels: role in channel function. Trends Neurosci 21:148-54

Walz W. 1989. Role of glial cells in the regulation of the brain ion microenvironment. Prog Neurobiol 33:309-33

Walz W, MacVicar B. 1988. Electrophysiological properties of glial cells: comparison of brain slices with primary cultures. Brain Res 443:321-4

Wang D, Yan B, Rajapaksha WR, Fisher TE. 2009. The expression of voltage-gated ca2+ channels in pituicytes and the up-regulation of L-type ca2+ channels during water deprivation. J Neuroendocrinol 21:858-66

Wang G, Dayanithi G, Kim S, Hom D, Nadasdi L, et al. 1997. Role of Q-type Ca2+ channels in vasopressin secretion from neurohypophysial terminals of the rat. J Physiol 502 (Pt 2):351-63

Wang G, Dayanithi G, Newcomb R, Lemos JR. 1999. An R-type Ca(2+) current in neurohypophysial terminals preferentially regulates oxytocin secretion. J Neurosci 19:9235-41

Watkins LR, Milligan ED, Maier SF. 2001. Glial activation: a driving force for pathological pain. Trends Neurosci 24:450-5

Weick JP, Groth RD, Isaksen AL, Mermelstein PG. 2003. Interactions with PDZ proteins are required for L-type calcium channels to activate cAMP response element-binding protein-dependent gene expression. J Neurosci 23:3446-56

West AE, Chen WG, Dalva MB, Dolmetsch RE, Kornhauser JM, et al. 2001. Calcium regulation of neuronal gene expression. Proc Natl Acad Sci U S A 98:11024-31
Westenbroek RE, Ahlijanian MK, Catterall WA. 1990. Clustering of L-type Ca2+ channels at the base of major dendrites in hippocampal pyramidal neurons. Nature 347:281-4
Westenbroek RE, Bausch SB, Lin RC, Franck JE, Noebels JL, Catterall WA. 1998a. Upregulation of L-type Ca2+ channels in reactive astrocytes after brain injury, hypomyelination, and ischemia. J Neurosci 18:2321-34
Westenbroek RE, Hell JW, Warner C, Dubel SJ, Snutch TP, Catterall WA. 1992. Biochemical properties and subcellular distribution of an N-type calcium channel alpha 1 subunit. Neuron 9:1099-115
Westenbroek RE, Hoskins L, Catterall WA. 1998b. Localization of Ca2+ channel subtypes on rat spinal motor neurons, interneurons, and nerve terminals. J Neurosci 18:6319-30
Westenbroek RE, Sakurai T, Elliott EM, Hell JW, Starr TV, et al. 1995. Immunochemical identification and subcellular distribution of the alpha 1A subunits of brain calcium channels. J Neurosci 15:6403-18
Westerink RH, Ewing AG. 2008. The PC12 cell as model for neurosecretion. Acta Physiol (Oxf) 192:273-85
Wickman K, Clapham DE. 1995. Ion channel regulation by G proteins. Physiol Rev 75:865-85
Wilhelm A, Volknandt W, Langer D, Nolte C, Kettenmann H, Zimmermann H. 2004. Localization of SNARE proteins and secretory organelle proteins in astrocytes in vitro and in situ. Neurosci Res 48:249-57
Williams ME, Brust PF, Feldman DH, Patthi S, Simerson S, et al. 1992. Structure and functional expression of an omega-conotoxin-sensitive human N-type calcium channel. Science 257:389-95
Williams PJ, MacVicar BA, Pittman QJ. 1990. Electrophysiological properties of neuroendocrine cells of the intact rat pars intermedia: multiple calcium currents. J Neurosci 10:748-56
Williams PJ, Pittman QJ, MacVicar BA. 1991. Ca(2+)- and voltage-dependent inactivation of Ca2+ currents in rat intermediate pituitary. Brain Res 564:12-8
Williams PJ, Pittman QJ, MacVicar BA. 1993. Blockade by funnel web toxin of a calcium current in the intermediate pituitary of the rat. Neurosci Lett 157:171-4
Wiser O, Bennett MK, Atlas D. 1996. Functional interaction of syntaxin and SNAP-25 with voltage-sensitive L- and N-type Ca2+ channels. EMBO J 15:4100-10
Witcher DR, De Waard M, Sakamoto J, Franzini-Armstrong C, Pragnell M, et al. 1993. Subunit identification and reconstitution of the N-type Ca2+ channel complex purified from brain. Science 261:486-9

Wittemann S, Mark MD, Rettig J, Herlitze S. 2000. Synaptic localization and presynaptic function of calcium channel beta 4-subunits in cultured hippocampal neurons. J Biol Chem 275:37807-14

Wu L, Bauer CS, Zhen XG, Xie C, Yang J. 2002. Dual regulation of voltage-gated calcium channels by PtdIns(4,5)P2. Nature 419:947-52

Wu LG, Westenbroek RE, Borst JG, Catterall WA, Sakmann B. 1999. Calcium channel types with distinct presynaptic localization couple differentially to transmitter release in single calyx-type synapses. J Neurosci 19:726-36

Xu W, Lipscombe D. 2001. Neuronal Ca(V)1.3alpha(1) L-type channels activate at relatively hyperpolarized membrane potentials and are incompletely inhibited by dihydropyridines. J Neurosci 21:5944-51

Yokoyama CT, Westenbroek RE, Hell JW, Soong TW, Snutch TP, Catterall WA. 1995. Biochemical properties and subcellular distribution of the neuronal class E calcium channel alpha 1 subunit. J Neurosci 15:6419-32

Young SM, Jr., Neher E. 2009. Synaptotagmin has an essential function in synaptic vesicle positioning for synchronous release in addition to its role as a calcium sensor. Neuron 63:482-96

Yu FH, Catterall WA. 2004. The VGL-chanome: a protein superfamily specialized for electrical signaling and ionic homeostasis. Sci STKE 2004:re15

Zamponi GW, Bourinet E, Nelson D, Nargeot J, Snutch TP. 1997. Crosstalk between G proteins and protein kinase C mediated by the calcium channel alpha1 subunit. Nature 385:442-6

Zhang H, Fu Y, Altier C, Platzer J, Surmeier DJ, Bezprozvanny I. 2006. Ca1.2 and CaV1.3 neuronal L-type calcium channels: differential targeting and signaling to pCREB. Eur J Neurosci 23:2297-310

Zhang H, Maximov A, Fu Y, Xu F, Tang TS, et al. 2005. Association of CaV1.3 L-type calcium channels with Shank. J Neurosci 25:1037-49

Zhang Q, Pangrsic T, Kreft M, Krzan M, Li N, et al. 2004. Fusion-related release of glutamate from astrocytes. J Biol Chem 279:12724-33

Zhang W, Star B, Rajapaksha WR, Fisher TE. 2007. Dehydration increases L-type Ca(2+) current in rat supraoptic neurons. J Physiol 580:181-93

Zhao Y, Xu J, Gong J, Qian L. 2009. L-type calcium channel current up-regulation by chronic stress is associated with increased alpha(1c) subunit expression in rat ventricular myocytes. Cell Stress Chaperones 14:33-41

Zhong H, Yokoyama CT, Scheuer T, Catterall WA. 1999. Reciprocal regulation of P/Q-type Ca2+ channels by SNAP-25, syntaxin and synaptotagmin. Nat Neurosci 2:939-41

Zhuchenko O, Bailey J, Bonnen P, Ashizawa T, Stockton DW, et al. 1997. Autosomal dominant cerebellar ataxia (SCA6) associated with small polyglutamine expansions in the alpha 1A-voltage-dependent calcium channel. Nat Genet 15:62-9

Zucker RS. 1993. Calcium and transmitter release. J Physiol Paris 87:25-36

Appendix

Preparation of plasmid DNA by alkaline lysis with SDS: maxipreparation

Day1, streak DYT-antibiotic plate with bacteria and grow in incubator at 37°C. Day 2, take one colony and inoculate 5 ml of Terrific Broth (antibiotic +) at 37 °C, shake 250 rpm about 4h. Day 3, take 5ml of bacterial solution into 300 ml of TB (add antibiotic) and grow at 37°C, shake 250rpm about 16 h. Split 300 ml culture into 2 bottles (250 ml), and spin cells at 5000 g (4000 rpm) for 15 min at 4°C. Remove supernatant.and suspend pellet with 50 ml of ice-cold 1XSTE for each bottle. Centrifuge at 4000 rpm for 15 min at 4 °C. Resuspend pellet into 10ml of solution I, fully mixed with pipette. Add 20 ml of solution II, mix well by gently inverting the bottle 3-5 times to lyses the cell. Sticky genomic DNA should been seen. Add 20 ml of Solution III for each bottle and mix well by shaking 8-10 times, massive white denatured protein should been seen. Store the mixture on ice for 5 min, and centrifuge at 4000rpm for 15 min at 4°C. Filter supernatant through 4 layers of cheesecloth into new centrifuge bottle (250 ml). A light yellow clear solution of about 50ml is obtained. Add about 30 ml of isopropanol and mix well at room temperature. (Isopropanol: filtered solution = 0.6:1), put at RT for 30 min. Centrifuge at 4000 rpm for 15 min at 4°C. Discard supernatant and rinse pellet (Plasmid DNA in it) carefully with 2 ml of 85% ethanol. Drain off the ethanol and air dry the pellet for 5 min. Dissolve pellet in 3 ml of T.E. Solution (pH 8.0). Transfer DNA suspension into 15 ml cortex tube, add 4.8 ml of cold 5 M LiCl,

vortex thoroughly for 10 sec. Centrifuge at 1000 rpm or 9000 g for 10 min at 4°C.Transfer supernatant to a 30 ml cortex tube and add 30 ml of isopropanol, and mix well (DNA suspension : Isopropanol=1:1). Centrifuge at 1000rpm for 10 min at 4 °C. Discard supernatant and rinse pellet with 2 ml of 85% Ethanol by gently rotate the cortex tube. Drain off ethanol and air dry for 10 min (make sure minimally residual ethanol). Dissolve pellet (Plasmid DNA in it) with 500 µl of T.E. Solution (pH 8.0) and add 5 µl of RNase (10mg/ml) put for 30 min at RT. (Optional: at this point DNA solution can been stored at -20 °C). Add 400 µl of 1.6 M NaCl (with 13% (w/v) PEG800).Mix well and centrifuge at 12000g for 1-2 min at 4°C. Discard supernatants; dissolve the pellets (DNA in it) with 500 µl of T.E. (pH 8.0).

Following steps are further purification of DNA. a) Extract DNA solution with 500 µl of phenol, mix well by vortex 10 sec and spin at 5000rpm for 5 min. (white protein layer should be seen between aqueous layer and phenol); b) Transfer supernatant carefully into a new Eppendorf tube, add 500 µl of Chloroform, mix well vortex 10 sec and spin at 5000rpm for 5 min at RT; c) Transfer top aqueous layer to a new tube. Repeat step a-c at least once; d) Once the clear DNA solution is obtained, add 5M NaCl to a final concentration to 125mM; (for example, for 400 µl of DNA solution, about 10 µl of 5M NaCl is added) e) Add 800 µl of 100% ethanol into 400 µl of DNA solution (ethanol: DNA solution =1:2), keep on ice for at least 30 min, then white cloudy precipitation of DNA should be seen. (the more long fibrous precipitation, the

better purity) f) Centrifuge at 12000g for 5 min at 4°C. g) Carefully remove the supernatant and rinse the pellet (Pure DNA) with 200 µl of 85% ethanol, vortex briefly and spin again at 12000g for 2 min at 4°C h) Discard supernatant and evaporate all ethanol i) Dissolve pellet with pure water or T.E. (if subclone is not expected); Spectrophotometer Reading: dilute sample at ratio 1:200 in ddH_2O, 1OD λ260nm=50µg/µl.